THE SCALE DEPENDENCE OF DISPERSIVITY IN UNSATURATED MILL TAILINGS

by

Deborah L. McElroy

Submitted in Partial Fulfillment of
the Requirements for the Degree of
Master of Science in Hydrology

New Mexico Institute of Mining and Technology
Socorro, New Mexico

May, 1987

ABSTRACT

The two goals of this experiment were to determine the dispersivity of copper mill tailings under unsaturated flow conditions and to investigate the dependence of dispersivity on the scale of the experiment. A field-scale column, 336 cm in length, was packed with a homogeneous copper mill tailings sand and used to conduct a solute-transport experiment. After unsaturated flow was initiated and steady-state conditions established, a pulse of a bromide-tracer solution was applied. Bromide concentrations were then obtained over time, at four different depths along the column, to determine changes in dispersivity as a function of transport distance. Two smaller-scale (30 cm in length) column experiments were also conducted under similar unsaturated flow conditions, to provide an additional comparison of dispersivity to the scale of the experiment.

The field-scale column yielded dispersivities of 3.1, 4.1 and 1.2 cm for depths of 63, 126 and 252 cm, repectively, and failed to demonstrate a trend in the dispersivity values with transport distance. The mean dispersivity of 2.8 cm for the field-scale column was larger than the 0.47 cm dispersivity for the 30 cm long column, but was within one order of magnitude. This difference was attributed to the difference in the packing procedure for each column. Unlike the smaller column which was packed as one continuous lift, the field-scale column was packed in a series of 5 cm lifts, which imposed a stratification upon the porous medium. This stratification resulted in a heterogeneity of a larger-scale that existed in the smaller column, and consequently yielded a higher dispersivity. Thus, the relationship between dispersivity and the scale of the experiment was closely associated with the scale of the heterogeneities present.

TABLE OF CONTENTS

LIST OF FIGURES

LIST OF TABLES

LIST OF APPENDICES

ACKNOWLEDGEMENTS

The progress and completion of this investigation was made possible through the support and assistance of many sources.

I wish to thank my advisor, Dan Stephens, for his guidance and insightful comments and suggestions during the course of this study.

I also wish to acknowledge two principle sources of funding for this research: The United States Bureau of Mines under the Mining and Minerals Resources Research Institute, Generic Center Program and the Department of Energy, under the Master's Thesis Research Program on Nuclear Waste Management.

Dr. Pete Weirenga, of NMSU Dept. of Crop and Soil Sciences, provided invaluable technical advice and the use of his laboratory. Technical assistance from Greg Lewis, Stephen Conrad, Warren Cox, and Joe Vincent helped me through numerous phases of frustration in the laboratory. Mary Stollenwertz risked neck and limbs in packing the column, and Robert Mace provided tireless assistance with the sampling.

Continual encouragement was provided by fellow graduate students, including Peggy Barrol, Ken Harris, Gary Johnson, Julie Mattick, and Cindi Ardito. My officemates Swen Magnuson and Neil Blandford supplied me with dubious role-models, lots of humour, and kept graduate school in its proper perspective. A special thanks to my good friend Swen, for his unflagging support.

A very special thank-you is also extended to my family, who have maintained a strong emotional and sometimes financial support during my college career.

I. INTRODUCTION

PURPOSE OF INVESTIGATION

Seepage from mill tailings impoundments may contaminate both surface and ground-water systems. Tailings are composed of host rock that have been crushed during the milling process to facilitate ore extraction. In general, the mill waste solids are transported as a slurry from the mill area and deposited in a tailings pond. Over the course of time, the solids settle out and impoundments are formed. Precipitation may generate seepage through the tailings, and the subsequent leachate that forms is of environmental concern, especially if the leachate exits the tailings and enters the surface or ground water system.

In semi-arid climates, it is often assumed that dissolution of soluble chemical constituents of the tailings by infiltrating water is negligible, due to low annual precipitation and high evaporation rates. However, infiltration may not, in fact, be negligible even when annual rates of potential evaporation exceed precipitation. In a numerical simulation of infiltration into uranium mill tailings under semi-arid conditions, Klute and Herman (1978) indicated that long term recharge to an underlying aquifer can occur. Moreover, many of the tailings impoundments in semi-arid regions of the United States do not have adequate controls for drainage or surface run-off. Hydrologic characterization of the mill tailings can provide needed information about the transport of leached solutes within the tailings.

Larson (1984) characterized the beach-sand faction of

copper mill tailings by evaluating the saturated hydraulic conductivity, soil moisture characteristic curves, and relative hydraulic conductivity. Lewis (1986) then evaluated water and solute movement in the same tailings fraction, through infiltration and diffusion experiments. He found that diffusion could account for significant solute movement at low water contents, and that definite net downward movement of infiltrating precipitation did occur in unvegetated tailings in a semi-arid climate.

Lewis (1986) also determined the dispersivity of tailings, a property of the medium that influences the distribution of chemical concentrations in fluids which drain from the tailings.

The purposes of the current investigation were:

1) to obtain a field-scale dispersivity under unsaturated flow conditions, and
2) to investigate the dependence of dispersivity on the scale of the experiment.

LITERATURE REVIEW

In semi-arid climates, unsaturated conditions exist within abandoned tailings impoundments for much of the year. As dissolved chemical species are transported through the tailings (assuming no further chemical interactions with the tailings), their movement is affected by the hydrological characteristics of the medium, such as texture, particle-size distribution, water content, pressure heads, and hydraulic conductivity. These

characteristics influence the processes of dispersion and diffusion, which characterize the mixing and dilution of the solutes percolating through the tailings. The dispersion process can be quantified by determining the coefficient of hydrodynamic dispersion, which embodies dispersivity. The hydrodynamic dispersion coefficient is an important parameter used to describe the physics of the transport of chemicals through the copper mill tailings, for predictive modeling purposes.

Hydrodynamic dispersion is the result of both microscopic and macroscopic effects. At the microscopic scale, fluid velocity variations (in magnitude and direction) within and between pore-water channels cause a spreading of the solute. An initially close group of solute 'particles' will spread further apart as different flow paths are taken and as the particles travel at different velocities. For convenience, the flow velocities are averaged at the microscopic scale, because it would prove too complex to define the total flow pattern in detail. Advection describes the mean pore-fluid velocity, whereas hydrodynamic dispersion describes the variation about that mean.

At the macroscopic, or field-scale, heterogeneities within the medium are likely to exist, which result in additional velocity variations. The spread of the solute is no longer controlled by the local microscopic-scale dispersion, but rather by the larger-scale velocity variations. Layering of soils with different hydraulic conductivities and soil textures can change the spreading pattern of a solute. In field-scale studies,

dispersion appears to be the result of the heterogeneity of the profile (Anderson, 1979; Mercado, 1967; Pickens and Grisak, 1981, Sudicky et al., 1983), and the microscopic effects become insignificant.

Schwartz (1977), simulated macroscopic dispersion for a heterogeneous porous medium by using a statistical model of dispersion. He found that the

> "magnitude of dispersion is controlled by the contrast in hydraulic conductivity between the inclusions and the mode of aggregation. Generally, dispersivity is found to decrease as the conductivity contrast decreases and the structure of the medium is regularized."

Thus, the characteristics of a porous medium that influence dispersion depend on the scale of the representative elementary volume (REV). At the microscopic scale, pore-size and geometry are the dominating factors. At the macroscopic scale, hydraulic conductivity variations and contrasts within a formation govern the dispersion. At a megascopic scale, inter-formational hydraulic conductivity contrast would be the major factor.

The scale chosen for the REV averaging can influence the value of the dispersivity. Field-scale dispersivities have been observed that are several orders of magnitude larger than the dispersivities obtained from laboratory columns. This has been well-researched for the saturated case (Gelhar et al., 1979; Sauty, 1980; Anderson, 1979). Pickens and Grisak (1981) tabulated dispersivity results from various saturated field tests and obtained dispersivities that ranged from 0.012 to 15.2 m. These were compared to laboratory column results from repacked granular media, which gave a range of dispersivity values from 0.01 to 1.0

cm. The laboratory column dispersivities were several orders of magnitude smaller than the larger-scale field dispersivities.

There is a paucity of data which demonstrates the scale-dependence of dispersivity for unsaturated flow. Unsaturated flow experiments, especially at a field scale, are generally more difficult to run than comparably sized saturated experiments. Because of lower flow velocities, an experiment under unsaturated conditions is more time consuming than under saturated conditions, and the larger-scale experiments magnify the time difference. In addition, the apparatus and methodology used to conduct an unsaturated solute-transport experiment is more complex than for a saturated experiment. Unsaturated flow is also more complex than saturated flow due to the occurrence of three phases (air, soil, water). Furthermore, the relationship between dispersivity and water content is not well defined for a partially saturated medium.

Van de Pol et al. (1977) studied solute and water movement to a depth of 70 cm, in an unsaturated field soil consisting of clay to silty clay, over a medium sand. They found both pore-water velocity and hydrodynamic dispersion to be log-normally distributed, with mean values of 3.78 cm/day and 36.65 cm^2/day, respectively, which yielded a mean dispersivity of 9.7 cm. An approximate averaged water content of 34% was determined from the water content versus depth graph included in the article. The log-normal distriution indicated that extremes in solute displacement could occur in natural, heterogeneous field soils, due to the pore-water velocity distribution and spatial variability

of the soil. For comparison to this field result, unsaturated solute-transport experiments in repacked columns of 20 to 95 cm in length yielded dispersivities ranging from 0.03 to 1.2 cm, for varying water contents and soil types (Yule and Gardner, 1978; Kirda, et al., 1973; Gaudet, et al., 1977; De Smedt and Wierenga, 1984, van Genuchten and Wierenga, 1977).

Warrick, et al. (1971) conducted a solute-transport, field experiment in Panoche clay loam, over a 180 cm depth. This experiment yielded a dispersivity of 2.7 cm for a volumetric water content of 38%. It was observed that the hydrodynamic dispersion coefficient from small times or small distances increased with time or distance traveled.

A field study was conducted by Kies (1981), to measure and simulate solute transport in unsaturated Glendale clay loam, over a 450 cm depth. The dispersion coefficients and solute velocities that were obtained were also log-normally distributed, indicating large spatial variability. The dispersion coefficient and pore-water velocity both increased with depth, but there was no clear trend with depth for the dispersivities. However, the overall dispersivity of 14.3 cm was an order of magnitude larger than the dispersivities reported in the literature from unsaturated, repacked column experiments (Yule and Gardner, 1978; Kirda, et al., 1973; Gaudet, et al., 1977; De Smedt and Wierenga, 1984; van Genuchten and Wierenga, 1977).

Bresler and Dagan (1979) applied a conceptual model of solute transport to an unsaturated, heterogeneous field soil to determine concentration distributions for vertical, steady-state

flow. The spread of solute in a heterogeneous field soil was found to be much larger than the spread caused by using the microscopic, pore-scale hydrodynamic dispersion model. They concluded that advection and heterogeneity of the medium was the main mechanism for the solute spread modeled in the field soil, and that the pore-scale hydrodynamic dispersion could be neglected, in such a case.

SUMMARY OF OBJECTIVES OF INVESTIGATION

From the literature reviewed relevant to the scale-dependence of dispersivity for partially saturated media, two major points were suggested: 1) dispersivity may increase as a function of time or distance traveled, 2) dispersivity may increase as a function of the increasing heterogeneity of the medium. The objectives of this research are to provide insight into the first of those points as well as to obtain a value of dispersivity at a scale approximating that encountered in the field, for the copper mill tailings.

To summarize the scope of work in this study, a column (16.2 cm x 336 cm) was packed with a homogeneous, copper mill tailings sand. After steady-state, unsaturated flow conditions were established, a pulse of a conservative tracer was applied. Tracer (bromide) concentrations were obtained at several depths along the column to determine changes in dispersivity as a

function of travel distance. Two small-scale (30 cm) repacked column experiments were also run under similar unsaturated conditions for an additional comparision of dispersivity to scale of the experiment.

This study will be presented in the following sequence. First the theoretical basis for dispersion will be discussed, especially as it applies to unsaturated flow. Next, methods of determining the appropriate transport parameters will be reveiwed, including problems specific to unsaturated flow conditions. Flow and transport characterization of the mill tailings will follow, which includes results of the short and long-column, solute-transport experiments conducted in the laboratory under unsaturated flow conditions.

II. BACKGROUND IN SOLUTE TRANSPORT PROCESSES

DISPERSION

Dispersion refers to the mixing and spreading of a solute with the soil water during transport. This mixing results in a decrease in solute concentration and a more diffuse solute-soil water interface. As in Figure 1, an injection of a pulse of nonreactive solute into a flow field would show dilution and spreading, with time or distance. Hydrodynamic dispersion is attributed to a combination of processes: mechanical dispersion and molecular diffusion. Mechanical dispersion results from the motion of the fluid whereas molecular diffusion is a consequence of solute concentration gradients.

Molecular Diffusion

Diffusion results in a more uniform spatial distribution of the solute concentration in the soil water. Over time, random thermal motion of the molecules will cause a decrease in concentration gradients (Figure 2a). Because of the need to quantify diffusion, the coefficient of molecular diffusion was developed. Fick's first law states that the rate of diffusion is proportional to the concentration gradient. In bulk water (no soil) at rest, this is represented by

$$J_d = -D_o \, (dC/dx) \qquad (1)$$

where J_d is the diffusive flux, D_o the diffusion coefficient (L^2T^{-1}) and dc/dx the concentration gradient of a solute in the x-direction.

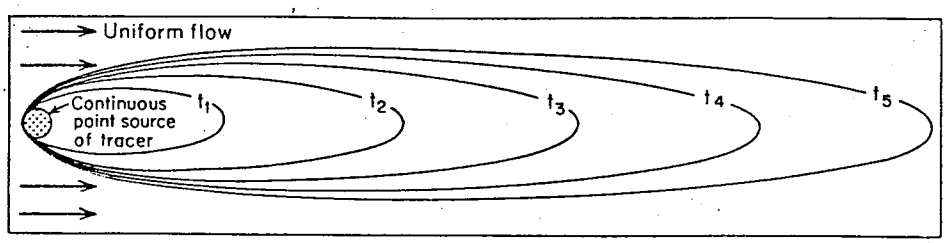

(a)

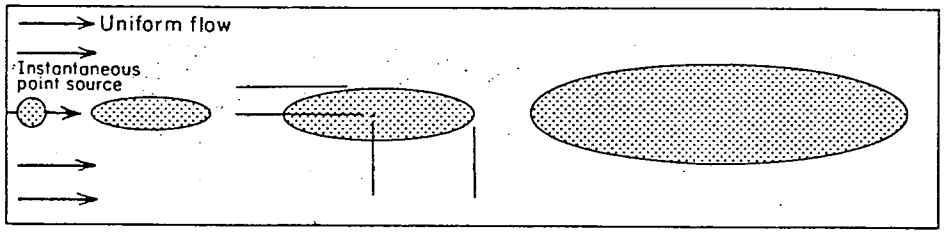

(b)

Figure 1. Spreading of a tracer in a two-dimensional uniform flow field in an isotropic sand. (a) Continuous tracer feed (b) instaneous point source. (from Freeze and Cherry, 1979)

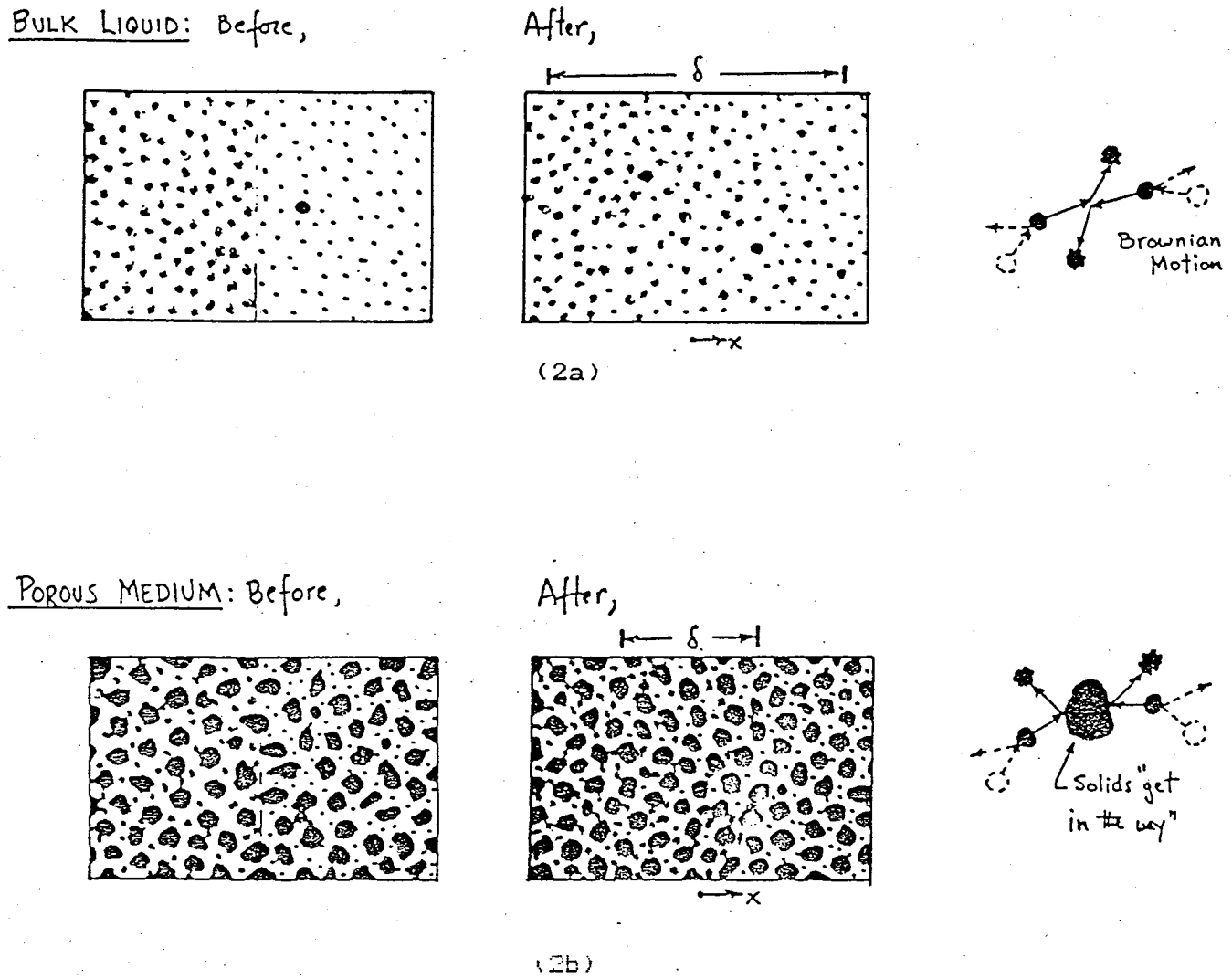

Figure 2. Spreading of tracer due to molecular diffusion. (a) in bulk water; (b) in porous medium. (from Wilson, 1985)

However, in the unsaturated zone, diffusion occurs in soil water rather than bulk water (Figure 2b). The molecular diffusion coefficient in soil water, D*, is less than the diffusion coefficient in bulk water, D_o. In addition, D* is a function of water content, θ. According to Hillel (1980), as water content decreases in an unsaturated soil, the number of water-connected pores decreases, causing the water channels to become more tortuous or branching. This in turn increases the actual path length over which diffusion must occur. Coupled with soil particle interference at the molecular level, the decreasing water content effectively decreases the molecular diffusion coefficient for soil water. Equation (1) can be rewritten, for unsaturated conditions as

$$J_d = -\theta D^* \nabla C \qquad (2)$$

$$D^* = D_o \Upsilon \qquad (3)$$

where Υ is the tortuosity factor (the straight path length divided by the actual path length for a diffusing molecule). Tortuosity, a dimensionless quantity, commonly ranges from 0.5 to 0.01 for a porous medium (Freeze and Cherry, 1979, p. 104).

Mechanical Dispersion Coefficient

Mechanical dispersion is primarily a function of flow velocity, or more specifically of irregularities in the distribution of pore-water velocities on a microscopic scale. These variations in magnitude and direction of pore-water velocities are caused by differences in the size and geometry of the pores,

as well as frictional effects (Figure 3). Small changes in pore radius will reflect large changes in volumetric discharge (Poiseuille's law), which increases the microscopic-scale velocity variations within the soil water (Figure 3b). Water will move faster at the center of a pore than along the pore walls, due to the viscous drag along the rough surfaces of the 'channel' walls (Figure 3a). Irregularities in grain sizes may cause eddies to occur. Increased tortuousness of pore channels will tend to vary the pore-water velocities even more.

Mechanical dispersion can be described in a manner similar to (1) for diffusion, such that

$$J_d = -\theta D_h \ (dC/dx) \tag{4}$$

where D_h is the mechanical dispersion coefficient (L^2/T) and J_h describes the transport by mechanical dispersion (Baer, 1972). The mechanical dispersion coefficient is a function of fluid velocity and saturation. The relationship of D_h to velocity for a saturated medium is (Freeze & Cherry, 1979):

$$D_h = a_L v^m \tag{5}$$

where a_L is the dispersivity in the direction of flow, and v is the mean pore-water velocity (q/θ), where q is the Darcy velocity, and θ is the volumetric water content. The exponent m is an empirically determined constant, usually between 1 and 2 for saturated media. The dispersivity, a_L, is an empirical parameter and a property of the porous medium. It is usually treated as a constant for a particular medium. However, dispersivity appears

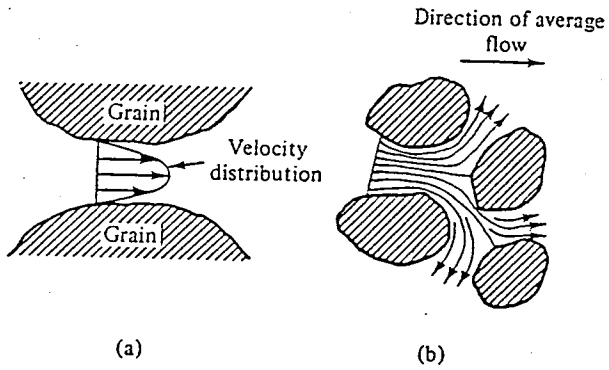

Figure 3. Spreading due to mechanical dispersion. (a) frictional effects; (b) variations in pore sizes and flow paths. (from Baer, 1979)

to vary with increasing travel distance or heterogeneity of the medium (Sauty, 1980), under saturated flow conditions. The variation of dispersivity with travel distance and the relationship between dispersivity and velocity has not been clearly established for unsaturated soils.

Hydrodynamic Dispersion Coefficient

Molecular diffusion and mechanical dispersion coefficients are combined to form the hydrodynamic dispersion coefficient, D'

$$D' = av^m + D^* \tag{6}$$

The use of different terms for D' found in the literature is a source of confusion. It is referred to as the hydrodynamic dispersion coefficient (Freeze & Cherry, 1979; Baer, 1979), the apparent diffusion coefficient (Gaudet, et al., 1977), and the diffusion-dispersion coefficient (Hillel, 1980). In this study, D' will be referred to as the hydrodynamic dispersion coefficient.

Molecular diffusion and mechanical dispersion occur simultaneously in miscible displacement. However, their significance in the dispersive process varies with velocity. At large flow velocities, the contribution of molecular diffusion to D' is small, compared to mechanical dispersion (Biggar & Nielsen, 1962; Baer, 1979). Conversely, in regions of very small velocities as found in unsaturated flow, the diffusional contribution may be large. The relationship between mechanical dispersion and molecular diffusion can be expressed by the porous medium Peclet

number,

$$P_e = vd / D^* \tag{7}$$

where d is defined as the average particle diameter (Freeze & Cherry, 1979) or a characteristic pore length (Baer, 1979). Laboratory experiments for saturated conditions have established curves for Peclet numbers versus the D'_L/D^* ratio, as shown in Figure 4, (Freeze & Cherry, 1979). D'_L is the longitudinal dispersion coefficient (where longitudinal refers to the direction of flow). The relationship between the Peclet number and D'_L/D^* depends on the particular medium and fluid. Increased pore-water velocity causes the porous medium Peclet number to increase and reach a velocity for which the molecular diffusion coefficient contribution is negligible. For most cases of saturated groundwater movement, diffusion is negligible. For sandy loam samples infiltrated at varying velocities, Kirda et al. (1973) determined that the contribution of molecular diffusion was not significant for pore-water velocities greater than 0.01 cm/min. According to Baer (1979), the general relationships shown by Figure 4 can be extrapolated to unsaturated conditions, and the respective components are recognized as functions of water content as well as pore-water velocities.

Dispersion In a Partially Saturated Medium

Dispersion in a partially saturated medium is influenced by factors beyond those of a saturated medium, which increases the complexity of the mixing process. Under unsaturated flow

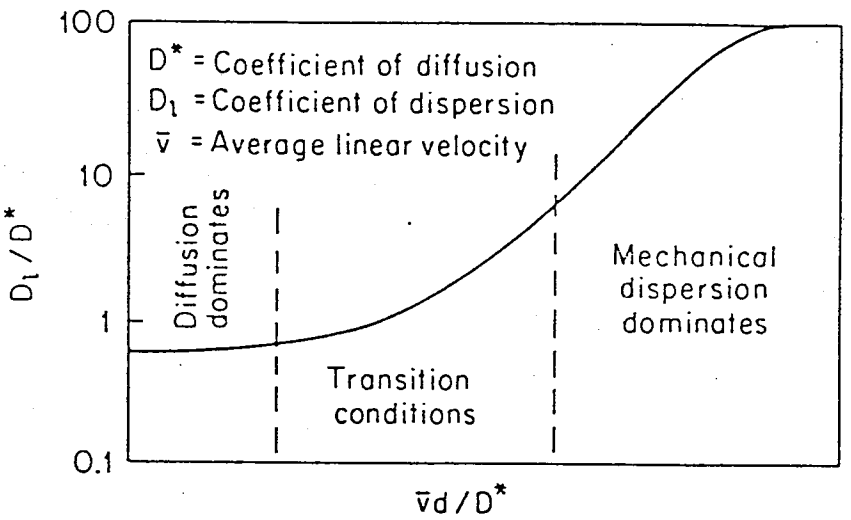

Figure 4. Relation between the porous medium Peclet number and the ratio of longitudinal dispersion coefficient and the coefficient of molecular diffusion in a sand of uniform-sized grains. (from Freeze and Cherry, 1979)

conditions, the hydrodynamic dispersion coefficient appears to be a function of the microscopic pore structure, the water content, and the pore-water velocity. Wilson and Gelhar (1974) demonstrated that the hydrodynamic dispersion coefficient determined under unsaturated flow conditions can exceed the dispersion coefficient for saturated flow in the same medium, for a particular range of water contents.

A decrease in water content creates zones of stagnant water which are not a full part of the advective flow (Krupp & Elrick, 1968; Nielsen & Biggar, 1961). Water may be trapped by the air phase, and cut off from the advective flow field; or it may be held to the soil surface by adhesive forces. Decreasing the saturation of the porous medium increases the fraction of immobile water in the pores (Nielsen & Biggar, 1961) and affects the dispersive process.

Krupp and Elrick (1968) describe three phases of the mixing process, under unsaturated flow conditions. At high water contents, most of the water in the system is mobile and participates in the advective flow. This provides a uniform flow field, and solute displacement occurs predominantly within the mobile phase. In contrast, wide velocity distributions (and non-uniform flow) occur at lower water contents which posses significant fractions of both mobile and stagnant water. The water-filled pores will conduct water and solute more quickly than the partially-filled, stagnant pores, thus widening the dispersed concentration zone. At much lower water contents, the immobile fraction dominates, and displacement primarily occurs within the

partially-filled pores. According to Krupp and Elrick (1968), the transport becomes more uniform at the very low water contents.

Wilson and Gelhar (1974) suggested the behavior of the hydrodynamic dispersion coefficient may be influenced by the pore-size distribution of the porous medium. In Figure 5, the variance of the pore-size distribution is shown as a function of the degree of saturation, S_e. When all the pores are water-filled, the variance of the pore-size distribution is small, and the majority of pores contribute equally to flow. As the pores are desaturated, both water-filled and partially-saturated pores exist, and the variance of the pore size distribution increases. As saturation approaches zero, only the smallest pores contain fluid, and the variance decreases.

Wilson and Gelhar (1974) developed an analytical model for unsaturated, solute displacement, which he applied to a statistical analysis of solute transport through a soil with a uniform moisture content. He calculated that, for a constant Peclet number, as the effective saturation decreased, the hydrodynamic dispersion coefficient increased, reached a maximum, and then decreased.

Using the results of Krupp and Elrick's (1968) solute-transport experiments through glass beads, Wilson (1974) then plotted the ratio D'/vl as a function of effective saturation (Figure 6). In a manner similar to the behavior of the pore size distribution, the highest dispersion occurs in the mid-saturation zone, and lowest dispersion at the greatest S_e. The second

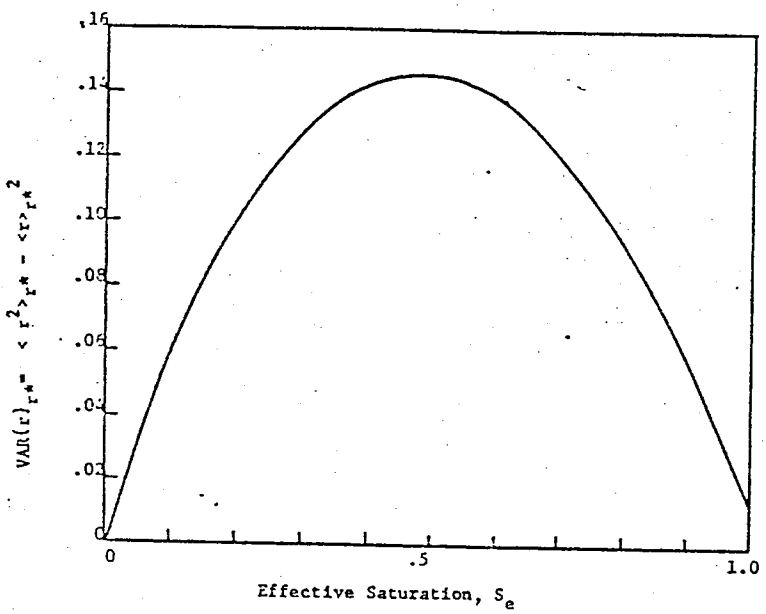

Figure 5. Variance of the pore size distribution: glass beads. (from Wilson and Gelhar, 1974)

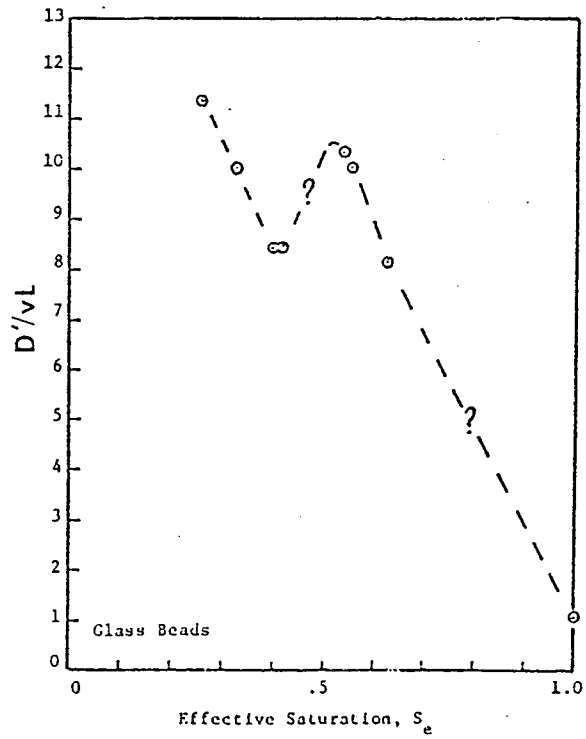

Figure 6. Dispersion coefficients as a function of saturation, evaluated with data of Krupp and Elrick (1968). (from Wilson and Gelhar, 1974)

maxima of the Krupp and Elrick (1968) data was not clearly understood, and data for the lower water contents was not available. The theoretical model of Wilson and Gelhar (1974) may be misleading at the lower contents, and the second rise evidenced by Krupp and Elrick's results may be due to a more complex pore geometry than expected.

Dispersivity, at least conceptually, was also shown to be a function of water content for unsaturated media by the model of Wilson and Gelhar (1974). In Figure 7, dispersivity was plotted as a dimensionless quantity (a_L/L) versus effective saturation for three different porous medium Peclet numbers, P_e. Wilson and Gelhar (1974) found that dispersivity increased to a maximum and then decreased as the effective saturation decreased. Each maxima was a function of the Peclet number (equation 7) and the higher maxima corresponded to the higher porous medium Peclet numbers. The dependence of dispersivity on water content was important at the lower water contents, but less important at higher water contents, closer to saturation (Wilson and Gelhar, 1974).

ADSORPTION

In addition to dispersive processes, solute concentration may be altered due to chemical reactions, biochemical reactions, or radioactive decay. Adsorption (Appendix A) is one chemical reaction that can have a significant effect on the transport of a

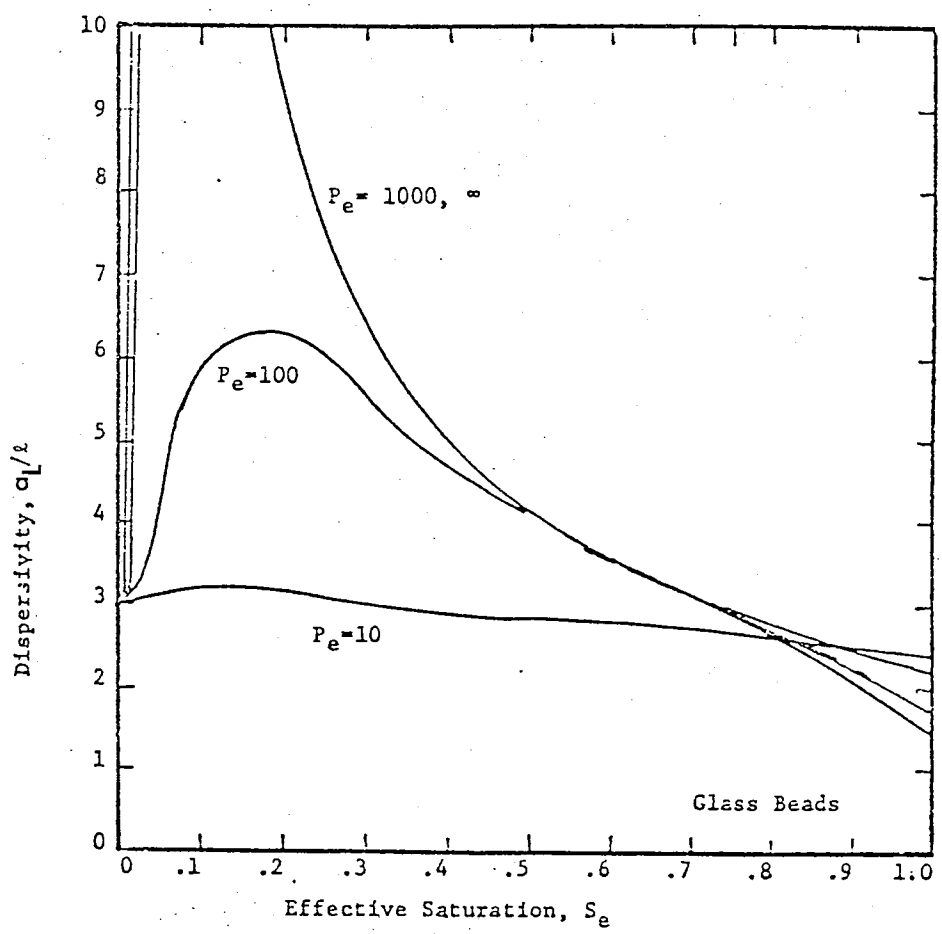

Figure 7. Dispersivity as a function of the degree of saturation. (from Wilson and Gelhar, 1974)

tracer.

Adsorption batch experiments can be run in the laboratory to determine the mass of the chemical constituent adsorbed on the the solid per unit mass of solids (S). According to the relationship

$$S = K_d C^b \tag{8}$$

where C is the solute concentration and K_d and b are coefficients which depend on the solute species and the porous medium. If b=1, the relationship becomes linear,

$$dS/dC = K_d \tag{9}$$

and the distribution coefficient, K_d, can be used to describe the ratio of the amount of an adsorbed ion to its concentration in the solution. The use of K_d to describe this process is limited to fast, reversible reactions and the linear S versus C relation. If a solute is affected by adsorption, the solute front may advance more slowly than the bulk mass of water. This retardation of the solute front relative to the movement of the bulk mass of water can be described by

$$v/v_c = 1 + (\rho_b K_d/\theta) \tag{10}$$

where v_c is the velocity of the $C/C_o = 0.5$ point of the concentration profile, and ρ_b is the bulk density. Without adsorption, $K_d = 0$, and R = 1.

As cations are adsorbed by the solid, the tracer front migrates at a slower rate than the ideal tracer movement (Figure

8) and is characterized by a retardation factor, R, greater than one. If the solute or tracer moves as an ideal substance and does not undergo any adsorption or other chemical reactions, the retardation factor equals one. It is also possible to have a retardation factor of less than one, which occurs when only a portion of the water phase contributes to the solute movement by either anion exclusion or presence of an immobile water phase (van Genuchten, 1980). Anion exclusion is the process in which negatively charged clays may repel anions from water held in the vicinity of the clay surface.

If the adsorption reaction is irreversible, the exchange reaction is slow relative to the velocity, or if the distribution coefficient does not describe a linear process, non-equilibrium conditions exist, and the retardation factor connot be used to accurately describe the movement of the adsorbed front.

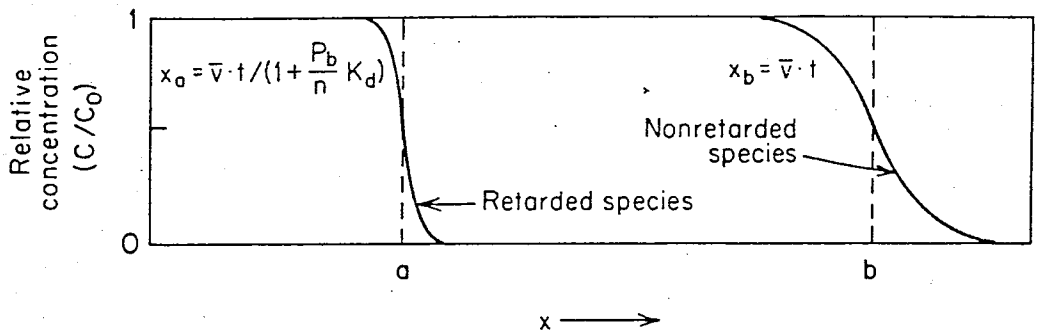

Figure 8. Advance of adsorbed and nonadsorbed solutes through a column of porous materials. Partitioning of adsorbed species is described by K_d. (from Freeze and Cherry, 1979)

III. METHODOLOGY AND ANALYSIS OF SOLUTE-TRANSPORT EXPERIMENTS

The dispersivity of porous media can be determined from both laboratory column experiements and in-situ field experiments. The laboratory column experiments, in which effluent is analyzed during solute-displacement, are more convenient than field experiments in terms of time and complexity. However, an increase in dispersivity usually results when methods of analyzing solute-transport in the laboratory are then applied to field experiments (Anderson, 1984). This section discusses methods for determining dispersivity from repacked column experiments and approaches which address the discrepancy in dispersivities between laboratory column results and the results of transport under field conditions.

SOLUTE TRANSPORT IN LABORATORY COLUMNS

Dispersion can be analyzed in the laboratory by means of soil columns, through which a tracer solution is added. For example, a vertical soil column is uniformly packed as a homogeneous medium. A constant flux of water is applied to the column, until steady state flow conditions and a uniform moisture content are established (Figure 9a). Then a continuous supply of a non-reactive tracer is introduced into the flowstream at the top of the column. Effluent samples can be obtained at the bottom of the column over time and these samples are analyzed for tracer concentration. The relation between concentration and time at a fixed point is termed a breakthrough curve (BTC).

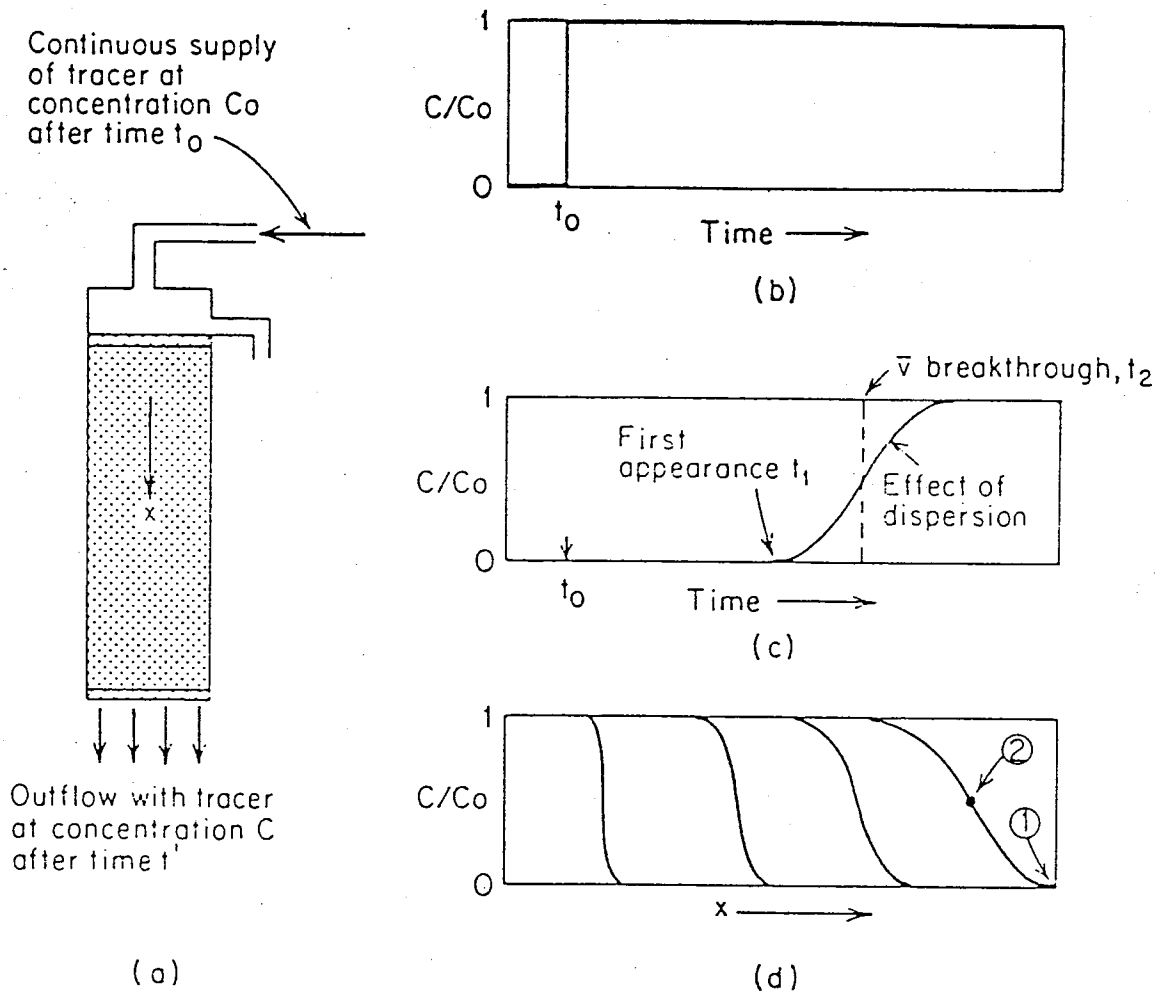

Figure 9. Longitudinal dispersion of a tracer passing through a column of porous medium. (a) Column with steady flow and continuous supply of tracer after time t; (b) stepfunction-type tracer input relation; (c) relative tracer concentration in outflow from column (dashed line indeicates piston flow and solid line illustrates effect of mechanical dispersion and molecular diffusion); (d) concentration profile in the column at various times. (from Freeze and Cherry, 1979)

Figure 9c shows a hypothetical breakthrough curve, assuming that the concentration of tracer in the column was zero prior to input. Concentration measured from the effluent is C, and concentration of the introduced tracer is C_o. Thus C/C_o gives the relative effluent concentration values, ranging from 0 to 1. When plotting breakthrough curves, concentration is often plotted versus number of pore volumes of effluent (T), which is the dimensionless ratio of the volume of effluent to the total volume of water held in the column,

$$T = Qt/\theta AL \tag{11}$$

where Q is the volumetric flux, and t is time. It is assumed that volumetric flux can be determined from the measured input rates, or it may be computed as the product of the Darcy velocity and cross-sectional area, or 'qA'.

Figure 9b illustrates the tracer input condition as a step function, which describes an instantaneous change in tracer concentration at the input boundary. The tracer concentration in the column, prior to tracer introduction, is zero in this example. Looking at the BTC (Figure 9c), one can see the first appearance, or breakthrough, of the tracer (at t_1) and follow the gradual concentration increase with time until $C/C_o = 1$, at the tail. Dispersion has created the transition zone, between $C/C_o = 0$ and $C/C_o = 1$. The dashed line in Figure 9c shows the tracer movement without dispersional effects and represents a piston-type displacement. In Figure 9d, the spread of the solute front extended as the tracer moved through the column, suggesting

that both time and distance increased the effects of dispersion.

Theoretically, a breakthrough curve which describes a non-reactive, conservative tracer will reach the 50% concentration at one pore volume. At this pore volume, all the original water in the column has been replaced by the tracer solution, and the 50% concentration (which averages the dispersed zone concentrations) has reached the column exit.

Designing and implementing a solute-transport, column experiment under unsaturated conditions presents special problems, such as the non-linearity of flow where hydraulic conductivity, K, is a function of pressure head. For flow through vertical columns of uniform porous material, some of the complexity of unsaturated flow can be circumvented by the establishment of steady-state flow conditions and consequent uniform water contents.

For one-dimensional, vertical flow

$$q = -K(\Psi)\ (dH/dz) \tag{12}$$

where q is the Darcy flux in the z direction, K the hydraulic conductivity, is the pressure head, H is the hydraulic head, and z the vertical distance coordinate (positive downward). Separating hydraulic head H, into its components of elevation or gravitational head, z, and pressure head, Ψ,

$$q = -K(\Psi)\ (d\Psi/dz - 1) \tag{13}$$

with a unit gravitational head gradient for one-dimension-

al vertical flow.

If the relationship of pressure head, Ψ, to water content, θ, is known (from experimental θ-Ψ curves) and the pressure head gradient is expanded by the chain rule,

$$q = -K(\theta)\ \left(\left(\frac{d\Psi}{d\theta}\frac{d\theta}{dz}\right) - 1\right) \tag{14}$$

If steady-state flow conditions are established in the vertical column, and the inflow rate equals the outflow rate, then the water content should be uniform throughout the column ($d\theta/dz = 0$). Flow becomes gravity driven, and

$$q = K(\theta) \tag{15}$$

The unsaturated hydraulic conductivity is still a function of water content. However, the constant water content establishes a constant hydraulic conductivity and simplifies the flow and transport analysis.

DETERMINING TRANSPORT PARAMETERS

Advection-Dispersion Equation

The advection-dispersion equation is used to decribe the solute transport process in a porous medium. The derivation of the equation is based on the law of conservation of mass, and assumes a homogeneous and isotropic porous medium. Steady-state, uniform flow conditions exist, and Darcy's law applies. Incompressibility of the medium and the fluid is also assumed, and

there are no sources or sinks.

With the assumption that Darcy's law applies, the transport of a solute is defined on a macroscopic scale, by the average linear velocity. This is a macroscopic parameter which describes the advective path of a solute. But, the dispersion process is based on microscopic paramenters (local velocity inhomogeneities and pore size differences) which cause the solute to deviate from the advective path. Hence, the equation for solute transport needs to accounts for advection on a macroscopic scale and dispersion on a microscopic scale.

As derived in Appendix B, the advection-dispersion equation in one dimension is (Freeze and Cherry, 1979, P. 551):

$$D_L' \frac{\partial^2 C}{\partial \ell^2} - v \frac{\partial C}{\partial \ell} = \frac{\partial C}{\partial t} \tag{16}$$

Ion-exchange and subsequent BTC delay can be included in the advection-dispersion equation by the retardation factor, such that

$$D_L' \frac{\partial^2 C}{\partial \ell^2} - v \frac{\partial C}{\partial \ell} = R \frac{\partial C}{\partial t} \tag{17}$$

The coefficient of dispersion D', is used as a constant in the advection-dispersion equation for a specific pore-water velocity. Under unsaturated flow conditions, there is a further dependency of D' on the water content (Krupp and Elrick, 1968). Therefore, the use of the advection-dispersion equation may be limited to a D' which is valid only for the specific velocity and water content for which it was determined.

The classical advection-dispersion equation (17) has

successfully described solute transport for unsaturated media, with constant water contents and pore-water velocities (Kirda et al., 1973; Bresler & Laufer, 1974; Yule & Gardner, 1978). In these experiments, however, a higher hydrodynamic dispersion coefficient was obtained than for comparible saturated experiments. De Smedt & Wierenga (1984), Krupp & Elrick (1968), Gupta et al. (1973), and Gaudet et al. (1973) obtained BTC's that could not be successfully described by the advection-dispersion equation (17), due to early breakthrough and tailing. A model using mobile-immobile water phases was suggested to explain the divergence, and was incorporated into the advection-dispersion equation to account for the differences observed (De Smedt & Wierenga, 1984; Wilson, 1984, van Genuchten & Wierenga, 1977).

Application of Analytical Solutions

Analytical solutions of the advection-dispersion equation provide a method of determining solute transport parameters such as the hydrodynamic dispersion coefficient and the retardation factor. The type of boundary conditions which best describe an experiment will dictate the choice of the most appropriate analytical solution to be used. Improper use of boundary conditions may generate poor approximations of the transport parameters, especially for column Peclet numbers less than five (van Genuchten and Wierenga, 1986). The column Peclet number, P_c (as opposed to the porous medium Peclet number, P_e), is defined as

$$P_c = vL/D' \tag{18}$$

Inlet boundary conditions are of two types; the first- or concentration-type and the third- or flux-type. The first-type of input boundary condition is

$$C_r(0,t) = C_o \tag{19}$$

where C_r is the resident concentration and C_o the input concentration. This assumes the concentration is continuous across the inlet boundary and the input solution is well-mixed (Parker and van Genuchten, 1984). However, in reality a boundary layer may exist in the region contiguous and external to the porous medium, which renders the first type boundary condition inappropriate.

A discontinuity in concentration across the inlet boundary is implied by the third-type or flux-type boundary condition

$$C_r - \frac{D'}{v}\frac{\partial C_r}{\partial x}\bigg|_{x=0} = C_{in}(t) \tag{20}$$

where $C_{in}(t)$ is the concentration of the injection fluid as a function of time. The third-type boundary condition specifies the solute flux at the inlet boundary and accounts for a transition zone in which the dispersivity and concentration vary continuously, at the microscopic scale. Van Genuchten and Parker (1984) describe the third-type boundary condition as most correct in terms of conservation of mass across the inlet boundary.

Subject to the initial and lower boundary conditions of

$$C_r(x,0) = 0 \qquad (x > 0) \tag{21}$$

$$\frac{\partial C}{\partial x}(\infty,t) = 0 \tag{22}$$

and the third-type boundary condition, the solution to the

advection-dispersion equation (17) for a pulse-type injection (Lindstrom et al., 1967), is

$$\frac{C}{C_o} = \frac{1}{2}\mathrm{erfc}\left(\frac{Rx-vt}{2(D'Rt)^{1/2}}\right)+\left(\frac{v^2t}{\pi D'R}\right)^{1/2} \exp\left(-\frac{(Rx-vt)^2}{4D'Rt}\right) - \frac{1}{2}\left(1+\frac{vx}{D'} + \frac{v^2t}{D'R}\right) \exp\left(\frac{vx}{D'}\right)\mathrm{erfc}\left(\frac{Rx+vt}{2(D'Rt)^{1/2}}\right) \tag{23}$$

where

$$C(x,t) = \begin{cases} C(x,t) & 0<t<t' \\ C(x,t) - C(x,t-t') & t>t' \end{cases} \tag{24}$$

Van Genuchten and Parker (1984) recommend that the solution of Lapidus and Amundson (1952) be used to calculate effluent BTC's for flux-averaged concentration distributions from finite columns or semi-infinite field profiles, and that the solution of Lindstrom et al. (1967) be reserved to evaluate volume-averaged, in situ concentrations. For the case in which breakthrough curves are obtained by means of porous cup samplers or other extraction systems, the most correct concentration mode is not clear. The observed data are unlikely to be either strictly flux-averaged concentrations or volume-averaged concentrations (van Genuchten & Parker, 1984).

Five different methods for determining transport parameters through the use of analytical solutions are reviewed by van Genuchten and Weirenga (1986). These include graphical techniques as well as a least-squares, non-linear curve fit to the effluent curve. They conclude the computer approach based on a non-linear least-squares curve fit gives the most accurate results and is the most convenient method to use.

Other Methods of Determining Transport Parameters

In equation (4), dispersion is represented by an equation analogous to Fick's law of diffusion and therefore defined as a Fickian process. In order to describe a Fickian process, the concentration-distance distribution curve should approximate a normal or Gaussian distribution, except at early time. The variance of the concentration distribution should increase linearly with time or distance, and dispersivity should remain a constant for the porous medium (Anderson, 1984). The classical Fickian form is not valid for early times, when the dispersion process is not fully developed. Gelhar et al. (1979) propose that the observed dependence of dispersivity on the scale of the field experiment may be a reflection of this early-time behavior, before transport becomes Fickian.

The length of time or distance needed to obtain Fickian transport has not been determined. Gelhar and Axness (1981) suggest such distances as equal to 10 to 100 times the value of dispersivity, for heterogeneous systems in the field. Using this criteria for cases in which dispersivities are on the order of 100 meters, transport may not be Fickian until transport distances are on the order of kilometers. Smith and Schwartz (1980) suggest dispersion may never become Fickian for some cases in which mixing is caused by spatial heterogeneities in hydraulic conductivity.

In the derivation of the advection-dispersion equation the dispersive flux is defined at a microscopic pore-scale. Dispersivities determined from small, repacked columns in the labora-

tory, with short travel distances and homogeneous porous mediums, are more representative of this local scale than dispersivities determined from field experiments. The field tests generally measure equivalent or averaged dispersivities from the injection point to the measuring point, yielding values which are not representative of the local dispersivities. In such cases, transport may not be Fickian.

For instances in which dispersion is non-Fickian, the classical advection-dispersion equation with a constant dispersivity may not apply (Anderson, 1984). Gelhar et al. (1979) presented a one-dimensional modified form of the advection-dispersion equation which solved for solute transport for initial, non-Fickian times through large, Fickian times. Other investigators use the standard advection-dispersion equation, but with time- or travel-dependent dispersivities (Anderson, 1984).

Another approach to describing the dispersion process is the stochastic approach. Because dispersion describes the deviation from the mean velocities and is influenced by pore geometry, characterizing the porous medium in terms of hydraulic conductivity could help to define the velocity field. Field determination of the velocity field at all points would be inordinately time-consuming, and beyond practical benefit. Therefore, Gelhar et al. (1979), Gelhar and Axness (1981), and Dagan (1981) propose using methods which rely on the statistical properties of hydraulic conductivity to define dispersivity.

Smith and Schwartz (1980) developed an approach which

defined the velocity field in detail by using stochastic methods to describe the spatial heterogeneity in hydraulic conductivity. However, for the realistic quantities of hydraulic conductivity data that would be available to describe a site, considerable uncertainty resulted in the transport modeling (Smith and Schwartz, 1981). Dagan (1982) also found that a high degree of uncertainty was associated with concentration predictions which relied on stochastic modeling of solute transport.

IV. FLOW AND TRANSPORT CHARACTERISTICS OF COPPER MILL TAILINGS

CHARACTERIZATION OF COPPER MILL TAILINGS

The copper mill tailings used in these experiments were obtained from the Phelps Dodge Corporation, Tyrone Branch in Southwestern New Mexico (see location map, Figure 10). Collection was from the beach sand fraction of the dam crest, which yielded a fairly homogeneous medium.

The results of a particle size analysis on the collected tailings, by Lewis (1986) are shown in Table 1. The particle size distributions (Figure 11) exhibit a well-graded distribution and an average uniformity coefficient of 18. The uniformity coefficient is the ratio of the diameter which includes 60% of the particles (d_{60}) to the smaller d_{10} which includes 10% of the particles (by weight). The more uniform the particles are in size, the closer is the uniformity coefficient to unity. The samples classify as a loamy sand or sandy loam, according to the U.S.D.A. textural classification in Figure 12.

A particle density analysis was also carried out by Lewis, the results of which are shown in Table 2 along with corresponding porosities obtained from the relationship

$$n = 1 - (\rho_b/\rho_s) \tag{25}$$

where ρ_b is the dry bulk density and ρ_s is the particle density.

The dry bulk density used for the porosity analysis, of 1.45 g/cc, was used for disturbed, repacked tailings. Larson (1984) found an average dry bulk density of 1.40 g/cc for undisturbed cores, from the same sampling areas. However, columns

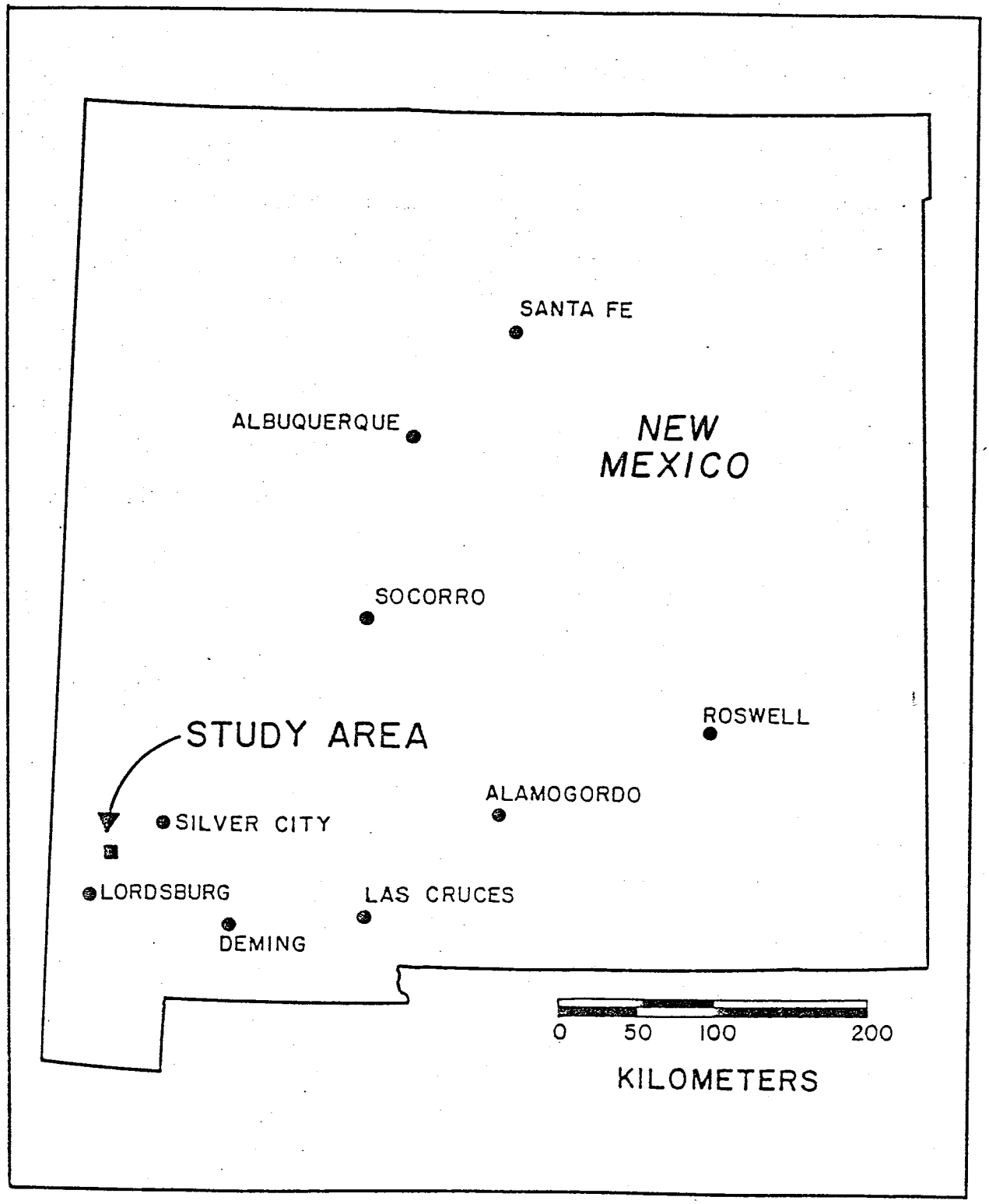

Figure 10. General location map of copper mill tailings source. (from Lewis, 1986)

Table 1. Particle Size Analysis

Parameter	Sample # 1	2	3	4	Avg	Sample SDEV
D_{10}	0.0063	0.010	0.009	0.008	0.0083	0.0016
D_{50}	0.12	0.12	0.12	0.12	0.12	0.00
D_{60}	0.15	0.15	0.15	0.15	0.15	0.00
C_c	4.89	3.27	3.84	4.69	4.17	0.75
Cu	23.81	15.00	16.70	18.80	18.58	3.82
% clay	6.0	5.0	7.0	6.0	6.0	0.82
% silt	22.0	15.0	15.0	15.0	16.75	3.50
% sand	72.0	80.0	78.0	79.0	77.25	3.59

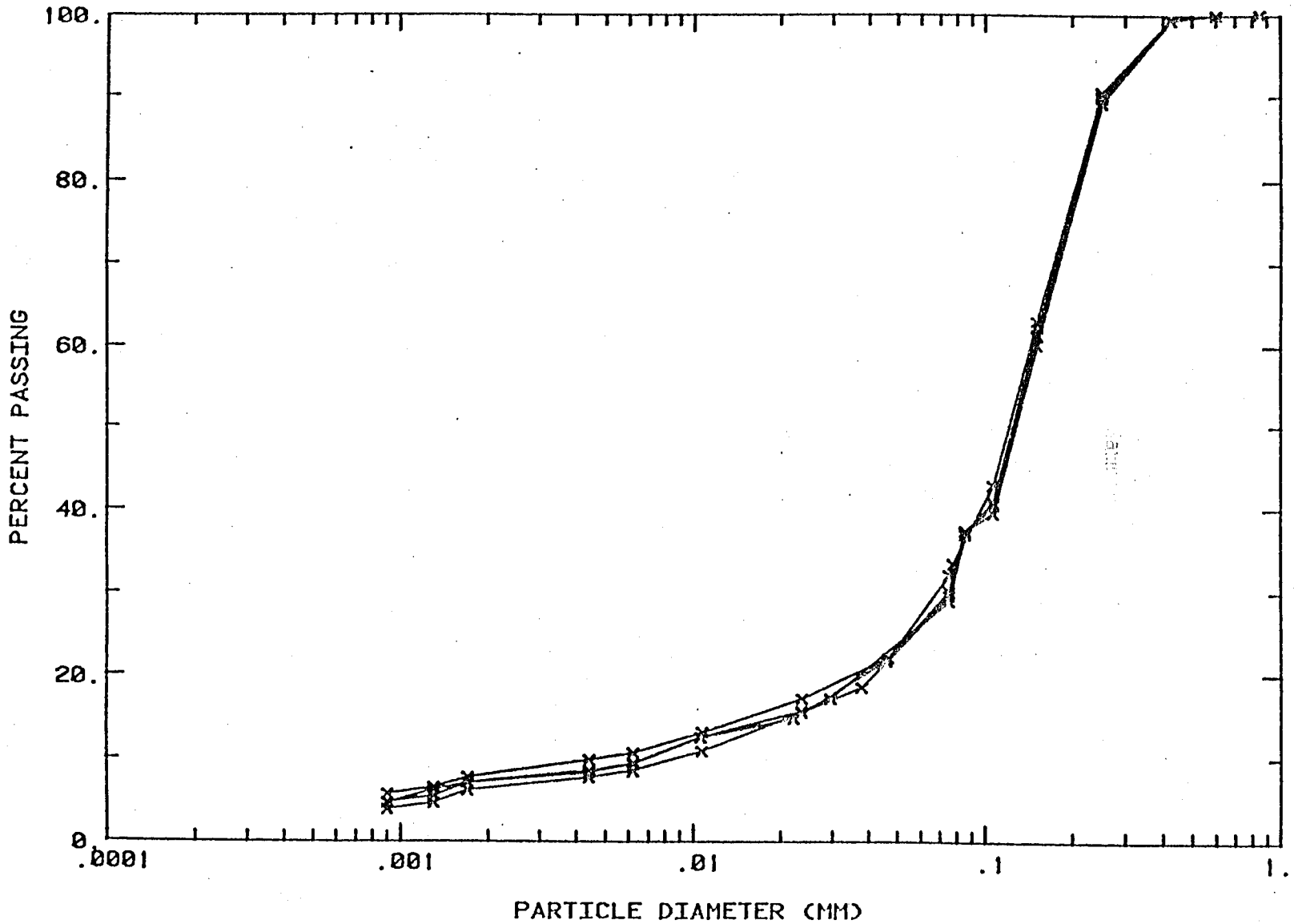

Figure 11. Particle size distribution of disturbed tailings collected at the dam crest. (from Lewis, 1986)

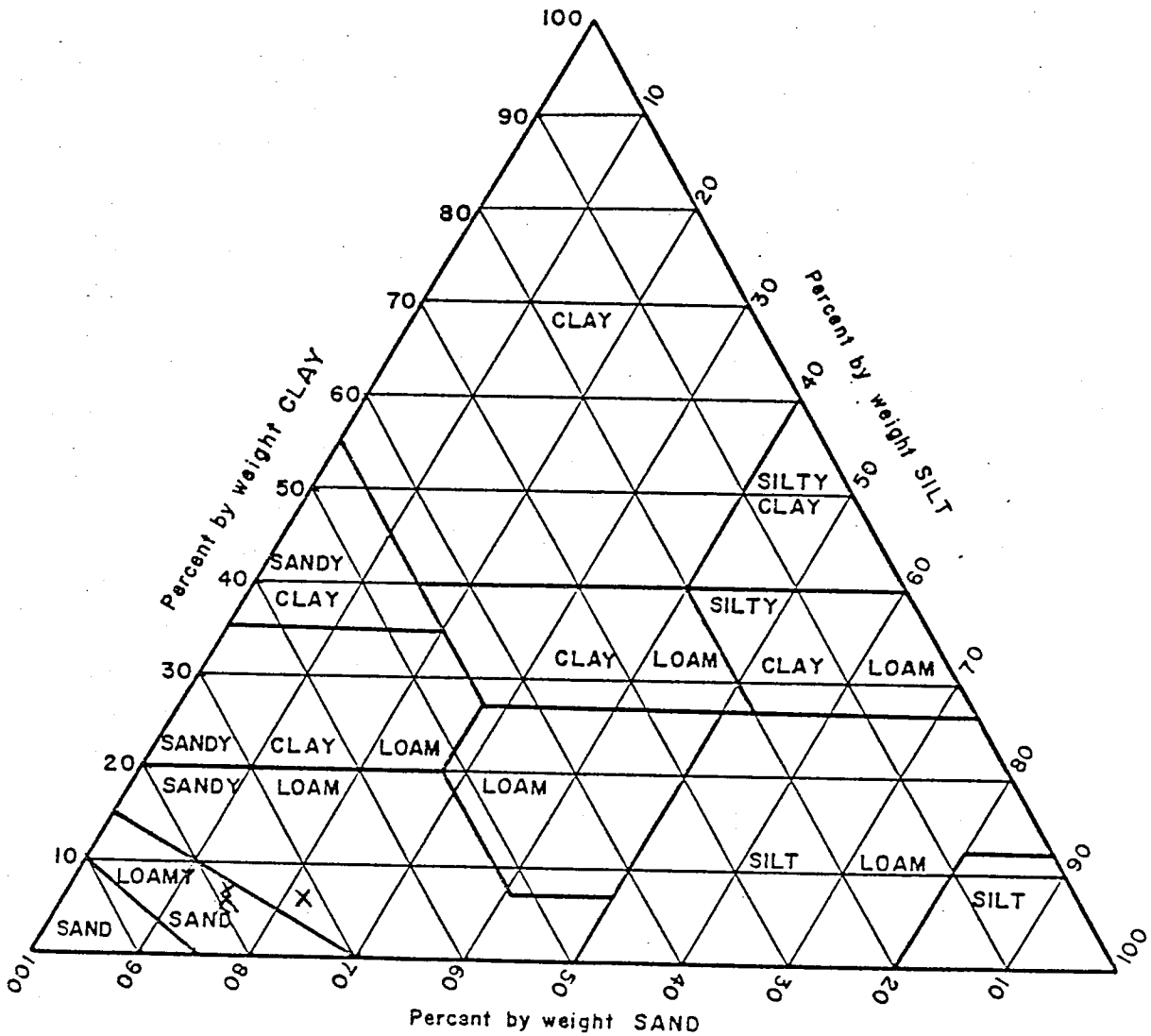

Figure 12. U.S.D.A. soil textural triangle, showing tailings composition of dam-crest material. (from Lewis, 1986)

Table 2. Results of average particle density analysis.

Sample	1	2	3	4	5	6	7	8	Avg	SDEV
Particle Density (ρ_s)	2.71	2.81	2.66	2.82	2.77	2.84	2.90	2.85	2.80	0.08
Porosity (n) (ρ_b = 1.45g/cc)	0.465	0.484	0.455	0.486	0.477	0.489	0.500	0.491	0.482	0.015

packed at the 1.40 g/cc dry bulk density exhibited compaction after saturation and drainage, whereas those packed at 1.45 g/cc did not (Lewis, 1986). In order to prevent consolidation and subsequent particle redistribution during the wet-up or solute transport processes, the repacked dry bulk density of 1.45 g/cc was adopted for all experimental work.

Saturated hydraulic conductivities were determined from disturbed, repacked ring samples, a disturbed, repacked column, and from in-situ field tests. The results are presented in Table 3.

The difference in saturated hydraulic conductivity between the ring and column samples, for disturbed and repacked tailings was attributed to a larger amount of entrapped air in the longer column and the increased effect of preferental flow along sample container walls for the smaller ring samples (Lewis, 1986). The differences in conductivities between the in situ bore-hole

TABLE 3. Hydraulic conductivities from repacked ring samples, repacked columns, and in-situ testing.

Sample	Number Samples	Average Sat. Hyd. Cond.
Disturbed, repacked (Lewis, 1984)		
A Ring Samples (100cc)	3	1.83E-03 cm/sec
B Column Samples (15 X 152cm)	4	5.47E-04 cm/sec
In Situ (Larson, 1984)		
C Bore-hole Infiltration	1	7.00E-04 cm/sec
D Instantaneous Profile Test	1	4.20E-03 cm/sec

infiltration and instantaneous profile test were also attributed chiefly to entrapped air by Larson (1984). The packing procedure for the disturbed and repacked column (Sample B) was identical to the procedure to be used for the long-column solute transport experiments, and the REV for the same sample (B) was larger than that of the ring samples. Therefore, the saturated hydraulic conductivity for the disturbed, repacked column of 5.47E-04 cm/sec was the most appropriate value to use in the long-column experiments.

An analysis of the clay-size fraction was carried out for samples obtained from the dam crest of the impoundment, and collected from 10 to 140 cm depths. Of the clay-sized fraction (<2 microns) 60-70% was identified as illite, 30% as kaolinite, and less than 10% as both smectites and mixed-layer illite-smectite. Jarosite, a potassium iron hydrous silicate, was also found in all the samples. The clay fraction composed 5-6% (by weight) of the sample.

TRACER SELECTION

An ideal tracer is one that is not sorbed or attenuated, is conservative (not subject to degradation or alteration during the experiment), and is found at very low background levels in the natural system (Davis, et al., 1980). Hence, the ideal tracer moves entirely with the liquid or traced phase. With these criteria in mind, bromide was chosen as a tracer for the tail-

ings. In addition, it is easily detectable by use of a specific ion electrode and inexpensive.

Lewis (1986) conducted batch-shaker experiments, to test for recovery of bromide in the copper mill tailings. A loss of bromide was discovered, which was attributed to complexation of the bromide with metal ions in the soil solution. The specific ion electrode, which measures free bromide ions in solution, could not detect the bromide ions which had complexed with the metal ions. Adsorption was also considered as a cause of bromide ion depletion, but did not appear to be a significant factor, for several reasons:

1. Chloride ions (smaller ionic radius), at a concentration 100 times that of the bromide ion, were added to the solution, with no detectable change in bromide concentration.
2. Tailings are composed of only 6% (by weight) clays.
3. The tailings soil solution ranged from pH's of 4.1 to 5.0, which was generally lower than the zero point of charge for the clays.
4. Bromide is highly soluble, therefore has less tendency to be adsorbed.

With the shaker-batch experiments a relationship was established between the observed bromide concentrations after mixing with the tailings and the actual bromide concentrations of the reference solution (Figure 13). A curve was fit to the

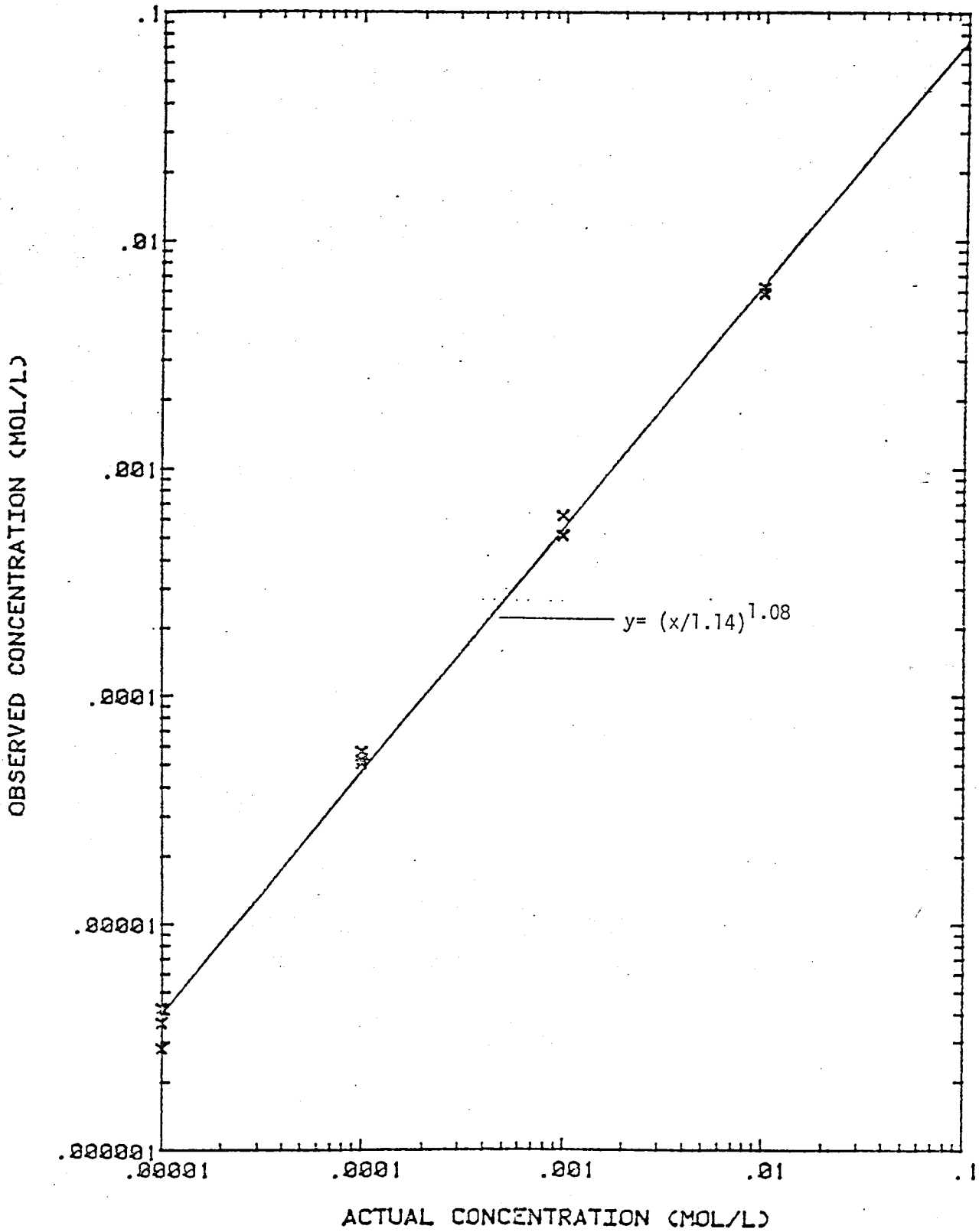

Figure 13. Actual (known) concentration versus observed (measured) concentration and fitted power curve from batch-shaker experiments. (from Lewis, 1986)

data and yielded an equation of the form:

$$C_a = 1.14C_o^{0.93} \tag{26}$$

where C_a is the known, actual concentration of the reference solution (moles/liter), and C_o is the observed bromide concentration after mixing with the copper tailings (moles/liter). This equation (1) can be used to correct for the bromide concentration data, obtained in the tailings experiments.

UNSATURATED FLOW AND TRANSPORT IN A SHORT COLUMN

A small-scale (30 cm), unsaturated, solute-transport experiment on a small scale, (30 cm) was conducted for later comparison of dispersivity values with the larger-scale (330 cm), unsaturated column experiment. These experiments were conducted at NMSU (Las Cruces, NM), using the laboratory and equipment of Dr. P. Weirenga, of the Dept. of Crop and Soil Sciences.

Methodology

First, the column packing procedure and design is described. This is followed by a discussion of the experimental procedure and the method of analysis for the transport parameters.

Two plexiglass columns (30 cm X 5.1 cm) were packed with copper mill tailings which had been sieved (16 mm sieve) and air dried. First, a steel porous plate was placed at the bottom of each column. Then, the tailings were funneled through a ~60 cm tube (which contained two offset screens). The 60 cm tube led into the plexiglass column, which was clamped to a shaker that vibrated the column as the tailings were poured into the column. The vibration settled and consolidated the tailings to a bulk density of 1.44 g/cm^3. This bulk density (1.44 g/cm^3) is slightly less than the desired 1.45 g/cm^3. The screens and tube provided a more homogeneous mixing by ensuring consistency in the packing procedure.

The general design of the experimental apparatus is shown in

Figure 14. A syringe pump pulled eluent from a reservoir and discharged it onto the soil surface via a plastic capillary tube. The pump stroked on timed intervals, pushing a specified volume through the capillary tube with each stroke. The discharge tube at the base of each column was connected to a vacuum chamber. Sampling vials were placed in a circular rack within the vacuum chamber for effluent collection. The sample rack rotated on a timed basis, repositioning a new vial under the column discharge tube after each rotation. With this arrangement, samples could be collected without interrupting the vacuum system or experiment. Two tensiometers were placed at the upper and lower sections of the column to monitor the pressure heads.

The columns were wet-up at a flux of 1.43E-04 cm/sec (12.37 cm/day). However, water ponded momentarily at the soil surface, with each stroke. Therefore, the flux was changed to 1.63E-04 cm/sec (14.04 cm/day), which allowed for more strokes per set time interval, but less volume emitted per stroke. This latter flux was used for the duration of the experiment.

One column was administered a 0.01N $Ca(NO_3)_2$ eluent and the other was given an eluent of distilled water. Distilled water replicated the large-scale (330 cm) column experiment, which also used a distilled water eluent. The results of the $Ca(NO_3)_2$ eluent column were compared with results from the 30 cm length, distilled-water column, since solute-transport laboratory experiments often use eluents other than distilled water (Biggar and Nielsen, 1962; Van de Pol and Weirenga, 1979), in order to more closely approximate the conditions found in nature.

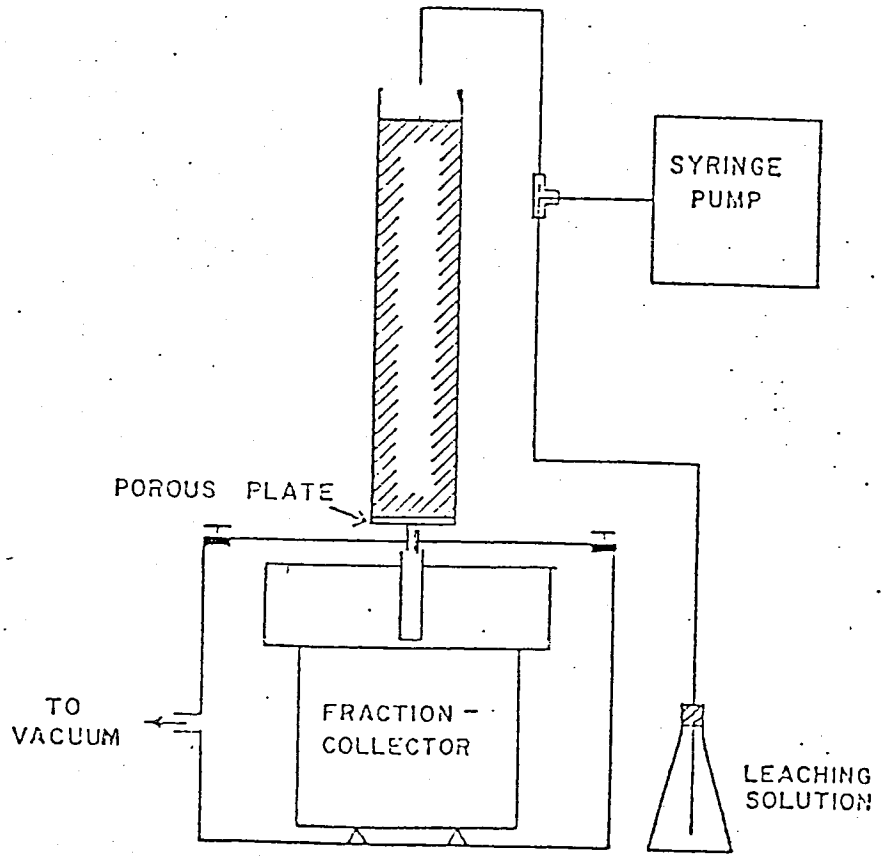

Figure 14. Schematic diagram of experimental apparatus for solute-transport in small repacked laboratory experiments. (from van Genuchten and Wierenga, 1985.)

During the wet-up procedure, shrinkage of the tailings medium was noted in the $Ca(NO_3)_2$ eluent column. Consequently, this column was repacked. However, shrinkage was again observed during the wet-up, and the column was repacked once again. Although some shrinkage was still noted, this final repacking of the $Ca(NO_3)_2$ eluent column was used for the duration of the experiment.

Both tritium and bromide were used as tracers in this experiment. Approximately one pore volume of 0.1M bromide and 0.2 μCi/ml tritium tracer solution was introduced to each column (0.995 pore volume for the distilled, 1.04 pore volume for the $Ca(NO_3)_2$ eluent). This was followed with the distilled water and $Ca(NO_3)_2$ eluents, respectively. The tritium was measured with a Beckman LS-100C liquid scintillation system, using the average of three measurements, and the bromide with an Orion specific electrode ion analyzer (Orion Research, Inc., Cambridge, MA).

Establishing a unit gradient for the experiment proved difficult, due primarily to time constraints. The tensiometer revealed pressure-head differences of about 10 cm of water and 4 cm of water for the distilled-water eluent and $Ca(NO_3)_2$ eluent columns, respectively (Appendix C). Gravimetric water contents of 33% and 32% were determined for the distilled and $Ca(NO_3)_2$ eluent columns. These water contents were obtained by comparing the dry and wet mass of the columns prior to wet-up and at the end of the experiment.

After effluent samples were obtained and measured, correc-

tions were made to the bromide effluent data to account for measurement error due to complexation (see Tracer Selection section). The possibility of nitrate (from the $Ca(NO_3)_2$ eluent) interference with the free bromide measurement was also considered. For this reason, a series of bromide concentration comparisons were made between a specified mass of bromide in distilled water with an identical bromide mass in the $Ca(NO_3)_2$ eluent. There was no measurable difference in bromide concentration for either the $Ca(NO_3)_2$ or distilled water eluents.

A curve-fitting computer model, CFITM (van Genuchten, 1980) (listed in Appendix D) was used to analyze the effluent tracer concentration data and to determine dispersivity. CFITM performs a non-linear, least-squares fit of an analytical solution to the breakthrough data, by varying three parameters: the column Peclet number (P_c) and retardation factor (R) (equations 19 and 10, respectively), and the dimensionless pulse length (T'), where

$$T' = vt'/L \tag{27}$$

and t' is the duration of the pulse of tracer added to the column. All three parameters can be obtained by the curve fit; or if one parameter is known, the other two can be optimized. The analytical solution of Lindstrom et al. (1967) (equation 23) was fit to the effluent data. The solution applies a third-type (or flux-type) boundary condition to a semi-infinite system. The CFITM is an equilibrium model which assumes the adsorption reaction is reversible and occurs quickly relative to the flow velocity. The distribution coefficient is also assumed to

describe a linear process.

CFITM was optimized for two parameters, R and P_c. The pulse length, T', was determined by dividing the volume of the tracer pulse introduced into the column (V_p), by the volume of water held in the column (V_w), so that:

$$T' = V_p / V_w \tag{28}$$

Presentation of Results

The results of the small-scale (30 cm), unsaturated, solute-transport experiment are presented in this section. First, the BTC's associated and mass balance calculations for each column and tracer are presented. Then, the transport parameters T, P_c and R are determined along with the pore-water velocity, hydrodynamic dispersion and dispersivity results.

Breakthrough curves for each column, in terms of pore volume versus relative concentration are shown in Figures 15 and 16 and the relevant data is tabulated in Appendix E. The arrival time of the tritium is almost identical to that of the bromide, within each column. However, the bromide curve peaks at a relative concentration greater than that of the tritium peak.

A comparison of BTC's between the distilled-water and $Ca(NO_3)_2$ eluent columns is shown for each tracer (bromide in Figure 17, tritium in Figure 18). The distilled-water eluent BTC shows a slightly later arrival, less tailing as the tracer concentration decreases, and a narrower peak width for both the tritium and bromide tracers. In addition, the BTC from the

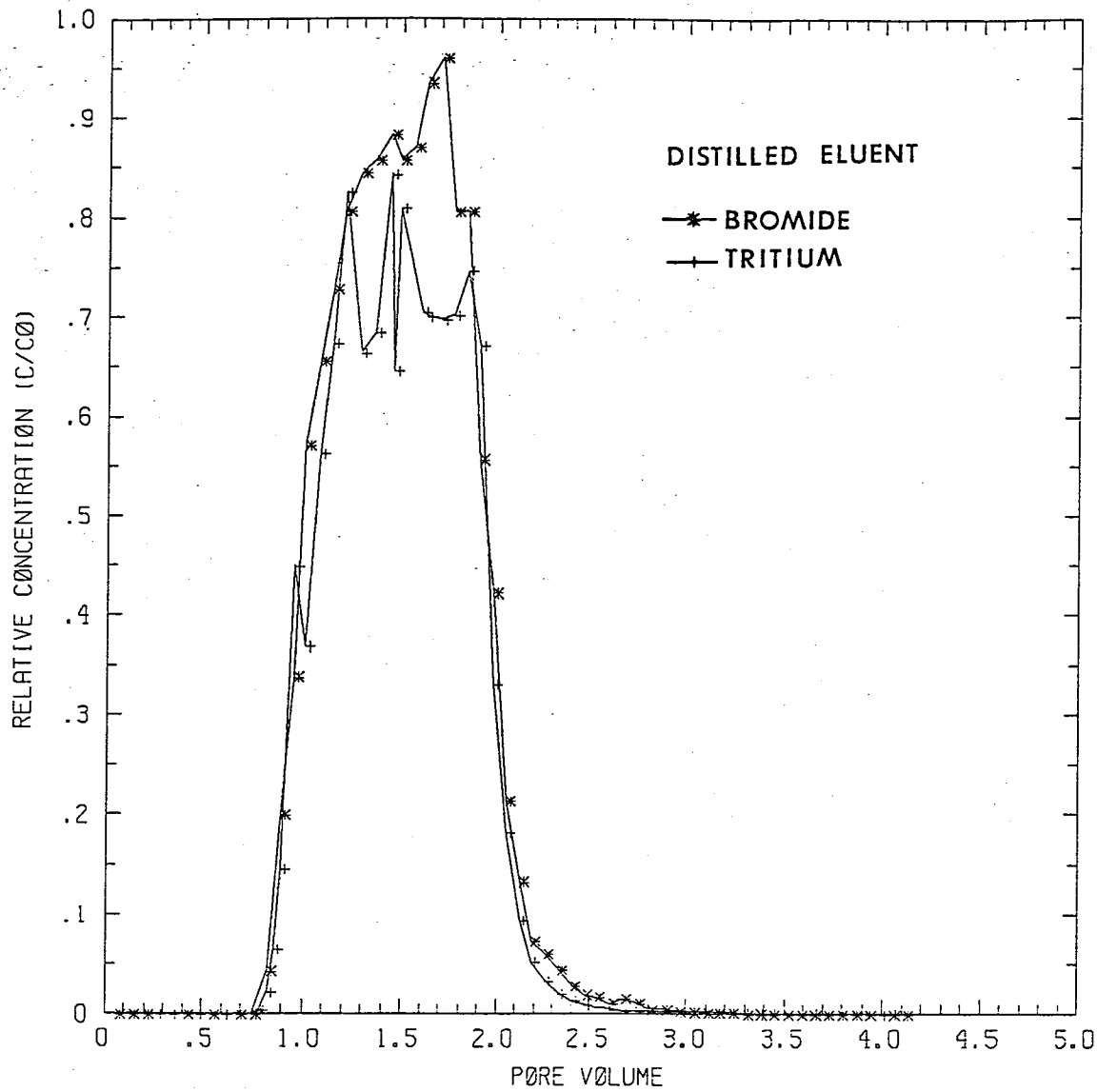

Figure 15. BTC's for bromide and tritium, distilled water eluent column.

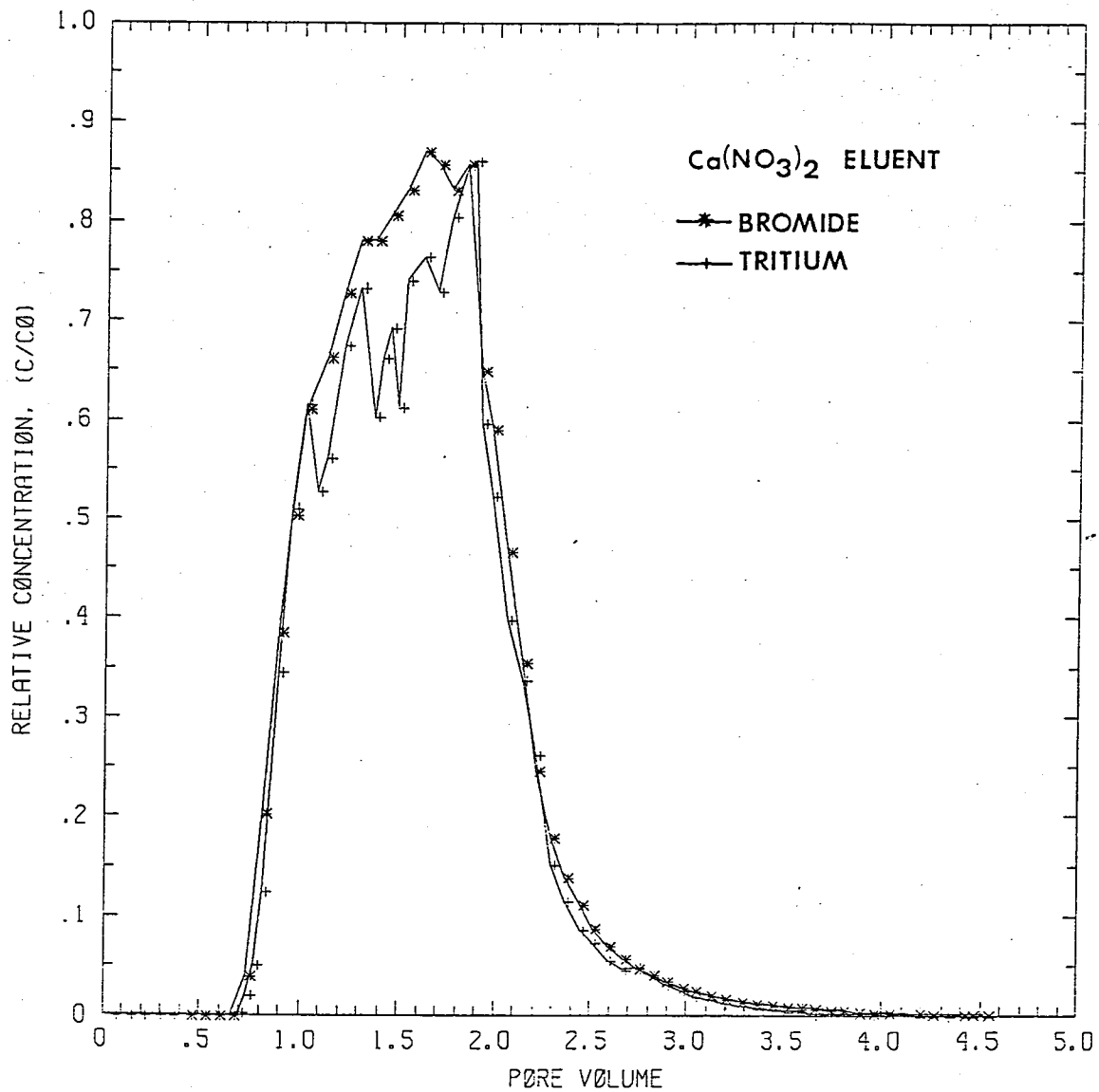

Figure 16. BTC's for bromide and tritium, $Ca(NO_3)_2$ eluent column.

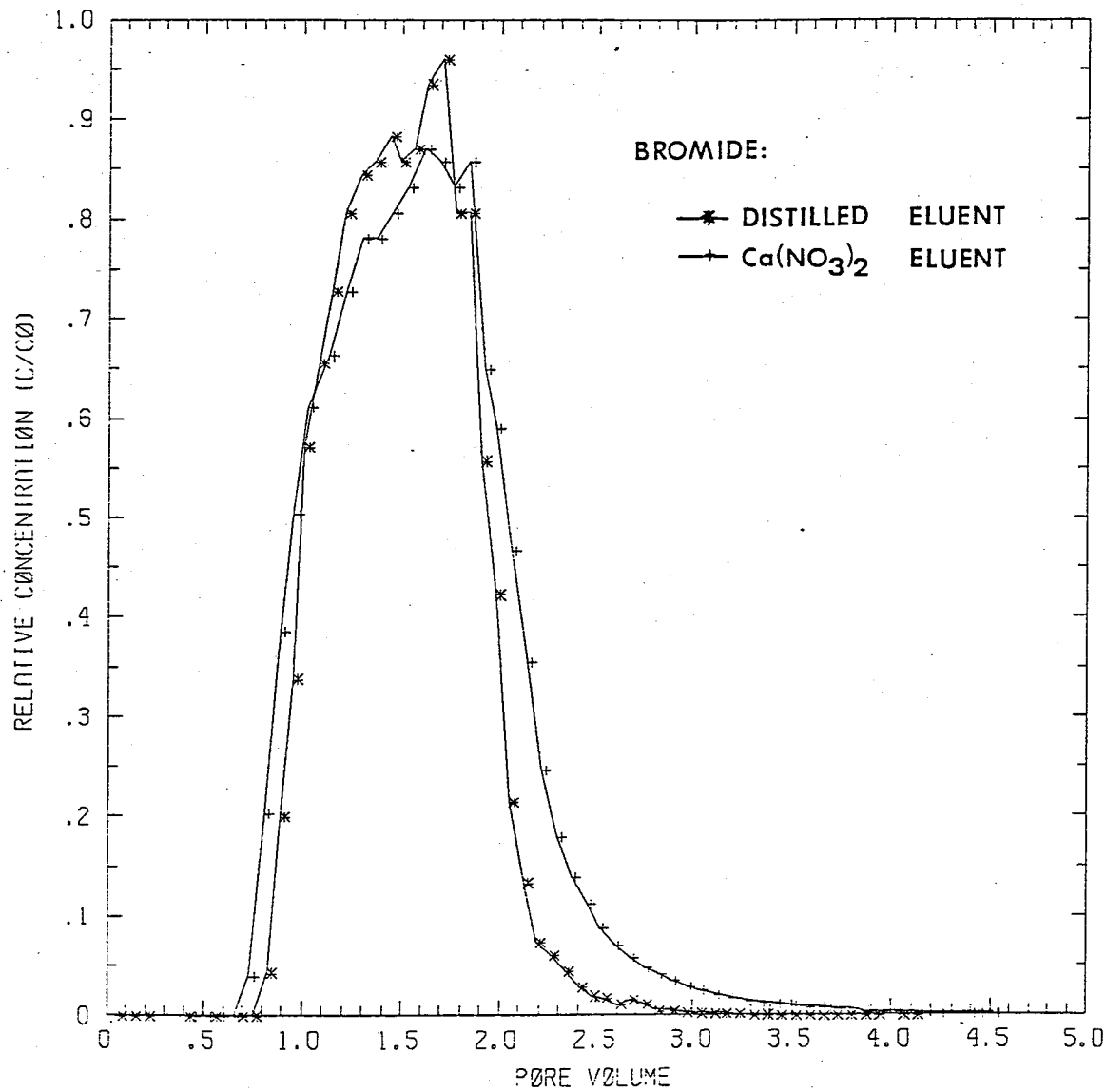

Figure 17. Bromide BTC's from distilled and $Ca(NO_3)_2$ eluent columns.

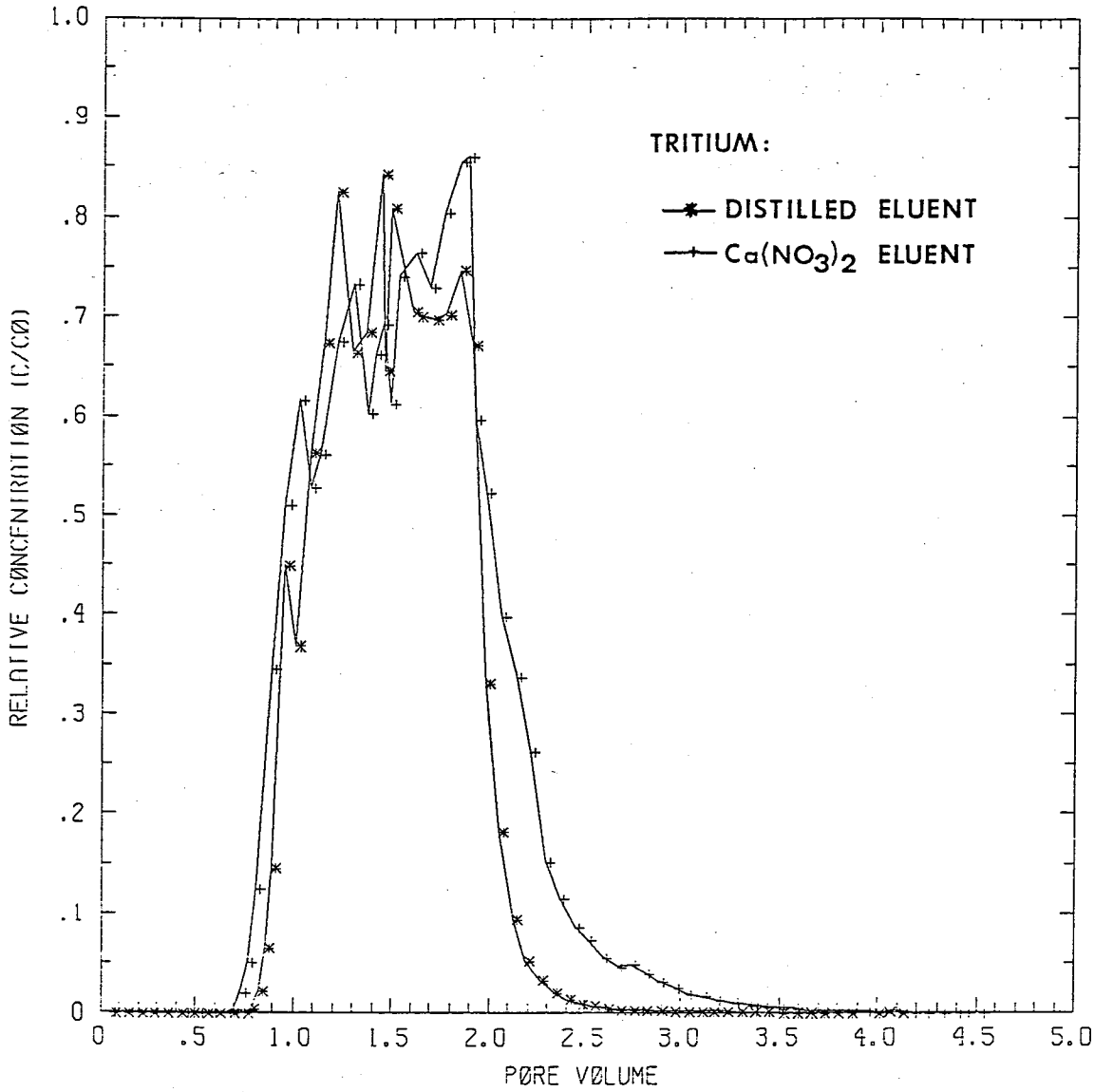

Figure 18. Tritium BTC's from distilled and $Ca(NO_3)_2$ eluent columns.

distilled water case is more symmetric than that of the $Ca(NO_3)_2$ eluent column.

A mass balance was calculated for each BTC, by comparing the integrated area under the BTC to the calculated area of 100% bromide or tritium mass retrieval. Thus, if all tracer mass was conserved

$$A_i / A_c = 1.0 \tag{29}$$

where A is the integrated area under the BTC and A_c is the area calculated for 100% bromide or tritium mass return. The mass balance results are shown in Table 4. All mass balance calculations were lower than 100%, however, the bromide yielded a greater percentage of mass recovery than the tritium.

Table 4. Mass balance for each breakthrough curve.

Tracer	Column Eluent	Mass Balance (%)
Bromide	distilled	88
Tritium	distilled	76
Bromide	$Ca(NO_3)_2$	98
Tritium	$Ca(NO_3)_2$	87

As described in the methodology section, the curve-fitting computer model, CFITM (Van Genuchten, 1980), was used to describe the breakthrough data from these unsaturated 30 cm column experiments. Since T' was known, CFITM was optimized for the two parameters, R and P_c, and the resulting curve fits are shown in Figures 19, 20, 21 and 22. A three-parameter fit was also tried but the results were not markedly different. The retardation factor, column Peclet number and pulse lengths are presented in Table 5 and the computer outputs are included in Appendix F.

Table 5. Results of CFITM curve-fit. Pulse length (T') is known, column Peclet number (P_c) and retardation factor (R) are optimized.

Tracer	Column Eluent	T'	P_c	R
Bromide	distilled	0.995	58.43	0.985
Tritium	distilled	0.995	26.56	1.000
Bromide	$Ca(NO_3)_2$	1.040	21.94	1.000
Tritium	$Ca(NO_3)_2$	1.040	15.97	1.050

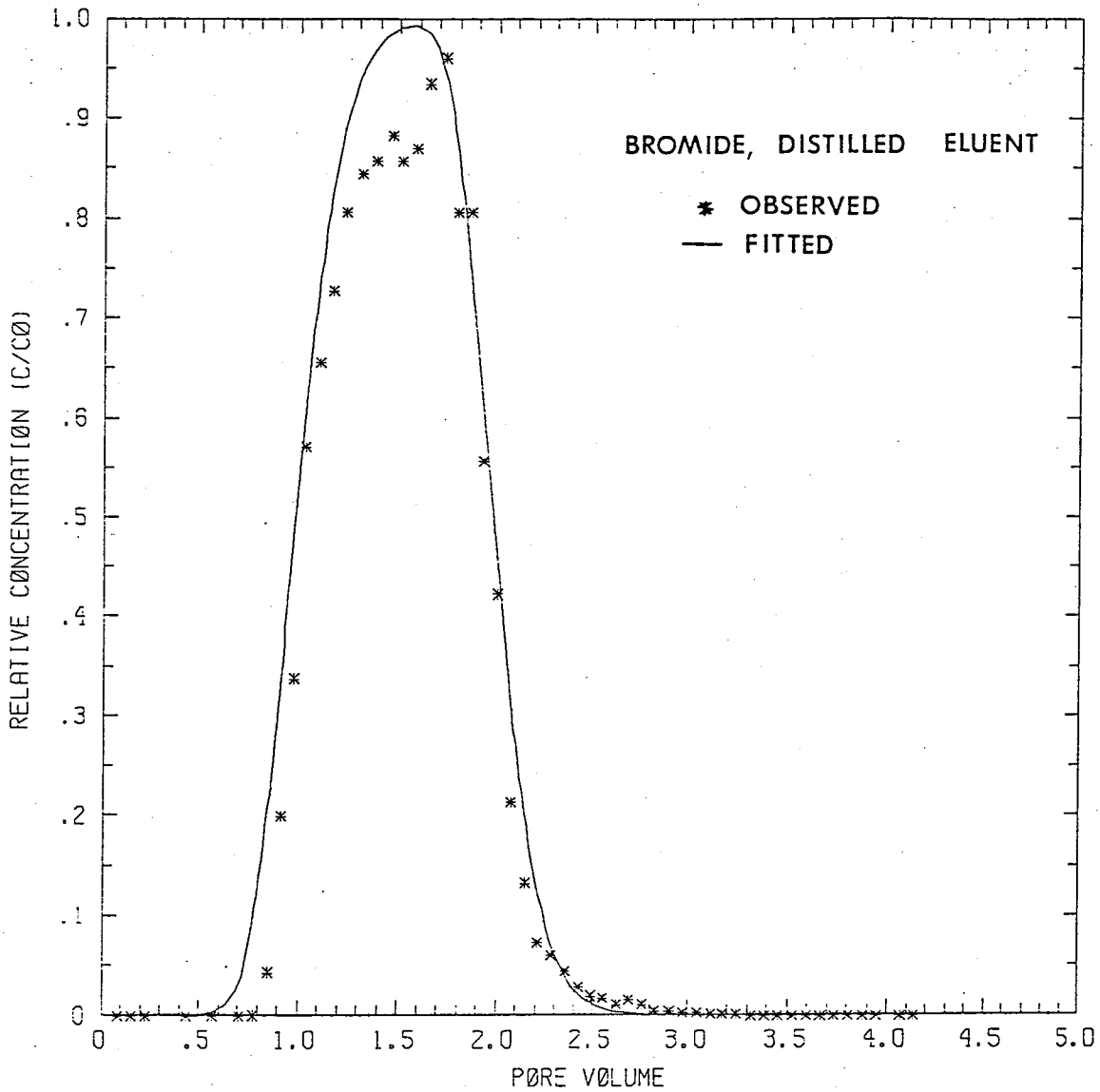

Figure 19. Bromide breakthrough data and CFITM fitted curve (two-parameter optimization), for distilled eluent column.

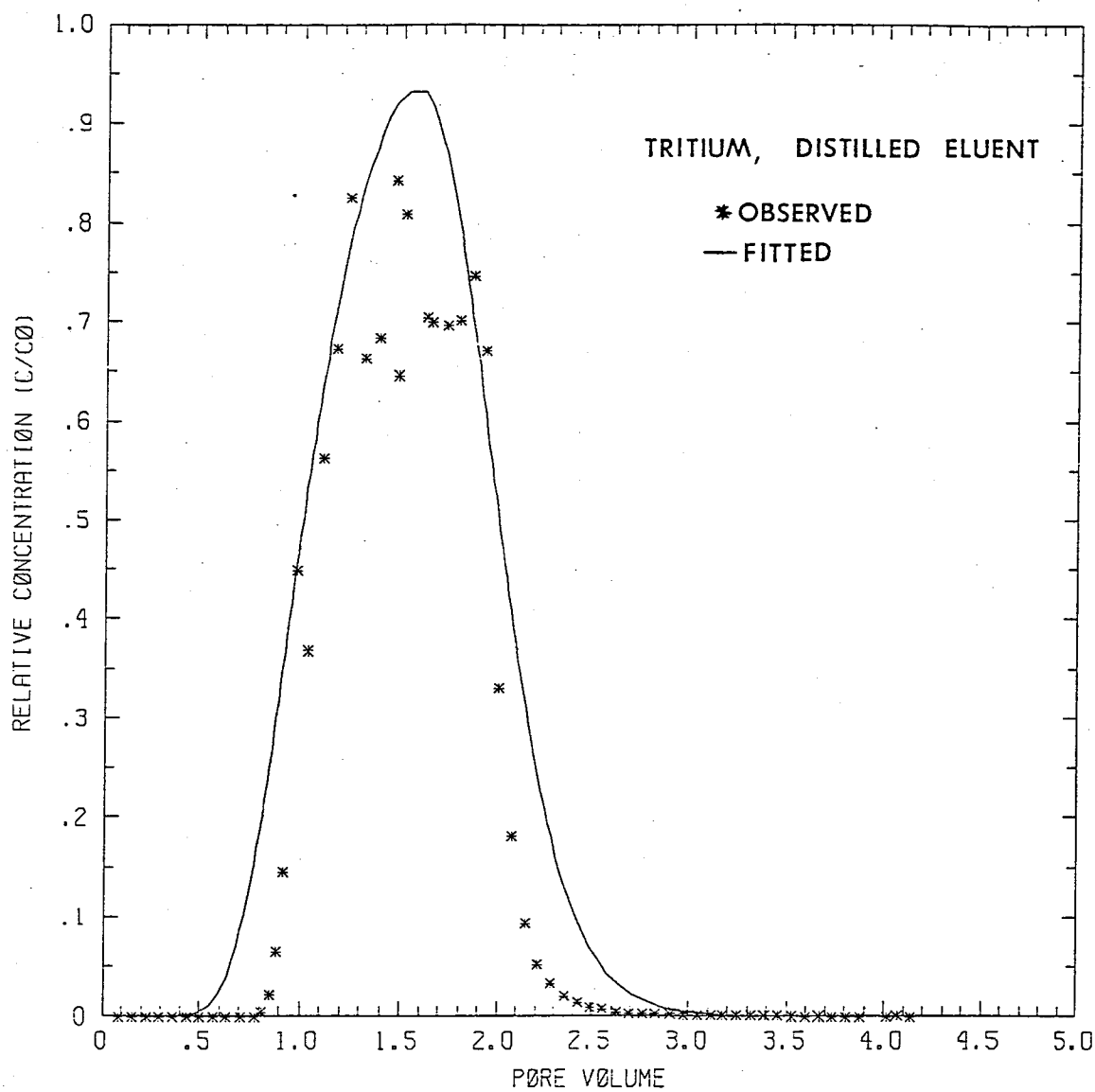

Figure 20. Tritium breakthrough data and CFITM fitted curve (two-parameter optimization) for distilled eluent column.

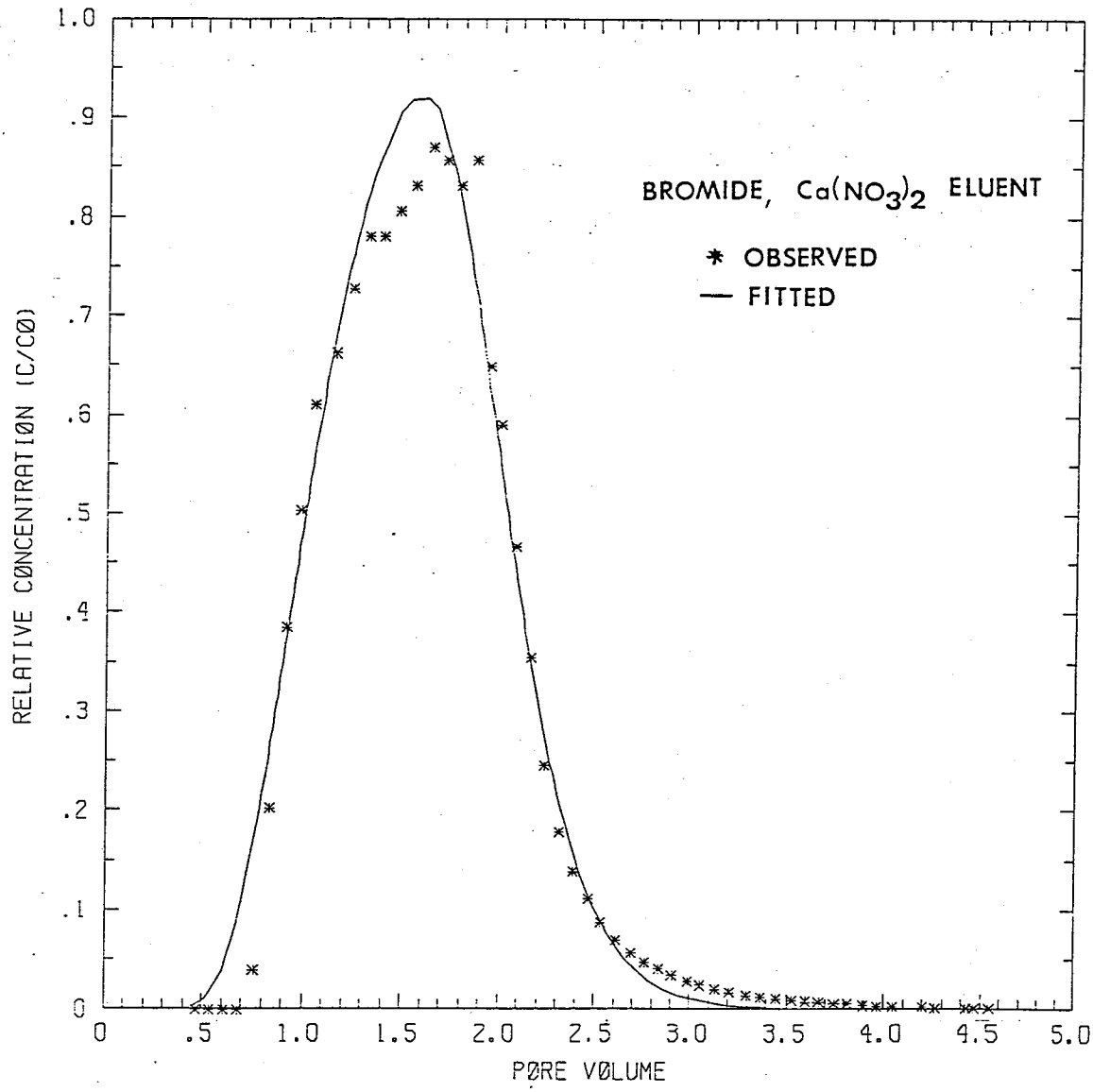

Figure 21. Bromide breakthrough data and CFITM fitted curve (two-parameter optimization) for $Ca(NO_3)_2$ eluent column.

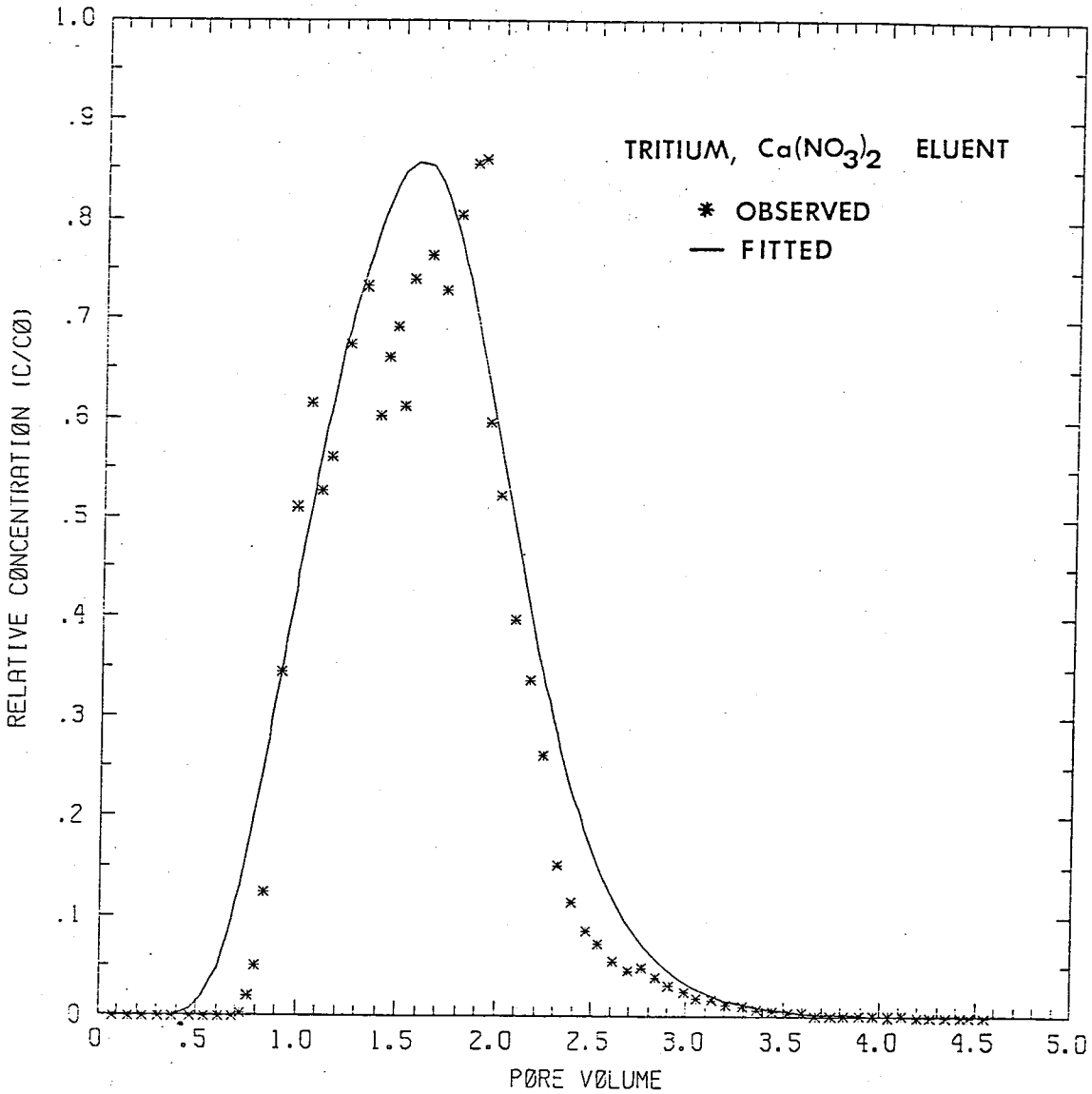

Figure 22. Tritium breakthrough data and CFITM fitted curve (two-parameter optimization) for $Ca(NO_3)_2$ eluent column.

The pore-water velocities, hydrodynamic dispersion coefficients and dispersivities are presented in Table 6. Using the relationship for pulse length in equation (27), the pore-water velocity for each column was calculated with a t' of 691 minutes and L of 27.7 and 26.9 cm for the distilled water and $Ca(NO_3)_2$ eluent columns, respectively. The hydrodynamic dispersion coefficients and dispersivities were determined from the fitted P_c, using equations (5) and (18) and assuming molecular diffusion was insignificant.

Table 6. Values of pore-water velocities (v), hydrodynamic dispersion coefficients (D') and dispersivities (a_L).

Tracer	Column Eluent	v (cm/min)	D' (cm^2/min)	a_L (cm)
Bromide	distilled	0.0399	0.0189	0.47
Tritium	distilled	0.0399	0.0416	1.04
Bromide	$Ca(NO_3)_2$	0.0405	0.0497	1.23
Tritium	$Ca(NO_3)_2$	0.0405	0.0682	1.68

The validity of disregarding the molecular diffusion coefficient can be demonstrated by a comparison of the dispersivity which included the molecular diffusion coefficient to the dispersivity which neglected molecular diffusion. An unsaturated, molecular diffusion coefficient, $D(\theta)^*$, of 4.13E-05 cm^2/min was calculated for the bromide-tracer, distilled-water eluent column, using the relationship suggested by Wilson and Gelhar (1974)

$$D(\theta)^* = 1/3\ (\theta/n)^2\ D_s^* \qquad (30)$$

and using a saturated molecular diffusion coefficient (D_s^*) of 5.55E-04 cm^2/min (Appendix G), a θ of 33% and n of 44%. A dispersivity of 0.47 cm was obtained from both the addition and the omission of molecular diffusion. Therefore, at these fluxes, the diffusion coefficient was not significant and could be disregarded.

The pore-water velocities in Table 6 were compared to the pore-water velocities of the tracers (v_{tr}). The tracer pore-water velocities were determined by dividing the column length by the time of the arrival of the 50% relative concentration of the tracer in the effluent. The results are shown in Table 7.

Table 7. Comparison of input pore-water velocity (v) and the velocity of the tracer (v_{tr}), where 't' is time for 50% tracer concentration to reach effluent.

Tracer	Column Eluent	v (cm/min)	t (min)	v_{tr} (cm/min)
Bromide	distilled	0.0399	694.2	0.0399
Tritium	distilled	0.0399	728.9	0.0380
Bromide	$Ca(NO_3)_2$	0.0405	697.4	0.0386
Tritium	$Ca(NO_3)_2$	0.0405	697.4	0.0386

Discussion

This discussion investigates the presence (or absence) of adsorption, the difference in results between the distilled and $Ca(NO_3)_2$ eluent columns and compares the results from the bromide and tritium tracers to determine the better tracer for these copper mill tailings. A representative dispersivity for these unsaturated copper mill tailings, at a laboratory scale, is chosen.

Adsorption did not appear to be an influential factor for either tracer, in this experiment. In Table 5, the retardation factors were either 1.0 or very close to 1.0, indicating neither adsorption nor ion exclusion was a problem. The low clay content of the copper mill tailings (6%) and pH range of the leachate (3.9 t0 4.1) would have severely limited the occurrence of adsorption (see Tracer selection section).

The two columns show distinct differences in BTC shapes and dispersivity values. The greater peak width, earlier tracer

arrival, more extensive tailing and higher dispersivity of the $Ca(NO_3)_2$ eluent column (for both tritium and bromide tracers) is similar to BTC's observed with dead-end pores, or stagnant water in the flow path (De Smedt and Wierenga, 1984). This might be accounted for by packing differences between the two columns or by the use of different eluents.

The occurrence of chemical reactions that would differ between the two columns is very likely, since a different eluent was used in each column. As a divalent cation, calcium (from the $Ca(NO_3)_2$) eluent) may preferentially adsorb on to the soil surface and allow flocculation of the clays to occur (Hillel, 1980). The flocculation of clays may change the porosity and/or the permeability of the porous medium as the clay double-layer contracts. Clay content of the tailings is less than 6% by weight, minimizing the amount of flocculation that could exist. However, as noted in the experimental procedures section, a shrinkage of the porous medium was observed during the initial wet-up of the $Ca(NO_3)_2$ column. This change in the structure of the tailings matrix would undoubtedly have an effect on water movement through the tailings. The more asymmetric shape and higher dispersivity of the $Ca(NO_3)_2$ curves, as compared to the distilled-water eluent BTC's, may be from the change in the structure of the tailings matrix.

Had both columns produced similar breakthrough curves, the choice between using a distilled-water eluent or a $Ca(NO_3)_2$ eluent would be mute. However, there was a distinct difference in BTC's which cannot be addressed in full because of lack of

experimental data. With only one column of each eluent type, it could not be accurately ascertained whether the difference in BTC's between columns was due to packing differences between the columns or to the use of different eluents.

Bromide responded as a more conservative tracer than did the tritium, for both columns. The mass balance of the BTC's yielded a greater percentage of bromide recovery than tritium recovery, for each column. The reason for the lack of full recovery was not clear. Irreversible adsorption was not considered a factor in the tritium or bromide loss. Retardation factors of 1.0 and 1.05 for the distilled and $Ca(NO_3)_2$ eluent columns indicate no adsorption occurred. Undoubtedly, measurement error played a part in the tritium loss, since scatter was observed in the BTC data at the peaks of the tritium curves. Despite the uncertainty as to the cause of the tracer loss, the results do indicate that bromide acted as the most conservative tracer, for the copper mill tailings.

The pore-water velocity comparisons between v and v_{tr} (Table 7) demonstrated that both tracers closely followed the bulk movement of water, with a 5% difference, at most, between v and v_{tr}. However, the v_{tr} of the bromide in the distilled water column predicted the bulk movement of water most accurately.

Tritium yielded higher dispersivities than the bromide-tracer, distilled-water eluent column (0.47 and 1.04cm, for bromide and tritium, respectively) and the $Ca(NO_3)_2$ column (1.23 and 1.68cm for bromide and tritium, respectively). Another look at the fit of the CFITM curves to the breakthrough data in

Figures 19, 20, 21 and 22 provides some insight. The CFITM tritium curves are poor matches for the actual data; the observed data arrives later and recedes more sharply than the fitted curves. The bromide curves are in better agreement with the observed data, and subsequently yield parameters of less uncertainty.

The poor fit of the CFITM curves to the tritium data may be related to the peak height and mass balance of the breakthrough curves. The tritium BTC's yielded a lower mass balance than their bromide counterparts. The CFITM model had to widen the tritium peak width because of the low BTC peak height, in order to conserve mass under the curve. The fitted curve could not describe the tritium mass lost during the experiment, which was crucial to defining the parameters.

The dispersivity of 0.47 cm for the bromide-tracer, distilled-water eluent column was chosen to describe these unsaturated, copper mill tailings at the laboratory (~30 cm) scale. The dispersivity values of greatest confidence were calculated from the bromide data, for both columns. Furthermore, a distilled-water eluent and bromide tracer were also used in the larger-scale column experiments (336 cm), and therefore, the bromide-tracer, distilled-water column was the most useful for comparitive purposes. This dispersivity value (0.47 cm) was well within the range of magnitude of other dispersivities also obtained in unsaturated, laboratory experiments of a similar scale (Yule and Gardner, 1978; Kirdat, etal., 1973; Gaudet, et al., 1977; De Smedt and Wierenga, 1984; van Genuchten and Wierenga, 1977).

Summary

The short-column (30 cm) experiments provided a reference for comparison of dispersivities with the long-column (336 cm) experiment to follow. A dispersivity of 0.47 cm was obtained, for a 32% volumetric water content and a flux of 1.625E-04 cm/sec using a bromide tracer and distilled-water eluent. This dispersivity was within the range of other unsaturated laboratory experiments. The molecular diffusion coefficient was not significant in the calculation of the dispersion coefficient.

Bromide proved to be an good tracer for the copper tailings, with no adsorption, a larger mass balance return than the tritium, and a pore-water velocity determined from the tracer movement that matched the measured input velocity. In addition, the bromide tracer yielded dispersivities of greater certainty than the dispersivities from the tritium, due to poor agreement between the CFITM curves and the tritium BTC. The $Ca(NO_3)_2$ column exhibited a different hydrodynamic character than the distilled water column, with earlier tracer arrival, greater tailing, and higher dispersivities than the distilled-water eluent column.

UNSATURATED FLOW AND TRANSPORT IN A LONG COLUMN

The scale chosen for a solute-transport experiment may influence the value of dispersivity. For saturated media, this scale dependence is well documented and is a function of the scale of the heterogeneities present in the media. For the unsaturated solute-transport case, there is insufficient data from which to draw the same conclusions. Dispersivities determined from various unsaturated, solute-transport experiments found in the literature are shown in Figure 23 and listed in Table 8. These experiments were conducted at varying vertical scales and water contents and with different porous media. Unlike the laboratory experiments which were conducted with homogeneous repacked soils, the field experiments were conducted with in-situ soils. Figure 23 suggests dispersivity may increase with transport distance in the unsaturated case, but additional data, especially at the field scale, is needed for comparison.

A laboratory experiment was conducted to determine the dispersivity for unsaturated copper tailings and to evaluate the dependence of dispersivity on distance of transport, under unsaturated conditions. The porous medium was homogeneous, hopefully eliminating the variable of field-scale heterogeneity from the experiment. The scale dependence of dispersivity was examined by sampling for a tracer at several depths along the column, and determining the dispersivity at each of those depths. The dispersivity values were then compared to the unsaturated, smaller-scale (30 cm in length) column experiment

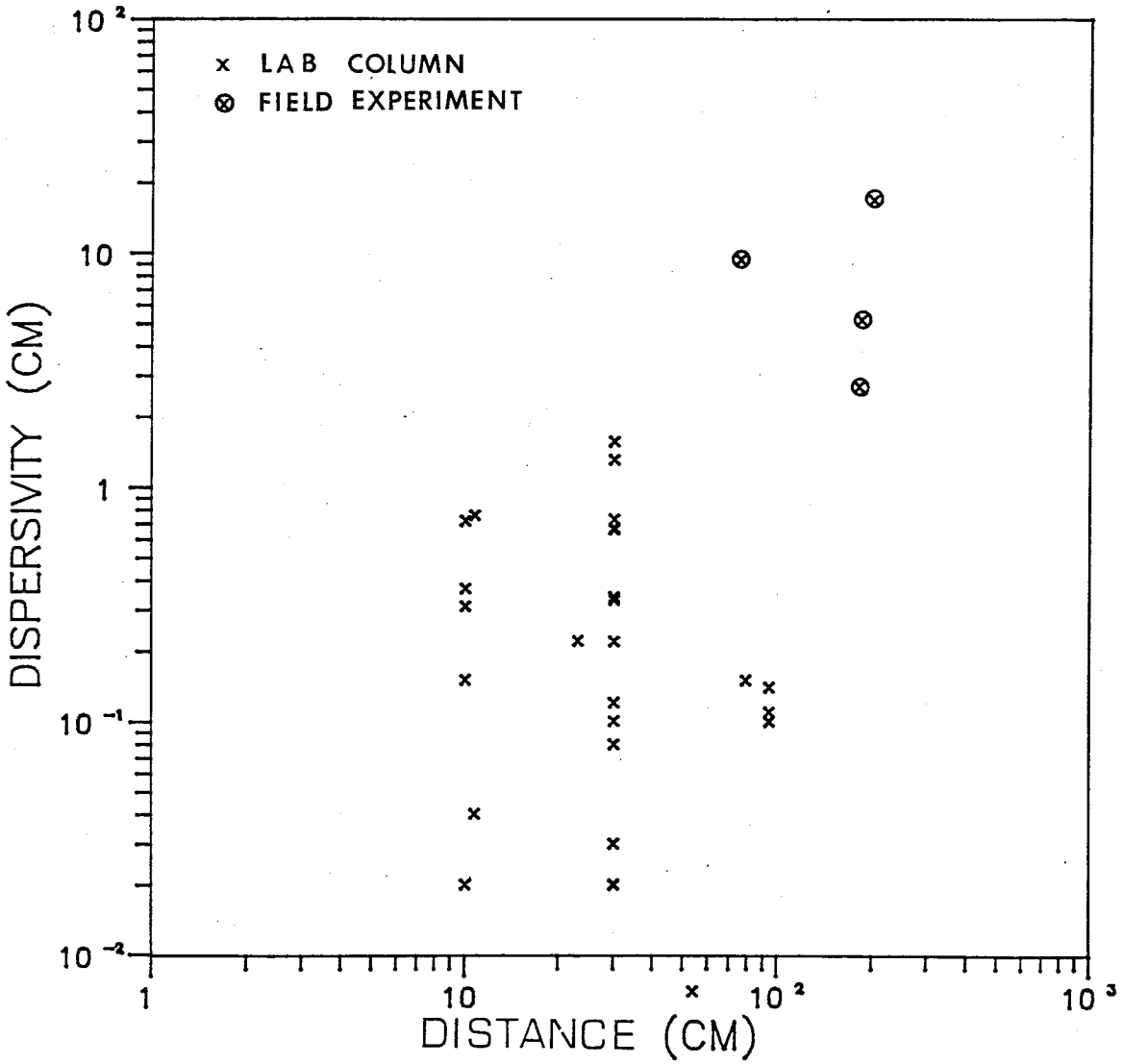

Figure 23. Dispersivities from both repacked laboratory column and in-situ field solute-transport experiments, under unsaturated flow conditions. Dispersivities determined from literature cited in Table I.

TABLE 8. Dispersivity results from various unsaturated laboratory and field solute-transport experiments; * indicates a field experiment.

Author	Soil	Vertical Scale (cm)	Dispersivity a_l (cm)
Krupp and Elrick,	glass beads	10.0	0.02
Mansel, et al., (1979)	Oldsmar fine sand	10.0	0.37 0.72 0.15 0.31
Elrick, et al., (1966)	glass beads	10.7	0.04 0.76
Yule and Gardner, (1978)	Plainfield sand	23.0	0.22
De Smedt and Wierenga, (1979)	glass beads	30.0	0.02
De Smedt and Wierenga, (1984)	glass beads	30.0	0.03 0.03 0.03 0.02 0.02 0.08
Nielsen and Biggar, (1962)	Oakley sand	30.0	0.22 0.34
	glass beads	30.0	0.12
	Aiken clay loam	30.0	1.57 0.10
van Genuchten, et al., (1977)	Glendale clay	30.0	0.33
	small aggregates		0.73
	large aggregates		0.67 0.66 1.31
Gupta, et al., (1973)	glass beads	54.0	0.007
Van de Pol, et al,	field soil	75.5	9.40
Hildebrand and Himmelblau, (1977)	sand	79.0	~0.15
Gaudet et al., (1977)	sand	94.0	0.14 0.10 0.11 0.10
Warrick, et al., (1971)	field soil, (Panoche clay loam)	180.0	2.70
Biggar and Nielsen, (1976)	Panoche	183.0	5.20
Kies, (1981)	field soil	200.0	16.90

described in the previous section of this paper, and to dispersivity values from unsaturated experiments found in the literature. An additional comparison was made to the dispersivity determined from a saturated, solute-transport experiment through copper mill tailings at a similar scale by Lewis, (1986) (Appendix H).

Methodology

First this section describes the column set-up, packing procedure, and instrumentation. Experimental procedures are then discussed for saturating the column, leaching under unsaturated conditions, and conducting solute-transport experiments in the long-column.

Column description. One long, plexiglass column (Figure 24), 336 cm in length and 16.2 cm diameter, was composed of three sections which were bolted together at the flanges with neoprene gaskets for seals. A blind flange was affixed to the bottom section. A 1.27 cm hole was drilled and tapped into the blind flange, and a reducer was then fitted to the hole. Tygon tubing was connected to the reducer, and this was used for effluent collection. The entire plexiglass column was supported vertically by a metal tripod, which was bolted to the cement floor.

The set-up of the column was changed to accommodate different stages of the experiment. For the saturated parts of this experiment, a polypropylene felt filter was placed between the flange and the tailings, to prevent loss of tailings through the

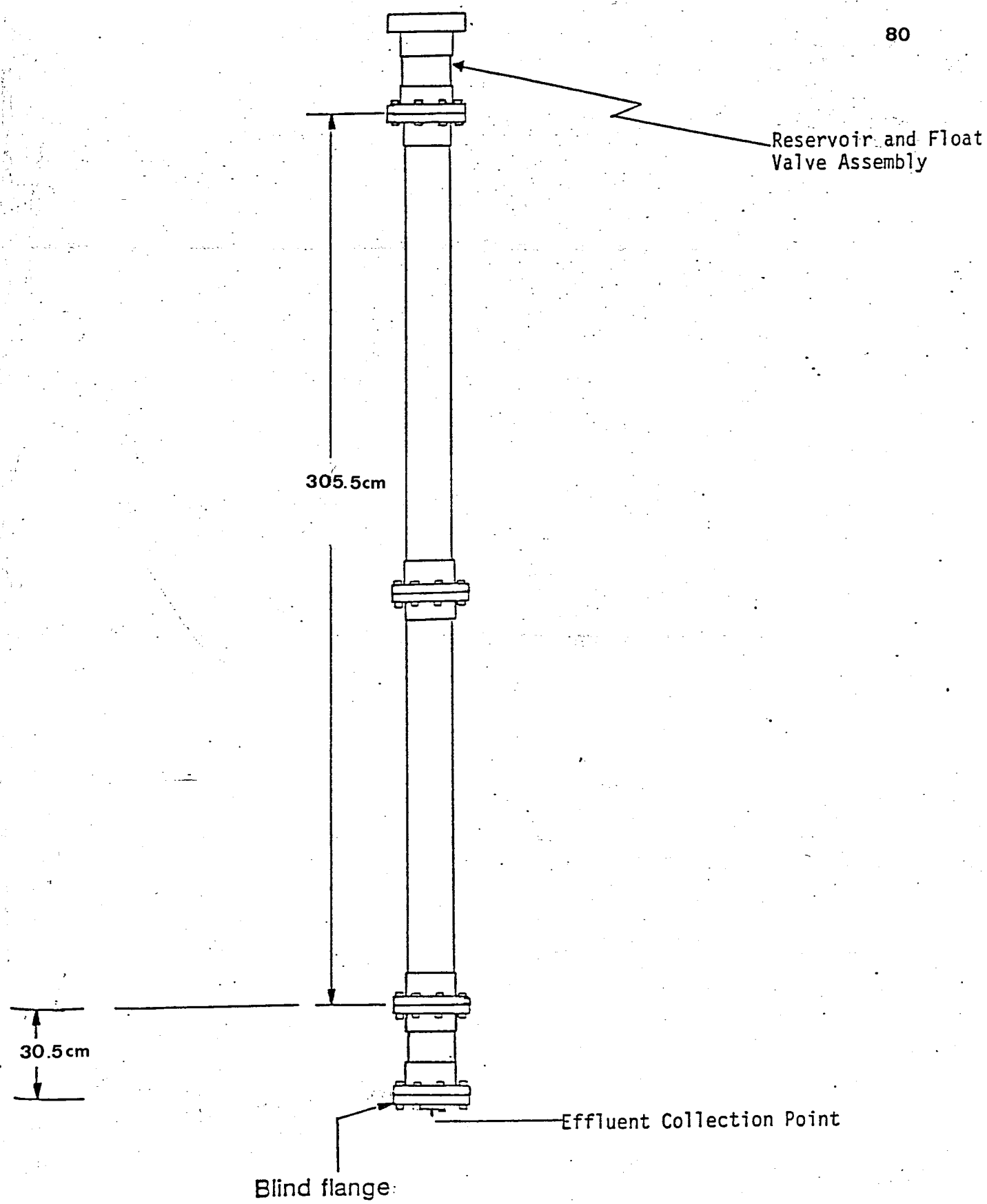

Figure 24. Long-column diagram.

outlet. In addition, 30.5 cm plexiglass section was temporarily bolted to the top of the soil column to allow storage for a head of water, during the initial column wet-up and subsequent leaching process. The unsaturated, displacement portion of the experiment required the use of a ceramic porous plate and flange assemblage at the bottom of the column. A hydraulic conductivity of 1.0E-06 cm/sec was obtained for the one-bar porous plate (Lewis, 1986). The blind flange was ground out and the porous plate seated flush with the flange surface, as shown in Figure 25. A space of 5 mm was maintained between the porous plate and the inner seat of the flange, to allow optimum eluent removal across the entire surface area.

The copper tailings were packed into the column in five centimeter increments to a field density of 1.44 g/cm^3, slightly less than the optimum bulk density of 1.45 g/cm^3. Before packing, the tailings were sieved through a 16 mm sieve to sort out the dried aggregates, and then they were air-dried. Next, the tailings were poured into a funnel connected to a 2.5 cm diameter PVC pipe about 160 cm in length. Each interval was then tamped down to a 5 cm lift by using an aluminum disc, 16 cm in diameter, that was attached to a long metal pipe for handling. The entire column length, 336 cm, was packed in the aforementioned manner.

Instrumentation. In preparation for the unsaturated solute-transport experiment, instrumentation was designed and implemented to handle some of the problems inherent in the unsaturated

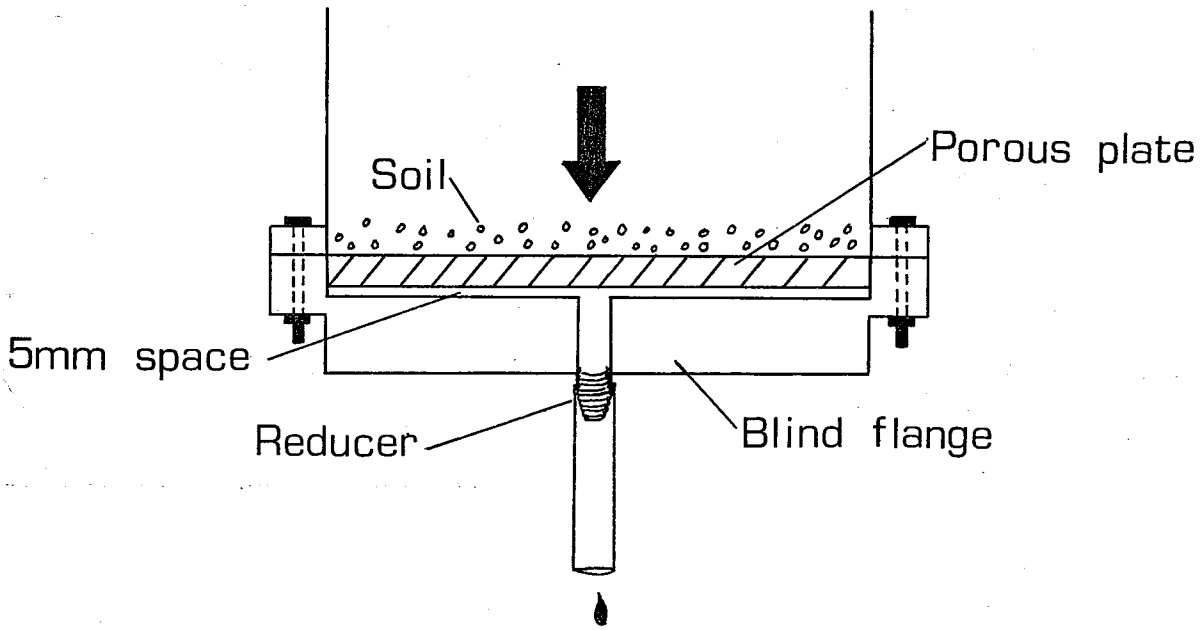

Figure 25. Flange and ceramic porous plate assemblage at the bottom of the column.

flow process. Monitoring of pressure heads to ensure a constant water content was necessary. A method of extracting soil-water solution during the experiment, at several depths along the column, was needed. Instrumentation was needed to apply a continuous, long-term vacuum at the bottom of the column to allow for effluent discharge while under negative pressure heads. Finally, the introduction of the tracer solution needed to be considered carefully.

The input system consisted of a pump, reservoir and fluid distribution device. A reciprocating, positive-displacement pump (Model RP-G20, FMI Labs, New York) was used to input the distilled water and tracer solution at a specified flux. A Mariot syphon (Figure 26) was used upstream of the pump, to insure pumping rates would not be affected by the level of the water in the reservoir. The device used to distribute the input fluid uniformly across the soil surface is shown in Figure 27. Nine 0.159 cm (0.0625 in) plastic, capillary tubes distributed water from the pump onto the surface of the tailings. All capillary tubes were equal in diameter and length, and the outflow ends were placed at equal heights above the manifold. Therefore, the volumetric fluxes through each of the tubes were equivalent. This was corroborated by experimental data, which measured equivalent fluxes for the top and the bottom capillary tubes.

A vacuum was established at the bottom of the column, by means of an aquarium pump (Whisper 1000, Willinger Bros., Inc.) housed in a well-sealed desiccator (Figure 28). An air hose was directed from the vacuum pump through the desiccator to

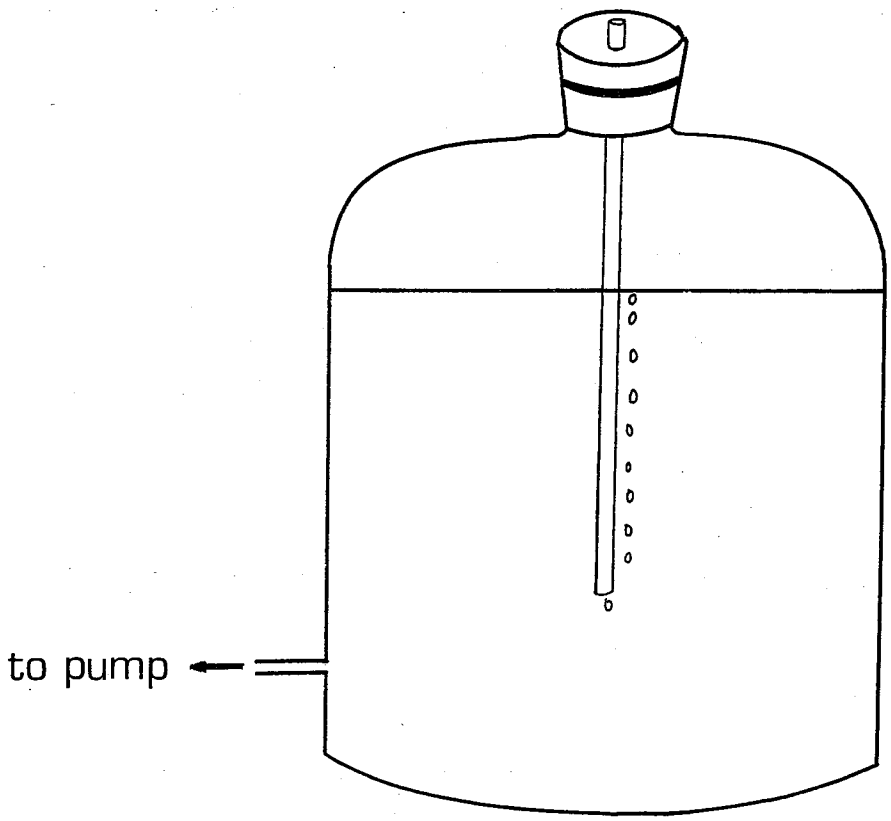

Figure 26. Constant level reservoir, upstream of input pump.

INPUT DEVICE

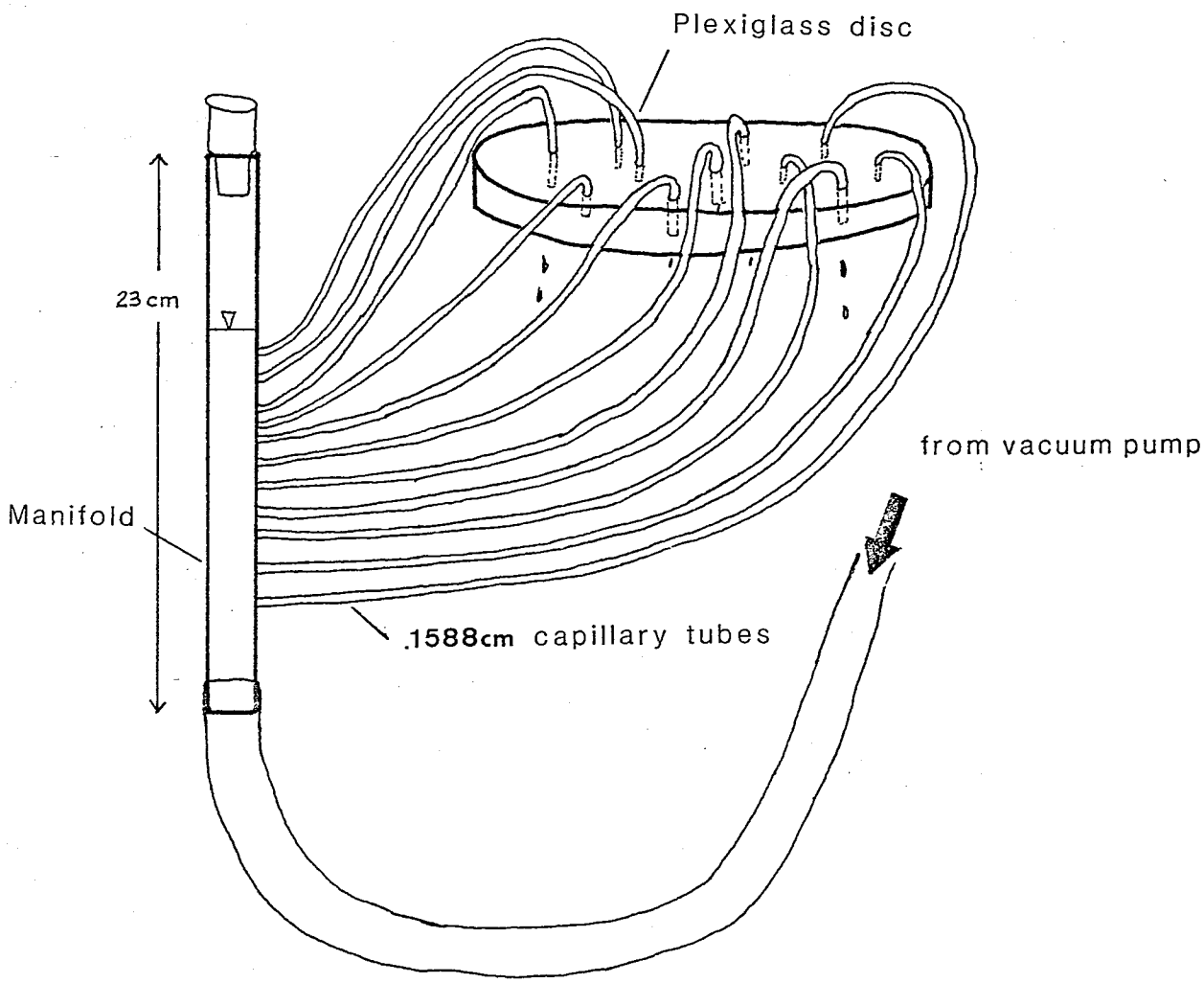

Figure 27. Device used to distribute tracer solution across the soil surface, at the top of the column.

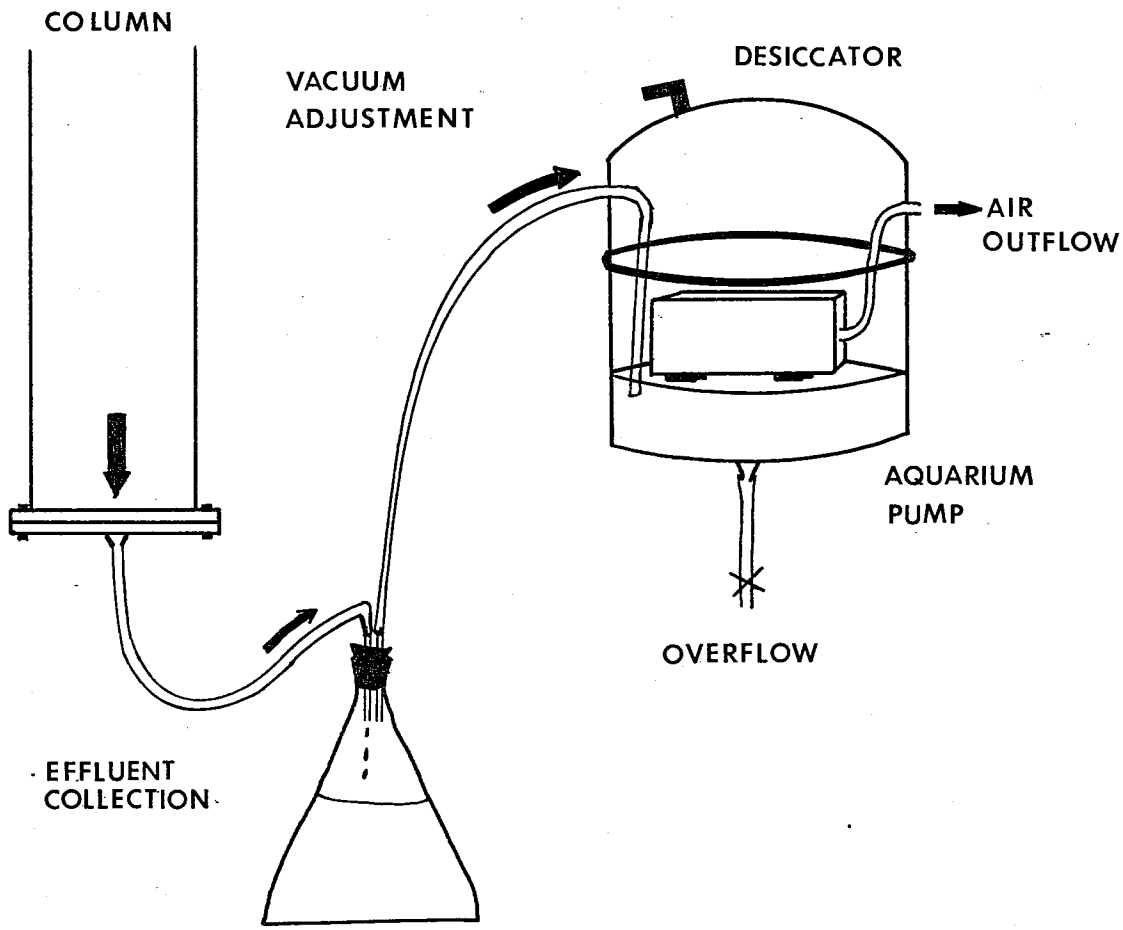

Figure 28. Vacuum system and apparatus for bottom of the column.

the outside air. A small air-escape valve was placed on the desiccator wall, to allow for vacuum adjustment. The vacuum was measured by a mercury manometer attached to the vacuum-pump and desiccator assemblage. A vacuum tube from the desiccator was connected to the column effluent tube and applied a vacuum across the porous plate. An Erlenmeyer flask was connected to the vacuum line, between the column and the vacuum pump, to collect the effluent.

To monitor the pressure heads during the experiment, tensiometers were placed along the length of the column, as shown in Figure 29. Small porous ceramic cups (3.18 cm or 1 1/4 in length, 0.95 cm or 3/8 cm width), were epoxied on to 0.64 cm (1/4 in) glass tubing. De-aired water was sucked into the tensiometer, through the porous cup, by means of a vacuum pump. A septum stopper was placed at the top of the glass tubing and sealed with silica gel. Holes were drilled into the column wall and hand bored into the tailings for tensiometer placement. The glass tubing of each tensiometer had been inserted through rubber stoppers (#2), which seated the tensiometers firmly to the column wall. To measure the pressure, a hand-held pressure transducer (Tensimeter, SMS, Las Cruces, NM) was used.

To obtain soil-water samples for tracer concentration analyses during the solute transport experiment, five porous cup samplers were installed along the length of the column (Figure 29). These samplers (Figure 30), were constructed with high-flow, porous ceramic cups (6.99 cm or 2 3/4 in length, 2.22 cm or 7/8 in width) of one bar air entry pressure, which were epoxied

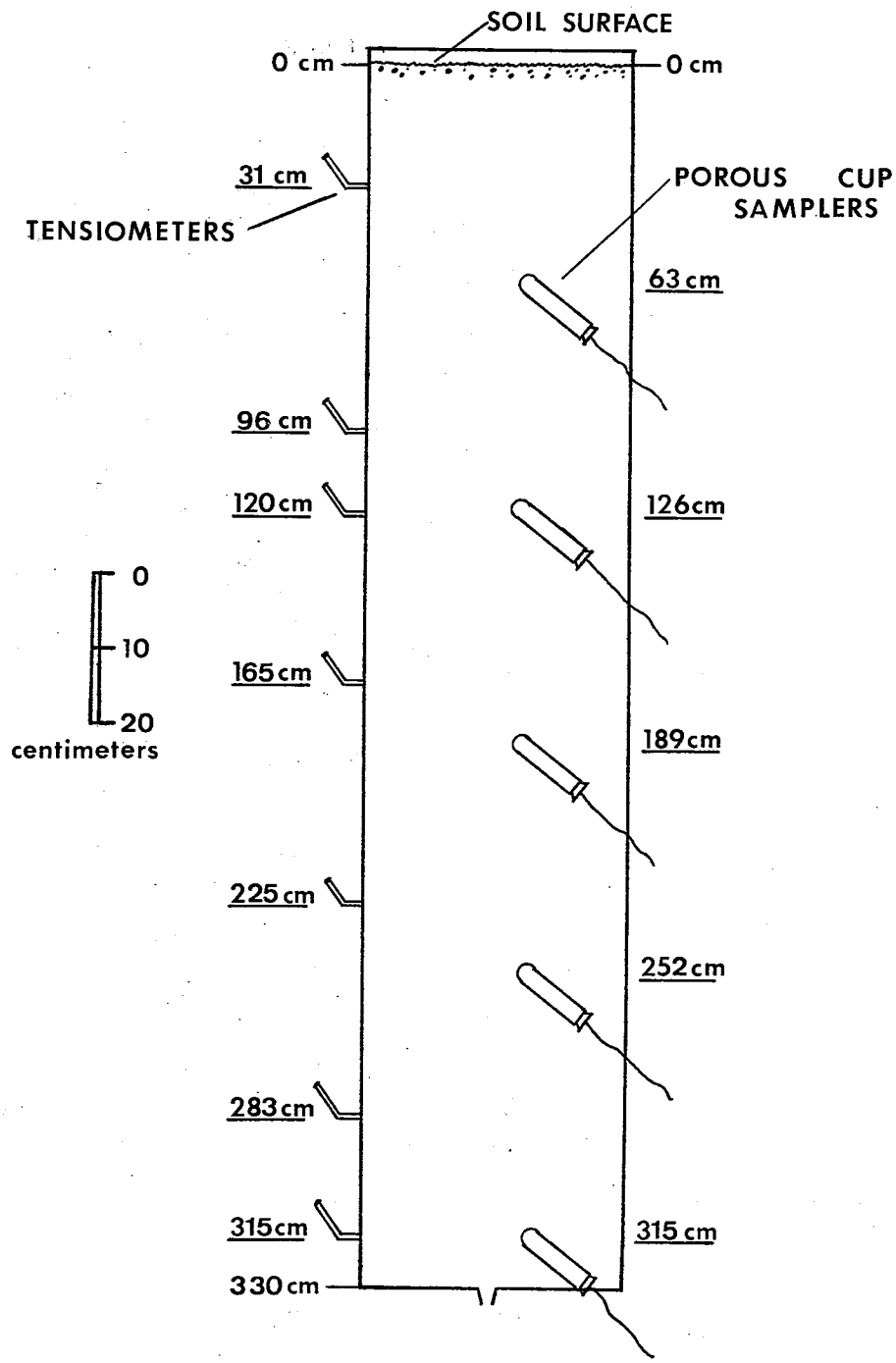

Figure 29. Location of tensiometers and porous cup samplers with depth, in the long column.

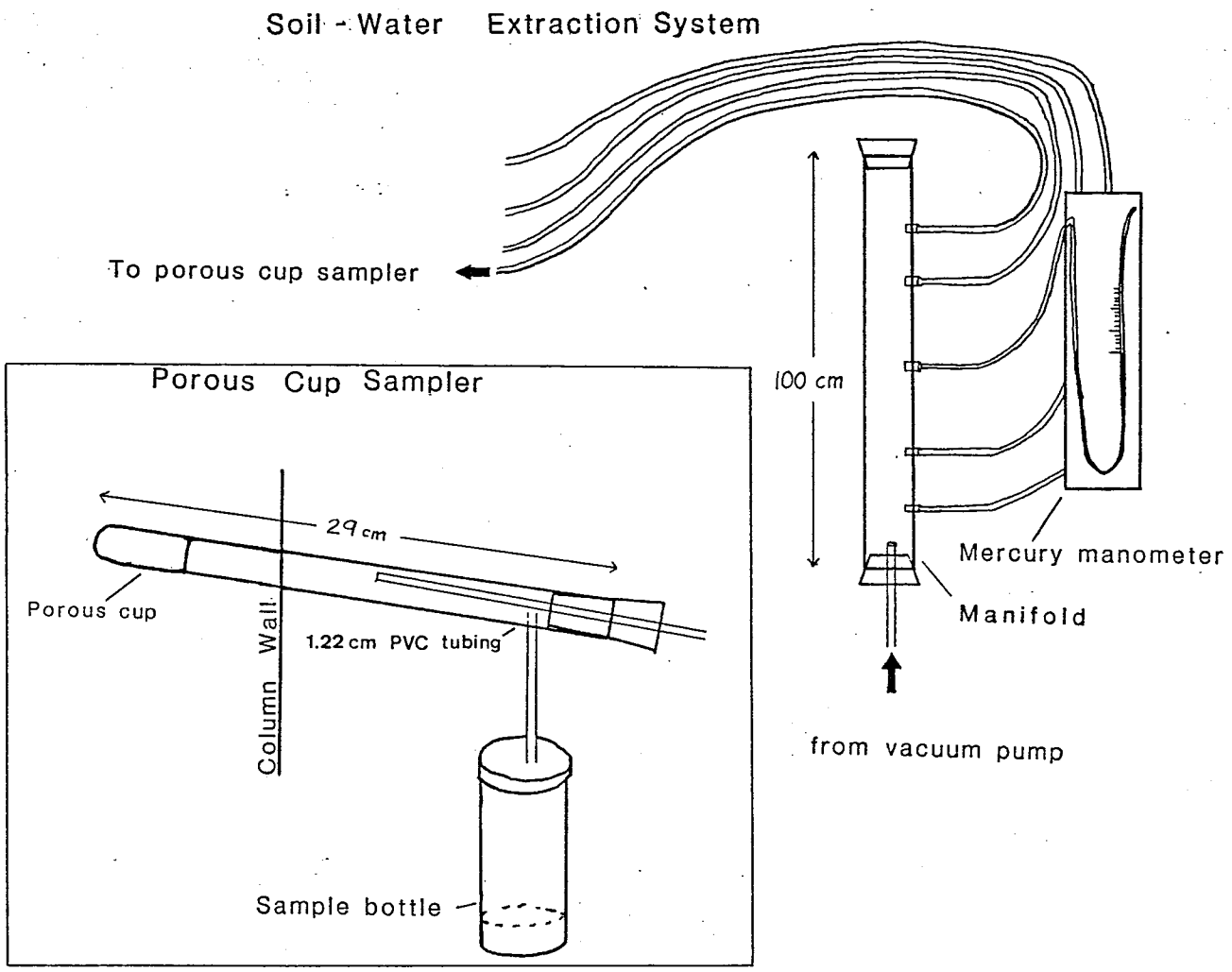

Figure 30. Soil-water extraction system. Vacuum established by vacuum pump, through manifold and capillary tubes to porous cup samplers. Sampler shown in inset.

onto the ends of 1.27 cm (1/2 in) inside diameter, clear, PVC tubes. A rubber stopper (#0), with 0.32 cm (1/8 in) diameter tubing through the center, was placed at the open end of each PVC tube. The other end of the tubing connected to a vacuum system. At the end of the PVC tube distal to the porous ceramic cup, a hole was drilled, to which 0.32 cm (1/8 in) diameter tubing was fit. This tubing led to a pill bottle with a snap-top lid which was used to collect the soil-water during extraction.

Holes were drilled into the column wall to allow sampler placement and hand-bored into the tailings with an augered drill bit. The porous cup samplers were then inserted into the holes, with the porous cup as close to the middle of the column as possible. They were inserted at an angle, with the porous cup higher than the end of the PVC tube, to facilitate drainage of water down through the tube. Silica gel was packed between the PVC tube and the column wall, to prevent leakage out the column wall.

Pore-fluid was extracted from the tailings with porous cup samplers which were connected to a vacuum manifold. The manifold was constructed from clear, acrylic tube was drilled and plugged with rubber stoppers, one for each sampler. The top of the manifold tube was blocked off, and the bottom was connected to a vacuum pump. Each rubber stopper had a 0.32 cm (1/8 in) tubing through it; one end of the 0.32 cm tubing was connected to the vacuum manifold, and the other end was connected to the porous cup sampler. Each sampler could be connected to the same vacuum system, and one, all, or any combination thereof could be

serviced by the vacuum at one time. The vacuum was initiated by a vacuum pump, which applied a vacuum to the samplers which were connected. The amount of vacuum was measured by a mercury manometer, which was also connected to the vacuum manifold. The soil-water sample was collected at the lower end of the clear PVC tube where it could be easily seen, and it drained into the pill container when the vacuum was removed.

Procedure for infiltration and leaching. The objectives of the initial wet-up were to determine the saturated hydraulic conductivity of the tailings and to leach soluble chemicals from the tailings as much as possible, prior to conducting the tracer experiment. To saturate the column, a reservoir of distilled water was connected to a float valve assembly, which in turn fed the distilled water into the column. A constant head of 352 cm of water was maintained, where 'z' is zero at the bottom of the column. The column was saturated, leached with distilled water over a period of 10 days, and then drained for a 3 month period. During the drainage period, instrumentation for the unsaturated part of the experiment was installed. However, drying occurred to a greater extent than expected during this time, and the column was re-saturated for 6 days and drained again for 5 days.

In preparation for the unsaturated leaching of the tailings, I replaced the filter cloth and flange with the porous plate-flange assemblage after the final 5 day drainage period. Distilled water was then pumped into the column at a flux much less

than the saturated hydraulic conductivity of the tailings. Adjustment of the input flux and the vacuum at the bottom of the column was required to obtain steady-state conditions and uniform water content throughout the column. Ten days after initiation of unsaturated leaching, a stabilized input and effluent flux of 8.09E-05 cm/sec (1.0 ml/min) was obtained for the unsaturated column leaching. This input flux was later decreased (71 days after initiation of unsaturated leaching) to 6.87E-05 cm/sec (0.85 ml/min) in order to equal a decreased effluent flux. The decrease in the effluent flux was due to a loss of vacuum efficiency by the aquarium pump.

At a flux of 1.0 ml/min, ponding developed at the top of the column, even though the sediments were unsaturated. This suggested that a low-permeability clogging layer had developed at the upper surface of the tailings. The upper 39 cm of the column were repacked, and the original tailings were examined for microbes. No evidence of microbial activity was recognized under microscopic scrutiny of soil-water slides. A small hole near the bottom of the column was opened to prevent air pressure build-up ahead of the wetting front. However, ponding again developed after the repacking. This was probably a consequence of using wet, rather than air-dried, tailings during the repacking procedure, which raised the bulk density and lowered the permeability of the medium. The top 43 cm of the column were then repacked with air-dried tailings, in an identical manner as the original packing procedure, and no further ponding at the soil surface was evidenced.

During the unsaturated leaching period (76 days), the electrical conductivity and pH of the eluent was closely monitored, to document chemical changes. Soil water pressure heads were monitored by the tensiometers. Generally, the tensiometers functioned properly for one to two week intervals. Input and discharge fluxes were also measured.

Procedure for solute-transport experiment. After 76 days of unsaturated leaching and steady-state flow conditions were established, a 17.9L pulse of 1.00E-01 M bromide solution was introduced to the column. The bromide solution was prepared by dissolving 196.2 g of $CaBr_2.H_2O$ solid in 18 L of distilled water. At the time of tracer introduction, uniform pressure-heads of -26.0, -27.0 and -26.0 cm of water were recorded for the 31, 165, and 283 cm depths, respectively. The pulse of tracer was introduced at 0.85 ml/min over an 17 day period, followed by a distilled water eluent. The distilled water eluent was continued for 101 more days. Less than ten minutes were required to rinse and refill the reservoir with the appropriate solution.

Extraction of soil water for tracer concentration analysis was initiated 24 hours after the tracer was introduced. To obtain a soil-water sample, an induced suction of 40 cm of water was used. Extraction time varied between 1 to 2.5 hours and sample volumes varied from 2 to 8 ml. The influence of the induced suction on the flow field was considered and is reviewed in Appendix I. Sampling frequency varied according to the peak concentration location. As the solute front moved past a

sampler, up to four measurements were taken over a 24 hour period. Sampling was less frequent (once a day) after the main bulk of the breakthrough curve had passed (1200 hrs after introduction of the tracer) and concentrations were more stable.

Only three of the five porous cup samplers were used. Porous cup sampler #3 (189 cm depth along the column) only transmitted a few drops of soil-water, not enough for concentration analysis. The sampler was replaced, but it still did not extract enough soil-water and was omitted from the experiment. Due to leakage problems at the tube-column junction, the lowest sampler (315 cm depth) was also omitted from the experiment.

Effluent volume was measured at the beginning and end of each soil-water extraction period. Length of sampling time, temperatures and sample volumes were also recorded. The bromide concentration was measured by an Orion Ion Analyzer, as explained in the previous unsaturated, short-column experiment.

Results and Discussion

Infiltration. During the period of saturation, the calculated hydraulic conductivity, K_s, was 5.40E-04 cm/sec for the packed tailings. K_s was determined using the measured volumetric discharge rate (Q) of 0.12 ml/sec obtained from the bottom eluent, a column area (A) of 206.1 cm^2, a head change of 352 cm over a 330 cm porous medium length for a hydraulic gradient (i) of 1.07, and Darcy's Law

$$K_s = Q/Ai \tag{31}$$

The K_s of 5.40E-04 cm/sec agrees with the K_s of 5.47E-04 cm/sec determined from repacked, laboratory-column permeability experiments of Lewis (1986) for the same copper tailings medium. In addition, the K_s of 5.40E-04 cm/sec is very close to the K_s of 7.4E-04 cm/sec Lewis (1986) determined from his solute-transport experiment under saturated conditions in which he used similar packing procedures to those in the present investigation.

During the period of saturation, effective porosity (n_e) was estimated by noting the distance, L, the wetting front moved in a specified amount of time, and assuming piston-type displacement. The distance, L, was the change in the depth of the wetting front from 265.8 to 254.0 cm in a 154.5 minute time period. The volume of water, V_w input over the same 154.5 minute period was calculated by multiplying the area of the column (206.1 cm^2) by the change in water level at the top of the column (4.3 cm). Using the relationship

$$n_e = V_w / L A \tag{32}$$

with a V_w of 886.2 ml and L of 11.8 cm, an effective porosity of 36% was calculated. The 3.0% residual moisture content (obtained by oven-drying samples of the tailings before packing) of the air-dried tailings increased the porosity to 39%. Entrapped air might cause the actual porosity to be somewhat higher. Therefore, an effective porosity of 40%, as used by Greg Lewis (1986) for the same tailings and packing density, appeared to be a reasonable estimate for porosity.

Influx and efflux. According to Freeze and Cherry (1979), steady-state flow occurs when the magnitude and direction of the flow velocities are constant with time, at any point within the flow field. Under the unsaturated flow conditions of this column experiment, the recharge and discharge rates should be equal as well as constant over time, in order to prevent water storage or loss during the experiment.

From Figure 31, it is obvious that the inflow and outflow rates during 194 days of the experiment were not constant throughout the experiment, nor were they always equal to each other. The time period shown extends from the initiation of unsaturated leaching to the end of the solute-transport experiment. The inflow and outflow rates are listed in Appendix J. There was a widespread variation in flow rates, especially prior to the introduction of the tracer at 1828.2 hrs. After the introduction of the tracer, the outflow rates more closely followed the trend of the inflow rates.

Because the outflow rate was lower than the inflow rate, an increase in water stored in the column occurred. To illustrate, the cumulative volume of water flowing out of the column was plotted versus time in Figure 32, and the data is listed in Appendix K. The solid, straight line represents the cumulative volume into the column at a constant rate of 0.85 ml/min. If the inflow and outflow rates were equal, the slopes of the two lines would parallel each other. It can be seen that the slope of the outflow rate generally paralleled the slope of the inflow rate (shown by the dashed line), with the exception of two events at

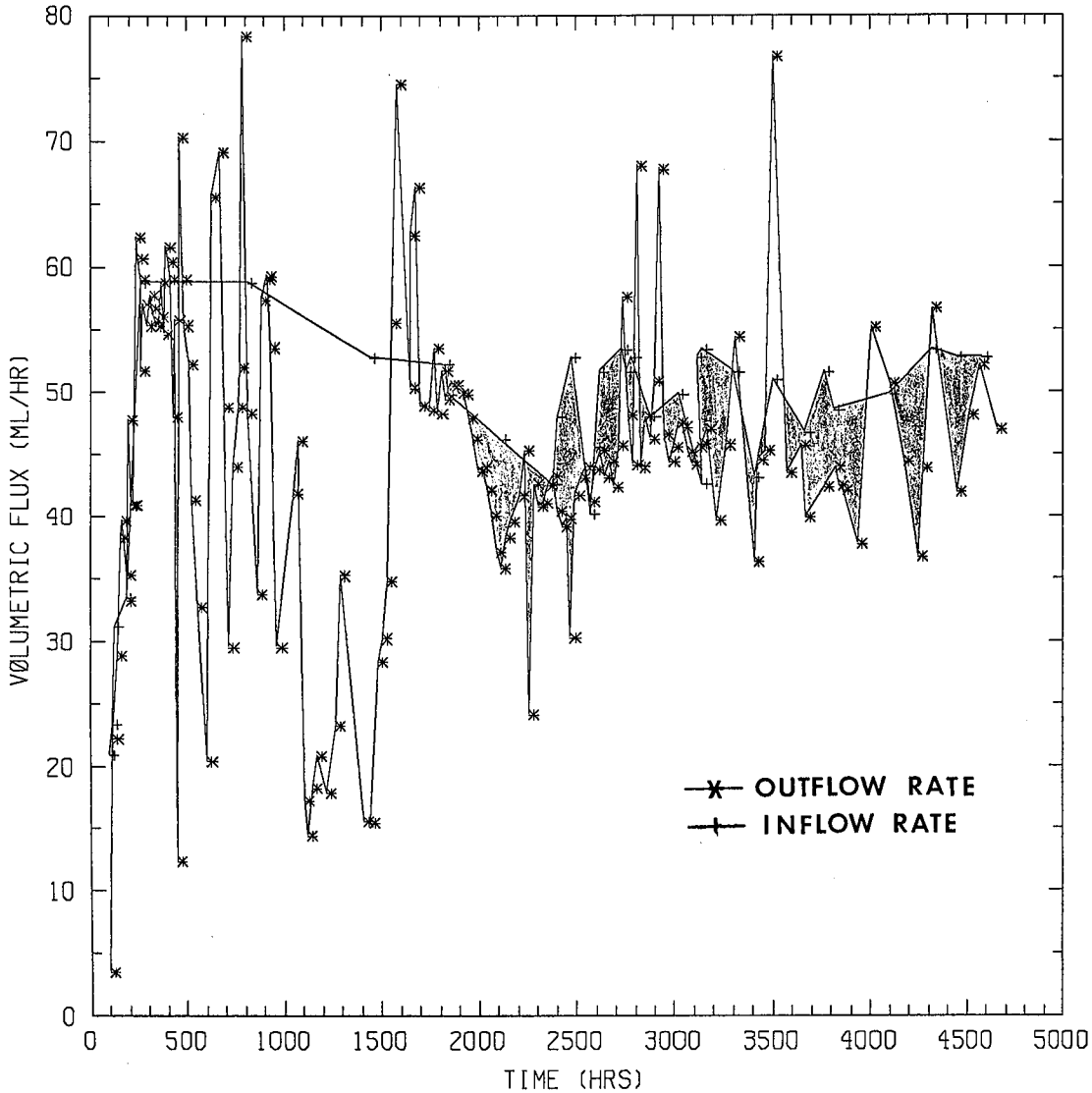

Figure 31. Inflow and outflow rates, over time. Time is 0 at initiation of unsaturated leaching.

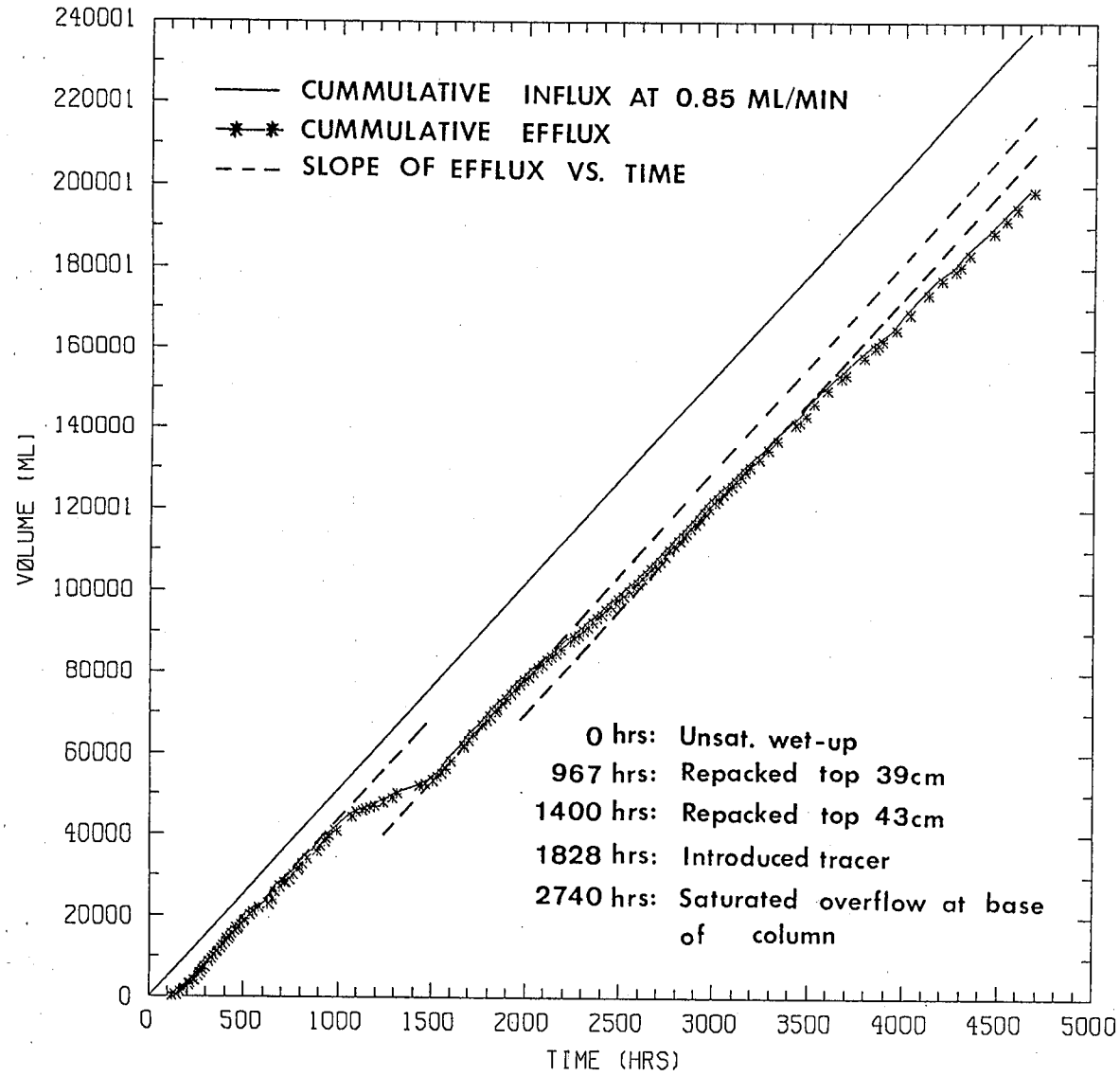

Figure 32. Comparison of efflux and influx volumes, over time. Time is 0 at initiation of unsaturated leaching.

967 hrs and 2000 hrs.

The first departure of the outflow slope from that of the inflow, at 967 hrs, coincides with the repacking of the top 39 cm of tailings. As suggested in the procedural section, these repacked tailings acted as a clogging layer, and the ponding that resulted decreased the infiltration and outflow rates. After the second repacking event at 1400 hrs, the outflow slope again paralleled the inflow slope. Steady-state conditions were thus established for the initiation of the solute-transport experiment at 1828 hrs, as verified by tensiometric data presented in the following Flow field section.

The second departure of outflow and inflow slopes is shown at about 2000 hrs, during the solute-transport experiment. Two explanations were explored to account for the difference in outflow and inflow rates.

One possible cause for difference was through removal of soil-water from the system via the sampling procedure. Figure 33 compares the cumulative sampling volume obtained over time (listed in Appendix L) to the cumulative volume out of the column as a function of time. The dashed line represents the cumulative volume into the column, at an assumed constant inflow rate of 0.85 ml/min. However, the sampling volume accumulated (1420 ml) cannot account for the total difference between inflow and outflow (10,500 ml; obtained by graphical integration of the shaded area in Figure 31).

The decrease in outflow at 2000 hrs also may have been caused by an increase in storage in the lower part of the column

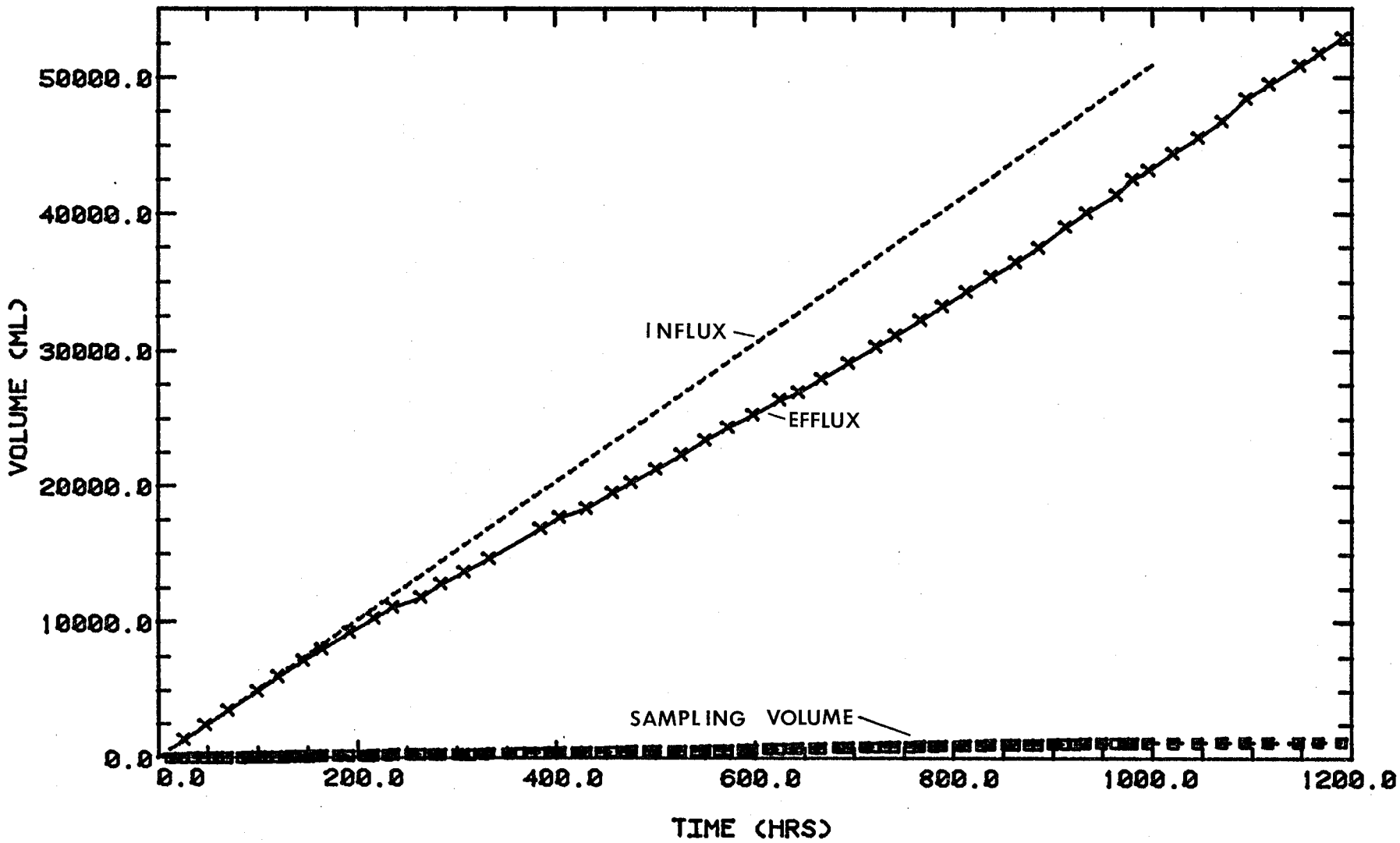

Figure 33. Cummulative sampling volume over time, relative to influx and efflux volumes. Time at 0 corresponds to introduction of the tracer.

due to the decrease in the efficiency of the vacuum pump (see Procedures section). As the basal sediments saturated, water leaked from a small hole near the base of the column. This leakage was included in the effluent volume measurements and was accounted for in the cumulative effluent volume shown in Figure 38. After this overflow occurred (first noted at 2740 hrs), it can be seen that outflow rate nearly equaled the inflow rate. The hole near the base of the column established a lower boundary condition, which limited the depth of saturation at the base of the column. Leakage occurred whenever the depth of saturation height was sufficient to generate the head necessary to force water through the hole. Thus, an equilibrium was re-established for the duration of the experiment, albeit a different (wetter) condition than at the introduction of the tracer.

The soil-water sampling regime and saturation of the basal portion of the column probably affected the amount and distribution of the increased storage (10,500 ml). The sampling volume (1420 ml) that never reached the effluent was subtracted from the increase in storage (10,500 ml), and a revised storage increase of 9080 ml was calculated.

Some of the 9080 ml of additional storage would be located in the saturated basal portion of the column. The saturated basal portion of the column accounted for 417 ml of the additional storage. This was determined by subracting the volume of water ($A*\theta*L$) at a water content of 33% from the volume of water held at saturation (40%). The hole through which leakage occurred was located 18 cm above the bottom of the column (L), and the

area of the column (A) was 206.1 cm^2.

The change in storage at the bottom of the column (417 ml) was subtracted from the total increased storage (9080 ml), and a net storage increase of 8663 ml resulted. The increase in storage was probably distributed along the column length and resulted in a subsequent increase in water content of the copper tailings. As discussed in the following flow field section, the tensiometric data also suggested an increase in water content within the column profile over time.

Flow field. Several aspects of the flow field for the long-column experiment are considered in this section. The uniformity of the pressure heads and water contents and the relationships between pressure heads, water contents and hydraulic conductivity are discussed. Saturated hydraulic conductivity and porosity estimates are also included.

Pressure-head measurements from the time of tracer introduction to the end of the experiment are shown in Figure 34 and included in Appendix M. These measurements were obtained from the tensiometers installed along the column wall, at the depths indicated in Figure 34. Unconnected points indicate tensiometer failure, and subsequent lack of data for that time period. Pressure heads from the top, middle, and bottom tensiometers (31, 165, and 283 cm, respectively) gave the most complete, uninterrupted data sets. Additional data sets for the 96, 120 and 225 cm tensiometers were incomplete, but provided ancillary data.

From Figure 34 it appears that the uniformity of pressure

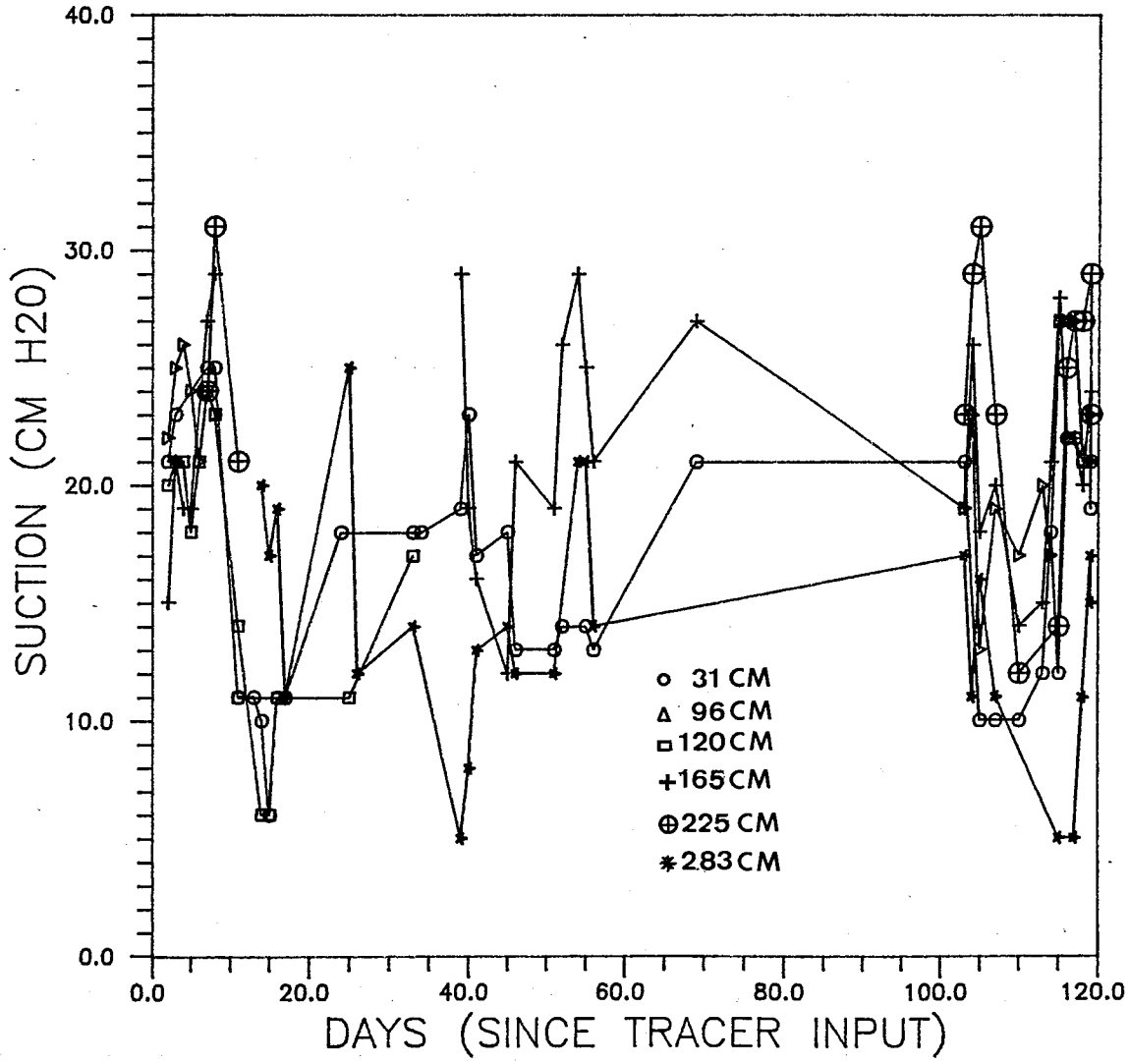

Figure 34. Suction measured at discrete depths. Time is 0 at the introduction of the tracer.

head measurements, which existed at the time of tracer introduction, began to decrease about 10 days after the introduction of the tracer. During the remainder of the experiment, pressure head differences of up to 23 cm of water occurred on days 39 and 115. The deepest tensiometer at the 283 cm depth generally recorded the lowest suctions, whereas the tensiometers at the 165 and 225 cm depths consistently recorded the highest suctions.

The vacuum used for sample extraction did not appear to strongly affect the suction measurements. The most intensive sampling (up to four times per 24 hour period) occurred from one to 15 days. During that time the suctions showed an overall decrease in value, which indicated an unexpected increase in water contents. An increase in suction would have occurred if the system had responsed to the applied suction and subsequent removal of soil-water from the system.

The tensiometric data exhibited definite trends over time (Figure 34). Ten days after introduction of the tracer, the suction measurements decreased. This decrease coincided with the major increase in storage observed in Figure 32, at 2060 hrs or 10 days after the introduction of the tracer at 1828.2 hrs. The suctions appeared to stabilize at approximately 36 days into the solute-transport experiment, and storage was also stabilized at approximately the same time (2700 hrs in Figure 32, which correlates to 871.8 hrs or 36.3 days in Figure 34). The abrupt change in suctions which occurred at 104 days in Figure 34 was not supported by a related sharp change in storage in Figure 32. In fact, a gradual increase in storage was observed from approxi-

mately 3600 hrs (74 days after introduction of tracer) through to the end of the experiment.

The suction variations and changes that were observed from 104 to 117 days into the solute-transport experiment were probably caused by procedural maintainence problems. The vacuum pump was mistakenly not connected with the outflow tubes on the 102nd day of the experiment, and saturated overflow occurred through the hole near the base of the column. On the 103rd day, the input system was not connected and no inflow occurred for a 24 hour period. By the 119th day, the suctions were re-established at values similar to those of day 103, prior to the inflow and vacuum connection problems.

Mean pressure-heads for each depth in the column were calculated using the following relationship

$$\overline{\Psi}_d = \sum_{i=1}^{n} \Psi_i/n \qquad (33)$$

where n is the number of observations for each tensiometer and $\overline{\Psi}_d$ is the mean pressure-head at a specific depth. These mean pressure-heads are listed in Table 9.

Table 9. Mean pressure heads for long-column flow field.

Depth (cm)	Mean Pressure Head (cm of H20), $\overline{\Psi}_d$
49.0	-16.3
114.0	-22.0
138.0	-16.0
182.0	-21.5
242.0	-24.2
301.0	-13.8

An overall pressure-head average ($\overline{\Psi}$) for the entire column of -18.6 cm of water was then calculated by weighting the mean pressure-head measurements ($\overline{\Psi}_d$) according to the number of measurements for each depth (n_d),

$$\overline{\Psi} = \frac{1}{N}\sum_{d=1}^{6} \Psi_d n_d \tag{34}$$

where d was the number of tensiometers and N was the summed total of tensiometric observations from all depths.

At the completion of the experiment the tailings were sampled for volumetric water content, θ_v. A hand sampler was used to collect seven 5.1 cm X 5.0 cm ring samples from different depths along the column, over a two-hour period. Compaction of the ring samples occurred during the sampling procedure, especially with the deeper, more inaccessible samples. The metering pump and vacuum system were turned off before sampling. Although redistribution of water with the column probably occurred, the bottom outflow tube was clamped off and no water exited the system as effluent during the destructive sampling. The volumetric water content was calculated using the $\theta_v = W\rho_b/\rho_w$ relationship, where ρ_b is the dry bulk density, W the gravimetric water content, and ρ_w the density of water. The ring samples were weighed before and after oven drying for 24 hours at 105°C, to obtain M_w, the mass of water held by the samples. The gravimetric water content ($W = M_w/M_s$) was calculated, where M_s is the mass of dried soil. The volumetric water contents (θ_v) were then obtained, using a dry bulk density of 1.44 g/cc (the column packing density). These values are shown in Figure 35 and listed

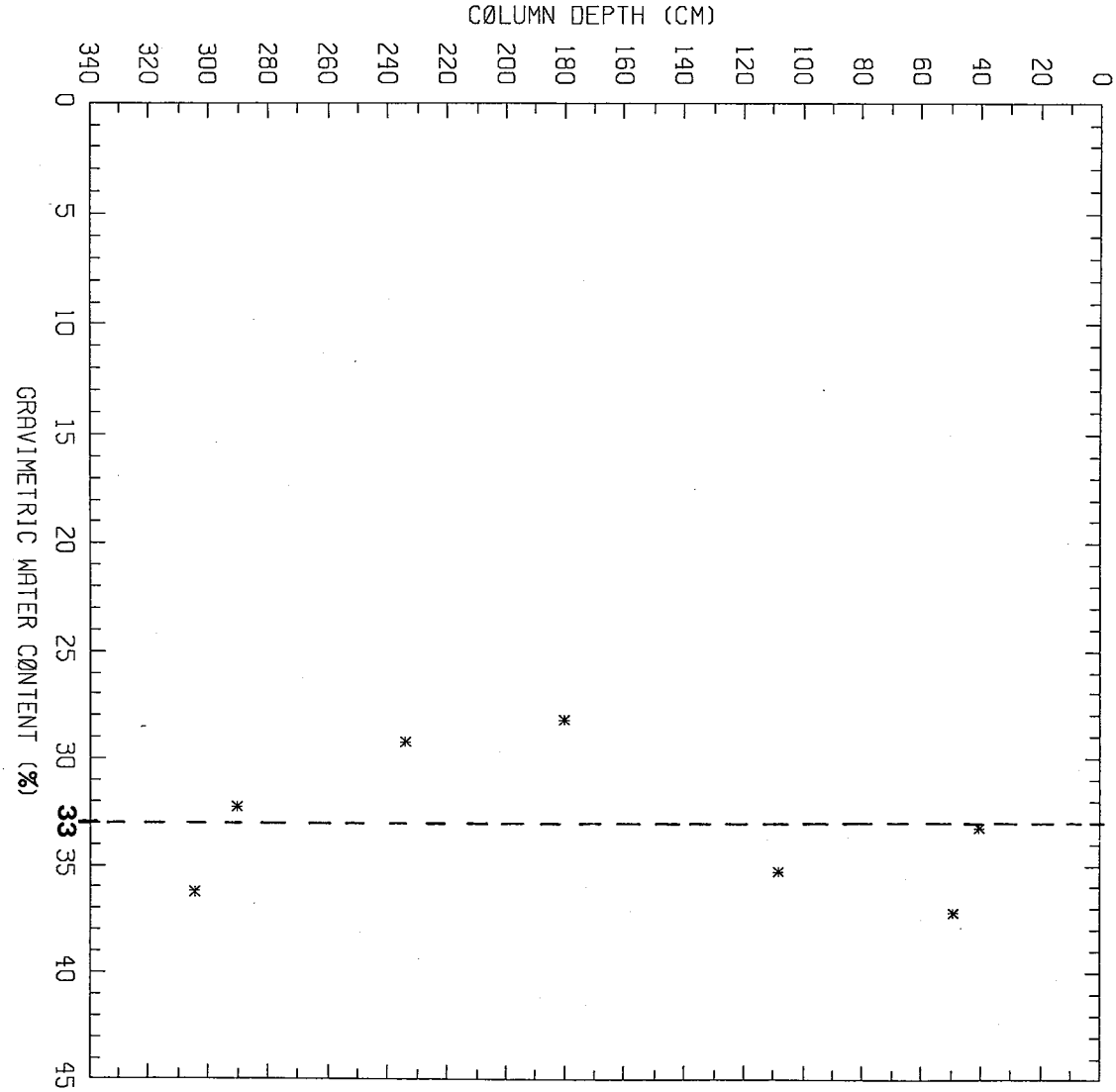

Figure 35. Volumetric water content with column depth, determined by hand-core sampling.

in Appendix N, and yielded a mean volumetric water content ($\bar{\theta}_v$) of 33%.

A drier section existed towards the lower middle portion of the column (140 to 280 cm depths), as evidenced by the decreased water content. This is in good agreement with the pressure-head measurements which were lower for tensiometers at the 165 and 225 cm depths. Saturation at the bottom of the column was not indicated by the water contents. However, redistribution of water within the column during the ring sampling procedure may have affected samples from the bottom of the column, because they were obtained at the end of the two hour sampling period.

The mean water content and pressure head measurements were applied to the soil-moisture characteristic curve (θ/Ψ curve) for these copper tailings (Lewis, 1986), shown in Figure 36. The curve shows the relationship between volumetric water content and suction (which is the negative of pressure head). The mean pressure head of -18.6 cm of water (obtained from tensiometers) was applied to this curve, and yielded volumetric water contents in the 33.0 to 38.5% range (wetting and drying curves, respectively). Hysteresis probably occurred during the wet-up and drainage procedure, thus an intermediate θ_v of 35.8% was chosen as representative. This is a good approximation of the $\bar{\theta}_v$ of 33% obtained by the ring samples (an 8% difference).

The flux (6.87E-05 cm/sec) used in this experiment (where $q=K(\theta)$) was compared to the hydraulic conductivity, $K(\theta)$, of the copper tailings at the $\bar{\theta}_v$ of 33%. Figure 37 shows the relationship between hydraulic conductivity and volumetric water content

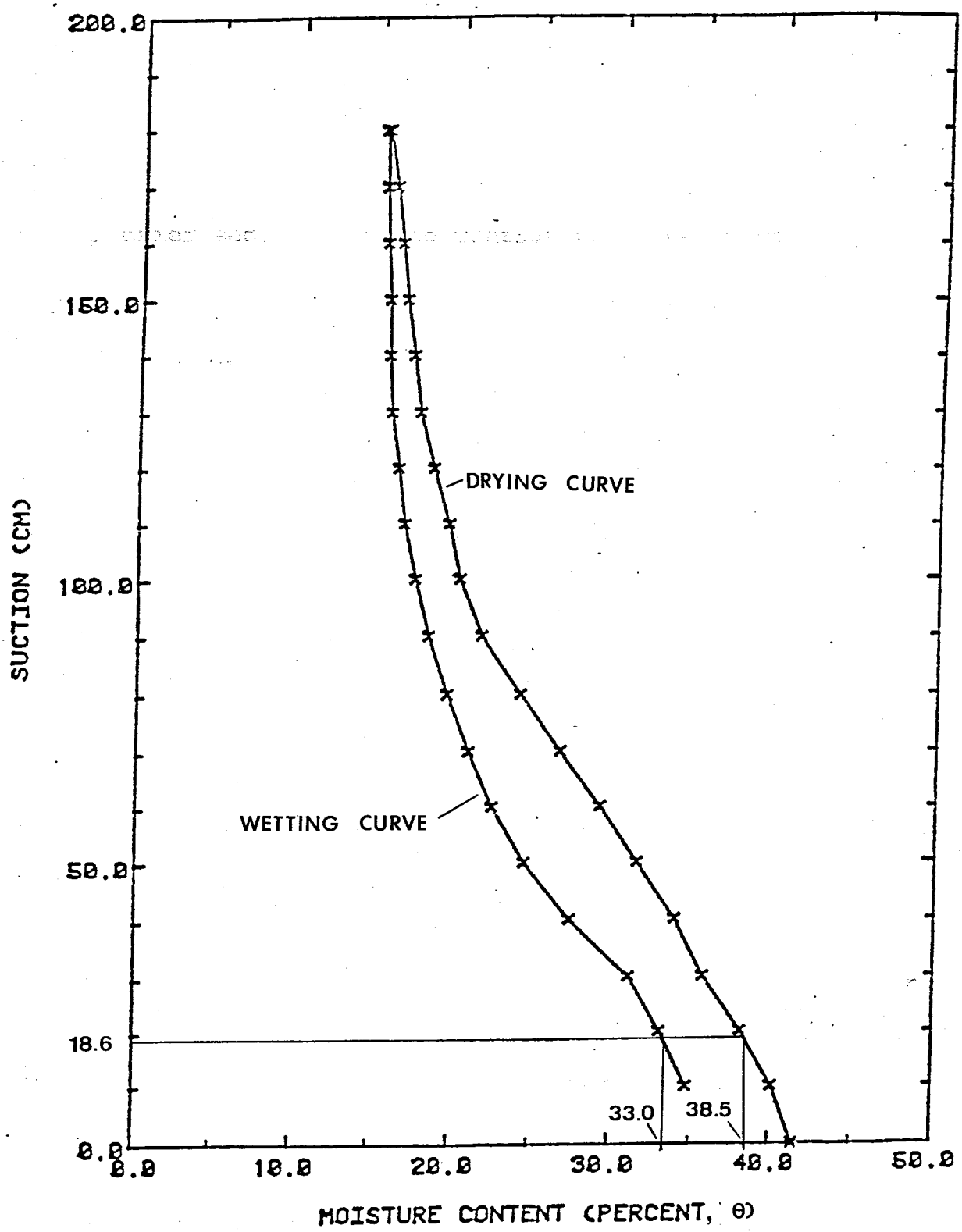

Figure 36. Water contents of both wetting and drying soil moisture characteristic curves for mean suction of 18.6 cm of H_2O. Characteristic curve for copper mill tailings, beach sand fraction, from Lewis (1986).

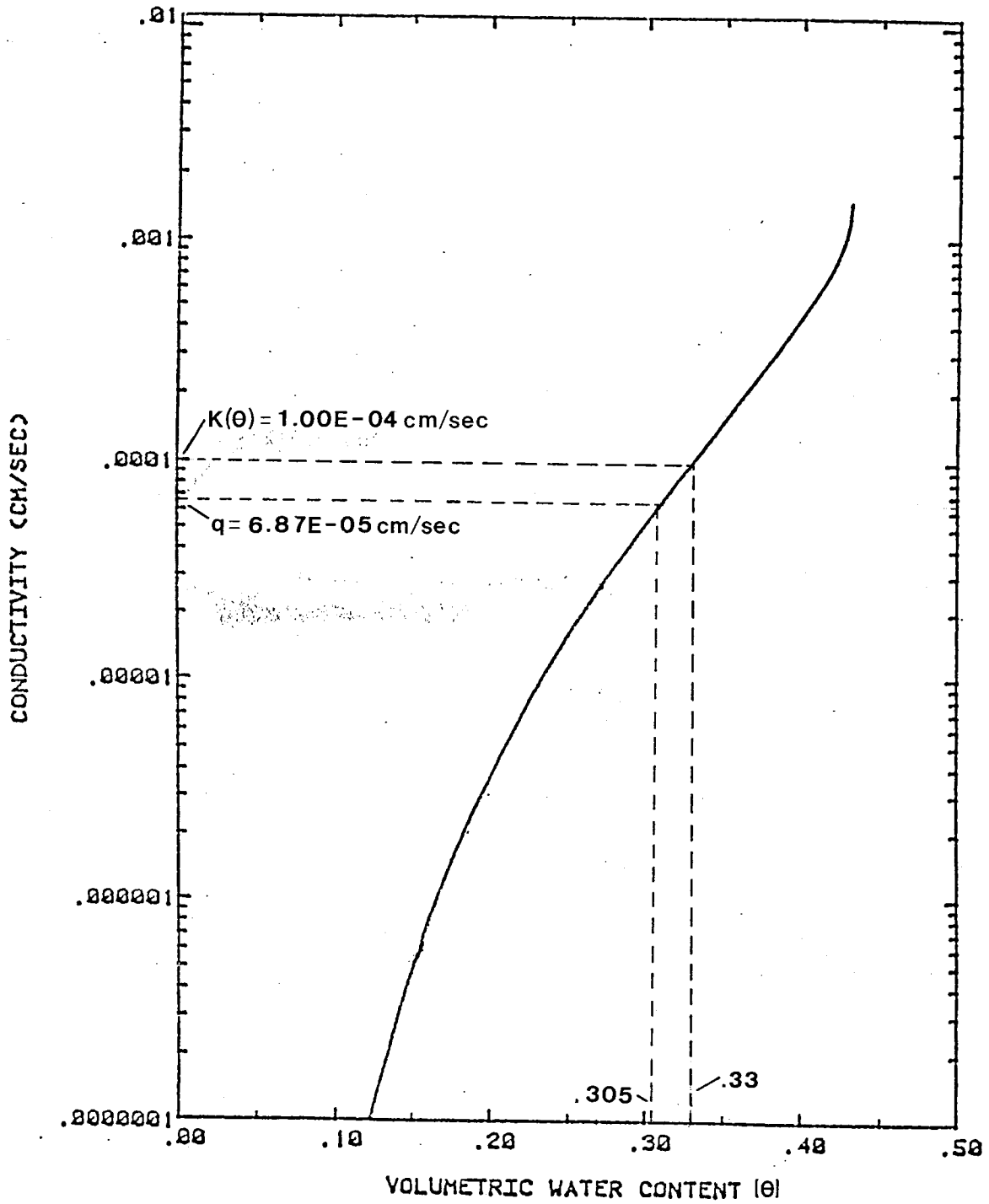

Figure 37. Comparison of input flux (q = 6.87E-05 cm/sec) to K(θ) determined from measured mean water content of long column. Projected water content at input flux (30.5%) also included for comparison with measured mean water content (33%). K-θ curve for beach sand fraction of copper mill tailings from Lewis (1986).

for these copper tailings (Lewis, 1986). At a $\bar{\theta}_v$ of 33%, a K(θ) of 1.00E-04 cm/sec results, which is well within an order of magnitude of the 6.87E-05 cm/sec flux used in the experiment. Also, the K-θ curve linked the 6.87E-05 cm/sec flux used in this experiment to a 30.5% water content. The mean water content of 33% actually measured from column samples was quite close to the 30.5% water content determined from the K-θ curve. The K-θ curve yielded a good approximation of the hydraulic conductivity or flux as well as the water contents used in this experiment.

Unsaturated leaching. Figures 38a and 39b show the measured electrical conductivity (EC) and pH values (listed in Appendix O) obtained during the unsaturated leaching of the column, prior to introduction of the tracer. Due to high initial concentrations of ions in the effluent as indicated by the high relative EC, the tracer was not introduced until decreased EC values of approximately 350 μmhos were demonstrated. This reduced chemical reactions between the tracer with the soil-water, such as complexation.

Solute-transport. From the results of the solute-transport experiment, BTC's were obtained for each sampling position along the column. The mass balance of each BTC was analyzed, seepage velocity comparisons were made, and the transport parameters were determined and analyzed. Comparisons of the dispersivities determined from the long column experiments were then examined in relation to transport distance. They were also compared to

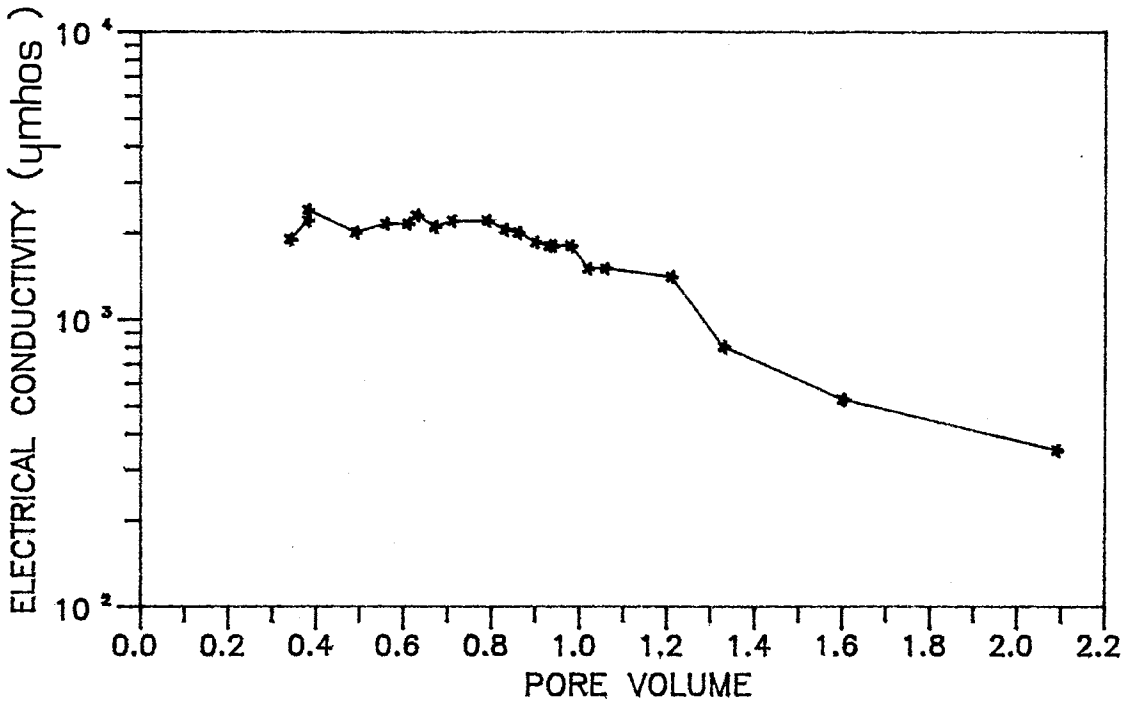

(a)

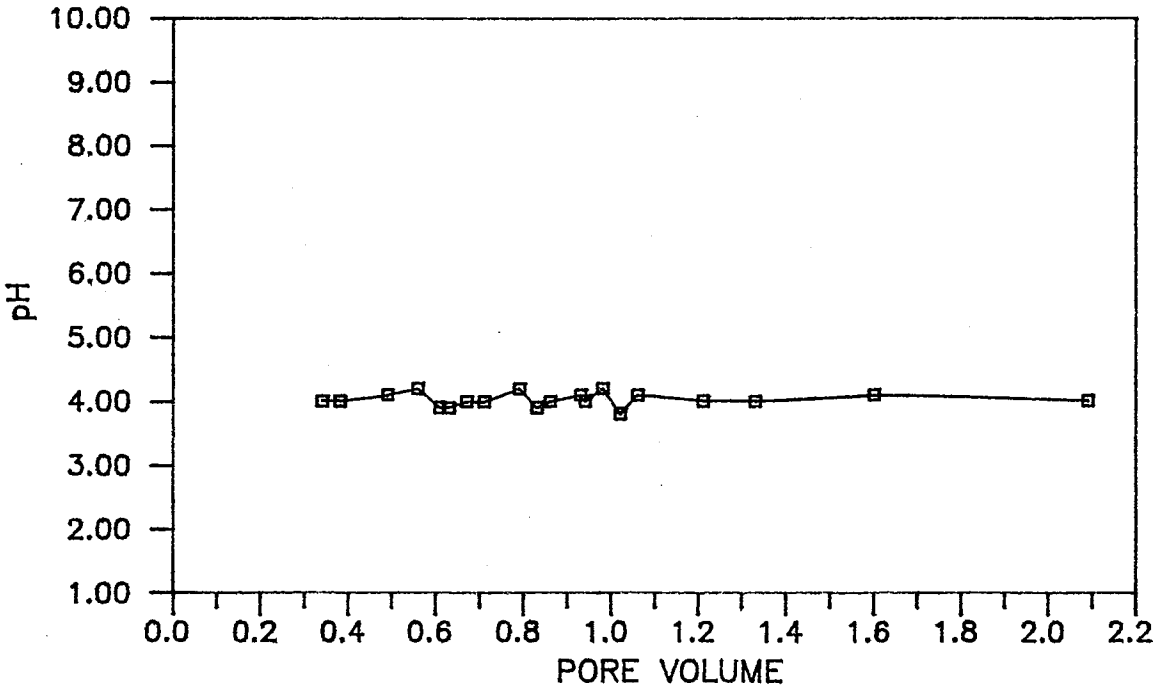

(b)

Figure 38. Electrical conductivity (a) and pH (b) as a function of pore volumes, during unsaturated leaching.

saturated long-column dispersivity results, unsaturated short-column dispersivity results, and to dispersivity results from unsaturated solute-transport experiments found in the literature.

Curves of relative concentration versus pore volume, time, and effluent volume at each sampling position along the column (63.0 cm, 126.0 cm, 252 cm, and 330.0 cm) are shown in Figures 39, 40, and 41, and the associated data is tabulated in Appendix P. Pore volumes were calculated as in equation (11), using the volumetric flux of 0.85 ml/min and the overall mean volumetric water content of 33% for each depth. The 330.0 cm BTC is effluent discharged from the bottom of the column, through the porous plate. The other three BTC's were obtained from porous cup sampler extraction system.

Corrections for complexation of the bromide ion, which interfered with measurements for the previous short columns, were not conducted for this experiment. For the long-column experiment, the bromide concentrations for the 63, 126 and 252 cm depths reached 100% of the input concentration, and corrections were therefore not necessary. The long-column experiment involved a long interval of leaching before introduction of the bromide tracer, and low concentrations of metal cations in the leachate prevented complexation with the bromide ions. The diffusion and short-column experiments, however, were conducted with little to no prior leaching. Thus metal ion concentrations in the leachate were sufficiently high to result in complexation of the bromide with the metal ions.

A mass balance was calculated for each BTC, by comparing the

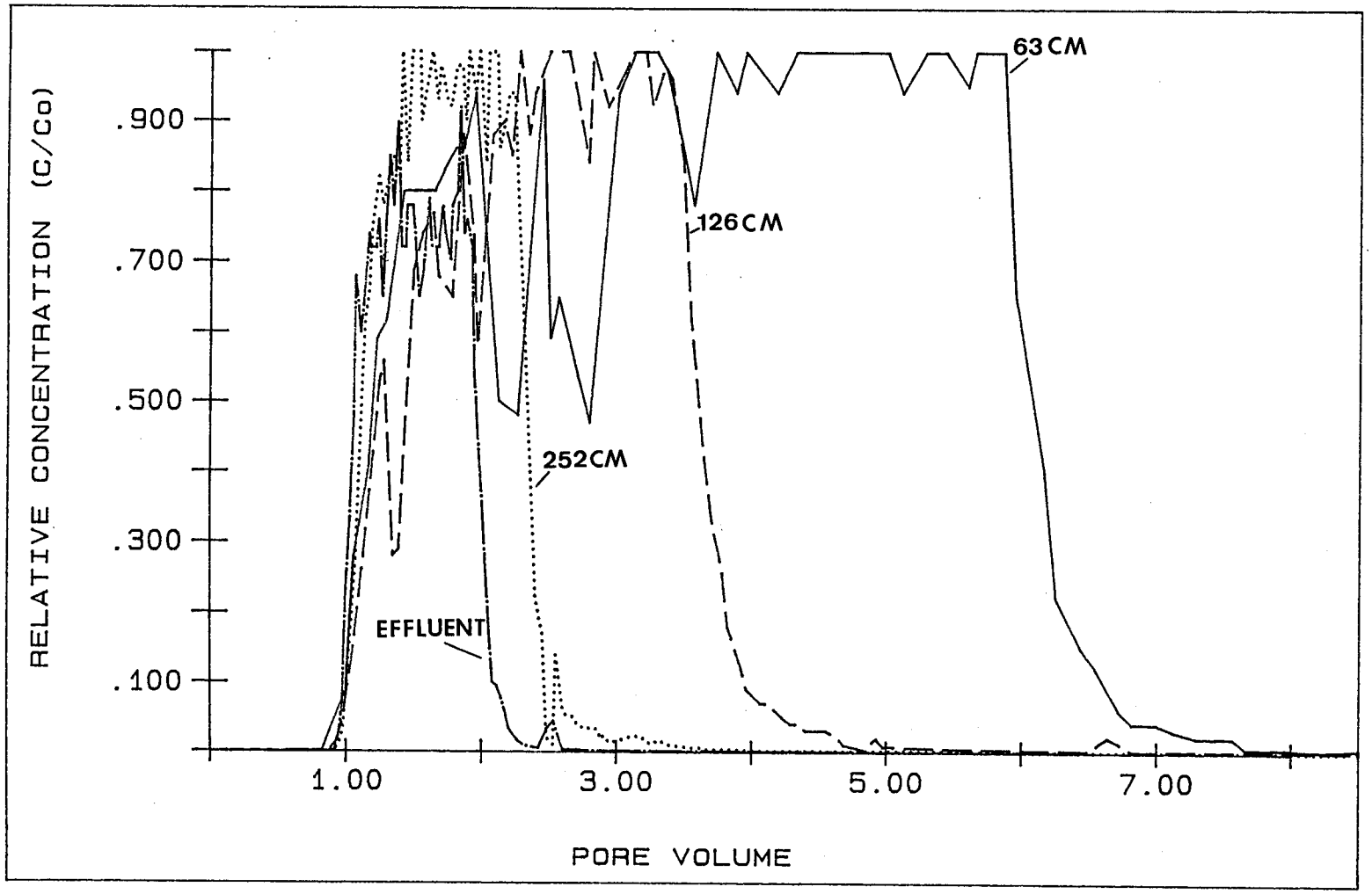

Figure 39. Relative concentration versus pore volume of sampling depth, at each sampling position.

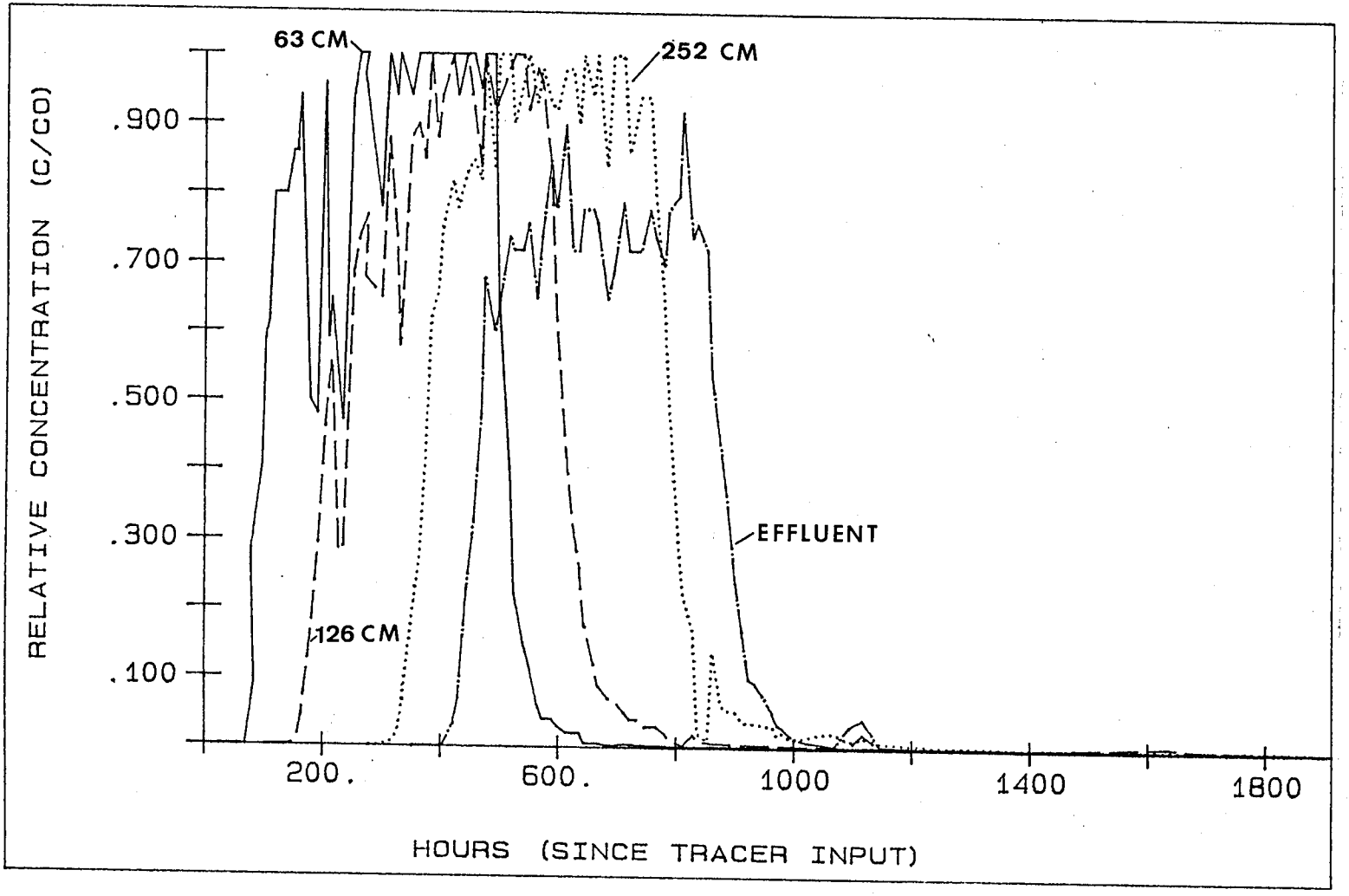

Figure 40. Relative concentration versus time, at each sampling position.

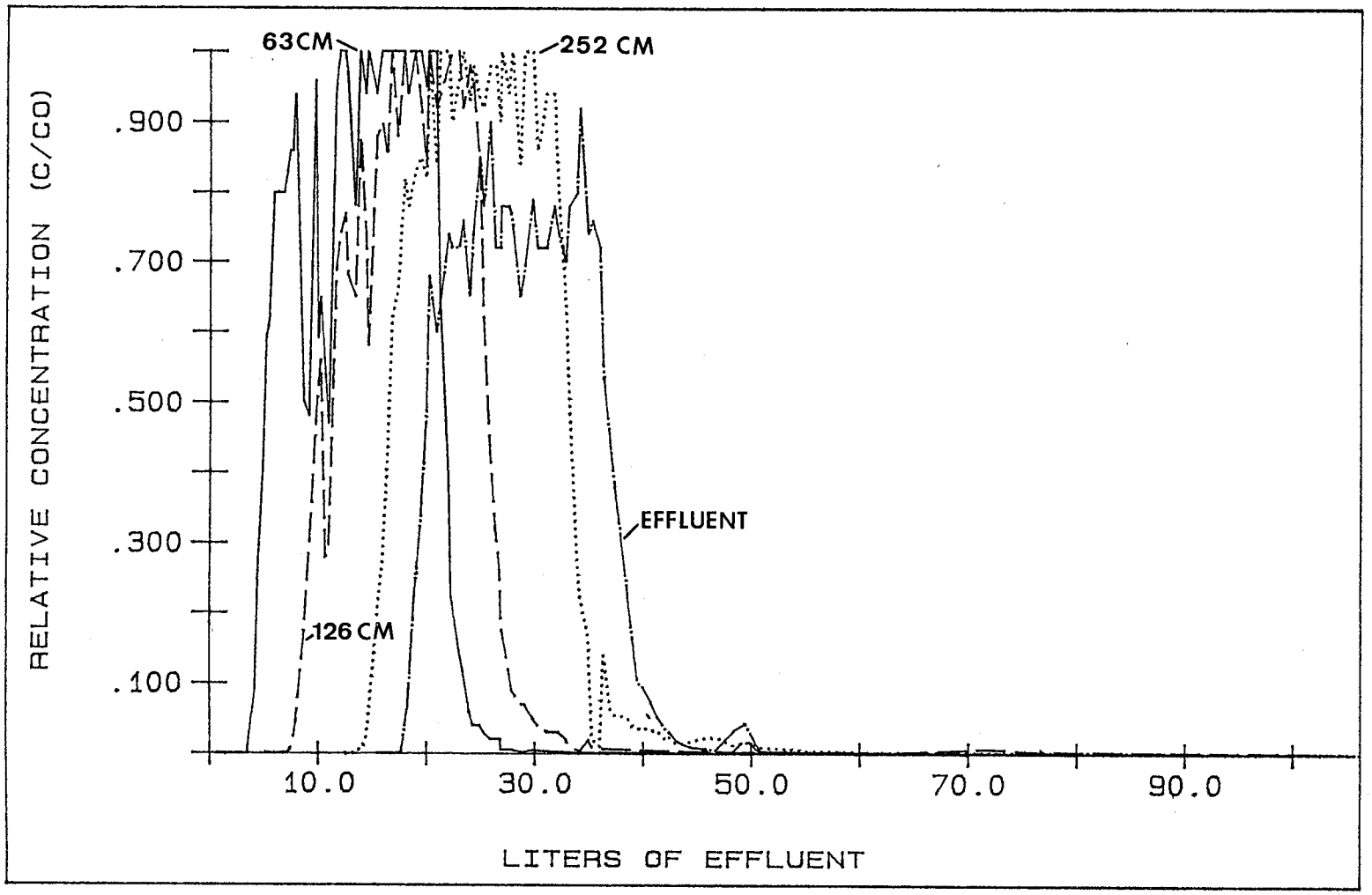

Figure 41. Relative concentration versus volume of effluent, at each sampling position.

integrated area under the BTC to the calculated area of 100% bromide mass retrieval. Thus, if all mass was conserved

$$A_i / A_c = 1.0 \tag{35}$$

where A_i is the integrated area under the BTC and A_c is the area calculated for 100% bromide mass return. Mass was conserved at the 63.0 cm, 126.0 cm, and 252.0 cm depths, but not in the effluent BTC at 330.0 cm (See Table 10).

The mass balance calculation reveals that only 94% of the bromide was discharged from the column at the effluent sampling point. As noted in the previous procedural section, water ponded on the porous plate at the base of the column, when the efficiency of the vacuum pump declined. Bromide solution leaking from an opening close to the bottom of the column, resulted in the mass return of only 94%. The zone of saturation which developed at the base of the column also created a mixing reservoir for concentrations of different times. For this reason, the bromide concentration values obtained from this curve should be viewed with caution.

TABLE 10. Mass balance of bromide, for each sampling depth.

Depth (cm)	% Mass Bromide Conserved
63.0	106
126.0	104
252.0	114
330.0	94

A comparison of pore-water velocities (q/θ) obtained from the movement of the bromide front with the experimental pore-water velocity, may indicate the extent to which the bromide traced the movement of water through the system. Average pore-water velocity is calculated from:

$$v = L/t \tag{36}$$

where L is the distance from the tracer input to the sampling point, and t is the time at which $C/C_o = 0.50$. The pore-water velocity of the bromide front was obtained for each sampling depth and listed in Table 11.

The pore-water velocities are reasonably consistent for the 126, 252, and 330 cm depths, but the shallowest depth of 63 cm exhibits the lowest velocity. This sampler was nearest the tracer input source and consequently may have been affected by pumping variability and by periods of pump shut-off, such as when volumetric pumping rates were measured. The deeper sampling depths, in contrast, may have been sufficiently distal from the source to dampen this input variability.

TABLE 11. Pore-water velocities, determined from tracer movement, and θ = 33%.

DEPTH (cm)	TIME (min) @ $C/C_o = 0.50$	V (cm/min)
63	9577.4	6.58E-03
126	12394.4	1.02E-02
252	22535.2	1.12E-02
330	27887.3	1.18E-02

The pore-water velocities of the bromide front were compared to the experimental pore-water velocity, which was calculated by dividing the input Darcian velocity (4.12E-03 cm/min) by the average water content of 33%, yielding a pore-water velocity of 1.25E-02 cm/min. The pore-water velocities for the tracer front (at each sampling depth) were only 6 to 18% lower than the experimental pore-water velocity of 1.25E-02 cm/min. The difference in velocities indicated the rate of tracer movement was slower than the rate of water movement. An inaccurate assumption of the volumetric water content during the tracer experiment could also cause a difference in pore-water velocities, but could not account for the full difference. A water content of 41% would be required to yield an experimental pore-water velocity in agreement with the averaged tracer-front velocity of 9.95E-03 cm/min. Since the porosity of the tailings was approximately 40%, a water content of 41% would have indicated a degree of saturation in excess of that observed throughout the column.

The input system may have been effective in lowering the pore-water velocity of the tracer front. The tracer was introduced at nine discrete points on the upper boundary of the column. Initially, separate tracer fronts moved down through the column, each emanating from individual injection points. At some point in the flow path these individual tracer fronts would merge, but an irregular tracer concentration front would still be present, in which zones of unequal concentration would exist radially, at the same depth. As the tracer solution moved down through the column and entered the porous cup, it became a

mixture of the higher and lower concentrations found at that depth, due to the irregularity of the front. Moreover, soil-water entered the cup from 360°. The solution below the cup, which was at a lesser concentration, lowered the overall concentration of the sample as it was drawn into the porous cup.

As transport continued, it might be expected that diffusion would smooth concentration gradients, create a more regular front, and yield tracer-front velocities closer to the experimental pore-water velocity. As seen in Table 11, the pore-water velocities of the tracer front did increase with depth and subsequently yielded values in better agreement with the experimental pore-water velocity.

The sustained vacuum used to extract the soil-water solution did not appear to be related to the lower pore-water velocity of the tracer front. If the induced suction had interrupted the flow field, decreased water contents or pressure-heads would have been observed at the time of sampling. However, as described in the flow field section of this paper, there was no evident correlation between pressure-heads (Figure 34) and sampling times or frequencies.

The curve-fitting program CFITM, as described in the short-column analysis section (p. 57), was used for the long-column analysis to determine the transport parameters. Curve-fitted BTC's, optimized for the column Peclet number, P_c (equation 18), dimensionless pulse length, T' (equation 27) and retardation factor, R (equation 5) are shown in Figures 42, 43, 44, and 45 for each column depth. Table 12 lists the parameters that were

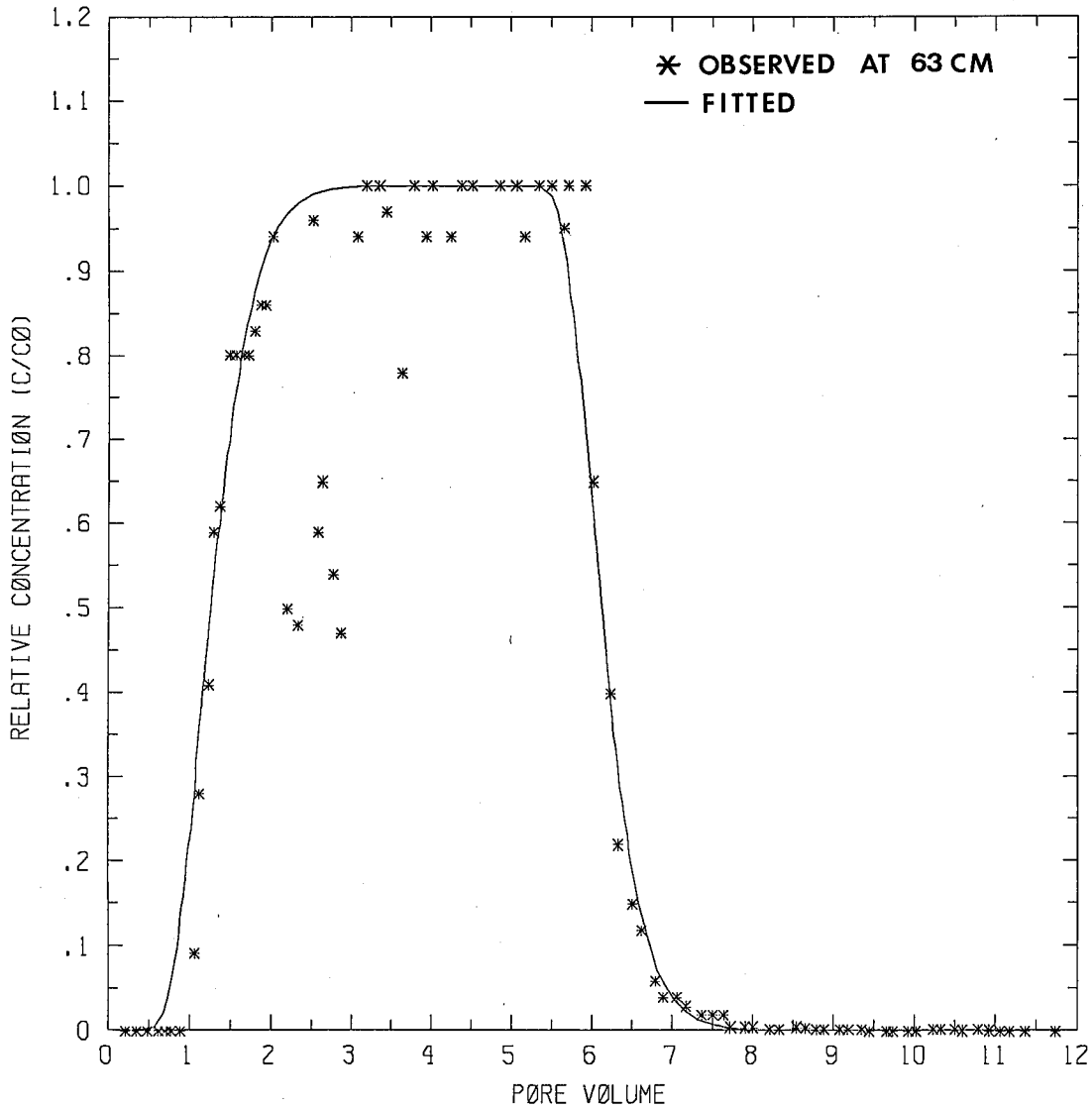

Figure 42. Observed data and CFITM curve fit for 63 cm depth.

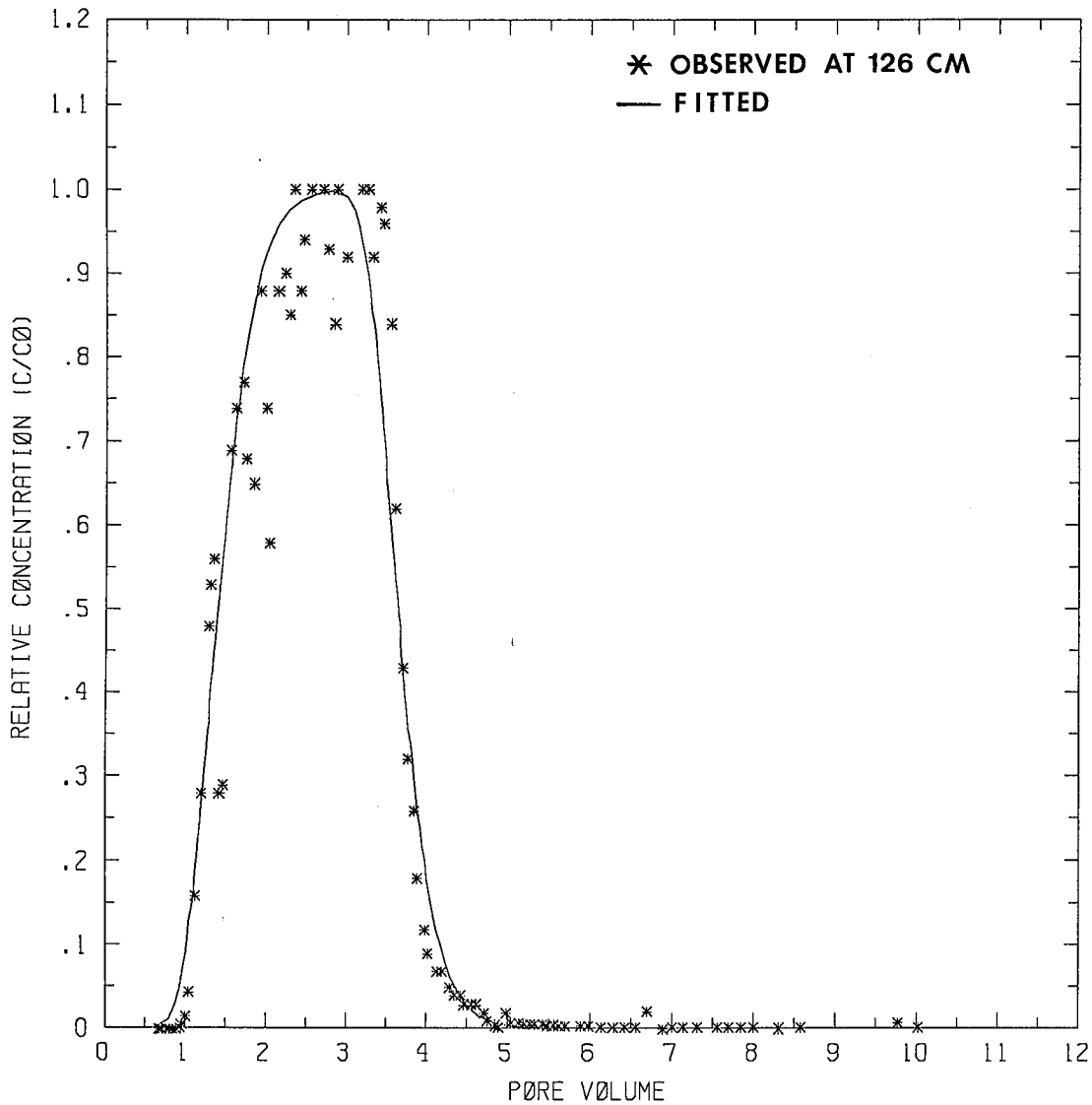

Figure 43. Observed data and CFITM curve fit for 126 cm depth.

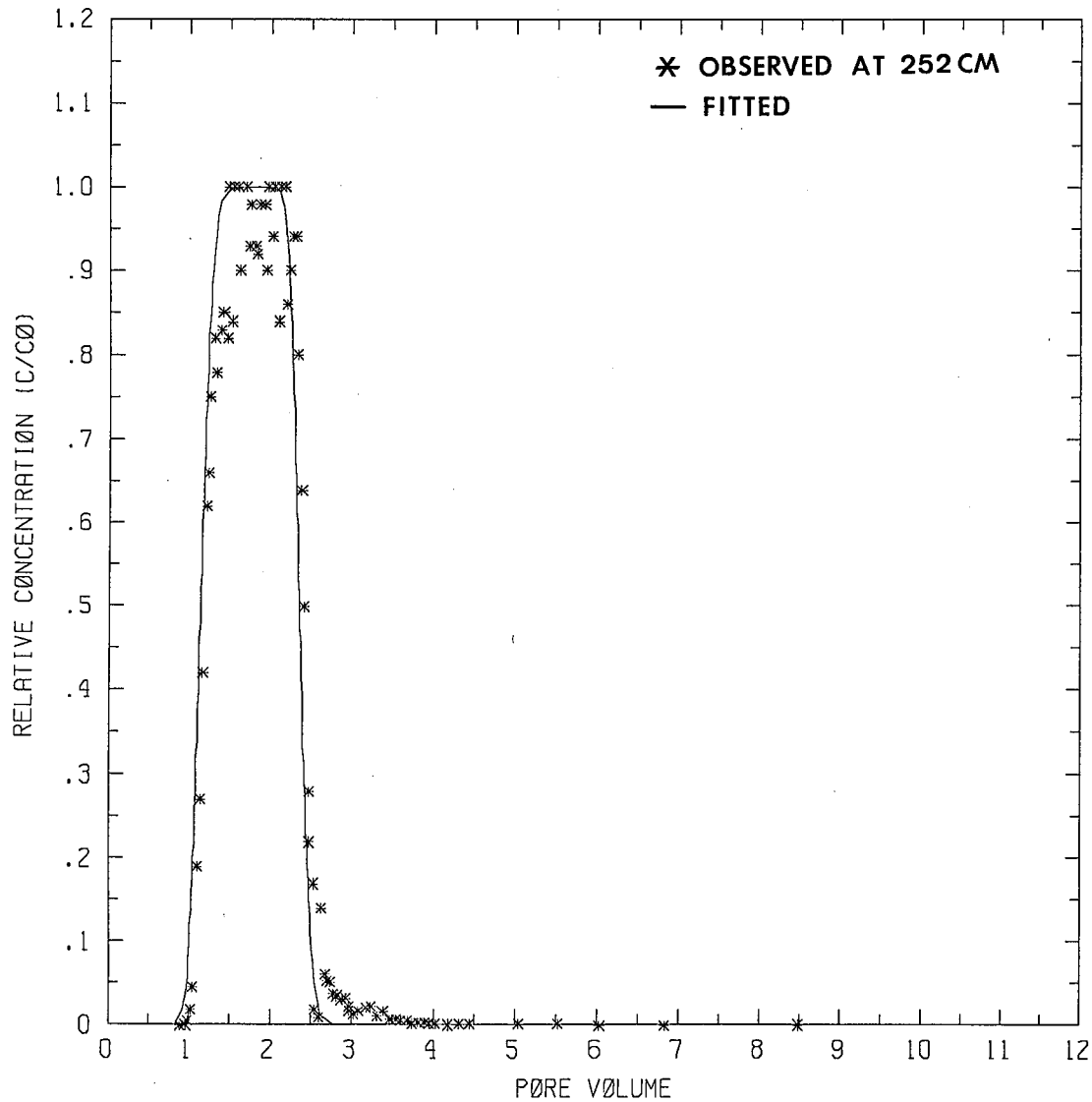

Figure 44. Observed data and CFITM curve fit for 252 cm depth.

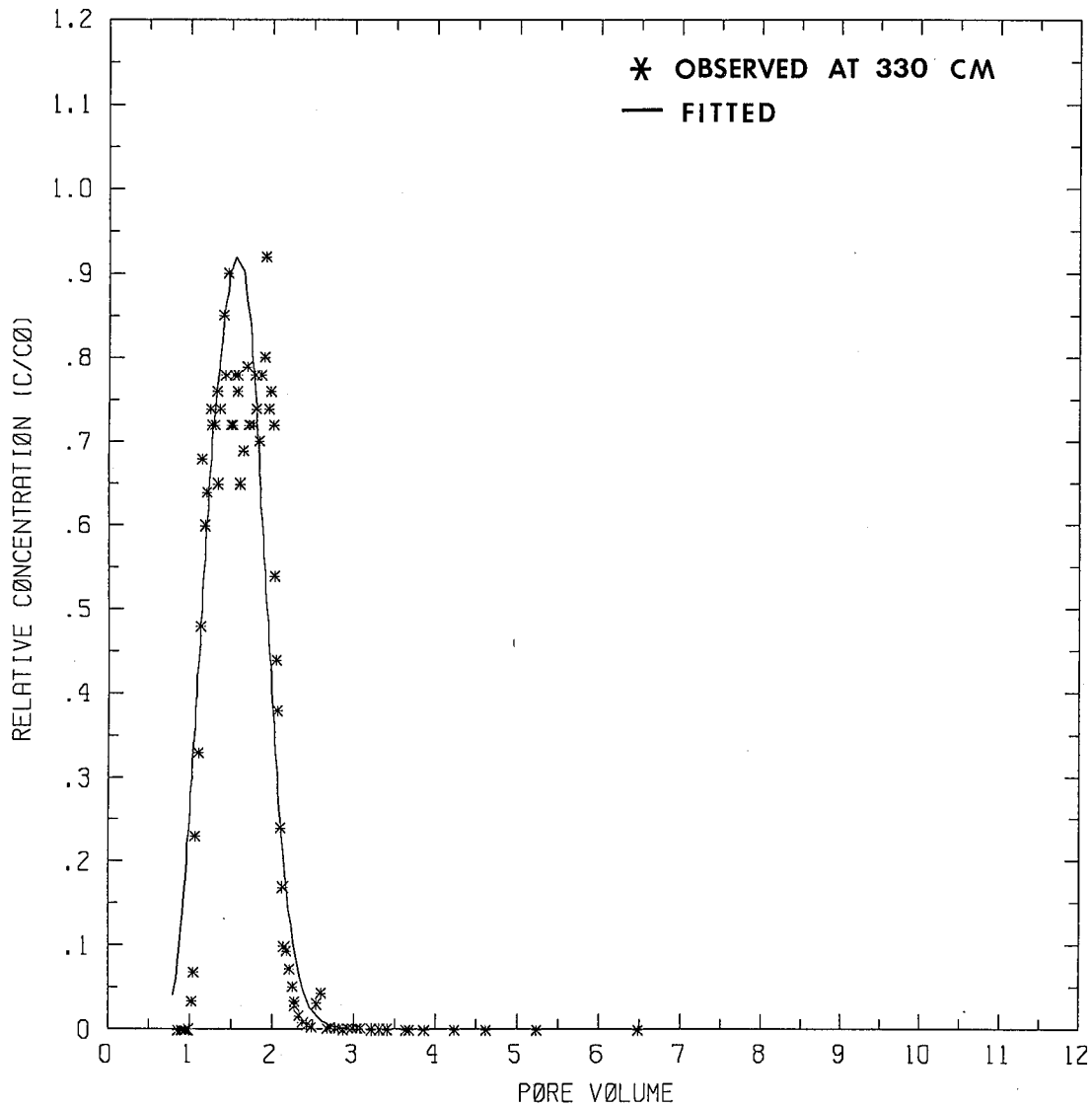

Figure 45. Observed data and CFITM curve fit for 330 cm depth (effluent).

TABLE 12. Parameters determined from CFITM analysis for column Peclet number (P_c), retardation factor (R) and dimensionless pulse length (T').

Depth (cm)	P	R	T'
63.0	20.49	1.26	4.85
126.0	30.89	1.40	2.25
252.0	214.96	1.14	1.21
330.0	48.20	1.13	0.80

obtained from the curve-fit, for each depth. The trend in T', which decreased with depth, is merely a function of the constant volume of the tracer pulse divided by an increasing depth. The computer outputs are listed in Appendix Q.

The fitted curves followed the general trend of the data, but appeared earlier than the observed data at each depth. The analytical, CFITM curves fit the BTC's better for the 63 and 126 cm depths than for the 252 and 330 cm depths.

There are several problems in the interpretation of the outflow concentration data. The mass balance of 94% for the outflow data (as calculated in a previous section) indicates the loss of tracer, which may have occurred when water and tracer leaked through the hole at the bottom of the column. However, CFITM assumes reversible chemical reactions in which the irreversible loss of tracer does not occur. Consequently, CFITM cannot reliably describe the results for the 330 cm effluent data. In addition, the saturated conditions which developed at the very

bottom of the column created a reservoir for mixing concentrations from different times. The large change in saturation (from 33% to 40%) also violated the assumption of uniform water contents needed for the CFITM analysis. For these reasons, the effluent data was not considered in the retardation factor or dispersivity analysis.

For the unsaturated, long-column experiment, an unexpected shift to the right is exhibited in each BTC for each sampling point. An ideal, conservative tracer reaches a relative concentration of 50% when one pore volume of water in the column is displaced, and yields a retardation factor of 1.0. For these experimental results (Table 12), all retardation factors, R, are greater than 1.0. The value of R may be influenced by several factors.

Adsorption can produce a R greater than 1. However, adsorption was not observed in the previous short-column experiment using bromide as a tracer in the copper mill tailings. In addition, a propogation of delayed tracer arrival with depth is not seen in the BTC's, as would be expected with a R greater than 1 due to adsorption. Figure 46 illustrates this effect. Using identical hydrodynamic dispersion coefficients and retardation factors (0.07 cm^2/min and 1.26, respectively), the BTC's in Figure 46 were generated for the 63, 126, 252, and 330 cm depths. It can be seen that the tracer arrival occurs at a greater pore volume for each progressive depth from 63 to 330 cm. The BTC's observed in the long-column solute-transport experiment (Figure 39) do not exhibit that propogation of delayed

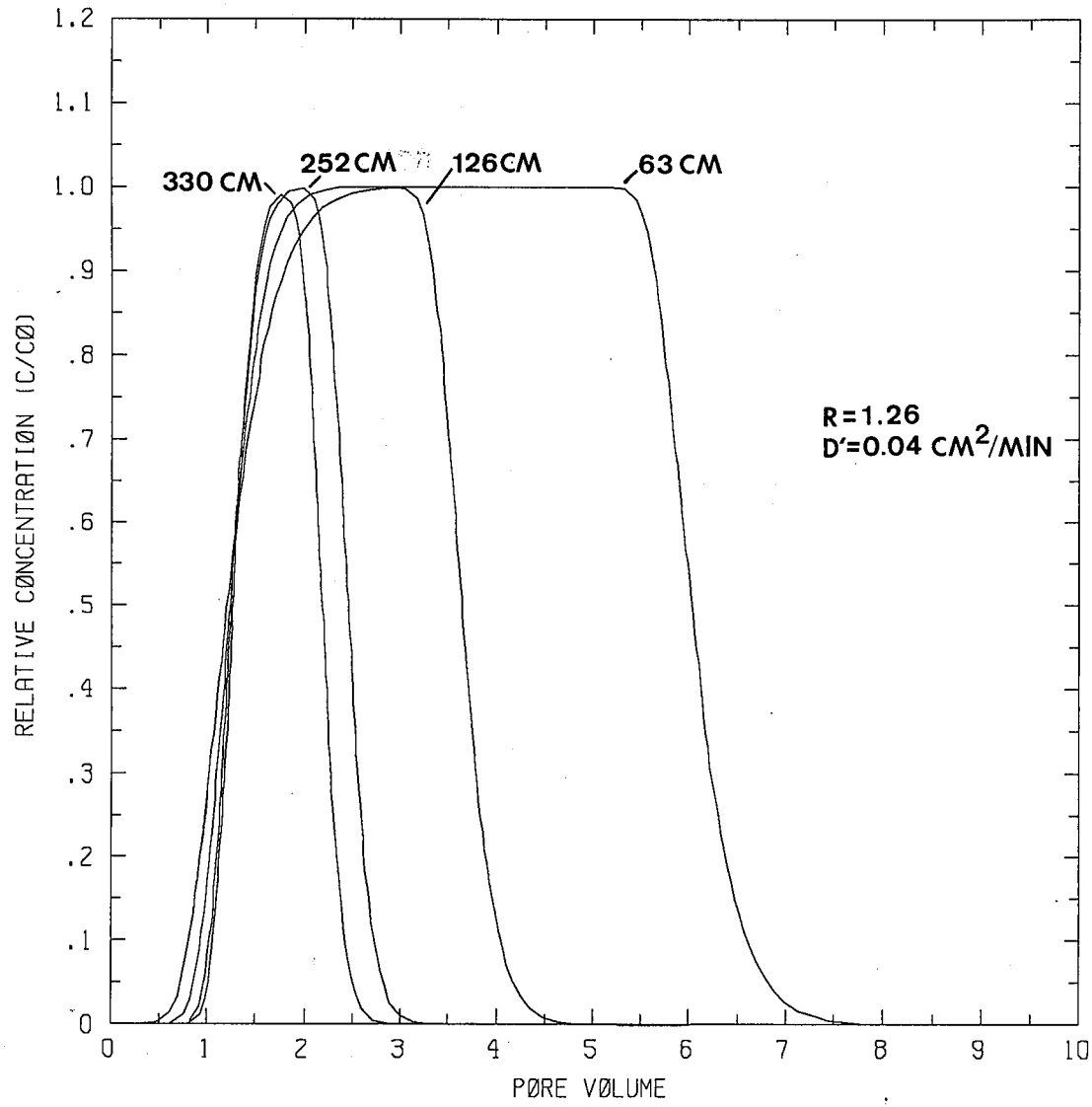

Figure 46. Analytical results showing changes in BTC's with depth, for a constant retardation factor.

tracer arrival and thus do not indicate adsorption.

The point injection of the input system, as discussed earlier in this paper, may have contributed to the delayed arrival of the tracer and the retardation of the BTC's. An irregular tracer front, as may be the case with the point injection system, could allow lower concentrations to be measured. A lowered tracer concentration for a particular pore volume would have resulted, and shifted the curve to the right.

The use of ceramic porous cups for soil-water extraction may also be a critical factor in the retardation factors results. Some soil-water is also held in the pores of the porous cups and is extracted with the sample when the vacuum is applied. Thus, the sample that is extracted does not completely represent the soil-water at that time, but rather the soil-water from two different sampling times. This mixture would occur each time sampling was initiated, and the observed tracer concentrations would be lower than the in-situ tracer concentrations. The lower concentrations would increase the retardation factor by shifting the BTC to the right of the BTC for which the retardation factor was one.

In comparison to flow and solute-transport in saturated media, the BTC for unsaturated conditions are commonly shifted to the left. For example, Nielsen and Biggar (1961), compared BTC's for unsaturated flow in 30 cm long columns at several pore velocities. A translation of the BTC to the left for slower flow velocities was observed in each case. This was in part attributed to a stagnant water phase, which did not participate in the

advective flow of water or contribute to the effluent volume measured, even though it represented a significant fraction of the pore volumes. The results of Gaudet et al. (1977), Coats and Smith (1964), and Krupp and Elrick (1968) are similar.

However, a shift of the unsaturated BTC to the left of the saturated BTC is not characteristic of these copper mill tailings, at the water contents investigated. The saturated long-column experiment with mill tailings (Lewis, 1986), exhibited a BTC which reached the 50% concentration at one pore volume. The BTC in the unsaturated (θ of 32%), short-column experiment was not displaced the left of the saturated BTC, although the first appearance of tracer in the unsaturated case was less than 0.1 pore volume earlier than the saturated flow case. Based on previous experiments at water contents similar to those of the long column, the shift of the BTC to the left and early tracer arrival may not be expected in long-column experiments in the copper tailings.

Table 13 lists the hydrodynamic dispersion coefficients and dispersivities calculated from the fitted transport parameters. The hydrodynamic dispersion coefficients, D', were calculated from the column Peclet number (equation 18), and the dispersivities, a_L, were calculated assuming molecular diffusion was not significant (equation 6). The dispersivities and dispersion coefficients did not demonstrate a clear trend with depth, nor did the dispersivities reach an asymptotic value.

In his laboratory experiment, using a tracer for saturated, radial flow, Lau et al. (1959) observed decreasing dispersivity

TABLE 13. Hydrodynamic dispersion coefficients (D') and dispersivities (a_L) determined for each sampling depth.

Depth (cm)	D' (cm_2/min)	a_L (cm)
63.0	0.04	3.1
126.0	0.05	4.1
252.0	0.01	1.2

values with increasing transport distance. He attributed the decrease to his sampling technique, which involved withdrawing pore-water solution with a hypodermic syringe at several depths. However, in the long-column experiment under investigation in this paper, the application of suction for sampling purposes did not appear to strongly influence the flow field. Even when sampling frequency was highest, pressure-heads were not responsive to the applied vacuum (Figure 34).

Gupta et al. (1973) determined hydrodynimic dispersion coefficients for 20 solute-transport experiments under unsaturated flow conditions, through a 54 cm column packed with glass beads. Uniform water contents were established for each experiment and these water contents ranged from 0.370 to 0.201. In situ tracer concentrations were measured with silver-silver chloride electrodes at 10 positions along the column length, and it was observed that the dispersion coefficients increased with

distance of transport.

Three factors were suggested by Gupta et al. (1973) which may have contributed to the observed trend in hydrodynamic dispersion coefficients with depth. The first was a variation in moisture content with depth, perhaps due to a non-uniform pressure head distribution within the porous medium. The second factor was the validity of Darcy's Law for the experiment, and the third factor was erroneous water content measurements.

Darcy's Law was valid for the pore-water velocity used in the long-column, unsaturated experiment. The measured water contents were certainly subject to experimental error such as sample compaction and water redistribution within the column during sampling. However, the values and trends observed in the water content data were well supported by the pressure-head data (see flow field section). The unsaturated flow conditions may have created zones of stagnant water which did not contribute to the advective flow and would have resulted in an effective water content which was lower than the measured water content. Although the presence of stagnant zones would have increased the hydrodynamic dispersion coefficients by increasing the seepage velocity and creating sinks for diffusion, they could not have accounted for the observed scatter in dispersivities with depth.

The non-uniformity of water content values in the column may have contributed to the variation in dispersivity with

depth. Wilson and Gelhar (1981) suggested :

> "nonuniform moisture content in space results in a stretching or contracting of a solute pulse as it propogates through the media. This effect is independent of the presence of mixing phenomenon, such as hydrodynamic dispersion."

They showed (numerically) that increasing moisture content in the direction of flow caused a contraction of the pulse, and a stretching of the pulse resulted when moisture contents decreased. The pulse contraction was measured as a smaller hydrodynamic dispersion coefficient, and the stretching of the pulse as a larger dispersion coefficient.

The dispersivities from the long-column solute-transport experiment appear to be related to the changing water contents within the column profile. In Figure 35, the water contents decreased with depth to at least 180 cm, and then increased again towards the saturated base of the column. Pressure-head data (Figure 34) exhibited a similar trend within the column profile. The lowest dispersivity value of 1.2 cm was determined at the 252 cm depth and was within the portion of the profile which contained the lowest water content and pressure-head values. The highest dispersivity value of 4.1 cm was determined at the 126 cm depth, which correlated with the higher water content and pressure-head portions of the column profile.

In contrast to the results of Wilson and Gelhar (1981), the dispersion coefficient for the mositure regime of the long-column experiment decreased with decreasing water content. However, as suggested by Wilson and Gelhar (1981) and Gupta et al. (1973),

these long-column results did indicate that water content was related to the hydrodynamic dispersion coefficient and dispersivity. The variation of water content within the column profile appeared to be the paramount factor in the variation of dispersivity with column depth.

A mean longitudinal dispersivity (a_l) of 2.8 cm was calculated by averaging the dispersivities at the 63, 126, and 252 cm depths. This mean dispersivity was compared 1) to the dispersivity from a saturated long-column experiment, 2) to the dispersivity of an unsaturated short-column experiment, and 3) to dispersivities from unsaturated solute-transport experiments found in the literature.

The saturated long-column experiment by Lewis (1986) used similar copper mill tailings (see Appendix H), and the dispersivity in the 330 cm long column was 2.2 cm. The unsaturated, long-column dispersivity of 2.8 cm was only slightly larger than the saturated dispersivity obtained for the same medium. Dispersivities from unsaturated, solute-transport laboratory experiments in the literature suggest a trend of increasing dispersivity with decreasing water content (Hildebrand and Himmelbaur, 1977; Yule and Gardner, 1978; Kirda et al., 1973; Nielsen and Biggar, 1961, 1962; Bresler and Laufer, 1974; Gupta et al., 1973; Krupp and Elrick, 1978; Gaudet et al., 1975. However, this same trend for the copper tailings cannot be concluded on the basis of this single comparison alone. In fact, these experimental results indicate that for a field-scale column and unsaturated flow conditions, the resulting dispersivity using

the classical hydrodynamic dispersion equation can be very similar to that of the saturated case.

A comparison of dispersivities was made between the unsaturated, short-column experiment and the unsaturated, long-column experiment. The short-column experiment was run at a water content similar to the long-column experiment with a water content of 33% for the long column, and a θ of 32% for the short column. The dispersivity obtained from the short-column experiment, using a bromide tracer and distilled water eluent, was 0.47 cm. The mean dispersivity of 2.8 cm from the long-column experiment was much larger, but by less than an order of magnitude.

The different packing processes involved in the column experiments may have contributed to the larger dispersivity for the long column. The short column was packed by vibrating the column as the tailings were introduced to obtain the specified density. In contrast, the long column was packed in 5 cm increments, and each lift should have been homogeneous and identical to all other lifts. However, stratification appeared to be inherent in this packing process. If the stratification caused heterogeneity of a larger-scale than microscopic pore-size variations, a larger dispersivity for the long column than for the small column may have been the result.

The result of the large-scale solute-transport experiment conducted under unsaturated flow conditions was compared to other experiments conducted at varying vertical scales, water contents, and with different porous mediums (Table 8, Figure 47). Three

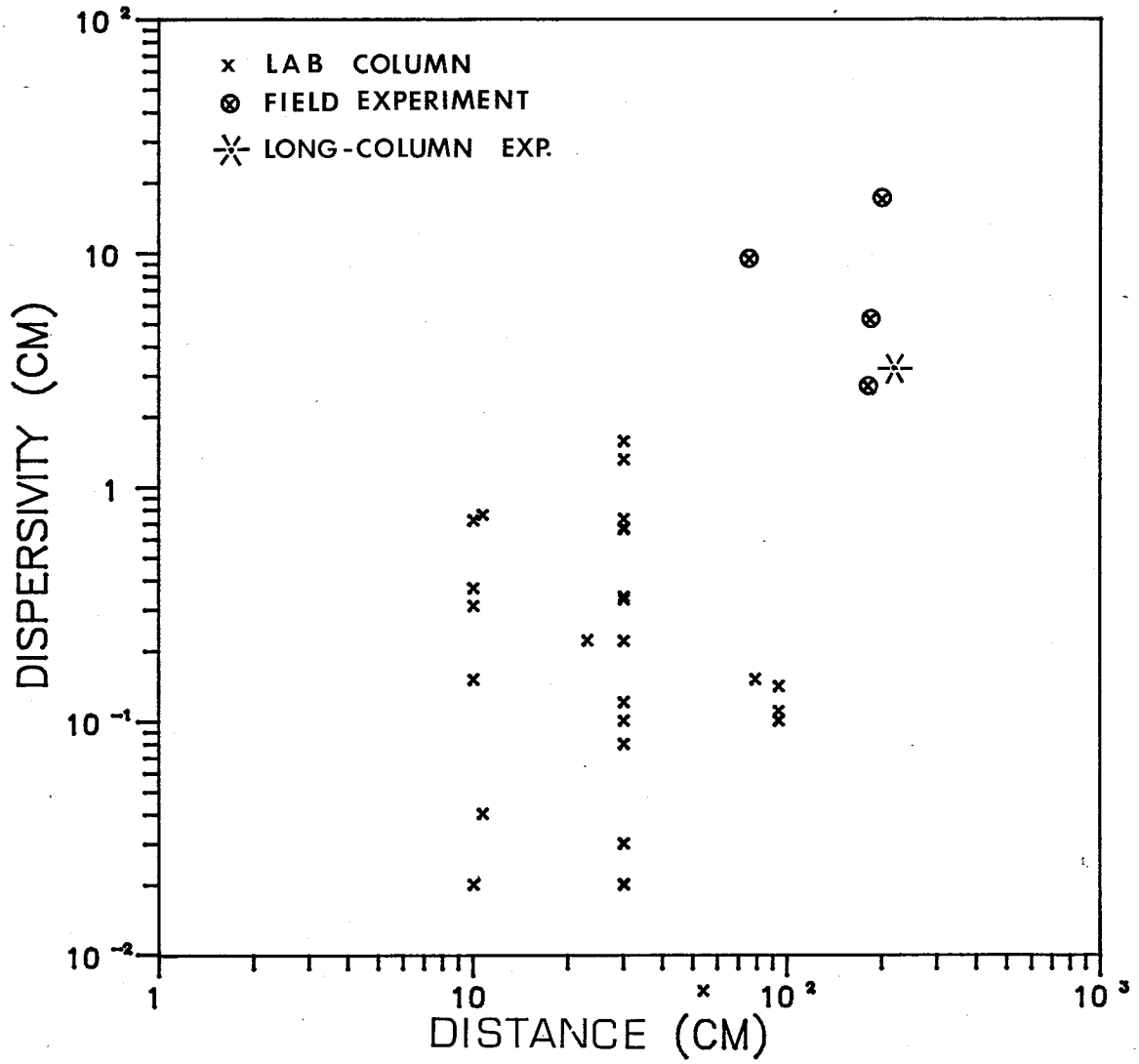

Figure 47. Dispersivity from long-column, unsaturated, solute-transport experiment compared with dispersivities determined from literature cited in Table 8.

of the field experiments were conducted at smaller vertical scales than the long-column experiment (Van De Pol, et al., 1977; Biggar and Nielsen, 1976; Kies, 1981) but yielded higher dispersivities than the long-column laboratory experiment. The field experiments were conducted in-situ in heterogeneous field soils, with naturally occurring stratification and hydraulic conductivity differences. The heterogeneity of the field medium appeared to influence the dispersivity to a greater degree than the scale of the experiment.

When compared to the cited laboratory experiments (Table 8) conducted with homogeneous media, the long-column, unsaturated laboratory experiment yielded the largest dispersivity. The difference in dispersivities between the column experiments in Table 8 and the long-column experiment was concluded to be a function of the heterogeneity of the long-column porous medium. The stratification inherent in the long-column packing procedure (packed in lifts) resulted in a heterogeneity and dispersivity of a larger scale than from the more homogeneously-packed small columns.

The 'scale-dependence' of dispersivity appears to be closely related to the scale of the heterogeneities present. Dispersion in the small laboratory column with a homogeneous medium is due to fluid velocity variations at the pore scale whereas dispersion at a field scale is predominantly due to velocity variations caused by stratification and hydraulic conductivity differences. As shown by this long-column experiment, the scale up of an experiment an order of magnitude from a

small column (30 cm in length) to a long column (over 300 cm in length) involved introducing heterogeneities caused by packing differences, although identical porous media were used. Increasing the column length ten times resulted in a increase in the dispersivity by six times amd the difference was concluded to be most strongly influenced by the heterogenieties within the long column.

V. SUMMARY AND CONCLUSIONS

Movement of solutes which originate and travel through mill tailing impoundments pose a potential contaminant threat to both surface and groundwater systems. Even in a semi-arid climate, net downward movement of infiltrating precipitation can occur (Lewis, 1984). Unsaturated conditions commonly exist in abandoned mill tailing impoundments in such climates, which may complicate transport prediction. In this investigation a bromide tracer was used to track solute movement through an unsaturated, copper mill-tailings medium, to obtain a transport parameter, dispersivity.

Two 30 cm laboratory columns, packed with copper mill tailings were used for the solute-transport investigation under unsaturated conditions. A dispersivity unique to that medium and water content was thus obtained, at a small scale.

A larger scale (330 cm) solute transport investigation was then undertaken, again with copper mill tailings as a porous medium and under unsaturated conditions. From this experiment a field-scale dispersivity was obtained for the mill tailings, specific to the water content of the experimental run; and the dependence of dispersivity on the scale of the experiment was also investigated.

From the above experiments, the following conclusions are drawn:

1.) Bromide is a good tracer for the copper mill tailings. Corrections for complexation must be made when high

metal ionic concentrations exist in the soil solution.

2.) For a large-scale, unsaturated experiment, the dispersivity for 83% of saturation can be similar to the saturated dispersivity, using the classical advection-dispersion equation.

3.) The mean dispersivity for the the long-column experiment under unsaturated flow conditions (3.1 cm) was slightly larger than that for the saturated case (2.2 cm). However, due to the lack of data at other water contents, no general trend was recognized for the relationship between saturated and unsaturated dispersivities within the same medium.

4.) The results of the field-scale column experiment under unsaturated flow conditions suggest dispersivity is a function of water content.

5.) Stratification of the porous medium (as in packing) may cause heterogeneity of a larger scale and significance than the microscopic pore-scale variations, leading to a larger dispersivity value.

6.) For a homogeneous medium, dispersivity does not always increase with time or distance traveled, after the initial developmental period is over.

VI. RECOMMENDATIONS FOR FUTURE WORK

In laboratory columns, undisturbed porous media have been found to yield higher dispersivity values than disturbed porous media (Cassel, 1974). It would be of value to conduct an in-situ solute-transport experiment at the mill tailings impoundment. The dispersivity value thus obtained would encompass heterogeneities not dealt with in the laboratory, and be useful for predictive modeling purposes.

The mill tailings have proved to be a sensitive medium in which to conduct solute-transport experiments, due to the chemical reactivity of the tailings. A less reactive medium, such as the Sevilleta sand which has been well-characterized (McCord, 1986; Byers and Stephens, 1983) would be a more stable, predictable, and convenient medium with which to conduct further experiments designed to examine solute-transport in unsaturated soils. Further long-column experiments, using a less reactive medium, to investigate the relationship between water content and dispersivity and the effect of heterogeneity of the porous medium on dispersivity would augment the sparse research of this nature under unsaturated flow conditions.

Some procedural and equipment changes which would improve the reliability and efficiency of such experiments, include:
1.) the use of in-situ tracer sampling equipment to preclude the sampling problems encountered in this investigation, 2.) the use of a bottom porous plate with a higher hydraulic conductivity than the one used in this investigation, in an effort to prevent

saturation at the exit boundary, and 3.) the use of a gamma-ray instrument for in-situ measurement of water content.

REFERENCES

Anderson, M.P., 1983. Movement of contaminants of groundwater, Groundwater transport: Advection and dispersion, in Groundwater Contamination: Product of a Technological Society. National Research Council, Geophysical Study, National Academy Press, Washington, D.C., 37-45.

Baer, J., 1979. Hydraulics of Groundwater. McGraw-Hill, Inc., New York, NY, 569pp.

Biggar, J.W., and Nielsen, D.R., 1962. Miscible displacement: II. Behavior of tracers. Soil Science Society of America Proceedings, 26, 125-128.

Biggar, J.W., and Nielsen, D.R., 1976. Spatial variability of the leaching characteristics of a field soil. Water Resources Research, 12, 78-84.

Bresler, E., and Dagan, G., 1979. Solute dispersion in unsaturated heterogeneous soil at field scale: II. Applications. Soil Science Society of America Journal, 43, 467-472.

Bresler, E., and Laufer,A., 1974. Anion exclusion and coupling effects in nonsteady transport through unsaturated soils: II. Laboratory and numerical experiments. Soil Science Society of America Proceedings, 38(2), 213-222.

Byers, E. and Stephens, D.B., 1983. Statistical and stochastic analyses of hydraulic conductivity and particle size in a fluvial sand, Soil Science Society of America Proc., 47(6), 1072-1080.

Coats, K.H., and Smith, B.D., 1964. Dead-end pore volume and dispersion in porous media, Society of Petroleum Engineers Journal, 4, 73-84.

Dagan, G., 1982. Stochastic modeling of ground water by unconditional and conditional probabilities, 2. The solute transport. Water Resources Research, 18, 835-848.

Davis, S.N., Thompson, G.M., Bentley, H.W., and Stiles, G., 1980. Ground-water tracers - a short review. Ground Water, 18(1), 14-23.

De Smedt, F., and Wierenga, P.J., 1979. Mass transfer in porous media with immobile water. Journal of Hydrology, 41, 59-67.

De Smedt, F., and Wierenga, P.J., 1984. Solute transfer through columns of glass beads. Water Resources Research, 20, 225-232.

Elrick, D.E., Erh, K.T., and Krupp, H.K., 1966. Applications of miscible displacement techniques to soils. Water Resources Research, 2, 717-724.

Gaudet, J.P., Jegat, H., Vachaud, G., and Wierenga, P.J., 1977. Solute transfer, with exchange between mobile and stagnant water, through unsaturated sand. Soil Science Society of America Journal, 41(4), 665-671.

Gelhar, L.W., and Axness, C.L., 1981. Stochastic analysis of macro-dispersion in three-dimensionally heterogeneous aquifers, Geophysical Research Center, Hydrology Research Program, Rep. No. H8, NMIMT, Socorro, NM, 140pp.

Gelhar, L.W., Gutjahr, A.L., and Naff, R.L., 1979. Stochastic analysis of macrodispersion in a stratified aquifer. Water Resources Research, 15, 1387-1397.

Gelhar, L.W., Mantoglou, A., Welty, C., and Rehfeldt, K.R., 1985. A review of field-scale physical solute transport processes in saturated and unsaturated porous media. Electric Power Research, Institute Report EA-4190, Palo Alto, CA.

Gupta, R.K., Millington, R.J., and Klute, A., 1973. Hydrodynamic dispersion in unsaturated porous media II. The stagnant zone concept and the dispersion coefficient. Journal of Indian Society of Soil Science, 21(2), 121-128.

Hildebrand, M.A., and Himmelbau, D.M., 1977. Transport of nitrate ion in unsteady unsaturated flow in porous media, A.I.Ch. Engineering Journal, 23, 326-335.

Hillel, D., 1980. Fundamentals of Soil Physics. Academic Press, New York, 413pp.

Kies, B., 1982. Solute transport in unsaturated field soil and in groundwater. Ph.D. dissertation, Department of Agronomy, New Mexico State University, Las Cruces, New Mexico.

Kirda, C., Nielsen, D.R., and Biggar, J.W., 1973. Simultaneous transport of chloride and water during infiltration. Soil Science Society of America Proceedings, 37, 339-345.

Klute, A., and Heermann, D.F., 1978. Water movement in uranium mill tailings profiles. U.S. Environmental Protection Agency Report ORP/LU788: National Technical Information Service Aquisition PB-291688. 98pp.

Krupp, H.K., and Elrick, D.E., 1968. Miscible displacement in an unsaturated glass bead medium, Water Resources Research, 4, 809-815.

Lapidus, L., and Amundson, N.R., 1952. Mathematics of adsorption in beds IV. The effect of longitudinal diffusion in ion-exchange chromatographic columns. J. Physical Chemistry, 56, 984-988.

Larson, M.B., 1984. A comparison of empirical/theoretical, laboratory and field techniques in evaluating unsaturated hydraulic properties of mill tailings. Unpublished Independent Study Paper, NMIMT, Socorro, NM, 183pp.

Lau, L.K., Kaufmann, W.J., and Todd, D.K., 1959. Dispersion of a water tracer in radial laminar flow through homogeneous porous media. Hydraulic Laboratory and Sanitary Engineering Research Laboratory, Progress Report, Canal Seepage, Univ. of California, Berkeley, 78pp.

Lewis, G., 1986. An analysis of infiltration and solute transport through abandoned mill tailings profiles. Unpublished Independent Study Paper, NMIMT, Socorro, MN, 262pp.

Lindstrom, F.T., Hague, R., Freed, V.H., and Boersma, L., 1967. Theory on the movement of some herbicides in soils: linear diffusion and convection of chemicals in soils. Environ. Sci. Technol., 1, 561-565.

Lloyd, J.W., and Heathcote, J.A., 1985. Natural Inorganic Hydrogeochemistry in Relation to Groundwater. Oxford University Press, New York, 296pp.

Mansell, R.S., Selim, H.M., Kanchanusut, P, Davidson, J.M., and Fiskell, J.G.A., 1977. Experimental and simulated transport of phosphorous through sandy soils. Water Resources Research, 13, 189-194.

McCord, J.T., 1986. Topographic controls on ground-water recharge. Unpublished Independent Study Paper, NMIMT, Socorro, NM, 89pp.

Mercado, A., 1967. The spreading pattern of injected water in a permeability stratified aquifer. Proceedings of Int. Assoc. Science Hydrology Symposium, Publ. No. 72, 23-26, Haifa.

Nielsen, D.R., and Biggar, J.W., 1961. Miscible displacement in soils: I. Experimental information, 25, 1-4.

Nielsen, D.R., and Biggar, J.W., 1962. Miscible displacement: III. Theoretical considerations. Soil Science Society Proceedings, 27, 216-221.

Parker, J.C., and van Genuchten, M.Th., 1984. Determining transport parameters from laboratory and field tracer experiments. Virginia Agricultural Experiment Station, Bulletin 84-3. 96p.

Pickens, J.F., and Grisak, G.E., 1981. Scale-dependent dispersion in a stratified aquifer, Water Resources Research, 17, 1191-1212.

Sauty, J.P., 1980. An analysis of hydrodispersive transfer in aquifers. Water Resources Research, 16(1), 145-158.

Saxena, S.K., Boersma, L, Lindstrom, F.T., and Young, J.L., 1974. Effect of pore-size on diffusion coefficients in porous media. Soil Acience, 117, 80-86.

Schwartz, F.W., 1977. Macroscopic dispersion in porous media: the controlling factors. Water Resources Research, 13(4), 743-752.

Smith, L., and Schwartz, F.W., 1980. Mass transport, 1, A stochastic analysis of macroscopic dispersion, Water Resources Research, 16, 303-313.

Smith, L., and Schwartz, F.W., 1981. Mass transport, 3, Role of hydraulic conductivity data in prediction. Water Resources Research, 17, 1463-1479.

Sudicky, E.A., 1983. An advection-diffusion theory of contaminant transport for stratified porous media. Ph. D. dissertation, Univ. of Waterloo, Waterloo, Ontario, Canada. 203pp.

Van de Pol, R.M., Wierenga, P.J., and Nielsen, D.R., 1977. Solute movement in a field soil. Soil Science Society of America Journal, 41, 10-13.

van Genuchten, M.Th., 1980. Determining transport parameters from solute displacement experiments. Research Report 118, USDA-SEA Salinity Lab, Riverside, CA. 37pp.

van Genuchten, M.Th., and Parker, J.C., 1984. Boundary conditions for displacement experiments through short laboratory soil columns. Soil Science Society of America Journal, 48, 703-708.

van Genuchten, M.Th., and Wierenga, P.J., 1977. Mass transfer studies in sorbing porous media, 2, Experimental evaluation with tritium (^3H_2O). Soil Science Society of America Journal, 41, 272-278.

van Genuchten, M.Th., and Wierenga, P.J., 1986. Determination of solute dispersion coefficients and retardation factors. In Press.

van Genuchten, M.Th., Wierenga, P.J., and O'Connor, G.A., 1977. Mass transfer studies in sorbing porous media, 3, Experimental evaluation with 2,4,5-T. Soil Science Society of America Proceedings, 41, 278-285.

Warrick, A.W., and Amoozegar-Fard A., 1977. Soil water regimes near porous cup water samplers. Water Resources Research, 13(1), 203-207.

Warrick, A.W., Biggar, J.W., and Nielsen, D.R., 1971. Simultaneous solute and water transfer for an unsaturated soil. Water Resources Research, 7(5), 1216-1225.

Wilson, J.L., 1985. Class handout. HYD 565, Groundwater Contamination Class, NMIMT, Socorro, NM.

Wilson, J.L., and Gelhar, L.W., 1974. Dispersive mixing in a partially saturated porous medium. Tech. Report 191, Ralph M. Parsons Laboratory for Water Resources and Hydrodynamics, Mass. Institute of Technology, Cambridge, Mass.

Wilson, J.L., and Gelhar, L.W., 1981. Analysis of longitudinal dispersion in unsaturated flow, 1, The analytical method. Water Resources Research, 17, 122-130.

Yule, D.F., and Gardner, W.R., 1978. Longitudinal and transverse dispersion coefficients in unsaturated Plainfield sand. Water Resources Research, 14, 582-588.

APPENDIX A.

ADSORPTION

Ion exchange is the replacement of one ion for another at the solid-solution interface. Adsorption refers to the process of accepting an ion at that surface and does not refer to the replacement of one ion for another. Adsorption and ion exchange describe surface phenomena. Porous media such as clays are often involved because of their large surface area to mass ratios. The specific area of clay minerals is on the order of 10^3 m^2/g in contrast to a clean sand, which can have a specific area of 10^{-3} m^2/g (Lloyd and Heathcote, 1985). When the effective diameter of a particle becomes small enough (as with most clays), surface effects become significant.

Clay minerals develop surface charges as a result of ionic substitutions within the crystal lattice (isomorphous replacement), and the unsatisfied valencies that exist on the silicate tetrahedron surfaces. The isomorphous replacement (such as Al^{3+} for Si^{4+}) results in a permanent negative charge to be satisfied. The charges that result from unsatisfied valencies at the surface are subject to change, depending on the PH of the solution. In alkaline solutions, the hydrogen atom (H+) tends to remain in solution, yielding a negative charge at the solid surface. In an acid solution,the hydrogen atoms move to the oxide sites, resulting in positive charges at the surface. The charge will be zero, at some intermediate pH, and this is called the zero point of charge. Each clay type may have a different zero point of charge, and can act differently at an equaivalent

pH.

Characteristics such as ionic radius and valence influence ionic preference for adsorption and the tightness of the molecular bonding that occurs. Generally, ions with a smaller hydrated radius and larger valence are adsorbed preferentially and held more tightly to the surface. However, other considerations such as ionic concentrations within the solution and the amount of adsorbed ions on the soil surface prior to introduction of the solution will have an effect. As a means of quantification, the cation exchange/adsorption capacity (CEC) can be measured for a specific material under chemically neutral conditions. This is a measure of the total number of cation charges available for exchange or adsorption.

As a means of quantification, the cation exchange/adsorption capacity (CEC) can be measured for a specific material, under chemically neutral conditons. This is a measure of the total number of cation charges available for exchange/adsorption.

Appendix B.

Derivation of the Advection-Dispersion Equation

The advection-dispersion equation is used to describe the solute-transport process in a porous medium. The derivation of the equation is based on the law of conservation of mass and assumes a homogeneous and isotropic porous medium. Steady-state, uniform flow conditions exist and Darcy's law applies. Incompressibility of the medium and fluid is also assumed and there are no sources or sinks.

Figure 1 represents an elemental volume of the porous medium, with dimensions Δx, Δy, and Δz. The pore-water velocity, v, is used to describe the advective rate of transport of the solute. The Darcian velocity through a surface perpendicular to the flow direction is q, or θv. Microscopic velocity varations, which deviate from advection, are represented by v^*, and the corresponding Darcian velocity is θv^*. The concentration of solute, C, is the mass per unit volume of solution and the mass flux is the mass of solute crossing a unit cross-sectional area per unit time. The advective and dispersive mass fluxes, for the x direction, are

$$\text{advective mass flux} = \theta C v \qquad (B1)$$

$$\text{dispersive mass flux} = \theta C v^* \qquad (B2)$$

As presented in an earlier section, the dispersive mass flux due to mechanical dispersion was defined analogous to Fick's law,

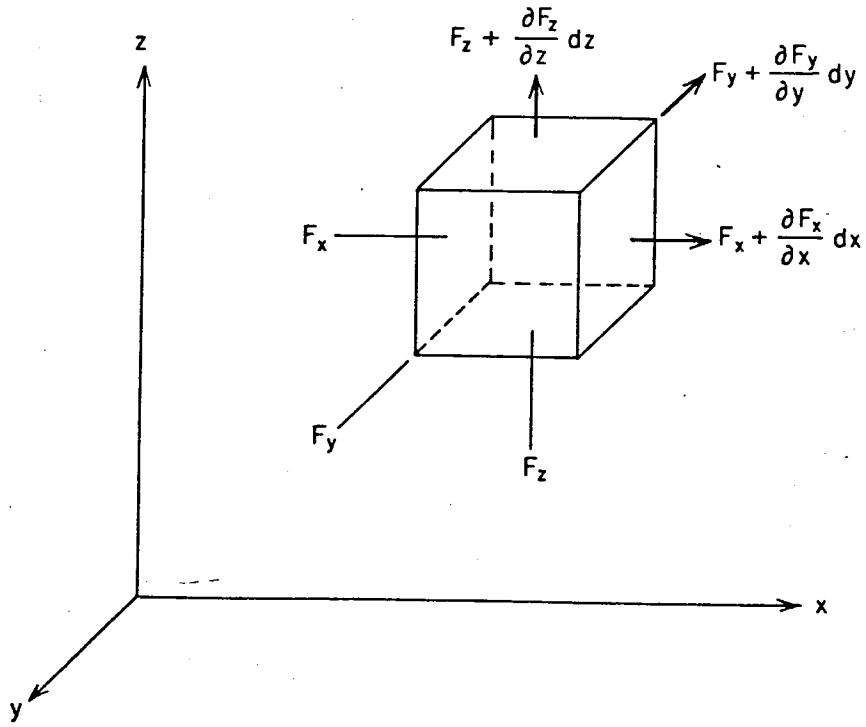

Figure 48. Mass balance in a cubic element.

such that

$$J_h = -\theta D_h \frac{\partial C}{\partial x} \tag{B3}$$

The rate of diffusion of a solute in a bulk medium,

$$J_d = -\theta D^* \frac{\partial C}{\partial x} \tag{B4}$$

can be added to the dispersive flux, to yield

$$\begin{aligned} J_h + J_d &= -\theta (D_h + D^*) \frac{\partial C}{\partial x} \\ J_h + J_d &= -\theta (D_x') \frac{\partial C}{\partial x} \end{aligned} \tag{B5}$$

where D'_x is the summed hydrodynamic dispersion coefficient in the x direction of flow. Since the dispersive mass flux was previously defined by (B2), it follows that

$$\theta C V_x^* = -\theta (D_x') \frac{\partial C}{\partial x} \tag{B6}$$

The total mass flux in the x direction, F_x, is the sum of the advective and dispersive fluxes:

$$F_x = \theta (C V_x + C V_x^*) \tag{B7}$$

Substituting in for the dispersive flux,

$$F_x = \theta \left(C V_x - D_x' \frac{\partial C}{\partial x} \right) \tag{B8}$$

The negative sign indicates the contaminant is moving towards the lower concentration zone. In a similar fashion, the dispersive fluxes for the y and z direction are

$$F_y = \theta \left(C V_y - D_y' \frac{\partial C}{\partial y} \right) \tag{B9}$$

and

$$F_z = \theta\left(CV_z - D_z' \frac{\partial C}{\partial z}\right) \tag{B10}$$

The mass flux across surface A is F($\Delta x \Delta z$). The exit flux, opposite surface A would equal the mass flux across A, plus any changes in mass flux as the solute moves through the elemental volume, $\frac{\partial F_y}{\partial y} \Delta y \Delta x \Delta z$. A similar analysis is applied to obtain the net solute amount in the x direction, $\frac{\partial F_x}{\partial x} \Delta x \Delta y \Delta z$, and the z direction, $\frac{\partial F_z}{\partial z} \Delta z \Delta x \Delta y$. The total difference between the exit and entrance mass fluxes is then

$$\left(\frac{\partial F_x}{\partial x} + \frac{\partial F_y}{\partial y} + \frac{\partial F_z}{\partial z}\right) \Delta x \Delta y \Delta z \tag{B11}$$

which represents the dissolved solute which accumulated in the elemental volume. Continuity requires that this amount equal the rate of mass change in the elemental volume,

$$-\theta \frac{\partial C}{\partial t} \Delta x \Delta y \Delta z \tag{B12}$$

The complete conservation of mass expression is

$$\frac{\partial F_x}{\partial x} + \frac{\partial F_y}{\partial y} + \frac{\partial F_z}{\partial z} = -\theta \frac{\partial C}{\partial t} \tag{B13}$$

Substitution of (B8), (B9), and (B10) into the conservation of mass expression, yields

$$\frac{\partial}{\partial x}\left[\theta C V_x - \theta D' \frac{\partial C}{\partial x}\right] + \frac{\partial}{\partial y}\left[\theta C V_y - \theta D_y' \frac{\partial C}{\partial y}\right] + \frac{\partial}{\partial z}\left[\theta C V_z - \theta D_z' \frac{\partial C}{\partial z}\right] = -\theta \frac{\partial C}{\partial t} \tag{B14}$$

Water content is assumed uniform and can be taken out of the derivative, and with simplification,

$$\left[\frac{\partial}{\partial x}\left(D_x' \frac{\partial C}{\partial x}\right) + \frac{\partial}{\partial y}\left(D_y' \frac{\partial C}{\partial y}\right) + \frac{\partial}{\partial z}\left(D_z' \frac{\partial C}{\partial z}\right)\right] - \left[\frac{\partial}{\partial x} C V_x + \frac{\partial}{\partial y} C V_y + \frac{\partial}{\partial z} C V_z\right] = \frac{\partial C}{\partial t} \tag{B15}$$

The homogeneous medium and steady-state conditions assumed inply v does not vary with space or time, D'_x, D'_y, and D'_z do not vary in space, and can be taken out of the derivative,

$$\left[D_x' \frac{\partial^2 C}{\partial x^2} + D_y' \frac{\partial^2 C}{\partial y^2} + D_z' \frac{\partial^2 C}{\partial z^2}\right] - \left[V_x \frac{\partial C}{\partial x} + V_y \frac{\partial C}{\partial y} + V_z \frac{\partial C}{\partial z}\right] = \frac{\partial C}{\partial t} \qquad (B16)$$

This is the advective-dispersive equation for three-dimensional flow, with the above assumptions of a honmogeneous, isostropic medium, steady-state flow and no sources or sinks. For the one-dimensional case, the equation becomes (Freeze and Cherry, 1979):

$$D_x' \frac{\partial^2 C}{\partial x^2} - V_x \frac{\partial C}{\partial x} = \frac{\partial C}{\partial t} \qquad (B17)$$

which is used to describe solute transport in one-dimensional laboratory experiments.

In the previous equation, the advection-dispersion equation contains no sources or sinks. Ion-exchange and subsequent BTC delay can be included in the advection-dispersion equation through the use of the retardation factor, in the following manner (Freeze and Cherry, 1979).

The rate at which the constituent is adsorbed is $\frac{\partial S}{\partial t}$, and the change in concentration in the fluid caused by adsorption or desorption is $\frac{\rho_b}{\theta} \frac{\partial S}{\partial t}$, where S is the mass of the chemical constituent adsorbed on the solid part of tthe porous medium per unit mass of solids. The amount of solute adsorbed by the medium is usually a function of the solute concentration in solution,

S = f(C), so that

$$\frac{\partial S}{\partial t} = -\left[\frac{\partial S}{\partial C} \cdot \frac{\partial C}{\partial t}\right] \tag{B18}$$

$$\frac{\rho_b}{\theta}\frac{\partial S}{\partial t} = -\left[\frac{\rho_b}{\theta}\frac{\partial S}{\partial C} \cdot \frac{\partial C}{\partial t}\right] \tag{B19}$$

The right-hand side of equation (B19) is included as a sink in the advection-dispersion equation,

$$D'\frac{\partial^2 C}{\partial x^2} - V\frac{\partial C}{\partial x} - \left[\frac{\rho_b}{\theta}\frac{\partial S}{\partial C} \cdot \frac{\partial C}{\partial t}\right] = \frac{\partial C}{\partial t} \tag{B20}$$

Moving the adsorption term to the left-hand side, and simplifying

$$D'\frac{\partial^2 C}{\partial x^2} - V\frac{\partial C}{\partial x} = \frac{\partial C}{\partial t}\left[1 + \frac{\rho_b}{\theta}\frac{\partial S}{\partial C}\right] \tag{B21}$$

Since $(1 + \frac{\rho_b}{\theta}\frac{\partial S}{\partial C})$ equals the retardation equation,

$$D'\frac{\partial^2 C}{\partial x^2} - V\frac{\partial C}{\partial x} = R\frac{\partial C}{\partial t} \tag{B22}$$

where R is the retardation factor.

Appendix C. Experimental information for short-column solute-transport experiment.

Column I (distilled eluent):

Pulse duration, t'= 691 min
Length of column, L = 27.7 cm
Pore volume, T = 0.995
Volumetric water content, 0 = 0.33

Date	Time	Applied Suction (cm of water)	Suction (top) (cm of water)	Suction (bottom) (cm of water)
4-1	13:05	---	27.0	26.0
	14:40	---	32.0	29.0
4-2	7:50	---	18.0	30.0
	9:15	---	21.0	23.0
	10;30	51.0	23.0	36.0
	10:55	52.0	21.0	35.0
	11:35	51.0	23.0	34.0
	13:45	51.0	20.0	35.0
	16:40	50.0	23.0	25.0
	22:25	51.0	21.0	29.0
4-3	7:15	60.0	21.0	30.0
	10:28	48.0	23.0	28.0
	15:23	46.0	19.0	27.0
	16:53	47.0	21.0	29.0
4-4	7:40	45.0	19.0	27.0
	11:30	46.0	20.0	29.0

Column II $Ca(NO_2)_3$:

Pulse duration, t' = 691 min
Length of column, L = 26.9 cm
Pore volume = 1.04
Volumetric water content = 0.32

4-1	13:05	---	20.0	20.0
	14:40	---	18.0	23.0
4-2	9:15	---	10.0	21.0
	10:30	51.0	28.0	24.0
	10:55	52.0	23.0	22.0
	11:17	51.0	28.0	15.0
	12:35	51.0	28.0	24.0
	13:45	51.0	28.0	26.0
	16:40	50.0	24.0	20.0
	22:25	51.0	23.0	21.0
4-3	7:15	60.0	22.0	31.0
	10:28	48.0	20.0	29.0
	15:23	46.0	18.0	25.0
	16:53	47.0	20.0	28.0
4-4	7:40	43.0	15.0	23.0
	11:30	46.0	15.0	25.0

```
C*********************************************************************
C*              NON-LINEAR LEAST SQUARES ANALYSIS CFITM              *
C*                                                                   *
C*                          WRITTEN BY                               *
C*                                                                   *
C*                     M. TH. VAN GENUCHTEN                          *
C*                                                                   *
C*********************************************************************

      IMPLICIT REAL*8(A-H,O-Z)
      DIMENSION Y(130),X(130),F(130),R(130),DELZ(130,5),B(10),E(5),
     $ TH(10),P(5),PHI(5),Q(5),LSORT(130),TB(10),A(5,5),BI(10),
     $ TITLE(20),D(5,5),INDEX(5),ZAP(130)


      DATA STOPCR/0.0005/

      OPEN(UNIT=21,DEVICE='DSK',FILE='P3LC4.INP',ACCESS='SEQIN')
      OPEN(UNIT=22,DEVICE='DSK',FILE='P3LC4.OUT',ACCESS='SEQOUT')
      OPEN(UNIT=44,FILE='OUT.GRF')

C  READ NUMBER OF CASES

      READ (21,*) NC
      DO 120 NCASE=1,NC

      WRITE(22,1000)

C  READ INPUT PARAMETERS

      READ(21,*) MODE,NDATA,MIT,NOB

      IF (MODE.EQ.0) THEN
      WRITE(22,1021)
      ELSE IF (MODE.EQ.1) THEN
      WRITE(22,1022)
      ELSE IF (MODE.EQ.2) THEN
      WRITE(22,1023)
      ELSE IF (MODE.EQ.3) THEN
      WRITE(22,1024)
      ELSE IF (MODE.EQ.4) THEN
      WRITE(22,1025)
      END IF

      READ(21,1001) TITLE
      WRITE(22,1002) TITLE

      IF (NDATA.EQ.0) GO TO 10

C  READ COEFFICIENTS NAMES
      READ(21,1004) (BI(I),I=1,6)

C  READ INITIAL ESTIMATES
      READ(21,*) (B(I),I=4,6)

C  READ INDICES
      READ(21,*) (INDEX(I),I=1,3)
      WRITE(22,1007)
```

```
      DO 4 I=1,3
      J=2*I-1
      WRITE(22,1008) I,BI(J),BI(J+1),B(I+3)
4     CONTINUE

C  READ AND WRITE EXPERIMENTAL DATA
      DO 6 I=1,NOB
      READ(21,*) X(I), Y(I)
6     CONTINUE

10    WRITE(22,1009)

      DO 12 I=1,NOB
      WRITE(22,1010) I, X(I), Y(I)
12    CONTINUE

      NP=0
      DO 14 I=4,6
      TB(I)=B(I)
      IF(INDEX(I-3).EQ.0) GO TO 14
      NP=NP+1
      K=2*NP-1
      J=2*I-7
      BI(K)=BI(J)
      BI(K+1)=BI(J+1)
      B(NP)=B(I)
      TH(NP)=B(NP)
14    TH(I)=B(I)

      GA=0.02
      NIT=0
      NP2=2*NP
      CALL MODEL (TH,F,NOB,X,INDEX,MODE)
      SSQ=0.

      DO 32 I=1,NOB
      R(I)=Y(I)-F(I)
32    SSQ=SSQ+R(I)*R(I)


      WRITE(22,1011) (BI(J),BI(J+1),J=1,NP2,2)
      WRITE(22,1012) NIT,SSQ,(B(I),I=1,NP)

C  BEGIN ITERATION
34    NIT=NIT+1
      GA=0.1*GA

      DO 38 J=1,NP
      TEMP=TH(J)
      TH(J)=1.01*TH(J)
      Q(J)=0
      CALL MODEL (TH,ZAP,NOB,X,INDEX,MODE)

      DO 36 I=1,NOB
      DELZ(I,J)=ZAP(I)-F(I)
36    Q(J)=Q(J)+DELZ(I,J)*R(I)

      Q(J)=100.*Q(J)/TH(J)
```

```
C  Q=XT*R (STEEPEST DESCENT)
38      TH(J)=TEMP

        DO 44 I=1,NP

        DO 42 J=1,I
        SUM=0

        DO 40 K=1,NOB
40      SUM=SUM+DELZ(K,I)*DELZ(K,J)

        D(I,J)=10000.*SUM/(TH(I)*TH(J))
42      D(J,I)=D(I,J)

44      E(I)=DSQRT(D(I,I))

50      DO 52 I=1,NP
        DO 52 J=1,NP
52      A(I,J)=D(I,J)/(E(I)*E(J))

C  A IS THE SCALED MATRIX MOMENT
        DO 54 I=1,NP
        P(I)=Q(I)/E(I)
        PHI(I)=P(I)
54      A(I,I)=A(I,I)+GA

        CALL MATINV(A,NP,P)

C  P/E IS THE CORRECTION VECTOR
        STEP=1.0
56      DO 58 I=1,NP
58      TB(I)=P(I)*STEP/E(I)+TH(I)

        DO 62 I=1,NP
        IF(TH(I)*TB(I))66,66,62
62      CONTINUE

        SUMB=0
        CALL MODEL(TB,F,NOB,X,INDEX,MODE)

        DO 64 I=1,NOB
        R(I)=Y(I)-F(I)
64      SUMB=SUMB+R(I)*R(I)

66      SUM1=0.0
        SUM2=0.0
        SUM3=0.0

        DO 68 I=1,NP
        SUM1=SUM1+P(I)*PHI(I)
        SUM2=SUM2+P(I)*P(I)
68      SUM3=SUM3+PHI(I)*PHI(I)

        ARG=SUM1/DSQRT(SUM2*SUM3)
        ANGLE=57.29578*DATAN2(DSQRT(1.-ARG*ARG),ARG)

        DO 72 I=1,NP
        IF(TH(I)*TB(I))74,74,72
72      CONTINUE
```

```
      IF(SUMB/SSQ-1.0)80,80,74
74    IF(ANGLE-30.0)76,76,78
76    STEP=0.5*STEP
      GO TO 56
78    GA=10.*GA
      GO TO 50

C  PRINT COEFFICIENTS AFTER EACH ITERATION
80    CONTINUE
      DO 82 I=1,NP
82    TH(I)=TB(I)

      WRITE(22,1012)NIT,SUMB,(TH(I),I=1,NP)

      DO 86 I=1,NP
      IF(DABS(P(I)*STEP/E(I))/(1.0D-20+DABS(TH(I)))-STOPCR)86,86,94
86    CONTINUE

      GO TO 96
94    SSQ=SUMB
      IF(NIT.LE.MIT) GO TO 34

C  END OF ITERATION LOOP
96    CONTINUE
      CALL MATINV(D,NP,P)

C  WRITE CORRELATION MATRIX
      DO 98 I=1,NP
98    E(I)=DSQRT(D(I,I))

      WRITE(22,1013) (I,I=1,NP)

      DO 102 I=1,NP
      DO 100 J=1,I
100   A(J,I)=D(J,I)/(E(I)*E(J))

102   WRITE(22,1014) I,(A(J,I),J=1,I)

C  CALCULATE 95% CONFIDENCE INTERVAL
      Z=1./FLOAT(NOB-NP)
      SDEV=DSQRT(Z*SUMB)
      TVAR=1.96+Z*(2.3779+Z*(2.7135+Z*(3.187936+2.466666*Z**2)))
      WRITE(22,1015)
      DO 108 I=1,NP
      SECOEF=E(I)*SDEV
      TVALUE=TH(I)/SECOEF
      TSEC=TVAR*SECOEF
      TMCOE=TH(I)-TSEC
      TPCOE=TH(I)+TSEC
      J=2*I-1
108   WRITE(22,1016) I,BI(J),BI(J+1),TH(I),SECOEF,TVALUE,TMCOE,TPCOE

C  PREPARE FINAL OUTPUT
      LSORT(1)=1
      DO 116 J=2,NOB
      TEMP=R(J)
      K=J-1

      DO 111 L=1,K
      LL=LSORT(L)
```

```
      IF(TEMP-R(LL)) 112,112,111
111   CONTINUE

      LSORT(J)=J
      GO TO 116
112   KK=J
113   KK=KK-1
      LSORT(KK+1)=LSORT(KK)
      IF(KK-L) 115,115,113
115   LSORT(L)=J
116   CONTINUE

      WRITE(22,1017)
      DO 118 I=1,NOB
      J=LSORT(NOB+1-I)
118   WRITE(22,1018) I,X(I),Y(I),F(I),R(I),J,X(J),Y(J),F(J),R(J)

C
C     SEND DATA TO PLOT FILE
       DO 334 I=1,NOB
        WRITE(44,333) X(I),Y(I)
333   FORMAT(3F10.4)
334   CONTINUE
      WRITE(44,*)
      DO 335 I=1,NOB
        WRITE(44,336) X(I),F(I)
336   FORMAT(2F10.4)
335   CONTINUE
      WRITE(44,*)
120   WRITE(22,1020)
C  END OF PROBLEM
1000  FORMAT(1H1,10X,82(1H*)/11X,1H*,80X,1H*/11X,1H*,10X,'NON-LINEAR
     $ LEAST SQUARES ANALYSIS',37X,1H*/11X,1H*,80X,1H*)
1001  FORMAT(20A4)
1002  FORMAT(11X,1H*,20A4,1H*/11X,1H*,80X,1H*/11X,82(1H*))
1004  FORMAT(5(A4,A2,4X))
1005  FORMAT(5F10.0)
1006  FORMAT(5I5)
1007  FORMAT(//11X,'INITIAL VALUES OF COEFFFICIENTS'/11X,30(1H=)/12X,
     $ 'NO',6X,'NAME',9X,'INITIAL VALUE')
1008  FORMAT(11X,I3,5X,A4,A2,4X,F12.3)
1009  FORMAT(//11X,'OBSERVED DATA',/11X,13(1H=)/11X,'OBS.NO.',5X,'PORE
     $ VOLUME',5X,'CONCENTRATION')
1010  FORMAT(11X,I5,5X,F12.4,4X,F12.4)
1011  FORMAT(//11X,'ITERATION',6X,'SSQ',4X,5(7X,A4,A2))
1012  FORMAT(11X,I5,5X,F11.7,2X,5F13.5)
1013  FORMAT(///,11X,'CORRELATION MATRIX',/11X,18(1H=)/14X,10(4X,I2,
     $ 5X))
1014  FORMAT(11X,I3,10(2X,F7.4,2X))
1015  FORMAT(1H1,10X,'NON-LINEAR LEAST SQUARES ANALYSIS, FINAL RESUL
     $ TS'/11X,48(1H=)//72X,'95% CONFIDENCE LIMITS'/11X,'VARIABLE',4X,
     $ 'NAME',8X,'VALUE',8X,'S.E.COEFF.',3X,'T-VALUE',5X,'LOWER',10X,
     $ 'UPPER')
1016  FORMAT(14X,I2,6X,A4,A2,2X,F12.5,5X,F9.4,4X,F8.2,2X,F9.4,6X,F9.4)
1017  FORMAT(//10X,9(1H-),'ORDERED BY COMPUTER INPUT',10(1H-),7X,
     $ 12(1H-),'ORDERED BY RESIDUALS',12(1H-)/18X,'PORE',6X,'CONCENTRA
     $ TION',6X,'RESI-',18X,'PORE',6X,'CONCENTRATION',6X,'RESI-'/10X,
     $ 'NO',4X,'VOLUME',6X,'OBS.',4X,'FITTED',6X,'DUAL',10X,'NO',4X,
     $ 'VOLUME',6X,'OBS.'4X,'FITTED',6X,'DUAL')
1018  FORMAT(10X,I3,4F10.3,10X,I3,4F10.3)
```

```
1020    FORMAT(///11X,'END OF PROBLEM'/11X,14(1H=))
1021    FORMAT(11X,1H*,10X,'INFINITE PROFILE',54X,1H*)
1022    FORMAT(11X,1H*,10X,'SEMI-INFINITE PROFILE, 1-TYPE BC',38X,1H*)
1023    FORMAT(11X,1H*,10X,'SEMI-INFINITE PROFILE, 3-TYPE BC',38X,1H*)
1024    FORMAT(11X,1H*,10X,'FINITE PROFILE, 1-TYPE BC',45X,1H*)
1025    FORMAT(11X,1H*,10X,'FINITE PROFILE, 3-TYPE BC',45X,1H*)
        STOP
        END

        SUBROUTINE EIGEN (G,P,MODE)

C  PURPOSE:TO CALCULATE THE EIGEN VALUES

        IMPLICIT REAL*8 (A-H,O-Z)
        DIMENSION G(20)
        BETA=0.1
        S=0.0
        IF(MODE.EQ.4) S=1.0
        DO 4 I=1,20
        J=0
1       J=J+1
        IF(J.GT.15) GO TO 3
        DELTA=-0.2*(-0.5)**J
2       BET2=BETA
        BETA=BETA+DELTA
        A=BET2*DCOS(BET2)+(0.25*(2.-S)*P-S*BET2**2/P)*DSIN(BET2)
        B=BETA*DCOS(BETA)+(0.25*(2.-S)*P-S*BETA**2/P)*DSIN(BETA)
        IF(A*B)1,3,2
3       G(I)=(BET2*B-BETA*A)/(B-A)
4       BETA=BETA+0.2
        RETURN
        END


        SUBROUTINE CONC (C,G,P,T,MODE)

C  PURPOSE: TO CALCULATE CONCENTRATION C FOR MODE 3,4

        IMPLICIT REAL*8 (A-H,O-Z)
        DIMENSION G(20)
        E=0.0
        TOL=0.00001
        S=DMIN1(1.D02,5.+40.*T)
        IF(P.GE.S) GO TO 4
        S=1
        IF (MODE.EQ.3)S=0.5

C  SERIES SOLUTION
        EX=0.5*P-0.25*P*T
        SUM=0.0
        DO 2 J=1,10
        DSUM=0.0
        DO 1 K=1,2
        I=2*J+K-2
        A=G(I)*DSIN(G(I))
        IF(DABS(A).LT.1.D-04) A=0.0
        EXP=EX-G(I)**2*T/P
1       DSUM=DSUM+A*EXF(EXP,E)/(G(I)**2+0.25*P*P+S*P)
        SUM=SUM+DSUM
        IF(DABS(DSUM/SUM).LT.TOL)GO TO 3
```

```
2       CONTINUE
        GO TO 4
3       C=1.-2.*SUM
        RETURN
4       AM=0.5*(1.-T)*DSQRT(P/T)
        AP=0.5*(1.+T)*DSQRT(P/T)
        A=0.5*EXF(E,AM)
        B=0.5*EXF(P,AP)
        D=DSQRT(.3183099*P*T)*EXF(-AM*AM,E)
        IF(MODE.EQ.3)C=A+(3.+P+P*T)*B-D
        IF(MODE.EQ.4)C=A+(3.+.5*P+.5*P*T)*D-(1.+3.*P+P*T*(4.+2.*AP**2))
     $  *B
        RETURN
        END

        FUNCTION EXF(A,B)

C  PURPOSE: TO CALCULATE EXP(A) ERFC(B)

        IMPLICIT REAL*8(A-H,O-Z)
        EXF=0.0
        IF((DABS(A).GT.170.).AND.(B.LE.0.)) RETURN
        C=A-B*B
        IF((DABS(C).GT.170.).AND.(B.GE.0.)) RETURN
        IF(C.LT.-170.) GO TO 3
        X=DABS(B)
        IF(X.GT.3.0) GO TO 1
        T=1./(1.+.3275911*X)
        Y=T*(.2548296-T*(.2844967-T*(1.421414-T*(1.453152-1.061405*T))))
        GO TO 2
1       Y=.5641896/(X+.5/(X+1./(X+1.5/(X+2./(X+2.5/X+1.)))))
2       EXF=Y*DEXP(C)
3       IF(B.LT.0.0) EXF=2.*DEXP(A)-EXF
        RETURN
        END

        SUBROUTINE MATINV (A,NP,B)

        IMPLICIT REAL*8(A-H,O-Z)
        DIMENSION A(5,5),B(10),INDEX(5,2)
        DO 2 J=1,5
2       INDEX(J,1)=0
        I=0
4       AMAX=-1.0

        DO 12 J=1,NP
        IF(INDEX(J,1)) 12,6,12

6       DO 10 K=1,NP
        IF(INDEX(K,1)) 10,8,10
8       P=DABS(A(J,K))
        IF(P.LE.AMAX) GO TO 10
        IR=J
        IC=K
        AMAX=P
10      CONTINUE
12      CONTINUE
```

```
      IF(AMAX) 30,30,14
14    INDEX(IC,1)=IR
      IF(IR.EQ.IC) GO TO 18

      DO 16 L=1,NP
      P=A(IR,L)
      A(IR,L)=A(IC,L)
16    A(IC,L)=P
      P=B(IR)
      B(IR)=B(IC)
      B(IC)=P
      I=I+1
      INDEX(I,2)=IC
18    P=1./A(IC,IC)
      A(IC,IC)=1.0

      DO 20 L=1,NP
20    A(IC,L)=A(IC,L)*P

      B(IC)=B(IC)*P

      DO 24 K=1,NP
      IF(K.EQ.IC) GO TO 24
      P=A(K,IC)
      A(K,IC)=0.0

      DO 22 L=1,NP
22    A(K,L)=A(K,L)-A(IC,L)*P
      B(K)=B(K)-B(IC)*P
24    CONTINUE

      GO TO 4

26    IC=INDEX(I,2)
      IR=INDEX(IC,1)

      DO 28 K=1,NP
      P=A(K,IR)
      A(K,IR)=A(K,IC)
28    A(K,IC)=P
      I=I-1
30    IF(I) 26,32,26
32    RETURN
      END


      SUBROUTINE MODEL(B,Y,NOB,X,INDEX,MODE)

C  PURPOSE: TO CALCULATE CONCENTRATIONS FOR A GIVEN PORE VOLUME

      IMPLICIT REAL*8(A-H,O-Z)
      DIMENSION B(10),Y(90),X(90),INDEX(5),G(20)
      E=0.
      K=0

      DO 2 I=4,6
      IF(INDEX(I-3).EQ.0) GO TO 2
      K=K+1
      B(I)=B(K)
2     CONTINUE
```

```
      P=B(4)
      R=B(5)
      IF((P.LE.100.).AND.(MODE.GE.3)) CALL EIGEN (G,P,MODE)

      DO 6 J=1,NOB
      DO 4 M=1,2
      C=0.0
      T=(X(J)+(1-M)*B(6))/R
      IF(T.LE.0.) GO TO 6
      AM=0.5*(1.-T)*DSQRT(P/T)
      AP=0.5*(1.+T)*DSQRT(P/T)
      IF(MODE.EQ.0) C=0.5*EXF(E,AM)
      IF(MODE.EQ.1) C=0.5*EXF(E,AM)+0.5*EXF(P,AP)
      IF(MODE.EQ.2) C=0.5*EXF(E,AM)+DSQRT(.3183099*P*T)*EXF(-AM*AM,E)-
     $ 0.5*(1.+P+P*T)*EXF(P,AP)
      IF(MODE.GE.3) CALL CONC(C,G,P,T,MODE)
      IF(M.EQ.2) GO TO 6
      Y(J)=C
4     CONTINUE
6     Y(J)=Y(J)-C
      RETURN
      END
```

Appendix E. Short-column (30 cm) solute-transport experiment results, bromide tracer in distilled water eluent.

Pore Volume	Concentration (observed, M/L)	Concentration (corrected, M/L)	Relative Conc. (C/Co)
0.060	0.00E+00	0.00E+00	0.00E+00
0.130	0.00E+00	0.00E+00	0.00E+00
0.199	0.00E+00	0.00E+00	0.00E+00
0.411	0.00E+00	0.00E+00	0.00E+00
0.546	0.00E+00	0.00E+00	0.00E+00
0.683	0.00E+00	0.00E+00	0.00E+00
0.752	4.07E-05	9.80E-05	9.80E-04
0.826	2.48E-03	4.42E-03	4.42E-02
0.890	1.28E-02	2.01E-02	2.01E-01
0.958	2.24E-02	3.39E-02	3.39E-01
1.010	3.94E-02	5.71E-02	5.71E-01
1.080	4.59E-02	6.57E-02	6.57E-01
1.150	5.13E-02	7.29E-02	7.29E-01
1.210	5.73E-02	8.07E-02	8.07E-01
1.290	6.03E-02	8.46E-02	8.46E-01
1.360	6.12E-02	8.59E-02	8.59E-01
1.440	6.32E-02	8.84E-02	8.84E-01
1.490	6.12E-02	8.59E-02	8.59E-01
1.560	6.22E-02	8.72E-02	8.72E-01
1.630	6.72E-02	9.36E-02	9.36E-01
1.710	6.92E-02	9.61E-02	9.61E-01
1.770	5.73E-02	8.07E-02	8.07E-01
1.840	5.73E-02	8.07E-02	8.07E-01
1.910	3.84E-02	5.58E-02	5.58E-01
1.980	2.86E-02	4.24E-02	4.24E-01
2.050	1.37E-02	2.15E-02	2.15E-01
2.120	8.23E-03	1.34E-02	1.34E-01
2.190	4.30E-03	7.33E-03	7.33E-02
2.260	3.51E-03	6.09E-03	6.09E-02
2.330	2.53E-03	4.50E-03	4.50E-02
2.400	1.56E-03	2.86E-03	2.86E-02
2.470	1.07E-03	2.02E-03	2.02E-02
2.530	8.92E-04	1.71E-03	1.71E-02
2.600	5.42E-04	1.08E-03	1.08E-02
2.670	8.14E-04	1.57E-03	1.57E-02
2.740	5.61E-04	1.11E-03	1.11E-02
2.800	2.41E-04	5.09E-04	5.09E-03
2.880	2.22E-04	4.71E-04	4.71E-03
2.950	1.64E-04	3.56E-04	3.56E-03
3.020	1.20E-04	2.67E-04	2.67E-03
3.090	7.00E-05	1.62E-04	1.62E-03
3.150	5.93E-05	1.39E-04	1.39E-03
3.220	4.97E-05	1.18E-04	1.18E-03
3.290	4.21E-06	1.20E-05	1.20E-04
3.360	3.80E-05	9.20E-05	9.20E-04
3.430	3.44E-05	8.40E-05	8.40E-04
3.500	3.05E-05	7.50E-05	7.50E-04
3.570	2.87E-05	7.10E-05	7.10E-04
3.640	2.57E-05	6.40E-05	6.40E-04
3.710	2.48E-05	6.20E-05	6.20E-04
3.780	2.31E-05	5.80E-05	5.80E-04
3.850	2.05E-05	5.20E-05	5.20E-04
3.920	1.80E-05	4.60E-05	4.60E-04
4.040	1.63E-05	4.20E-05	4.20E-04

4.110	1.63E-05	4.20E-05	4.20E-04

Appendix E. Short-column (30 cm) solute-transport experiment results, bromide tracer from column with (CaNo3)2 eluent.

Pore Volume	Concentration (measure, M/L)	Concentration (corrected, M/L)	Relative Conc. (C/Co)
0.442	0.00E+00	0.00E+00	0.00E+00
0.513	0.00E+00	0.00E+00	0.00E+00
0.588	0.00E+00	0.00E+00	0.00E+00
0.661	2.39E-05	6.00E-05	6.00E-04
0.735	2.24E-03	4.01E-03	4.01E-02
0.810	1.30E-02	2.04E-02	2.04E-01
0.889	2.58E-02	3.85E-02	3.85E-01
0.959	3.45E-02	5.05E-02	5.05E-01
1.030	4.24E-02	6.11E-02	6.11E-01
1.130	4.64E-02	6.64E-02	6.64E-01
1.220	5.13E-02	7.29E-02	7.29E-01
1.300	5.53E-02	7.81E-02	7.81E-01
1.370	5.53E-02	7.81E-02	7.81E-01
1.450	5.73E-02	8.07E-02	8.07E-01
1.530	5.93E-02	8.33E-02	8.33E-01
1.620	6.22E-02	8.72E-02	8.72E-01
1.690	6.12E-02	8.59E-02	8.59E-01
1.760	5.93E-02	8.33E-02	8.33E-01
1.840	6.12E-02	8.59E-02	8.59E-01
1.920	4.54E-02	6.51E-02	6.51E-01
1.980	4.09E-02	5.91E-02	5.91E-01
2.060	3.18E-02	4.68E-02	4.68E-01
2.140	2.36E-02	3.55E-02	3.55E-01
2.210	1.59E-02	2.46E-02	2.46E-01
2.290	1.13E-02	1.79E-02	1.79E-01
2.360	8.62E-03	1.40E-02	1.40E-01
2.440	6.85E-03	1.13E-02	1.13E-01
2.510	5.28E-03	8.87E-03	8.87E-02
2.590	4.10E-03	7.02E-03	7.02E-02
2.670	3.32E-03	5.77E-03	5.77E-02
2.740	2.73E-03	4.82E-03	4.82E-02
2.810	2.34E-03	4.17E-03	4.17E-02
2.880	1.97E-03	3.56E-03	3.56E-02
2.960	1.56E-03	2.86E-03	2.86E-02
3.030	1.35E-03	2.51E-03	2.51E-02
3.110	1.12E-03	2.10E-03	2.11E-02
3.180	9.31E-04	1.78E-03	1.78E-02
3.270	7.56E-04	1.47E-03	1.47E-02
3.340	6.59E-04	1.29E-03	1.29E-02
3.420	5.66E-04	1.12E-03	1.12E-02
3.500	4.85E-04	9.74E-04	9.74E-03
3.570	4.45E-04	8.98E-04	8.98E-03
3.640	3.87E-04	7.89E-04	7.89E-03
3.720	3.38E-04	6.96E-04	6.96E-03
3.790	3.09E-04	6.41E-04	6.41E-03
3.870	1.95E-04	4.18E-04	4.18E-03
3.940	1.69E-04	3.66E-04	3.66E-03
4.020	1.37E-04	3.01E-04	3.01E-03
4.170	1.23E-04	2.73E-04	2.73E-03
4.240	1.10E-04	2.47E-04	2.47E-03
4.400	9.40E-05	2.13E-04	2.13E-03
4.440	1.10E-04	2.47E-04	2.47E-03
4.520	1.10E-04	2.47E-04	2.47E-03

Appendix E. Short-column (30 cm) solute-transport experiment results, tritium tracer with distilled water eluent.

Pore Volume	Tritium Conc. (counts/min)	Relative Conc. (C/Co)
0.060	12.9	1.20E-04
0.130	10.9	7.00E-05
0.199	12.9	1.20E-04
0.270	8.3	0.00E+00
0.340	8.3	0.00E+00
0.411	10.9	7.00E-05
0.477	11.7	9.00E-05
0.546	8.3	0.00E+00
0.614	8.3	0.00E+00
0.683	8.3	0.00E+00
0.752	20.6	3.20E-04
0.787	175.3	4.34E-03
0.826	870.3	2.24E-02
0.857	2567.3	6.65E-02
0.890	5665.1	1.47E-01
0.958	17363.8	4.51E-01
1.010	14208.2	3.69E-01
1.080	21712.3	5.64E-01
1.150	25945.3	6.74E-01
1.210	31794.6	8.26E-01
1.290	25560.5	6.64E-01
1.360	26368.6	6.85E-01
1.440	32487.3	8.44E-01
1.460	24944.8	6.48E-01
1.490	31178.9	8.10E-01
1.600	27176.8	7.06E-01
1.630	27022.8	7.02E-01
1.710	26868.9	6.98E-01
1.770	27099.8	7.04E-01
1.840	28754.5	7.47E-01
1.910	25868.4	6.72E-01
1.980	12745.9	3.31E-01
2.050	7012.0	1.82E-01
2.120	3667.9	9.51E-02
2.190	2028.6	5.25E-02
2.260	1297.4	3.35E-02
2.330	801.0	2.06E-02
2.400	543.2	1.39E-02
2.470	394.2	1.00E-02
2.530	304.2	7.69E-03
2.600	199.9	4.98E-03
2.670	147.2	3.61E-03
2.740	129.1	3.14E-03
2.800	126.4	3.07E-03
2.880	116.0	2.80E-03
2.950	108.7	2.61E-03
3.020	94.8	2.25E-03
3.090	89.8	2.12E-03
3.150	62.5	1.41E-03
3.220	92.9	2.20E-03
3.290	57.9	1.29E-03
3.360	54.8	1.21E-03
3.430	52.5	1.15E-03

3.500	45.2	9.60E-04
3.570	43.7	9.20E-04
3.640	45.6	9.70E-04
3.710	37.5	7.60E-04
3.780	39.4	8.10E-04
3.850	27.9	5.10E-04
3.990	24.4	4.20E-04
4.040	58.3	1.30E-03
4.110	27.5	5.00E-04

Appendix . Short-column (30 cm) solute-transport experiment results, tritium tracer in (CaNO3)2 eluent.

Pore Volum	Tritium Concent. (Counts/min.)	Relative Conc. (C/Co)
0.053	15.0	6.50E-06
0.129	17.5	7.15E-05
0.205	15.0	6.50E-06
0.281	14.8	0.00E+00
0.357	14.8	0.00E+00
0.442	14.8	0.00E+00
0.513	14.8	0.00E+00
0.588	15.0	6.50E-06
0.661	22.7	2.06E-04
0.698	132.1	3.05E-03
0.735	846.0	2.16E-02
0.772	1985.0	5.12E-02
0.810	4825.0	1.25E-01
0.889	13291.1	3.45E-01
0.959	19702.3	5.12E-01
1.030	23758.3	6.17E-01
1.080	20371.9	5.29E-01
1.130	21680.3	5.63E-01
1.220	25990.3	6.75E-01
1.300	28260.8	7.34E-01
1.370	23219.6	6.03E-01
1.410	25490.0	6.62E-01
1.450	26683.0	6.93E-01
1.490	23604.4	6.13E-01
1.530	28530.1	7.41E-01
1.620	29453.7	7.65E-01
1.690	28145.3	7.31E-01
1.760	30993.0	8.05E-01
1.840	32955.6	8.56E-01
1.880	33148.0	8.61E-01
1.920	22988.7	5.97E-01
1.980	20179.5	5.24E-01
2.060	15369.2	3.99E-01
2.140	13021.8	3.38E-01
2.210	10135.6	2.63E-01
2.290	5902.5	1.53E-01
2.360	4478.7	1.16E-01
2.440	3351.2	8.67E-02
2.510	2881.7	7.45E-02
2.590	2173.6	5.61E-02
2.670	1796.5	4.63E-02
2.740	1904.2	4.91E-02
2.810	1561.7	4.02E-02
2.880	1269.3	3.26E-02
2.960	1011.4	2.59E-02
3.030	780.5	1.99E-02
3.110	680.5	1.73E-02
3.180	511.2	1.29E-02
3.270	434.2	1.09E-02
3.340	323.8	8.03E-03
3.420	259.1	6.35E-03
3.500	204.9	4.94E-03
3.570	192.2	4.61E-03
3.640	102.5	2.28E-03

3.720	97.9	2.16E-03
3.790	95.6	2.10E-03
3.870	70.5	1.45E-03
3.940	72.9	1.51E-03
4.020	57.9	1.12E-03
4.090	82.1	1.75E-03
4.170	50.9	9.40E-04
4.240	42.5	7.20E-04
4.320	35.5	5.39E-04
4.400	34.5	5.13E-04
4.440	33.5	4.87E-04
4.520	33.5	4.87E-04

```
*****************************************************************************
*
*          NON-LINEAR  LEAST SQUARES ANALYSIS
*
*          SEMI-INFINITE PROFILE, 3-TYPE BC
*distilled case, semi-inf, third bc, short col, br   pulse fixed
*
*****************************************************************************
```

INITIAL VALUES OF COEFFFICIENTS

NO	NAME	INITIAL VALUE
1	Peclet	14.050
2	RF	1.000
3	PULSE	0.995

OBSERVED DATA

OBS.NO.	PORE VOLUME	CONCENTRATION
1	0.0600	0.0000
2	0.1300	0.0000
3	0.1990	0.0000
4	0.4110	0.0000
5	0.5460	0.0000
6	0.6830	0.0000
7	0.7520	0.0010
8	0.8260	0.0442
9	0.8900	0.2008
10	0.9580	0.3387
11	1.0100	0.5712
12	1.0800	0.6571
13	1.1500	0.7291
14	1.2100	0.8070
15	1.2900	0.8458
16	1.3600	0.8587
17	1.4400	0.8844
18	1.4900	0.8587
19	1.5600	0.8716
20	1.6300	0.9357
21	1.7100	0.9613
22	1.7700	0.8070
23	1.8400	0.8070
24	1.9100	0.5579
25	1.9800	0.4236
26	2.0500	0.2152
27	2.1200	0.1338
28	2.1900	0.0733
29	2.2600	0.0608
30	2.3300	0.0450
31	2.4000	0.0286
32	2.4700	0.0202
33	2.5300	0.0171
34	2.6000	0.0108
35	2.6700	0.0157
36	2.7400	0.0111
37	2.8000	0.0051
38	2.8800	0.0047
39	2.9500	0.0036

40	3.0200	0.0027
41	3.0900	0.0016
42	3.1500	0.0014
43	3.2200	0.0012
44	3.2900	0.0001
45	3.3600	0.0009
46	3.4300	0.0008
47	3.5000	0.0007
48	3.5700	0.0007
49	3.6400	0.0006
50	3.7100	0.0006
51	3.7800	0.0006
52	3.8500	0.0005
53	3.9200	0.0005
54	4.0400	0.0004
55	4.1100	0.0004

ITERATION	SSQ	peclet	RF
0	0.5970093	14.05000	1.00000
1	0.2917959	25.09601	0.97697
2	0.1984256	38.50175	0.98845
3	0.1761113	49.03729	0.98615
4	0.1722616	54.97034	0.98533
5	0.1717819	57.34549	0.98481
6	0.1717353	58.15421	0.98461
7	0.1717321	58.41213	0.98455
8	0.1717321	58.43229	0.98454

CORRELATION MATRIX
==========

	1	2
1	1.0000	
2	0.1453	1.0000

NON-LINEAR LEAST SQUARES ANALYSIS, FINAL RESUL TS
==========

VARIABLE	NAME	VALUE	S.E.COEFF.	T-VALUE	95% CONFIDENCE LIMITS LOWER	UPPER
1	peclet	58.43229	7.8766	7.42	42.6330	74.2316
2	RF	0.98454	0.0084	116.68	0.9676	1.0015

ORDERED BY COMPUTER INPUT

NO	PORE VOLUME	CONCENTRA TION OBS.	FITTED	RESI-DUAL
1	0.060	0.000	0.000	0.000
2	0.130	0.000	0.000	0.000
3	0.199	0.000	0.000	0.000
4	0.411	0.000	0.000	0.000
5	0.546	0.000	0.001	-0.001
6	0.683	0.000	0.022	-0.022
7	0.752	0.001	0.070	-0.069
8	0.826	0.044	0.169	-0.124
9	0.890	0.201	0.290	-0.090
10	0.958	0.339	0.440	-0.102
11	1.010	0.571	0.555	0.017
12	1.080	0.657	0.693	-0.035

ORDERED BY RESIDUALS

NO	PORE VOLUME	CONCENTRATION OBS.	FITTED	RESI-DUAL
11	1.010	0.571	0.555	0.017
35	2.670	0.016	0.002	0.014
36	2.740	0.011	0.001	0.010
33	2.530	0.017	0.007	0.010
23	1.840	0.807	0.798	0.009
34	2.600	0.011	0.004	0.007
32	2.470	0.020	0.013	0.007
37	2.800	0.005	0.000	0.005
38	2.880	0.005	0.000	0.005
39	2.950	0.004	0.000	0.003
31	2.400	0.029	0.026	0.003
40	3.020	0.003	0.000	0.003

13	1.150	0.729	0.801	-0.072
14	1.210	0.807	0.870	-0.063
15	1.290	0.846	0.930	-0.084
16	1.360	0.859	0.961	-0.103
17	1.440	0.884	0.981	-0.097
18	1.490	0.859	0.988	-0.130
19	1.560	0.872	0.993	-0.122
20	1.630	0.936	0.989	-0.054
21	1.710	0.961	0.959	0.002
22	1.770	0.807	0.904	-0.097
23	1.840	0.807	0.798	0.009
24	1.910	0.558	0.656	-0.098
25	1.980	0.424	0.500	-0.076
26	2.050	0.215	0.354	-0.139
27	2.120	0.134	0.234	-0.100
28	2.190	0.073	0.145	-0.072
29	2.260	0.061	0.086	-0.025
30	2.330	0.045	0.048	-0.003
31	2.400	0.029	0.026	0.003
32	2.470	0.020	0.013	0.007
33	2.530	0.017	0.007	0.010
34	2.600	0.011	0.004	0.007
35	2.670	0.016	0.002	0.014
36	2.740	0.011	0.001	0.010
37	2.800	0.005	0.000	0.005
38	2.880	0.005	0.000	0.005
39	2.950	0.004	0.000	0.003
40	3.020	0.003	0.000	0.003
41	3.090	0.002	0.000	0.002
42	3.150	0.001	0.000	0.001
43	3.220	0.001	0.000	0.001
44	3.290	0.000	0.000	0.000
45	3.360	0.001	0.000	0.001
46	3.430	0.001	0.000	0.001
47	3.500	0.001	0.000	0.001
48	3.570	0.001	0.000	0.001
49	3.640	0.001	0.000	0.001
50	3.710	0.001	0.000	0.001
51	3.780	0.001	0.000	0.001
52	3.850	0.001	0.000	0.001
53	3.920	0.000	0.000	0.000
54	4.040	0.000	0.000	0.000
55	4.110	0.000	0.000	0.000

21	1.710	0.961	0.959	0.002
41	3.090	0.002	0.000	0.002
42	3.150	0.001	0.000	0.001
43	3.220	0.001	0.000	0.001
45	3.360	0.001	0.000	0.001
46	3.430	0.001	0.000	0.001
47	3.500	0.001	0.000	0.001
48	3.570	0.001	0.000	0.001
49	3.640	0.001	0.000	0.001
50	3.710	0.001	0.000	0.001
51	3.780	0.001	0.000	0.001
52	3.850	0.001	0.000	0.001
53	3.920	0.000	0.000	0.000
55	4.110	0.000	0.000	0.000
54	4.040	0.000	0.000	0.000
44	3.290	0.000	0.000	0.000
1	0.060	0.000	0.000	0.000
2	0.130	0.000	0.000	0.000
3	0.199	0.000	0.000	0.000
4	0.411	0.000	0.000	0.000
5	0.546	0.000	0.001	-0.001
30	2.330	0.045	0.048	-0.003
6	0.683	0.000	0.022	-0.022
29	2.260	0.061	0.086	-0.025
12	1.080	0.657	0.693	-0.035
20	1.630	0.936	0.989	-0.054
14	1.210	0.807	0.870	-0.063
7	0.752	0.001	0.070	-0.069
13	1.150	0.729	0.801	-0.072
28	2.190	0.073	0.145	-0.072
25	1.980	0.424	0.500	-0.076
15	1.290	0.846	0.930	-0.084
9	0.890	0.201	0.290	-0.090
17	1.440	0.884	0.981	-0.097
22	1.770	0.807	0.904	-0.097
24	1.910	0.558	0.656	-0.098
27	2.120	0.134	0.234	-0.100
10	0.958	0.339	0.440	-0.102
16	1.360	0.859	0.961	-0.103
19	1.560	0.872	0.993	-0.122
8	0.826	0.044	0.169	-0.124
18	1.490	0.859	0.988	-0.130
26	2.050	0.215	0.354	-0.139

END OF PROBLEM
==========

```
*****************************************************************************
*
*            NON-LINEAR  LEAST SQUARES ANALYSIS
*
*            SEMI-INFINITE PROFILE, 3-TYPE BC
*CANO3 CASE, SH COL. , BC #3, BROMIDE,                    , PULSE FIXED
*
*****************************************************************************
```

INITIAL VALUES OF COEFFFICIENTS

NO	NAME	INITIAL VALUE
1	PECLET	26.900
2	RF	1.000
3	PULSE	1.040

OBSERVED DATA

OBS.NO.	PORE VOLUME	CONCENTRATION
1	0.4420	0.0000
2	0.5130	0.0000
3	0.5880	0.0000
4	0.6610	0.0006
5	0.7350	0.0401
6	0.8100	0.2037
7	0.8890	0.3854
8	0.9590	0.5045
9	1.0300	0.6110
10	1.1300	0.6637
11	1.2200	0.7291
12	1.3000	0.7811
13	1.3700	0.7811
14	1.4500	0.8070
15	1.5300	0.8329
16	1.6200	0.8716
17	1.6900	0.8587
18	1.7600	0.8329
19	1.8400	0.8587
20	1.9200	0.6505
21	1.9800	0.5911
22	2.0600	0.4682
23	2.1400	0.3552
24	2.2100	0.2465
25	2.2900	0.1792
26	2.3600	0.1397
27	2.4400	0.1129
28	2.5100	0.0887
29	2.5900	0.0702
30	2.6700	0.0577
31	2.7400	0.0482
32	2.8100	0.0417
33	2.8800	0.0356
34	2.9600	0.0286
35	3.0300	0.0251
36	3.1100	0.0210
37	3.1800	0.0178
38	3.2700	0.0147
39	3.3400	0.0129

40	3.4200	0.0112
41	3.5000	0.0097
42	3.5700	0.0090
43	3.6400	0.0079
44	3.7200	0.0070
45	3.7900	0.0064
46	3.8700	0.0042
47	3.9400	0.0037
48	4.0200	0.0030
49	4.1700	0.0027
50	4.2400	0.0025
51	4.4000	0.0021
52	4.4400	0.0025
53	4.5200	0.0025

ITERATION	SSQ	PECLET	RF
0	0.0866530	26.90000	1.00000
1	0.0752620	21.81714	1.00081
2	0.0751682	21.96455	1.00285
3	0.0751676	21.94417	1.00278
4	0.0751676	21.94344	1.00279

CORRELATION MATRIX
==========

	1	2
1	1.0000	
2	0.1413	1.0000

NON-LINEAR LEAST SQUARES ANALYSIS, FINAL RESUL TS
==========

VARIABLE	NAME	VALUE	S.E.COEFF.	T-VALUE	95% CONFIDENCE LIMITS LOWER	UPPER
1	PECLET	21.94344	1.5217	14.42	18.8882	24.9986
2	RF	1.00279	0.0081	123.98	0.9866	1.0190

ORDERED BY COMPUTER INPUT

NO	PORE VOLUME	CONCENTRA TION OBS.	FITTED	RESI-DUAL
1	0.442	0.000	0.002	-0.002
2	0.513	0.000	0.010	-0.010
3	0.588	0.000	0.033	-0.033
4	0.661	0.001	0.077	-0.076
5	0.735	0.040	0.144	-0.104
6	0.810	0.204	0.233	-0.029
7	0.889	0.385	0.340	0.046
8	0.959	0.505	0.438	0.067
9	1.030	0.611	0.534	0.077
10	1.130	0.664	0.655	0.009
11	1.220	0.729	0.745	-0.016
12	1.300	0.781	0.809	-0.028
13	1.370	0.781	0.854	-0.073
14	1.450	0.807	0.893	-0.086
15	1.530	0.833	0.918	-0.085
16	1.620	0.872	0.919	-0.047
17	1.690	0.859	0.893	-0.035
18	1.760	0.833	0.844	-0.011

ORDERED BY RESIDUALS

NO	PORE VOLUME	CONCENTRATION OBS.	FITTED	RESI-DUAL
19	1.840	0.859	0.761	0.098
9	1.030	0.611	0.534	0.077
8	0.959	0.505	0.438	0.067
7	0.889	0.385	0.340	0.046
33	2.880	0.036	0.019	0.017
35	3.030	0.025	0.009	0.016
34	2.960	0.029	0.013	0.016
32	2.810	0.042	0.026	0.016
36	3.110	0.021	0.006	0.015
37	3.180	0.018	0.004	0.013
31	2.740	0.048	0.036	0.012
21	1.980	0.591	0.579	0.012
38	3.270	0.015	0.003	0.012
39	3.340	0.013	0.002	0.011
40	3.420	0.011	0.001	0.010
10	1.130	0.664	0.655	0.009
41	3.500	0.010	0.001	0.009
30	2.670	0.058	0.049	0.009

19	1.840	0.859	0.761	0.098	42	3.570	0.009	0.001	0.008
20	1.920	0.651	0.660	-0.010	43	3.640	0.008	0.000	0.007
21	1.980	0.591	0.579	0.012	44	3.720	0.007	0.000	0.007
22	2.060	0.468	0.473	-0.005	45	3.790	0.006	0.000	0.006
23	2.140	0.355	0.375	-0.020	46	3.870	0.004	0.000	0.004
24	2.210	0.246	0.300	-0.053	47	3.940	0.004	0.000	0.004
25	2.290	0.179	0.227	-0.048	48	4.020	0.003	0.000	0.003
26	2.360	0.140	0.176	-0.036	49	4.170	0.003	0.000	0.003
27	2.440	0.113	0.129	-0.016	53	4.520	0.002	0.000	0.002
28	2.510	0.089	0.097	-0.008	52	4.440	0.002	0.000	0.002
29	2.590	0.070	0.069	0.001	50	4.240	0.002	0.000	0.002
30	2.670	0.058	0.049	0.009	51	4.400	0.002	0.000	0.002
31	2.740	0.048	0.036	0.012	29	2.590	0.070	0.069	0.001
32	2.810	0.042	0.026	0.016	1	0.442	0.000	0.002	-0.002
33	2.880	0.036	0.019	0.017	22	2.060	0.468	0.473	-0.005
34	2.960	0.029	0.013	0.016	28	2.510	0.089	0.097	-0.008
35	3.030	0.025	0.009	0.016	20	1.920	0.651	0.660	-0.010
36	3.110	0.021	0.006	0.015	2	0.513	0.000	0.010	-0.010
37	3.180	0.018	0.004	0.013	18	1.760	0.833	0.844	-0.011
38	3.270	0.015	0.003	0.012	11	1.220	0.729	0.745	-0.016
39	3.340	0.013	0.002	0.011	27	2.440	0.113	0.129	-0.016
40	3.420	0.011	0.001	0.010	23	2.140	0.355	0.375	-0.020
41	3.500	0.010	0.001	0.009	12	1.300	0.781	0.809	-0.028
42	3.570	0.009	0.001	0.008	6	0.610	0.204	0.233	-0.029
43	3.640	0.008	0.000	0.007	3	0.588	0.000	0.033	-0.033
44	3.720	0.007	0.000	0.007	17	1.690	0.859	0.893	-0.035
45	3.790	0.006	0.000	0.006	26	2.360	0.140	0.176	-0.036
46	3.870	0.004	0.000	0.004	16	1.620	0.872	0.919	-0.047
47	3.940	0.004	0.000	0.004	25	2.290	0.179	0.227	-0.048
48	4.020	0.003	0.000	0.003	24	2.210	0.246	0.300	-0.053
49	4.170	0.003	0.000	0.003	13	1.370	0.781	0.854	-0.073
50	4.240	0.002	0.000	0.002	4	0.661	0.001	0.077	-0.076
51	4.400	0.002	0.000	0.002	15	1.530	0.833	0.918	-0.085
52	4.440	0.002	0.000	0.002	14	1.450	0.807	0.893	-0.086
53	4.520	0.002	0.000	0.002	5	0.735	0.040	0.144	-0.104

END OF PROBLEM
==========

```
*****************************************************************************
*
*           NON-LINEAR  LEAST SQUARES ANALYSIS
*
*           SEMI-INFINITE PROFILE, 1-TYPE BC
*           DISTILLED CASE, SEMI-INF,TRITIUM, SHORT COLUMNS, pulse FIXED
*
*****************************************************************************
```

INITIAL VALUES OF COEFFFICIENTS

NO	NAME	INITIAL VALUE
1	PECLET	14.050
2	RF	1.100
3	PULSE	1.010

OBSERVED DATA

OBS.NO.	PORE VOLUME	CONCENTRATION
1	0.0602	0.0001
2	0.1300	0.0001
3	0.1990	0.0001
4	0.2700	0.0000
5	0.3400	0.0000
6	0.4110	0.0001
7	0.4770	0.0001
8	0.5460	0.0000
9	0.6140	0.0000
10	0.6830	0.0000
11	0.7520	0.0003
12	0.7870	0.0043
13	0.8260	0.0224
14	0.8570	0.0665
15	0.8900	0.1465
16	0.9580	0.4506
17	1.0100	0.3692
18	1.0800	0.5640
19	1.1500	0.6738
20	1.2100	0.8263
21	1.2900	0.6645
22	1.3600	0.6848
23	1.4400	0.8442
24	1.4600	0.6476
25	1.4900	0.8096
26	1.6000	0.7058
27	1.6300	0.7019
28	1.7100	0.6977
29	1.7700	0.7034
30	1.8400	0.7470
31	1.9100	0.6720
32	1.9800	0.3310
33	2.0500	0.1822
34	2.1200	0.0951
35	2.1900	0.0525
36	2.2600	0.0335
37	2.3300	0.0206
38	2.4000	0.0140
39	2.4700	0.0100

40	2.5300	0.0077
41	2.6000	0.0050
42	2.6700	0.0036
43	2.7400	0.0031
44	2.8000	0.0031
45	2.8800	0.0028
46	2.9500	0.0026
47	3.0200	0.0023
48	3.0900	0.0021
49	3.1500	0.0014
50	3.2200	0.0022
51	3.2900	0.0013
52	3.3600	0.0012
53	3.4300	0.0012
54	3.5000	0.0010
55	3.5700	0.0009
56	3.6400	0.0010
57	3.7100	0.0008
58	3.7800	0.0008
59	3.8500	0.0005
60	3.9900	0.0004
61	4.0400	0.0013
62	4.1100	0.0005

ITERATION	SSQ	PECLET	RF
0	0.9121380	14.05000	1.10000
1	0.8465284	17.94012	1.05858
2	0.8240184	21.36509	1.05238
3	0.8173378	23.61546	1.04692
4	0.8152644	25.02607	1.04376
5	0.8146228	25.87385	1.04191
6	0.8144278	26.37305	1.04084
7	0.8143715	26.66368	1.04022
8	0.8143571	26.83182	1.03986
9	0.8143547	26.92875	1.03966
10	0.8143547	26.93572	1.03964

CORRELATION MATRIX
==========

	1	2
1	1.0000	
2	-0.2600	1.0000

NON-LINEAR LEAST SQUARES ANALYSIS, FINAL RESUL TS

VARIABLE	NAME	VALUE	S.E.COEFF.	T-VALUE	95% CONFIDENCE LIMITS LOWER	UPPER
1	PECLET	26.93572	5.2487	5.13	16.4362	37.4352
2	RF	1.03964	0.0221	47.01	0.9954	1.0839

ORDERED BY COMPUTER INPUT

NO	PORE VOLUME	CONCENTRA TION OBS.	FITTED	RESI-DUAL
1	0.060	0.000	0.000	0.000
2	0.130	0.000	0.000	0.000
3	0.199	0.000	0.000	0.000
4	0.270	0.000	0.000	0.000
5	0.340	0.000	0.000	0.000
6	0.411	0.000	0.000	0.000
7	0.477	0.000	0.002	-0.002
8	0.546	0.000	0.011	-0.011
9	0.614	0.000	0.033	-0.033
10	0.683	0.000	0.076	-0.076
11	0.752	0.000	0.142	-0.142
12	0.787	0.004	0.184	-0.180
13	0.826	0.022	0.236	-0.213
14	0.857	0.066	0.280	-0.214
15	0.890	0.147	0.329	-0.183
16	0.958	0.451	0.433	0.018
17	1.010	0.369	0.511	-0.142
18	1.080	0.564	0.608	-0.044
19	1.150	0.674	0.694	-0.020
20	1.210	0.826	0.757	0.069
21	1.290	0.664	0.825	-0.161
22	1.360	0.685	0.871	-0.186
23	1.440	0.844	0.910	-0.066
24	1.460	0.648	0.918	-0.270
25	1.490	0.810	0.927	-0.118
26	1.500	0.706	0.936	-0.230
27	1.630	0.702	0.929	-0.227
28	1.710	0.698	0.887	-0.189
29	1.770	0.703	0.832	-0.129
30	1.840	0.747	0.747	0.000
31	1.910	0.672	0.648	0.024
32	1.980	0.331	0.544	-0.212
33	2.050	0.182	0.443	-0.260
34	2.120	0.095	0.351	-0.256
35	2.190	0.053	0.272	-0.219
36	2.260	0.033	0.206	-0.172
37	2.330	0.021	0.153	-0.133
38	2.400	0.014	0.112	-0.098
39	2.470	0.010	0.081	-0.071
40	2.530	0.008	0.061	-0.053
41	2.600	0.005	0.043	-0.038
42	2.670	0.004	0.030	-0.026
43	2.740	0.003	0.021	-0.018
44	2.800	0.003	0.015	-0.012
45	2.880	0.003	0.010	-0.007
46	2.950	0.003	0.007	-0.004
47	3.020	0.002	0.004	-0.002
48	3.090	0.002	0.003	-0.001

ORDERED BY RESIDUALS

NO	PORE VOLUME	CONCENTRATION OBS.	FITTED	RESI-DUAL
20	1.210	0.826	0.757	0.069
31	1.910	0.672	0.648	0.024
16	0.958	0.451	0.433	0.018
61	4.040	0.001	0.000	0.001
56	3.640	0.001	0.000	0.001
50	3.220	0.002	0.001	0.001
58	3.780	0.001	0.000	0.001
53	3.430	0.001	0.000	0.001
55	3.570	0.001	0.000	0.001
54	3.500	0.001	0.000	0.001
57	3.710	0.001	0.000	0.001
52	3.360	0.001	0.001	0.001
62	4.110	0.001	0.000	0.000
59	3.850	0.001	0.000	0.000
60	3.990	0.000	0.000	0.000
51	3.290	0.001	0.001	0.000
1	0.060	0.000	0.000	0.000
3	0.199	0.000	0.000	0.000
2	0.130	0.000	0.000	0.000
4	0.270	0.000	0.000	0.000
5	0.340	0.000	0.000	0.000
30	1.840	0.747	0.747	0.000
6	0.411	0.000	0.000	0.000
49	3.150	0.001	0.002	-0.001
48	3.090	0.002	0.003	-0.001
47	3.020	0.002	0.004	-0.002
7	0.477	0.000	0.002	-0.002
46	2.950	0.003	0.007	-0.004
45	2.880	0.003	0.010	-0.007
8	0.546	0.000	0.011	-0.011
44	2.800	0.003	0.015	-0.012
43	2.740	0.003	0.021	-0.018
19	1.150	0.674	0.694	-0.020
42	2.670	0.004	0.030	-0.026
9	0.614	0.000	0.033	-0.033
41	2.600	0.005	0.043	-0.038
18	1.080	0.564	0.608	-0.044
40	2.530	0.008	0.061	-0.053
23	1.440	0.844	0.910	-0.066
39	2.470	0.010	0.081	-0.071
10	0.683	0.000	0.076	-0.076
38	2.400	0.014	0.112	-0.098
25	1.490	0.810	0.927	-0.118
29	1.770	0.703	0.832	-0.129
37	2.330	0.021	0.153	-0.133
17	1.010	0.369	0.511	-0.142
11	0.752	0.000	0.142	-0.142
21	1.290	0.664	0.825	-0.161

49	3.150	0.001	0.002	-0.001
50	3.220	0.002	0.001	0.001
51	3.290	0.001	0.001	0.000
52	3.360	0.001	0.001	0.001
53	3.430	0.001	0.000	0.001
54	3.500	0.001	0.000	0.001
55	3.570	0.001	0.000	0.001
56	3.640	0.001	0.000	0.001
57	3.710	0.001	0.000	0.001
58	3.780	0.001	0.000	0.001
59	3.850	0.001	0.000	0.000
60	3.990	0.000	0.000	0.000
61	4.040	0.001	0.000	0.001
62	4.110	0.001	0.000	0.000

END OF PROBLEM
==========

36	2.260	0.033	0.206	-0.172
12	0.787	0.004	0.184	-0.180
15	0.890	0.147	0.329	-0.183
22	1.360	0.685	0.871	-0.186
28	1.710	0.698	0.887	-0.189
32	1.980	0.331	0.544	-0.212
13	0.826	0.022	0.236	-0.213
14	0.857	0.066	0.280	-0.214
35	2.190	0.053	0.272	-0.219
27	1.630	0.702	0.929	-0.227
26	1.600	0.706	0.936	-0.230
34	2.120	0.095	0.351	-0.256
33	2.050	0.182	0.443	-0.260
24	1.460	0.648	0.918	-0.270

```
*****************************************************************************
*
*          NON-LINEAR  LEAST SQUARES ANALYSIS
*
*          SEMI-INFINITE PROFILE, 3-TYPE BC
*          DISTILLED CASE, SEMI-INF,TRITIUM, SHORT COLUMNS, pulse FIXED
*
*****************************************************************************
```

OBSERVED DATA
==========

OBS.NO.	PORE VOLUME	CONCENTRATION
1	0.0602	0.0001
2	0.1300	0.0001
3	0.1990	0.0001
4	0.2700	0.0000
5	0.3400	0.0000
6	0.4110	0.0001
7	0.4770	0.0001
8	0.5460	0.0000
9	0.6140	0.0000
10	0.6830	0.0000
11	0.7520	0.0003
12	0.7870	0.0043
13	0.8260	0.0224
14	0.8570	0.0665
15	0.8900	0.1465
16	0.9580	0.4506
17	1.0100	0.3692
18	1.0800	0.5640
19	1.1500	0.6738
20	1.2100	0.8263
21	1.2900	0.6645
22	1.3600	0.6848
23	1.4400	0.8442
24	1.4600	0.6476
25	1.4900	0.8096
26	1.6000	0.7058
27	1.6300	0.7019
28	1.7100	0.6977
29	1.7700	0.7034
30	1.8400	0.7470
31	1.9100	0.6720
32	1.9800	0.3310
33	2.0500	0.1822
34	2.1200	0.0951
35	2.1900	0.0525
36	2.2600	0.0335
37	2.3300	0.0206
38	2.4000	0.0140
39	2.4700	0.0100
40	2.5300	0.0077
41	2.6000	0.0050
42	2.6700	0.0036
43	2.7400	0.0031
44	2.8000	0.0031
45	2.8800	0.0028
46	2.9500	0.0026
47	3.0200	0.0023

48	3.0900	0.0021
49	3.1500	0.0014
50	3.2200	0.0022
51	3.2900	0.0013
52	3.3600	0.0012
53	3.4300	0.0012
54	3.5000	0.0010
55	3.5700	0.0009
56	3.6400	0.0010
57	3.7100	0.0008
58	3.7800	0.0008
59	3.8500	0.0005
60	3.9900	0.0004
61	4.0400	0.0013
62	4.1100	0.0005

ITERATION	SSQ	PECLET	RF
0	1.0873994	14.05000	1.10000
1	0.8740356	15.50051	0.99374
2	0.8320760	19.60063	1.00726
3	0.8203205	22.27736	1.00394
4	0.8166384	24.06618	1.00294
5	0.8155017	25.16307	1.00225
6	0.8151583	25.81566	1.00184
7	0.8150596	26.19670	1.00161
8	0.8150344	26.41692	1.00147
9	0.8150301	26.54346	1.00139
10	0.8150301	26.56157	1.00138
11	0.8150301	26.56157	1.00138

CORRELATION MATRIX
==========

	1	2
1	1.0000	
2	0.0887	1.0000

NON-LINEAR LEAST SQUARES ANALYSIS, FINAL RESUL TS

VARIABLE	NAME	VALUE	S.E.COEFF.	T-VALUE	95% CONFIDENCE LIMITS LOWER	UPPER
1	PECLET	26.56157	5.3002	5.01	15.9590	37.1641
2	RF	1.00138	0.0206	48.53	0.9601	1.0427

ORDERED BY COMPUTER INPUT

NO	PORE VOLUME	CONCENTRA TION OBS.	FITTED	RESI-DUAL
1	0.060	0.000	0.000	0.000
2	0.130	0.000	0.000	0.000
3	0.199	0.000	0.000	0.000
4	0.270	0.000	0.000	0.000
5	0.340	0.000	0.000	0.000
6	0.411	0.000	0.000	0.000
7	0.477	0.000	0.002	-0.002
8	0.546	0.000	0.011	-0.011
9	0.614	0.000	0.033	-0.033
10	0.683	0.000	0.076	-0.076
11	0.752	0.000	0.142	-0.142
12	0.787	0.004	0.184	-0.180
13	0.826	0.022	0.236	-0.213
14	0.857	0.066	0.280	-0.214
15	0.890	0.147	0.329	-0.183
16	0.958	0.451	0.433	0.018
17	1.010	0.369	0.511	-0.142
18	1.080	0.564	0.609	-0.045
19	1.150	0.674	0.695	-0.021
20	1.210	0.826	0.758	0.069
21	1.290	0.664	0.826	-0.161
22	1.360	0.685	0.872	-0.187
23	1.440	0.844	0.911	-0.067
24	1.460	0.648	0.918	-0.271
25	1.490	0.810	0.928	-0.118
26	1.600	0.706	0.936	-0.231
27	1.630	0.702	0.930	-0.228
28	1.710	0.698	0.887	-0.189
29	1.770	0.703	0.832	-0.129
30	1.840	0.747	0.747	-0.001
31	1.910	0.672	0.648	0.024
32	1.980	0.331	0.544	-0.213
33	2.050	0.182	0.443	-0.260
34	2.120	0.095	0.351	-0.256
35	2.190	0.053	0.271	-0.219
36	2.260	0.033	0.205	-0.172
37	2.330	0.021	0.152	-0.132
38	2.400	0.014	0.111	-0.097
39	2.470	0.010	0.080	-0.070
40	2.530	0.008	0.060	-0.052
41	2.600	0.005	0.042	-0.037
42	2.670	0.004	0.029	-0.026
43	2.740	0.003	0.020	-0.017
44	2.800	0.003	0.015	-0.012
45	2.880	0.003	0.009	-0.007
46	2.950	0.003	0.006	-0.004
47	3.020	0.002	0.004	-0.002
48	3.090	0.002	0.003	-0.001

ORDERED BY RESIDUALS

NO	PORE VOLUME	CONCENTRATION OBS.	FITTED	RESI-DUAL
20	1.210	0.826	0.758	0.069
31	1.910	0.672	0.648	0.024
16	0.958	0.451	0.433	0.018
61	4.040	0.001	0.000	0.001
50	3.220	0.002	0.001	0.001
56	3.640	0.001	0.000	0.001
53	3.430	0.001	0.000	0.001
58	3.780	0.001	0.000	0.001
55	3.570	0.001	0.000	0.001
54	3.500	0.001	0.000	0.001
57	3.710	0.001	0.000	0.001
52	3.360	0.001	0.001	0.001
62	4.110	0.001	0.000	0.000
59	3.850	0.001	0.000	0.000
51	3.290	0.001	0.001	0.000
60	3.990	0.000	0.000	0.000
1	0.060	0.000	0.000	0.000
3	0.199	0.000	0.000	0.000
2	0.130	0.000	0.000	0.000
4	0.270	0.000	0.000	0.000
5	0.340	0.000	0.000	0.000
6	0.411	0.000	0.000	0.000
30	1.840	0.747	0.747	-0.001
49	3.150	0.001	0.002	-0.001
48	3.090	0.002	0.003	-0.001
47	3.020	0.002	0.004	-0.002
7	0.477	0.000	0.002	-0.002
46	2.950	0.003	0.006	-0.004
45	2.880	0.003	0.009	-0.007
8	0.546	0.000	0.011	-0.011
44	2.800	0.003	0.015	-0.012
43	2.740	0.003	0.020	-0.017
19	1.150	0.674	0.695	-0.021
42	2.670	0.004	0.029	-0.026
9	0.614	0.000	0.033	-0.033
41	2.600	0.005	0.042	-0.037
18	1.080	0.564	0.609	-0.045
40	2.530	0.008	0.060	-0.052
23	1.440	0.844	0.911	-0.067
39	2.470	0.010	0.080	-0.070
10	0.683	0.000	0.076	-0.076
38	2.400	0.014	0.111	-0.097
25	1.490	0.810	0.928	-0.118
29	1.770	0.703	0.832	-0.129
37	2.330	0.021	0.152	-0.132
17	1.010	0.369	0.511	-0.142
11	0.752	0.000	0.142	-0.142
21	1.290	0.664	0.826	-0.161

49	3.150	0.001	0.002	-0.001
50	3.220	0.002	0.001	0.001
51	3.290	0.001	0.001	0.000
52	3.360	0.001	0.001	0.001
53	3.430	0.001	0.000	0.001
54	3.500	0.001	0.000	0.001
55	3.570	0.001	0.000	0.001
56	3.640	0.001	0.000	0.001
57	3.710	0.001	0.000	0.001
58	3.780	0.001	0.000	0.001
59	3.850	0.001	0.000	0.000
60	3.990	0.000	0.000	0.000
61	4.040	0.001	0.000	0.001
62	4.110	0.001	0.000	0.000

36	2.260	0.033	0.205	-0.172
12	0.787	0.004	0.184	-0.180
15	0.890	0.147	0.329	-0.183
22	1.360	0.685	0.872	-0.187
28	1.710	0.698	0.887	-0.189
32	1.980	0.331	0.544	-0.213
13	0.826	0.022	0.236	-0.213
14	0.857	0.066	0.280	-0.214
35	2.190	0.053	0.271	-0.219
27	1.630	0.702	0.930	-0.228
26	1.600	0.706	0.936	-0.231
34	2.120	0.095	0.351	-0.256
33	2.050	0.182	0.443	-0.260
24	1.460	0.648	0.918	-0.271

END OF PROBLEM
==========

```
*********************************************************************
*
*          NON-LINEAR  LEAST SQUARES ANALYSIS
*
*          SEMI-INFINITE PROFILE, 1-TYPE BC  PULSE
*CANO3 CASE, SHORT COLUMN, TR, SI-BC#1, ~~NO COEF~~. FIXED
*
*********************************************************************
```

INITIAL VALUES OF COEFFFICIENTS

NO	NAME	INITIAL VALUE
1	PECLET	14.050
2	RF	1.130
3	PULSE	1.040

OBSERVED DATA

OBS.NO.	PORE VOLUME	CONCENTRATION
1	0.0527	0.0000
2	0.1290	0.0001
3	0.2050	0.0000
4	0.2810	0.0000
5	0.3570	0.0000
6	0.4420	0.0000
7	0.5130	0.0000
8	0.5880	0.0000
9	0.6610	0.0002
10	0.6980	0.0030
11	0.7350	0.0216
12	0.7720	0.0512
13	0.8100	0.1250
14	0.8890	0.3455
15	0.9590	0.5116
16	1.0300	0.6167
17	1.0800	0.5289
18	1.1300	0.5626
19	1.2200	0.6751
20	1.3000	0.7341
21	1.3700	0.6031
22	1.4100	0.6624
23	1.4500	0.6931
24	1.4900	0.6129
25	1.5300	0.7409
26	1.6200	0.7648
27	1.6900	0.7306
28	1.7600	0.8048
29	1.8400	0.8560
30	1.8800	0.8609
31	1.9200	0.5971
32	1.9800	0.5240
33	2.0600	0.3994
34	2.1400	0.3375
35	2.2100	0.2629
36	2.2900	0.1526
37	2.3600	0.1158
38	2.4400	0.0867
39	2.5100	0.0745

40	2.5900	0.0561
41	2.6700	0.0463
42	2.7400	0.0491
43	2.8100	0.0402
44	2.8800	0.0326
45	2.9600	0.0259
46	3.0300	0.0199
47	3.1100	0.0173
48	3.1800	0.0129
49	3.2700	0.0109
50	3.3400	0.0080
51	3.4200	0.0063
52	3.5000	0.0049
53	3.5700	0.0046
54	3.6400	0.0023
55	3.7200	0.0022
56	3.7900	0.0021
57	3.8700	0.0014
58	3.9400	0.0015
59	4.0200	0.0011
60	4.0900	0.0017
61	4.1700	0.0009
62	4.2400	0.0007
63	4.3200	0.0005
64	4.4000	0.0005
65	4.4400	0.0005
66	4.5200	0.0005

ITERATION	SSQ	PECLET	RF
0	0.4083010	14.05000	1.13000
1	0.3985582	15.72349	1.11606
2	0.3978896	16.24501	1.11342
3	0.3978584	16.35372	1.11253
4	0.3978572	16.37832	1.11232
5	0.3978572	16.38108	1.11230

CORRELATION MATRIX
==========

	1	2
1	1.0000	
2	-0.3161	1.0000

NON-LINEAR LEAST SQUARES ANALYSIS, FINAL RESUL TS
==========

VARIABLE	NAME	VALUE	S.E.COEFF.	T-VALUE	95% CONFIDENCE LIMITS LOWER	UPPER
1	PECLET	16.38108	1.8273	8.96	12.7304	20.0318
2	RF	1.11230	0.0196	56.85	1.0732	1.1514

ORDERED BY COMPUTER INPUT

NO	PORE VOLUME	CONCENTRA TION OBS.	FITTED	RESI-DUAL
1	0.053	0.000	0.000	0.000
2	0.129	0.000	0.000	0.000
3	0.205	0.000	0.000	0.000
4	0.281	0.000	0.000	0.000

ORDERED BY RESIDUALS

NO	PORE VOLUME	CONCENTRATION OBS.	FITTED	RESI-DUAL
30	1.880	0.861	0.698	0.163
16	1.030	0.617	0.479	0.138
29	1.840	0.856	0.736	0.120
15	0.959	0.512	0.397	0.114

5	0.357	0.000	0.000	0.000
6	0.442	0.000	0.005	-0.005
7	0.513	0.000	0.016	-0.016
8	0.588	0.000	0.043	-0.043
9	0.661	0.000	0.087	-0.087
10	0.698	0.003	0.116	-0.113
11	0.735	0.022	0.149	-0.127
12	0.772	0.051	0.185	-0.134
13	0.810	0.125	0.225	-0.100
14	0.889	0.345	0.315	0.030
15	0.959	0.512	0.397	0.114
16	1.030	0.617	0.479	0.138
17	1.080	0.529	0.534	-0.005
18	1.130	0.563	0.586	-0.023
19	1.220	0.675	0.670	0.005
20	1.300	0.734	0.734	0.000
21	1.370	0.603	0.781	-0.178
22	1.410	0.662	0.805	-0.142
23	1.450	0.693	0.825	-0.132
24	1.490	0.613	0.841	-0.228
25	1.530	0.741	0.853	-0.112
26	1.620	0.765	0.858	-0.093
27	1.690	0.731	0.839	-0.108
28	1.760	0.805	0.800	0.005
29	1.840	0.856	0.736	0.120
30	1.880	0.861	0.698	0.163
31	1.920	0.597	0.657	-0.060
32	1.980	0.524	0.594	-0.070
33	2.060	0.399	0.509	-0.109
34	2.140	0.338	0.427	-0.090
35	2.210	0.263	0.361	-0.099
36	2.290	0.153	0.295	-0.142
37	2.360	0.116	0.244	-0.128
38	2.440	0.087	0.194	-0.108
39	2.510	0.074	0.158	-0.084
40	2.590	0.056	0.124	-0.068
41	2.670	0.046	0.097	-0.050
42	2.740	0.049	0.077	-0.028
43	2.810	0.040	0.061	-0.021
44	2.880	0.033	0.049	-0.016
45	2.960	0.026	0.037	-0.011
46	3.030	0.020	0.029	-0.009
47	3.110	0.017	0.022	-0.005
48	3.180	0.013	0.017	-0.005
49	3.270	0.011	0.013	-0.002
50	3.340	0.008	0.010	-0.002
51	3.420	0.006	0.007	-0.001
52	3.500	0.005	0.006	-0.001
53	3.570	0.005	0.004	0.000
54	3.640	0.002	0.003	-0.001
55	3.720	0.002	0.003	0.000
56	3.790	0.002	0.002	0.000
57	3.870	0.001	0.001	0.000
58	3.940	0.002	0.001	0.000
59	4.020	0.001	0.001	0.000
60	4.090	0.002	0.001	0.001
61	4.170	0.001	0.000	0.000
62	4.240	0.001	0.000	0.000
63	4.320	0.001	0.000	0.000
64	4.400	0.001	0.000	0.000

14	0.889	0.345	0.315	0.030
19	1.220	0.675	0.670	0.005
28	1.760	0.805	0.800	0.005
60	4.090	0.002	0.001	0.001
61	4.170	0.001	0.000	0.000
20	1.300	0.734	0.734	0.000
58	3.940	0.002	0.001	0.000
66	4.520	0.000	0.000	0.000
62	4.240	0.001	0.000	0.000
65	4.440	0.000	0.000	0.000
64	4.400	0.001	0.000	0.000
59	4.020	0.001	0.001	0.000
53	3.570	0.005	0.004	0.000
63	4.320	0.001	0.000	0.000
56	3.790	0.002	0.002	0.000
2	0.129	0.000	0.000	0.000
1	0.053	0.000	0.000	0.000
3	0.205	0.000	0.000	0.000
57	3.870	0.001	0.001	0.000
4	0.281	0.000	0.000	0.000
55	3.720	0.002	0.003	0.000
5	0.357	0.000	0.000	0.000
52	3.500	0.005	0.006	-0.001
54	3.640	0.002	0.003	-0.001
51	3.420	0.006	0.007	-0.001
49	3.270	0.011	0.013	-0.002
50	3.340	0.008	0.010	-0.002
48	3.180	0.013	0.017	-0.005
6	0.442	0.000	0.005	-0.005
47	3.110	0.017	0.022	-0.005
17	1.080	0.529	0.534	-0.005
46	3.030	0.020	0.029	-0.009
45	2.960	0.026	0.037	-0.011
44	2.880	0.033	0.049	-0.016
7	0.513	0.000	0.016	-0.016
43	2.810	0.040	0.061	-0.021
18	1.130	0.563	0.586	-0.023
42	2.740	0.049	0.077	-0.028
8	0.588	0.000	0.043	-0.043
41	2.670	0.046	0.097	-0.050
31	1.920	0.597	0.657	-0.060
40	2.590	0.056	0.124	-0.068
32	1.980	0.524	0.594	-0.070
39	2.510	0.074	0.158	-0.084
9	0.661	0.000	0.087	-0.087
34	2.140	0.338	0.427	-0.090
26	1.620	0.765	0.858	-0.093
35	2.210	0.263	0.361	-0.099
13	0.810	0.125	0.225	-0.100
38	2.440	0.087	0.194	-0.108
27	1.690	0.731	0.839	-0.108
33	2.060	0.399	0.509	-0.109
25	1.530	0.741	0.853	-0.112
10	0.698	0.003	0.116	-0.113
11	0.735	0.022	0.149	-0.127
37	2.360	0.116	0.244	-0.128
23	1.450	0.693	0.825	-0.132
12	0.772	0.051	0.185	-0.134
36	2.290	0.153	0.295	-0.142
22	1.410	0.662	0.805	-0.142

65	4.440	0.000	0.000	0.000	21	1.370	0.603	0.781	-0.178
66	4.520	0.000	0.000	0.000	24	1.490	0.613	0.841	-0.228

END OF PROBLEM
==========

```
*****************************************************************************
*                                                                           *
*          NON-LINEAR  LEAST SQUARES ANALYSIS                               *
*                                                                           *
*          SEMI-INFINITE PROFILE, 3-TYPE BC                                 *
*cano3 case, short column, si-bc#3, tr, no coef. fixed                      *
*                                                                           *
*****************************************************************************
```

OBSERVED DATA
==========

OBS.NO.	PORE VOLUME	CONCENTRATION
1	0.0527	0.0000
2	0.1290	0.0001
3	0.2050	0.0000
4	0.2810	0.0000
5	0.3570	0.0000
6	0.4420	0.0000
7	0.5130	0.0000
8	0.5880	0.0000
9	0.6610	0.0002
10	0.6980	0.0030
11	0.7350	0.0216
12	0.7720	0.0512
13	0.8100	0.1250
14	0.8890	0.3455
15	0.9590	0.5116
16	1.0300	0.6167
17	1.0800	0.5289
18	1.1300	0.5626
19	1.2200	0.6751
20	1.3000	0.7341
21	1.3700	0.6031
22	1.4100	0.6624
23	1.4500	0.6931
24	1.4900	0.6129
25	1.5300	0.7409
26	1.6200	0.7648
27	1.6900	0.7306
28	1.7600	0.8048
29	1.8400	0.8560
30	1.8800	0.8609
31	1.9200	0.5971
32	1.9800	0.5240
33	2.0600	0.3994
34	2.1400	0.3375
35	2.2100	0.2629
36	2.2900	0.1526
37	2.3600	0.1158
38	2.4400	0.0867
39	2.5100	0.0745
40	2.5900	0.0561

41	2.6700	0.0463
42	2.7400	0.0491
43	2.8100	0.0402
44	2.8800	0.0326
45	2.9600	0.0259
46	3.0300	0.0199
47	3.1100	0.0173
48	3.1800	0.0129
49	3.2700	0.0109
50	3.3400	0.0080
51	3.4200	0.0063
52	3.5000	0.0049
53	3.5700	0.0040
54	3.6400	0.0023
55	3.7200	0.0022
56	3.7900	0.0021
57	3.8700	0.0014
58	3.9400	0.0015
59	4.0200	0.0011
60	4.0900	0.0017
61	4.1700	0.0009
62	4.2400	0.0007
63	4.3200	0.0005
64	4.4000	0.0005
65	4.4400	0.0005
66	4.5200	0.0005

ITERATION	SSQ	PECLET	RF
0	0.5317237	14.05000	1.13000
1	0.4072428	13.93770	1.04164
2	0.3998415	15.52341	1.04755
3	0.3994771	15.86985	1.04594
4	0.3994611	15.95501	1.04565
5	0.3994610	15.97355	1.04557
6	0.3994610	15.97355	1.04557

CORRELATION MATRIX
==========

	1	2
1	1.0000	
2	0.0880	1.0000

NON-LINEAR LEAST SQUARES ANALYSIS, FINAL RESUL TS
==========

VARIABLE	NAME	VALUE	S.E.COEFF.	T-VALUE	95% CONFIDENCE LIMITS LOWER	UPPER
1	PECLET	15.97355	1.8388	8.69	12.3000	19.6471
2	RF	1.04557	0.0175	59.65	1.0106	1.0806

ORDERED BY COMPUTER INPUT

NO	PORE VOLUME	CONCENTRA TION OBS.	FITTED	RESI-DUAL
1	0.053	0.000	0.000	0.000
2	0.129	0.000	0.000	0.000
3	0.205	0.000	0.000	0.000
4	0.281	0.000	0.000	0.000

ORDERED BY RESIDUALS

NO	PORE VOLUME	CONCENTRATION OBS.	FITTED	RESI-DUAL
30	1.880	0.861	0.698	0.163
16	1.030	0.617	0.479	0.138
29	1.840	0.856	0.736	0.120
15	0.959	0.512	0.397	0.114

5	0.357	0.000	0.001	-0.001
6	0.442	0.000	0.005	-0.005
7	0.513	0.000	0.017	-0.017
8	0.588	0.000	0.044	-0.044
9	0.661	0.000	0.088	-0.088
10	0.698	0.003	0.117	-0.114
11	0.735	0.022	0.149	-0.128
12	0.772	0.051	0.186	-0.134
13	0.810	0.125	0.226	-0.101
14	0.889	0.345	0.315	0.030
15	0.959	0.512	0.397	0.114
16	1.030	0.617	0.479	0.138
17	1.080	0.529	0.534	-0.005
18	1.130	0.563	0.586	-0.023
19	1.220	0.675	0.670	0.005
20	1.300	0.734	0.734	0.000
21	1.370	0.603	0.782	-0.179
22	1.410	0.662	0.805	-0.143
23	1.450	0.693	0.825	-0.132
24	1.490	0.613	0.842	-0.229
25	1.530	0.741	0.853	-0.112
26	1.620	0.765	0.858	-0.093
27	1.690	0.731	0.839	-0.108
28	1.760	0.805	0.800	0.005
29	1.840	0.856	0.736	0.120
30	1.880	0.861	0.698	0.163
31	1.920	0.597	0.658	-0.061
32	1.980	0.524	0.595	-0.071
33	2.060	0.399	0.510	-0.110
34	2.140	0.338	0.428	-0.090
35	2.210	0.263	0.362	-0.099
36	2.290	0.153	0.295	-0.142
37	2.360	0.116	0.244	-0.128
38	2.440	0.087	0.194	-0.107
39	2.510	0.074	0.158	-0.083
40	2.590	0.056	0.123	-0.067
41	2.670	0.046	0.096	-0.050
42	2.740	0.049	0.076	-0.027
43	2.810	0.040	0.061	-0.020
44	2.880	0.033	0.048	-0.015
45	2.960	0.026	0.036	-0.011
46	3.030	0.020	0.029	-0.009
47	3.110	0.017	0.022	-0.004
48	3.180	0.013	0.017	-0.004
49	3.270	0.011	0.012	-0.001
50	3.340	0.008	0.009	-0.001
51	3.420	0.006	0.007	-0.001
52	3.500	0.005	0.005	0.000
53	3.570	0.005	0.004	0.001
54	3.640	0.002	0.003	-0.001
55	3.720	0.002	0.002	0.000
56	3.790	0.002	0.002	0.000
57	3.870	0.001	0.001	0.000
58	3.940	0.002	0.001	0.000
59	4.020	0.001	0.001	0.000
60	4.090	0.002	0.001	0.001
61	4.170	0.001	0.000	0.001
62	4.240	0.001	0.000	0.000
63	4.320	0.001	0.000	0.000
64	4.400	0.001	0.000	0.000

14	0.889	0.345	0.315	0.030
19	1.220	0.675	0.670	0.005
28	1.760	0.805	0.800	0.005
60	4.090	0.002	0.001	0.001
53	3.570	0.005	0.004	0.001
61	4.170	0.001	0.000	0.001
58	3.940	0.002	0.001	0.000
62	4.240	0.001	0.000	0.000
66	4.520	0.000	0.000	0.000
59	4.020	0.001	0.001	0.000
64	4.400	0.001	0.000	0.000
65	4.440	0.000	0.000	0.000
56	3.790	0.002	0.002	0.000
63	4.320	0.001	0.000	0.000
57	3.870	0.001	0.001	0.000
2	0.129	0.000	0.000	0.000
20	1.300	0.734	0.734	0.000
1	0.053	0.000	0.000	0.000
3	0.205	0.000	0.000	0.000
4	0.281	0.000	0.000	0.000
55	3.720	0.002	0.002	0.000
52	3.500	0.005	0.005	0.000
5	0.357	0.000	0.001	-0.001
51	3.420	0.006	0.007	-0.001
54	3.640	0.002	0.003	-0.001
49	3.270	0.011	0.012	-0.001
50	3.340	0.008	0.009	-0.001
48	3.180	0.013	0.017	-0.004
47	3.110	0.017	0.022	-0.004
6	0.442	0.000	0.005	-0.005
17	1.080	0.529	0.534	-0.005
46	3.030	0.020	0.029	-0.009
45	2.960	0.026	0.036	-0.011
44	2.880	0.033	0.048	-0.015
7	0.513	0.000	0.017	-0.017
43	2.810	0.040	0.061	-0.020
18	1.130	0.563	0.586	-0.023
42	2.740	0.049	0.076	-0.027
8	0.588	0.000	0.044	-0.044
41	2.670	0.046	0.096	-0.050
31	1.920	0.597	0.658	-0.061
40	2.590	0.056	0.123	-0.067
32	1.980	0.524	0.595	-0.071
39	2.510	0.074	0.158	-0.083
9	0.661	0.000	0.088	-0.088
34	2.140	0.338	0.428	-0.090
26	1.620	0.765	0.858	-0.093
35	2.210	0.263	0.362	-0.099
13	0.810	0.125	0.226	-0.101
38	2.440	0.087	0.194	-0.107
27	1.690	0.731	0.839	-0.108
33	2.060	0.399	0.510	-0.110
25	1.530	0.741	0.853	-0.112
10	0.698	0.003	0.117	-0.114
11	0.735	0.022	0.149	-0.128
37	2.360	0.116	0.244	-0.128
23	1.450	0.693	0.825	-0.132
12	0.772	0.051	0.186	-0.134
36	2.290	0.153	0.295	-0.142
22	1.410	0.662	0.805	-0.143

65	4.440	0.000	0.000	0.000	21	1.370	0.603	0.782	-0.179
66	4.520	0.000	0.000	0.000	24	1.490	0.613	0.842	-0.229

END OF PROBLEM

APPENDIX G.

MOLECULAR DIFFUSION EXPERIMENT

A diffusion experiment was conducted with the beach sand fraction of the copper mill tailings to determine the molecular diffusion coefficient for bromide in the tailings medium, under saturated conditions.

The copper tailings were screened through a number 16 sieve to remove aggregates and then air-dried to a 1-3% mass wetness. Two 5.0 cm X 30.0 cm columns were packed with a funnel and tube arrangement, through which the tailings were poured. As the tailings were poured, the side of the column was tapped to settle the contents to a dry bulk density of 1.44 g/cc.

The columns were saturated with distilled water by placing them in containers and allowing water to infiltrate through the bottom. After saturation was achieved, the bottom hose was clamped off, and water at the top of the column was siphoned off. Two centimeters of tracer-laden water (1.00E-01 M. bromide from $CaBr_2.H_2O$ solid dissolved in distilled water) was then placed at the top of the soil column and the column was sealed. The tracer solution was replenished once a week, but otherwise the columns were left undisturbed. After a period of approximately seven weeks (52 days for one column, 51 days for the second), the columns were sampled for bromide.

Sampling of the column was accomplished in the following manner. The soil in the column was sampled in increments (generally 2 cm) which were weighed and oven-dried (24 hours at

105°C) to obtain the gravimetric water contents. A measured volume (100 ml) of distilled water was added to each sample, stirred, and allowed to sit for 24 hours. This solution was then analyzed for free bromide concentration by means of a Orion Specific Ion Electrode. The number of moles of bromide were then calculated and divided by the mass of water originally held in the sampled section (determined by the previously mentioned oven drying), in order to calculate the bromide concentration of the sampled section. Corrections were made to the bromide concentration to account for complexation (see Tracer Selection section of this paper). The water content and bromide concentration data are tabulated in Table 14.

Table 14. Gravimetric water content, measured bromide concentraion, corrected bromide concentration at each depth, from column diffusion experiment. Original concentration is 1.00E-01 moles/liter.

	Depth (cm)	Water Content (%)	Concentration (meas., M/L)	Concentratn. (Corr., C/C_o)
COLUMN I:				
	1.0	30.0	1.33E-01	1.20E-02
	3.0	28.0	8.68E-02	6.27E-02
	5.1	29.0	4.95E-02	3.43E-02
	7.1	30.0	3.96E-02	2.70E-02
	9.0	33.0	3.51E-02	2.37E-02
	11.0	32.0	2.39E-02	1.57E-02
	13.0	30.0	1.85E-02	1.19E-02
	15.0	30.0	8.20E-03	4.96E-03
	17.0	29.0	1.02E-02	6.28E-03
	19.2	26.0	4.45E-03	2.60E-03
	21.5	29.0	2.86E-03	1.60E-03
	23.6	28.0	1.84E-03	9.94E-04
	25.7	27.0	1.24E-03	6.52E-04
	27.2	27.0	1.40E-03	7.44E-04
COLUMN II:				
	1.0	31.0	1.08E-01	7.96E-02
	3.0	30.0	8.20E-02	5.91E-02
	4.1	30.0	6.66E-02	4.72E-02
	7.1	30.0	4.30E-02	2.95E-02
	9.0	30.0	3.22E-02	2.16E-02
	11.0	31.0	2.17E-02	1.41E-02
	13.0	29.0	1.49E-02	9.48E-03
	15.0	28.0	1.19E-02	7.41E-03
	17.0	29.0	8.54E-03	5.18E-03
	19.3	29.0	5.47E-03	3.21E-03
	21.6	29.0	3.34E-03	1.89E-03
	23.7	28.0	3.29E-03	1.86E-03
	25.2	27.0	1.97E-03	1.07E-03
	27.2	27.0	3.19E-03	1.80E-03

The moles of bromide were plotted in Figures 49 and 50 in terms of relative concentrations versus depth of the column. Also shown in Figures 49 and 50 are curves generated by an analytical solution for varying the diffusion coefficient values. The analytical solution (Saxena et al., 1974), assuming a semi-infinite column length and a constant-concentration inlet boundary condition was:

$$C/C_o = \text{erfc}\ (z/2(D*t^{1/2})) \qquad \text{(G1)}$$

where z was depth, D was the diffusion coefficient, t was time, C was the measured concentration, and Co was the original input concentration.

It can be seen that no one curve fits the concentration values along the entire column depth. In addition, concentration measurements made at the column bottom show the tracer reached the bottom boundary during the experiment, which was inconsistent with the boundary conditions of the analytical solution.

Figures 49 and 50 each show a curve which was hand fitted to the observed measurements. These fitted curves yielded an approximate diffusion coefficient between 0.80 and 0.90 cm2/day, when fitted to the analytical curves of both columns. A final diffusion coefficient of 0.80 cm^2/day was determined by considering the upper half of the column measurements more valid, since these were not as affected by the aforementioned problem with the lower boundary.

In conclusion, the diffusion coefficient obtained for this saturated material ranged between 0.80 and 0.90 cm^2/day.

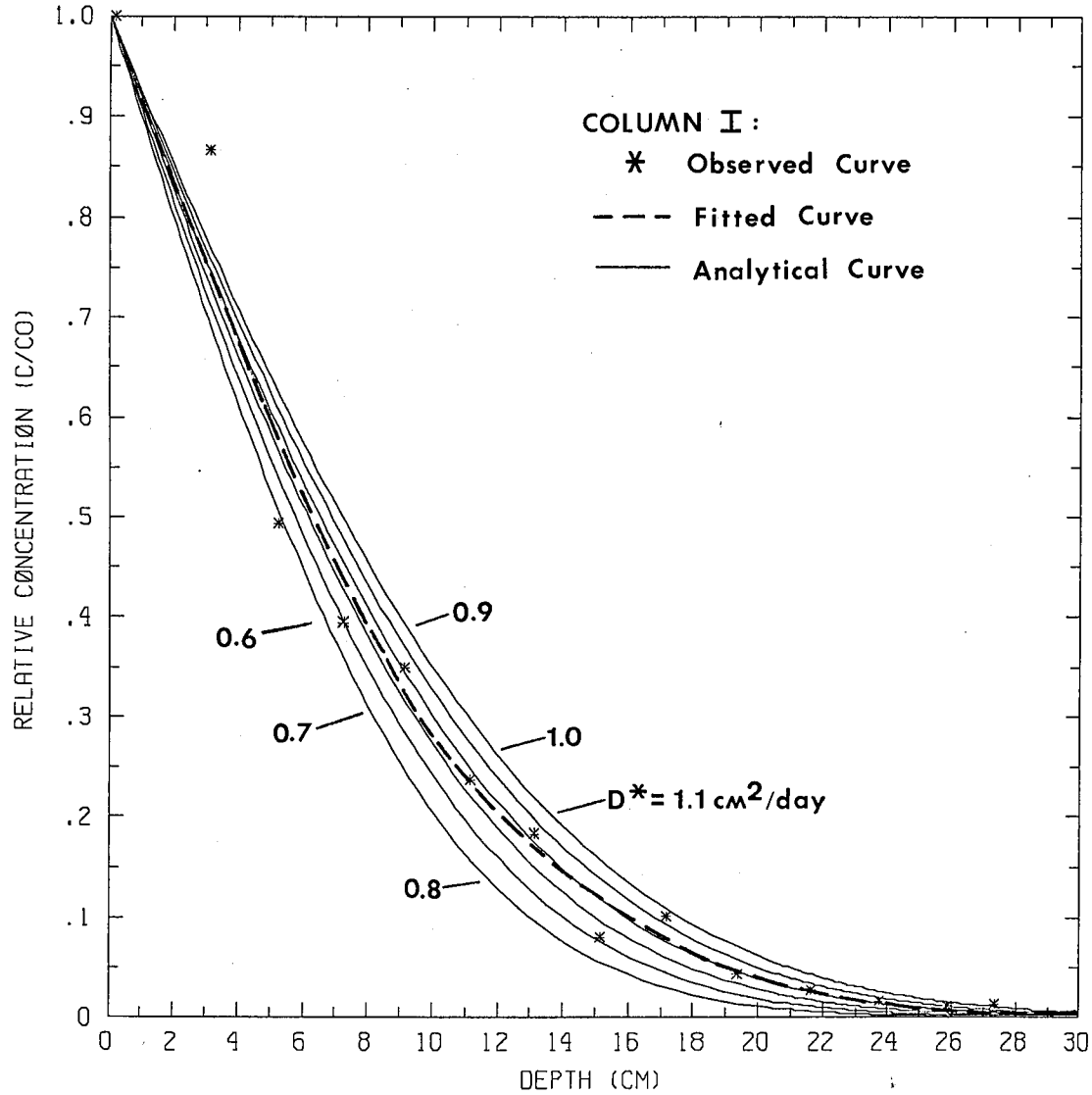

Figure 49. Relative bromide concentration versus depth, from diffusion experiment, Column I. Analytical curves generated for varying values of molecular diffusion coefficient are also shown. A molecular diffusion coefficient of 0.80 cm^2/day was determined.

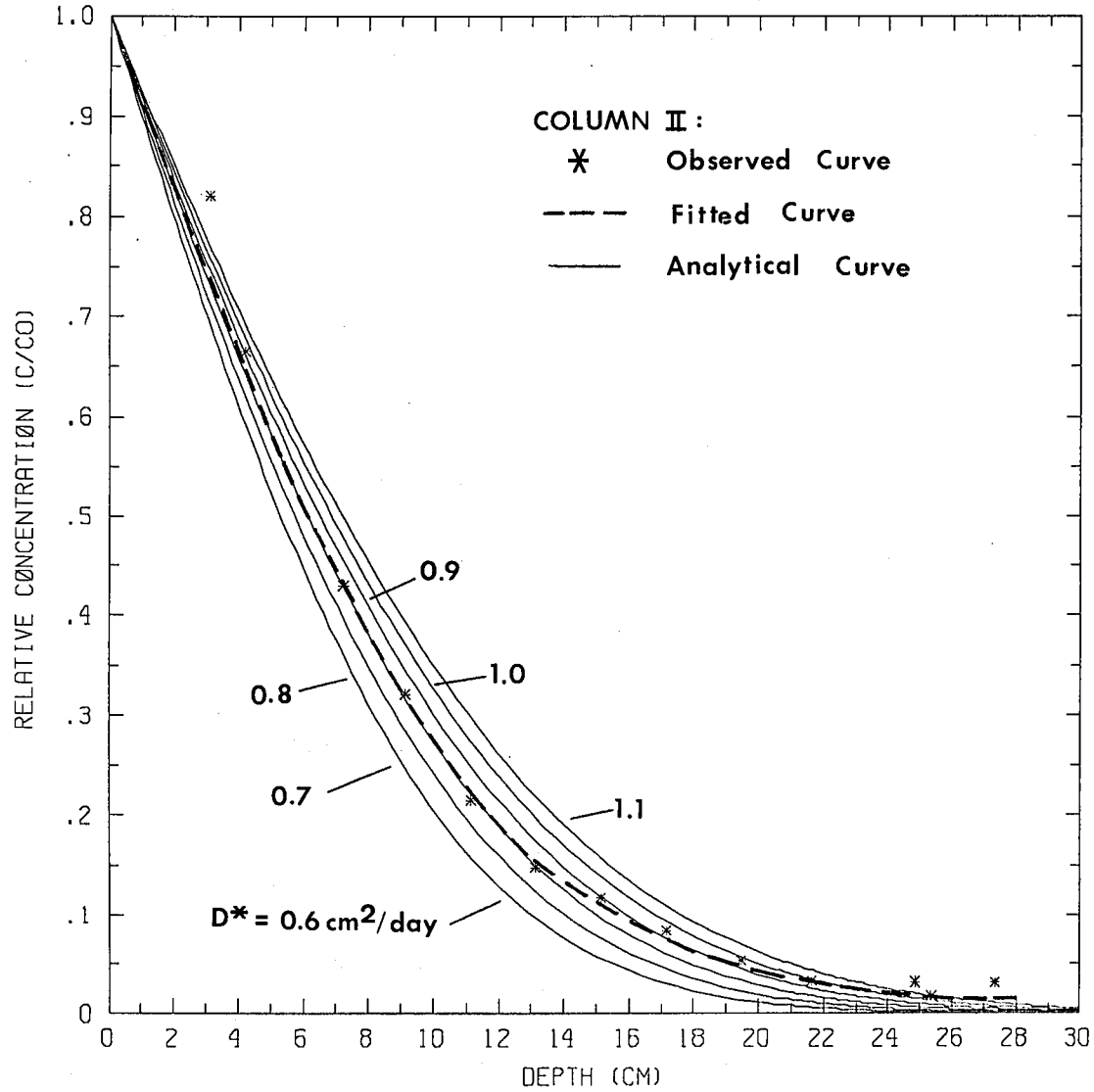

Figure 50. Relative bromide concentration versus depth, from diffusion experiment, Column II. Analytical curves generated for varying values of molecular diffusion coefficients are also shown. A molecular diffusion coefficient of 0.80 cm^2/day was determined.

However, the bromide found at the bottom of the column may well have influenced measurements in the lower part of the column, and thus the upper column measurements were given more weight when curve-fitting to the analytical solution. With this in mind, a final diffusion coefficient of 0.80 cm^2/day was determined. The experiment could have been improved by keeping the concentration constant at the upper boundary, and by termination of the experiment earlier to insure no bromide reached the lower boundary.

Appendix H.

SATURATED LONG-COLUMN SOLUTE-DISPLACEMENT EXPERIMENT

Lewis (1984) conducted a saturated solute-displacement experiment, using a long soil-column (335cm) and the beach sand fraction of the copper-mill tailings as a porous medium. The packing procedure was identical to that of the long-column unsaturated experiment, discussed in the Procedures section of the long-column experiment under unsaturated flow conditions, with 5 cm increments packed to a 1.45 g/cc dry bulk density. A reservoir and float valve assemblage fed distilled water and the tracer solution into the column, and maintained a constant height of ponding of 24 cm above the tailings surface.

Initially, the column was leached with distilled water. Effluent samples were collected and analyzed for copper, iron and sulfate concentrations as well as pH, temperature and electrical conductivity. One pore volume of a 1.0E-01 M bromide solution was introduced to the column after 10 days of leaching at a flux of 8.0E-04 cm/sec, and the effluent was analyzed during the bromide displacement.

Figure 51 shows the comparitive results of copper, total iron and sulfate, plotted as relative concentration versus pore volumes. The results of the bromide displacement were also included for comparison. All leached ions show a rapid decrease in concentration until a relatively constant concentration is reached at 0.6 pore volumes. Figure 52 shows a plot of electrical conductivity versus pore volumes. The shape of the electrical conductivity decrease is similar to that of the leached ion

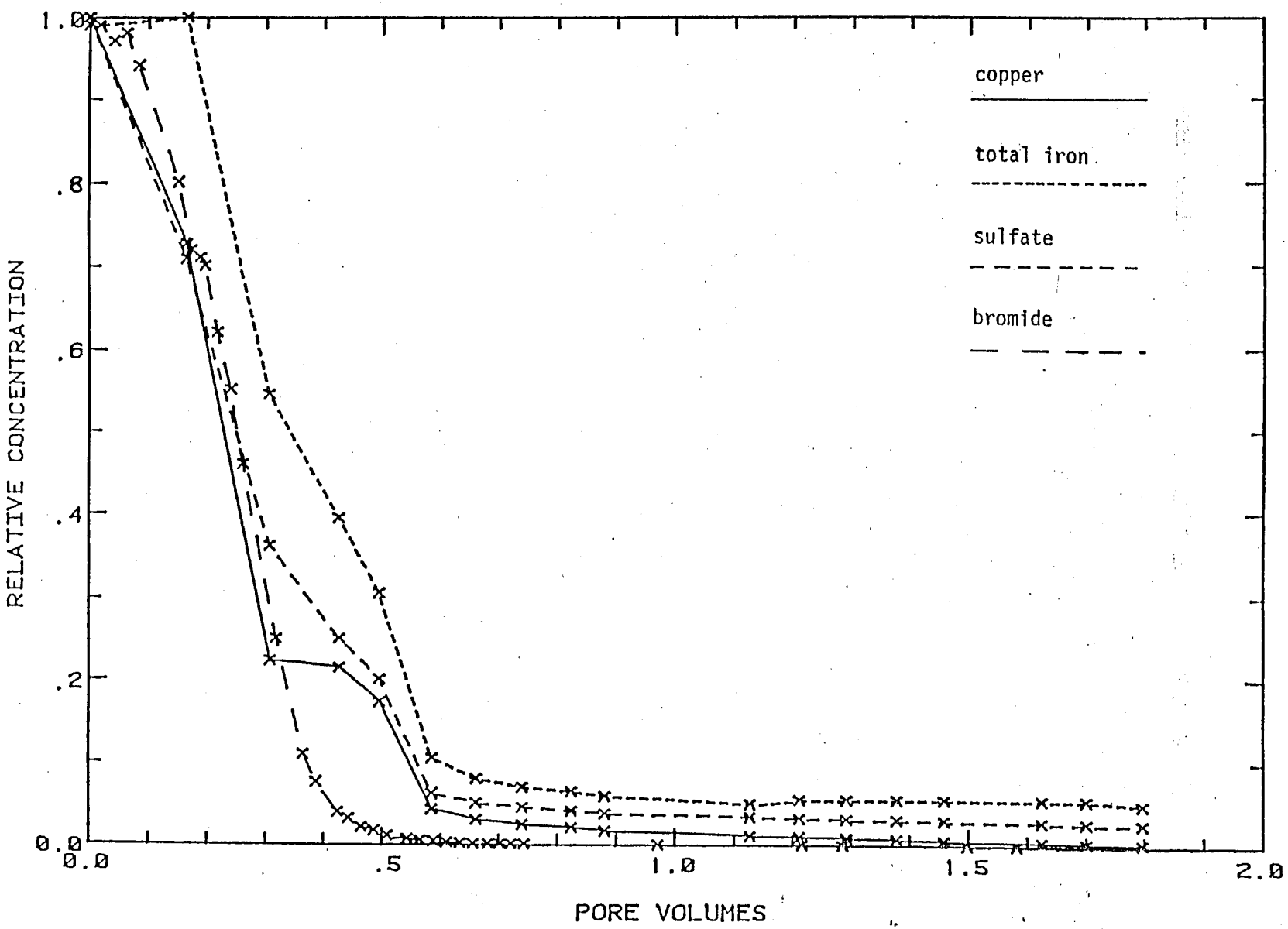

Figure 51. Relative concentration versus pore volumes from long-column leaching experiment (Cu, Fe, SO_4) and solute displacement experiment (Br). (from Lewis, 1986)

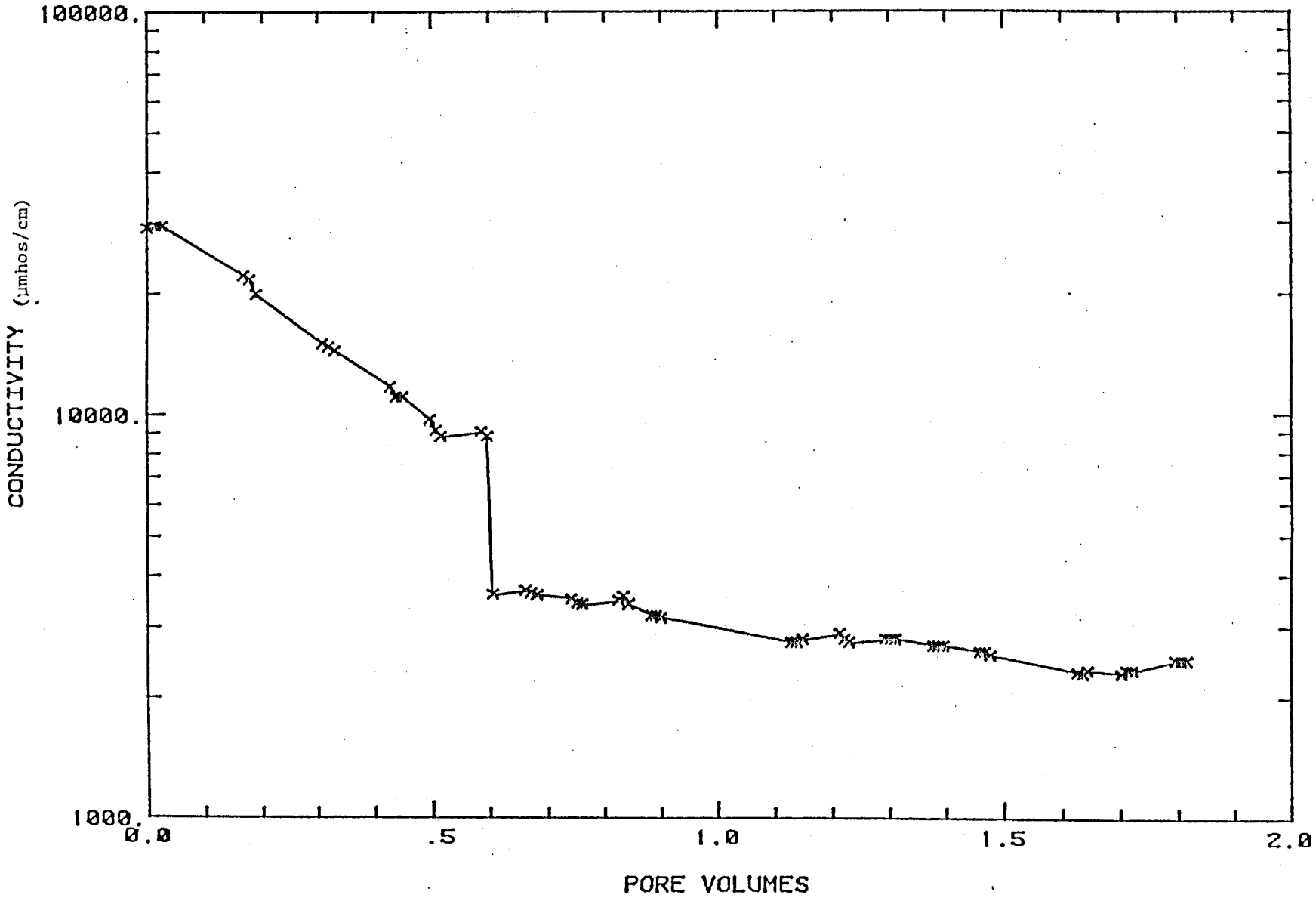

Figure 52. Electrical conductivity (logarithmic) of effluent versus pore volumes from long-column leaching experiment under saturated flow conditions. (from Lewis, 1986)

concentration decrease, both leveling off at about 0.6 pore volumes.

The bromide breadthrough curve is shown in Figure 53. A dispersivity of 2.17 cm was determined from the breakthrough curve using the CFITM non-linear, least-squares curve-fitting program (van Genuchten, 1980). A three parameter fit was obtained for the retardation factor (R) of 1.06, the column Peclet number (P_c) of 149.08, and a dimensionless pulse length (T') of 1.12. Minimal retardation was observed which suggested that bromide served as an excellent tracer.

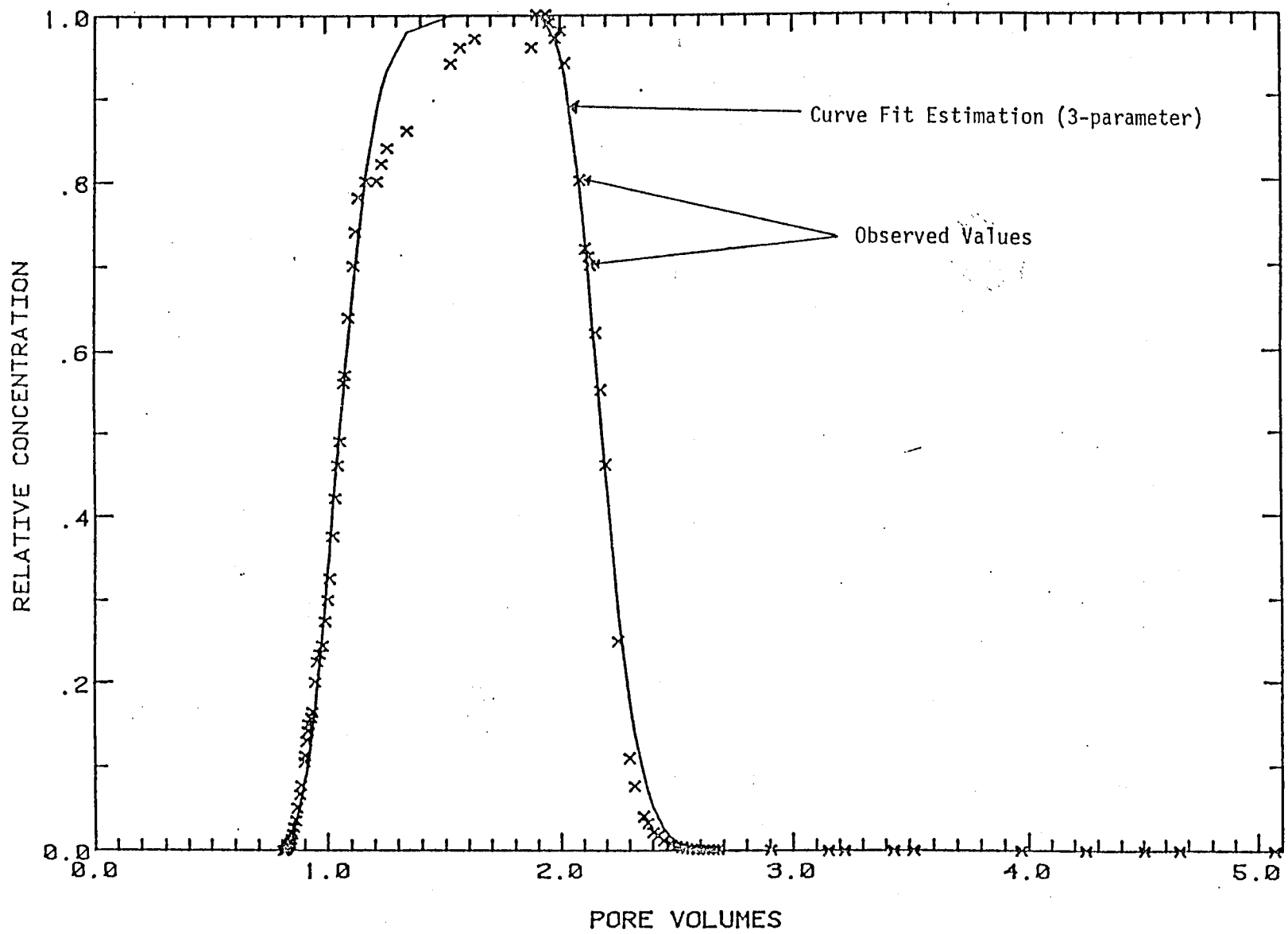

Figure 53. Relative bromide concentration versus pore volumes from long-column solute transport experiment under saturated conditions. (from Lewis, 1986)

APPENDIX I.

INFLUENCE OF EXTRACTION SUCTION ON FLOW FIELD IN COLUMN

The influence of induced suction on the flow field was considered, in order to determine the suction used for soil-water extraction by porous cups. Optimal conditions would be achieved by minimizing the portion of the flow field that was affected and decreasing the sampling time as much as possible.

Warrick and Amoozegar-Fard (1977) examined soil-water regimes near porous cup samplers. Analytical solutions were developed to determine Stokes stream potentials and hydraulic heads, as a function of soil-water pressure heads and extraction pressure heads for steady state conditions.

The solutions assume the following unsaturated hydraulic conductivity relationship

$$K(h) = K_s \exp(\alpha h) \qquad (I1)$$

to linearize the unsaturated flow equation, where K_s is the saturated hydraulic conductivity, is the slope of the $\ln(K_r)$ versus pressure head plot, h is the pressure head, and K_r is the relative hydraulic conductivity.

The solutions assume an infinite medium, which is not the case for the soil column used in this experiment. The upper and lower boundaries of the column cam be considered infinite, however the side boundaries are not. The solutions, then, are used as indications rather than absolute solutions for this case.

Stokes stream potentials and hydraulic heads within the flow

field were calculated for specific applied extraction suctions. Flow nets were then constructed which graphicaly depicted the influence of extraction of soil water on the flow field. Figure 54 shows a flow net for an extraction suction of 40 cm of H_2O and an initial soil suction of 30 cm of H_2O. Although this extion suction consumed more sampling time than a higher suction, the influence on the flow field was much less. Actual extraction time was between 1 to 2 1/2 hours for the 40 cm of H_2O extraction suction.

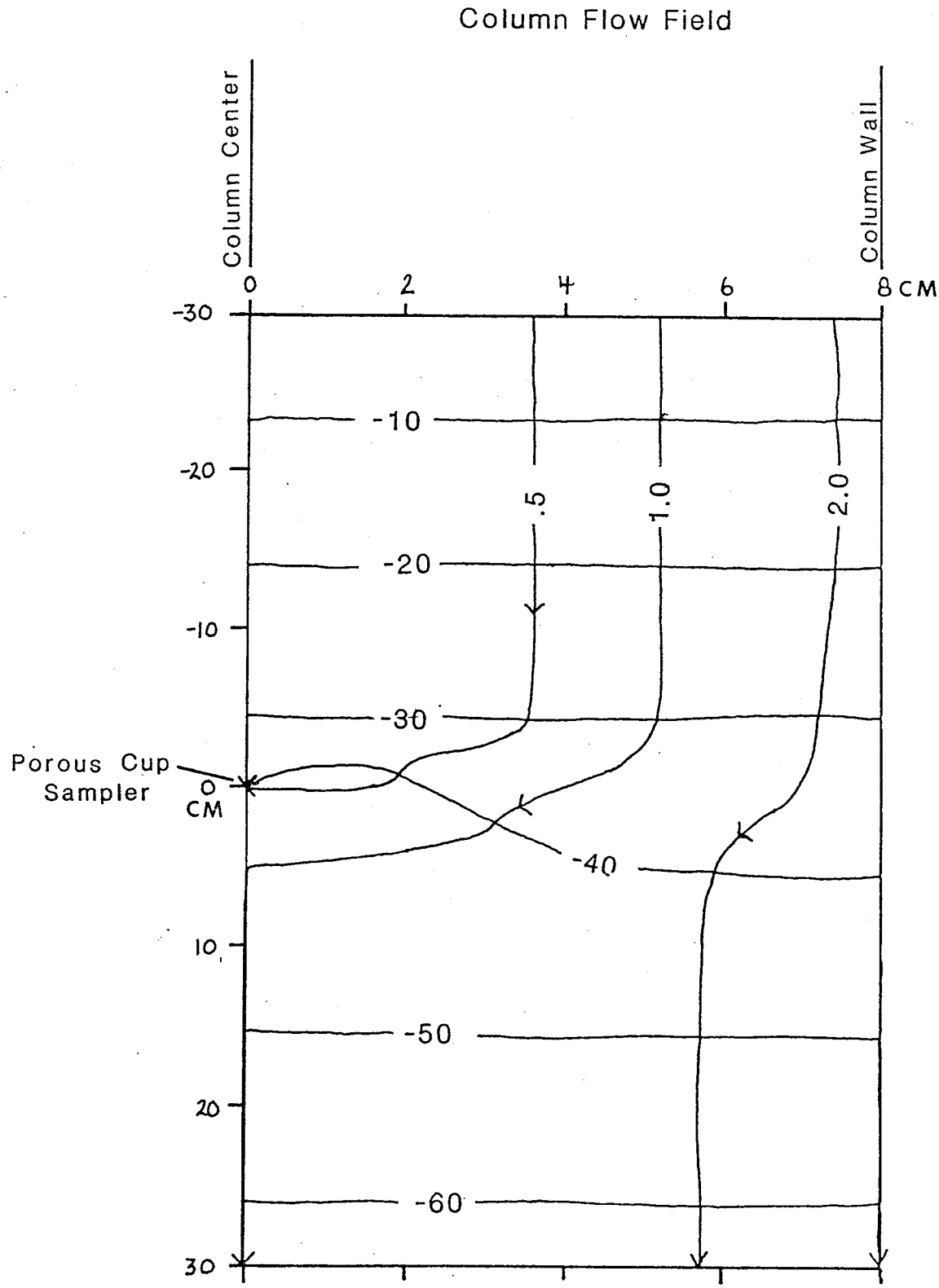

Figure 54. Flow net for long column.
Extraction Suction is 40cm H2O. Initial Suction is 30cm H2O.
Total Hydraulic Head (cm H2O) ———
Normalized Streamline ⟶

APPENDIX J. Volumetric inflow rates (ml/hr) from initiation of unsaturated leaching to the end of the long-column, solute-transport experiment.

Time (hrs)	Inflow Rate (ml/hr)
96.	21.
114.5	23.4
119.2	31.2
190.	33.6
256.5	58.8
812.2	58.8
1445.5	52.8
1829.2	52.2
1840.6	49.8
2112.5	46.2
2376.5	42.6
2400.5	48.
2472.5	52.8
2568.5	40.2
2592.5	45.6
2616.5	51.6
2735.5	53.4
2759.5	51.6
2783.5	52.8
2879.5	48.
3023.5	49.8
3143.5	42.6
3119.5	52.8
3143.5	53.4
3304.0	51.6
3404.8	43.2
3503.5	51.
3664.0	46.8
3762.5	51.6
3815.5	48.6
4100.8	49.8
4314.3	53.4
4444.1	52.8
4576.5	52.8

Appendix J. Volumetric outflow rates (ml/hr) for long-column experiment, from initiation of unsaturated leaching to the end of the solute-transport experiment.

Time (hrs)	Outflow Rate (ml/hr)
96.0	3.6
118.6	22.3
139.3	29.0
151.3	38.3
164.0	39.7
187.0	35.4
190.0	33.3
196.0	47.8
209.3	41.0
216.0	41.0
232.5	62.4
246.5	60.7
256.5	59.0
259.4	51.7
270.7	57.1
292.8	55.4
306.2	57.8
316.1	56.7
331.8	55.7
340.3	55.3
353.5	56.1
365.5	58.8
378.3	54.7
390.6	61.6
401.7	60.4
412.3	59.0
427.4	48.0
438.5	55.9
451.0	12.4
460.1	70.3
474.5	59.0
485.0	55.4
506.5	52.3
520.5	41.4
556.6	32.8
606.7	20.5
624.0	65.6
668.5	69.2
690.0	48.8
718.4	29.6
737.2	44.1
761.4	48.8
773.6	52.0
788.4	78.4
812.2	48.3
865.5	33.8
885.2	57.4
903.9	59.1
917.9	59.3
933.3	53.6
967.1	29.6
1054.3	41.9
1074.9	46.1

1104.8	17.3
1122.0	14.5
1145.8	18.3
1173.3	20.9
1220.5	18.0
1263.5	23.3
1291.8	35.3
1413.3	15.6
1445.5	15.5
1479.8	28.4
1509.5	30.3
1531.7	34.9
1553.3	55.6
1577.8	74.5
1648.3	50.4
1652.3	62.5
1673.7	66.4
1701.3	48.9
1746.3	48.6
1770.3	53.5
1791.2	48.3
1815.3	51.7
1828.2	49.5
1853.5	50.6
1875.4	50.6
1897.8	49.9
1926.9	49.8
1948.3	47.9
1974.1	46.2
1992.4	43.7
2019.9	44.0
2045.0	42.2
2063.9	40.1
2092.2	37.2
2112.6	35.9
2135.9	38.3
2160.9	39.6
2212.8	41.7
2232.0	45.3
2258.7	24.2
2285.5	42.6
2304.1	40.9
2328.5	41.1
2354.2	42.5
2378.2	43.3
2401.2	40.5
2426.2	39.2
2453.5	39.9
2471.8	30.4
2495.3	41.8
2522.4	43.2
2549.7	44.0
2569.3	41.3
2594.4	43.8
2616.5	45.3
2640.5	43.2
2665.2	44.5
2690.1	42.4
2713.1	45.7
2740.3	57.6

2761.4	48.2
2791.5	44.2
2808.2	68.0
2824.3	44.0
2848.5	48.0
2874.1	46.3
2897.9	50.8
2921.5	67.8
2944.9	46.6
2976.0	44.4
2995.5	45.6
3019.1	47.5
3045.5	47.2
3064.3	45.2
3088.9	44.2
3112.8	45.6
3137.1	45.9
3160.4	47.0
3213.5	39.7
3258.4	45.8
3305.1	54.4
3406.1	36.4
3424.1	44.6
3459.8	45.3
3500.5	76.7
3574.0	43.6
3646.2	45.7
3665.8	40.0
3762.5	42.4
3819.3	44.0
3836.3	42.5
3857.9	42.1
3929.3	37.8
4004.5	55.2
4102.1	50.7
4175.2	44.5
4240.5	36.8
4266.7	43.9
4314.3	56.7
4444.1	42.0
4507.4	48.2
4561.0	52.2
4649.8	47.0

Appendix K. Cumulative outflow from long-column experiment, from initiation of unsaturated leaching to the end of the solute-transport experiment.

Time (hrs)	Volume (ml)
96.0	348.0
118.6	852.2
139.3	1452.2
151.3	1912.2
164.0	2416.4
187.0	3231.4
190.0	3331.4
196.0	3618.4
209.3	4163.4
216.0	4438.4
232.5	5468.4
246.5	6318.4
256.5	6908.4
259.4	7058.4
270.7	7703.4
292.8	8928.4
306.2	9703.4
316.1	10264.4
331.8	11138.4
340.3	11608.4
353.5	12348.4
365.5	13053.4
378.3	13753.4
390.6	14511.4
401.7	15181.4
412.3	15806.4
427.4	16531.4
438.5	17151.4
451.0	17306.4
460.1	17946.4
474.5	18796.4
485.0	19378.4
506.5	20503.4
520.5	21082.4
556.6	22267.4
606.7	23292.4
624.0	24427.4
668.5	27507.4
690.0	28557.4
718.4	29397.4
737.2	30227.4
761.4	31407.4
773.6	32042.4
788.4	33202.4
812.2	34352.4
865.5	36152.4
885.2	37282.4
903.9	38387.4
917.9	39217.4
933.3	40042.4
967.1	41042.4
1054.3	44697.4
1074.9	45647.4
1104.8	46163.9

1122.0	46413.9
1145.8	46848.9
1173.3	47423.9
1220.5	48273.9
1263.5	49273.9
1291.8	50273.9
1413.3	52173.9
1445.5	52673.9
1479.8	53648.9
1509.5	54548.9
1531.7	55323.9
1553.3	56523.9
1577.8	58348.9
1648.3	61898.9
1652.3	62148.9
1673.7	63568.9
1701.3	64918.9
1746.3	67103.9
1770.3	68388.9
1791.2	69398.9
1815.3	70643.9
1828.2	71282.9
1853.5	72562.9
1875.4	73670.9
1897.8	74787.9
1926.9	76237.9
1948.3	77262.9
1974.1	78455.9
1992.4	79255.4
2019.9	80464.9
2045.0	81522.9
2063.9	82280.4
2092.2	83333.4
2112.6	84065.4
2135.9	84957.4
2160.9	85947.4
2212.8	88110.4
2232.0	88979.4
2258.7	89626.4
2285.5	90769.4
2304.1	91529.4
2328.5	92532.4
2354.2	93625.4
2378.2	94665.3
2401.2	95596.4
2426.2	96577.4
2453.5	97665.9
2471.8	98221.9
2495.3	99204.9
2522.4	100374.9
2549.7	101574.9
2569.3	102383.4
2594.4	103483.4
2616.5	104484.4
2640.5	105521.4
2665.2	106621.4
2690.1	107676.4
2713.1	108727.4
2740.3	110294.4
2761.4	111312.4

2791.5	112642.4
2808.2	113777.4
2824.3	114486.4
2848.5	115647.4
2874.1	116832.4
2897.9	118042.4
2921.5	119642.4
2944.9	120732.4
2976.0	122112.4
2995.5	123002.4
3019.1	124122.4
3045.5	125367.4
3064.3	126216.4
3088.9	127303.4
3112.8	128394.4
3137.1	129509.4
3160.4	130605.4
3213.5	132711.4
3258.4	134768.4
3305.1	137307.4
3406.1	140980.4
3424.1	141783.4
3459.8	143399.4
3500.5	146519.4
3574.0	149727.4
3646.2	153027.4
3665.8	153811.4
3762.5	157911.4
3819.3	160411.4
3836.3	161133.4
3857.9	162043.4
3929.3	164743.4
4004.5	168893.4
4102.1	173840.4
4175.2	177090.4
4240.5	179490.4
4266.7	180640.4
4314.3	183340.4
4444.1	188790.4
4507.4	191840.4
4561.0	194640.4
4649.8	198815.4

Appendix L. Time (hrs) and cumulative sampling volumes (ml) from all the porous cup samplers.

TIME (hrs)	CUMMULATIVE VOLUME (ml)
10.2	13.5
25.3	16.1
36.2	24.3
47.2	29.9
55.1	35.5
60.8	40.1
69.6	45.7
84.3	52.5
90.1	59.1
98.7	77.7
103.9	88.1
110.1	97.1
120.1	105.7
127.3	115.5
133.7	123.9
139.8	134.9
145.9	145.1
147.4	148.3
151.8	157.5
158.8	169.3
164.7	180.4
180.8	188.6
192.3	197.8
207.2	207.0
213.3	220.7
216.8	238.7
231.1	253.0
237.4	266.6
253.8	277.2
264.1	286.8
277.6	298.2
284.4	307.0
301.8	321.0
307.7	323.0
314.4	333.8
327.3	350.8
323.7	373.6
351.7	395.8
364.0	406.2
375.1	424.4
384.6	434.0
396.5	442.8
403.8	455.0
421.6	468.3
430.5	479.1
445.0	496.9
457.3	515.6
470.1	535.2
475.9	553.5

493.1
500.3
518.5
526.0
541.1
550.5
564.8
573.0
588.6
598.0
613.8
625.3
636.3
643.6
660.2
667.1
684.7
694.2
711.3
721.5
731.8
741.1
757.0
766.2
781.0
788.2
805.6
812.3
828.5
837.0
853.9
861.9
876.3
884.9
901.0
912.1
923.6
933.2
949.3
963.3
972.1
979.9
996.1
1021.3
1045.9
1069.7
1093.3
1116.7
1147.8
1167.3
1190.9
1217.3
1236.1
1260.7

567.7
580.4
586.8
605.0
609.3
625.5
638.9
649.9
667.9
703.4
725.8
749.4
771.0
793.0
811.0
821.0
836.4
848.2
873.4
886.6
901.2
915.0
926.4
937.2
954.0
973.4
993.6
1020.5
1031.8
1049.4
1067.8
1081.6
1092.2
1107.8
1116.4
1126.1
1134.1
1146.6
1156.8
1158.8
1159.8
1173.0
1186.0
1195.6
1204.0
1219.6
1222.4
1224.9
1235.2
1254.1
1265.5
1273.3
1280.9
1288.9

1284.6	1299.3
1308.9	1312.9
1332.2	1328.2
1385.3	1341.2
1430.2	1352.2
1476.9	1358.0
1577.9	1362.2
1631.6	1365.2
1694.1	1374.8
1837.6	1383.4
2008.1	1391.4
2273.9	1407.1
2830.5	1419.6

Appendix M. Pressure heads obtained from tensiometer readings during long-column (330 cm), unsaturated, solute-transport experiment. Time is from introduction of tracer to end of sampling.

DAY	PRESSURE HEADS (CM OF WATER) AT EACH DEPTH (CM)						
	31	96	120	165	225	283	315
2	-21.4	-22.0	-20.0	-15.0	-	-	-20.0
3	-23.4	-25.0	-21.0	-21.0	-	-	-24.0
4	-	-26.0	-21.0	-19.0	-	-	-30.0
5	-	-24.0	-18.0	-19.0	-	-	-43.0
6	-	-26.0	-21.0	-	-	-	-36.0
7	-25.2	-28.0	-24.0	-27.0	-24.0	-	-
8	-25.2	-14.0	-23.0	-29.0	-31.0	-	-
11	-11.0	-	-14.0	-	-21.0	-	-
13	-11.0	-	-	-	-	-	-
14	-10.0	-	-6.0	-	-	-20.0	-
15	-6.0	-	-6.0	-	-	-17.0	-
16	-11.0	-	-11.0	-	-	-19.0	-
17	-11.0	-	-11.0	-	-	-11.0	-
24	-18.0	-	-	-	-	-	-
25	-	-	-11.0	-	-	-25.0	-
26	-	-	-	-	-	-12.0	-
33	-18.0	-	-17.0	-	-	-14.0	-
34	-18.0	-	-	-	-	-	-
39	-19.0	-	-	-29.0	-	-5.0	-
40	-23.0	-	-	-19.0	-	-8.0	-
41	-17.0	-	-	-16.0	-	-13.0	-
45	-18.0	-	-	-12.0	-	-14.0	-
46	-13.0	-	-	-21.0	-	-12.0	-
51	-13.0	-	-	-19.0	-	-12.0	-
52	-14.0	-	-	-26.0	-	-12.0	-
54	-	-	-	-29.0	-	-21.0	-
55	-14.0	-	-	-25.0	-	-21.0	-
56	-13.0	-	-	-21.0	-	-14.0	-
69	-21.0	-	-	-27.0	-	-	-
103	-21.0	-19.0	-	-19.0	-23.0	-17.0	-15.0
104	-	-23.0	-	-26.0	-29.0	-11.0	-15.0
105	-10.0	-13.0	-	-18.0	-31.0	-16.0	-14.0
107	-10.0	-19.0	-	-20.0	-23.0	-11.0	0.0
110	-10.0	-17.0	-	-14.0	-12.0	-	-
113	-12.0	-20.0	-	-15.0	-	-	-
114	-18.0	-17.0	-	-21.0	-	-	-
115	-12.0	-27.0	-	-28.0	-14.0	-5.0	-
116	-22.0	-27.0	-	-22.0	-25.0	-	-
117	-22.0	-27.0	-	-22.0	-27.0	-5.0	-
118	-21.0	-21.0	-	-20.0	-27.0	-11.0	-3.0
119	-21.0	-23.0	-	-24.0	-29.0	-17.0	-5.0
119	-19.0	-21.0	-	-21.0	-23.0	-15.0	-4.0

APPENDIX N.

WATER CONTENTS (VOLUMETRIC), FROM 'RING' HAND-CORED SAMPLES TAKEN UPON COMPLETION OF LONG-COLUMN EXPERIMENT.

DEPTH (CM)	WATER CONTENT
33.0	40.
37.	49.
35.	108.
28.	180.
29.	234.
32.	290.
36.	304.

Appendix O. Electrical conductivity and pH of leachate for long-column, unsaturated leaching. Time equals zero for initiation of unsaturated leaching. At θ of 27%, L of 330 cm, and area of 206.1 cm^2, one pore volume was 18363.5 ml.

TIME (HRS)	PORE VOLUME	EC (μMHOS)	pH
246.5	0.34	1900.0	4.0
256.5	0.38	2200.0	4.0
259.4	0.38	2400.0	4.0
292.8	0.49	2000.0	4.1
316.1	0.56	2150.0	4.2
331.8	0.61	2150.0	3.9
340.3	0.63	2300.0	3.9
353.5	0.67	2100.0	4.0
365.5	0.71	2200.0	4.0
390.6	0.79	2200.0	4.2
401.7	0.83	2050.0	3.9
412.3	0.86	2000.0	4.0
427.4	0.90	1850.0	-
438.5	0.93	1800.0	4.1
451.0	0.94	1800.0	4.0
460.1	0.98	1800.0	4.2
474.5	1.02	1500.0	3.8
485.0	1.06	1500.0	4.1
556.6	1.21	1400.0	4.0
624.9	1.33	800.0	4.0
718.4	1.60	525.0	4.1
903.9	2.09	350.0	4.0

Appendix P. Time, volume of effluent, pore volumes and concentrations for 63 cm depth samples, long-column.

#	MIN	HOURS	LITERS	PV	MEAS. CONC	REL CONC
1	810.0	13.5	0.70	u 0.16	0.000E+00	0.000E+00
2	1518.0	25.3	1.28	0.30	0.000E+00	0.000E+00
3	2170.0	36.2	1.84	0.43	0.000E+00	0.000E+00
4	2831.0	47.2	2.39	0.56	0.000E+00	0.000E+00
5	3305.0	55.1	2.79	0.65	0.000E+00	0.000E+00
6	3650.0	60.8	3.07	0.72	0.000E+00	0.000E+00
7	4178.0	69.6	3.50	0.83	0.000E+00	0.000E+00
8	5057.0	84.3	4.25	1.01	0.921E-02	0.921E-01
9	4686.0	78.1	4.54	1.07	0.280E-01	0.280E+00
10	5920.0	98.7	4.95	1.18	0.410E-01	0.410E+00
11	6226.0	103.8	5.20	1.24	0.590E-01	0.590E+00
12	6607.0	110.1	5.50	1.31	0.620E-01	0.620E+00
13	7205.0	120.1	5.98	1.43	0.800E-01	0.800E+00
14	7637.0	127.3	6.34	1.51	0.800E-01	0.800E+00
15	8023.0	133.7	6.63	1.60	0.800E-01	0.800E+00
16	8385.0	139.8	6.89	1.66	0.800E-01	0.800E+00
17	8755.0	145.9	7.17	1.73	0.831E-01	0.831E+00
18	9105.0	151.8	7.43	1.81	0.861E-01	0.861E+00
19	9458.0	157.6	7.69	1.87	0.861E-01	0.861E+00
20	9854.0	164.2	7.97	1.96	0.941E-01	0.941E+00
21	10795.0	179.9	8.70	2.14	0.500E-01	0.500E+00
22	11500.0	191.7	9.18	2.28	0.480E-01	0.480E+00
23	12399.0	206.6	9.82	2.46	0.961E-01	0.961E+00
24	12692.0	211.5	10.03	2.52	0.590E-01	0.590E+00
25	13006.0	216.8	10.24	2.58	0.650E-01	0.650E+00
26	13682.0	228.0	10.71	2.72	0.540E-01	0.540E+00
27	14141.0	235.7	11.00	2.81	0.470E-01	0.470E+00
28	15230.0	253.8	11.70	3.02	0.941E-01	0.941E+00
29	15841.0	264.0	12.05	3.14	0.100E+00	0.100E+01
30	16646.0	277.4	12.54	3.30	0.100E+00	0.100E+01
31	17051.0	284.2	12.77	3.38	0.971E-01	0.971E+00
32	18067.0	301.1	13.45	3.58	0.780E-01	0.781E+00
33	18861.0	314.3	13.92	3.74	0.100E+00	0.100E+01
34	19615.0	326.9	14.42	3.89	0.941E-01	0.941E+00
35	19960.0	332.7	14.66	3.96	0.100E+00	0.100E+01
36	21100.0	351.7	15.45	4.19	0.941E-01	0.941E+00
37	21820.0	363.7	15.95	4.33	0.100E+00	0.100E+01
38	22505.0	375.1	16.38	4.47	0.100E+00	0.100E+01
39	24227.0	403.8	17.70	4.80	0.100E+00	0.100E+01
40	25296.0	421.6	17.99	5.01	0.100E+00	0.100E+01
41	25828.0	430.5	18.34	5.12	0.941E-01	0.941E+00
42	26700.0	445.0	18.96	5.29	0.100E+00	0.100E+01
43	27440.0	457.3	19.49	5.44	0.100E+00	0.100E+01
44	28207.0	470.1	20.01	5.60	0.951E-01	0.951E+00
45	28553.0	475.9	20.25	5.66	0.100E+00	0.100E+01
46	29586.0	493.1	20.92	5.87	0.100E+00	0.100E+01
47	30015.0	500.3	21.25	5.96	0.650E-01	0.650E+00
48	31112.0	518.5	22.03	6.17	0.400E-01	0.400E+00
49	31558.0	526.0	22.34	6.26	0.220E-01	0.220E+00
50	32468.0	541.1	22.99	6.44	0.150E-01	0.150E+00
51	33027.0	550.4	23.38	6.55	0.120E-01	0.120E+00
52	33889.0	564.8	23.99	6.72	0.601E-02	0.601E-01
53	34379.0	573.0	24.31	6.82	0.401E-02	0.401E-01
54	35315.0	588.6	24.94	7.00	0.401E-02	0.401E-01

55	35880.0	598.0	25.30	7.12	0.300E-02	0.300E-01
56	36826.0	613.8	25.90	7.30	0.200E-02	0.200E-01
57	37519.0	625.3	26.38	7.44	0.200E-02	0.200E-01
58	38180.0	636.3	26.84	7.57	0.200E-02	0.200E-01
59	38617.0	643.6	26.94	7.66	0.501E-03	0.501E-02
60	39609.0	660.2	27.63	7.85	0.501E-03	0.501E-02
61	40028.0	667.1	27.92	7.94	0.501E-03	0.501E-02
62	41082.0	684.7	28.67	8.15	0.200E-03	0.200E-02
63	41651.0	694.2	29.09	8.26	0.200E-03	0.200E-02
64	42675.0	711.3	29.84	8.47	0.501E-03	0.501E-02
65	43288.0	721.5	30.29	8.59	0.401E-03	0.401E-02
66	43947.0	732.4	30.77	8.72	0.300E-03	0.300E-02
67	44464.0	741.1	31.10	8.82	0.300E-03	0.300E-02
68	45390.0	756.5	31.82	9.01	0.200E-03	0.200E-02
69	45970.0	766.2	32.20	9.12	0.200E-03	0.200E-02
70	46857.0	780.9	32.89	9.29	0.200E-03	0.200E-02
71	47300.0	788.3	33.20	9.38	0.100E-03	0.100E-02
72	48333.0	805.6	33.95	9.59	0.500E-04	0.500E-03
73	48735.0	812.3	34.24	9.67	0.400E-04	0.400E-03
74	49717.0	828.6	34.98	9.86	0.100E-03	0.100E-02
75	50221.0	837.0	35.34	9.96	0.100E-03	0.100E-02
76	51232.0	853.9	36.05	10.16	0.200E-03	0.200E-02
77	51716.0	861.9	36.39	10.26	0.140E-03	0.140E-02
78	52576.0	876.3	37.05	10.43	0.140E-03	0.140E-02
79	53095.0	884.9	37.45	10.53	0.120E-03	0.120E-02
80	54062.0	901.0	38.54	10.72	0.140E-03	0.140E-02
81	54723.0	912.1	39.01	10.85	0.110E-03	0.110E-02
82	55413.0	923.6	39.60	10.99	0.100E-03	0.100E-02
83	55990.0	933.2	40.03	11.11	0.740E-04	0.740E-03
84	56958.0	949.3	40.74	11.30	0.740E-04	0.740E-03
85	58796.0	979.9	42.49	11.66	0.750E-04	0.750E-03
86	58765.0	979.4	43.20	11.66	0.580E-04	0.580E-03
87	61278.0	1021.3	44.36	12.16	0.580E-04	0.580E-03
88	62755.0	1045.9	45.55	12.45	0.750E-04	0.750E-03
89	64182.0	1069.7	46.76	12.73	0.750E-04	0.750E-03
90	67000.0	1116.7	49.45	13.28	0.260E-03	0.260E-02
91	68870.0	1147.8	50.83	13.66	0.291E-03	0.291E-02
92	70037.0	1167.3	51.72	13.89	0.660E-04	0.660E-03
93	71455.0	1190.9	52.84	14.17	0.730E-04	0.730E-03
94	73040.0	1217.3	54.09	14.49	0.920E-04	0.920E-03
95	74165.0	1236.1	54.93	14.71	0.880E-04	0.880E-03
96	75644.0	1260.7	56.02	15.00	0.680E-04	0.680E-03
97	77076.0	1284.6	57.11	15.29	0.720E-04	0.720E-03
98	78535.0	1308.9	58.23	15.57	0.720E-04	0.720E-03
99	79930.0	1332.2	59.32	15.85	0.700E-04	0.700E-03
100	83120.0	1385.3	61.43	16.48	0.980E-04	0.980E-03
101	85813.0	1430.2	63.49	17.02	0.760E-04	0.760E-03
102	88545.0	1475.8	66.02	17.56	0.100E-03	0.100E-02
103	94674.0	1577.9	69.70	18.77	0.940E-04	0.940E-03
104	100340.0	1672.3	75.24	19.90	0.800E-04	0.800E-03
105	110259.0	1837.6	82.53	21.87	0.620E-04	0.620E-03
106	120488.0	2008.1	89.85	23.89	0.440E-04	0.440E-03
107	136434.0	2273.9	102.56	27.06	0.400E-05	0.400E-04

Appendix P. Time, volume of effluent, pore volumes and concentrations for the 126 cm depth sampling point, long-column.

#	MIN	HOURS	LITERS	PV	MEAS. CONC	REL CONC
1	6235.0	103.9	5.21	0.62	0.000E+00	0.000E+00
2	6607.0	110.1	5.50	0.65	0.000E+00	0.000E+00
3	7205.0	120.1	5.98	0.71	0.000E+00	0.000E+00
4	7637.0	127.3	6.34	0.76	0.000E+00	0.000E+00
5	8023.0	133.7	6.63	0.79	0.000E+00	0.000E+00
6	8385.0	139.8	6.89	0.83	0.000E+00	0.000E+00
7	8842.0	147.4	7.24	0.88	0.170E-03	0.170E-02
8	9105.0	151.8	7.43	0.90	0.581E-03	0.581E-02
9	9458.0	157.6	7.69	0.94	0.160E-02	0.160E-01
10	9860.0	164.3	7.98	0.98	0.451E-02	0.451E-01
11	10803.0	180.0	8.70	1.07	0.160E-01	0.160E+00
12	11504.0	191.7	9.18	1.14	0.280E-01	0.280E+00
13	12417.0	207.0	9.83	1.24	0.480E-01	0.480E+00
14	12724.0	212.1	10.05	1.26	0.530E-01	0.530E+00
15	13006.0	216.8	10.24	1.29	0.560E-01	0.560E+00
16	13682.0	228.0	10.71	1.36	0.280E-01	0.280E+00
17	14141.0	235.7	11.00	1.40	0.290E-01	0.290E+00
18	15230.0	253.8	11.70	1.51	0.690E-01	0.690E+00
19	15841.0	264.0	12.05	1.57	0.740E-01	0.740E+00
20	16646.0	277.4	12.54	1.65	0.770E-01	0.770E+00
21	17051.0	284.2	12.77	1.69	0.680E-01	0.680E+00
22	18067.0	301.1	13.45	1.79	0.650E-01	0.650E+00
23	18861.0	314.3	13.92	1.87	0.881E-01	0.881E+00
24	19615.0	326.9	14.42	1.95	0.740E-01	0.740E+00
25	19960.0	332.7	14.66	1.98	0.580E-01	0.580E+00
26	21100.0	351.7	15.45	2.09	0.881E-01	0.881E+00
27	21820.0	363.7	15.95	2.17	0.901E-01	0.901E+00
28	22505.0	375.1	16.38	2.23	0.851E-01	0.851E+00
29	23075.0	384.6	16.83	2.29	0.100E+00	0.100E+01
30	23791.0	396.5	17.38	2.36	0.881E-01	0.881E+00
31	24227.0	403.8	17.70	2.40	0.941E-01	0.941E+00
32	25296.0	421.6	17.99	2.51	0.100E+00	0.100E+01
33	26700.0	445.0	18.96	2.65	0.100E+00	0.100E+01
34	27400.0	456.7	19.49	2.72	0.931E-01	0.931E+00
35	28207.0	470.1	20.01	2.80	0.841E-01	0.841E+00
36	28553.0	475.9	20.25	2.83	0.100E+00	0.100E+01
37	29586.0	493.1	20.92	2.94	0.921E-01	0.921E+00
38	31558.0	526.0	22.34	3.13	0.100E+00	0.100E+01
39	32468.0	541.1	22.99	3.22	0.100E+00	0.100E+01
40	33027.0	550.4	23.38	3.27	0.921E-01	0.921E+00
41	33889.0	564.8	23.99	3.36	0.981E-01	0.981E+00
42	34379.0	573.0	24.31	3.41	0.961E-01	0.961E+00
43	35315.0	588.6	24.94	3.50	0.841E-01	0.841E+00
44	35880.0	598.0	25.30	3.56	0.620E-01	0.620E+00
45	36826.0	613.8	25.90	3.65	0.430E-01	0.430E+00
46	37519.0	625.3	26.38	3.72	0.320E-01	0.320E+00
47	38180.0	636.3	26.84	3.79	0.260E-01	0.260E+00
48	38617.0	643.6	26.94	3.83	0.180E-01	0.180E+00
49	39609.0	660.2	27.63	3.93	0.120E-01	0.120E+00
50	40028.0	667.1	27.92	3.97	0.901E-02	0.901E-01
51	41082.0	684.7	28.67	4.07	0.701E-02	0.701E-01
52	41651.0	694.2	29.09	4.13	0.701E-02	0.701E-01
53	42675.0	711.3	29.84	4.23	0.501E-02	0.501E-01

54	43288.0	721.5	30.29	4.29	0.401E-02	0.401E-01
55	43947.0	732.4	30.77	4.36	0.401E-02	0.401E-01
56	44464.0	741.1	31.10	4.41	0.300E-02	0.300E-01
57	45390.0	756.5	31.82	4.50	0.300E-02	0.300E-01
58	45970.0	766.2	32.20	4.56	0.300E-02	0.300E-01
59	46857.0	780.9	32.89	4.65	0.200E-02	0.200E-01
60	47300.0	788.3	33.20	4.69	0.100E-02	0.100E-01
61	48333.0	805.6	33.95	4.79	0.501E-03	0.501E-02
62	48735.0	812.3	34.24	4.83	0.300E-03	0.300E-02
63	49717.0	828.6	34.98	4.93	0.200E-02	0.200E-01
64	50221.0	837.0	35.34	4.98	0.801E-03	0.801E-02
65	51232.0	853.9	36.05	5.08	0.801E-03	0.801E-02
66	51716.0	861.9	36.39	5.13	0.621E-03	0.621E-02
67	52576.0	876.3	37.05	5.21	0.641E-03	0.641E-02
68	53095.0	884.9	37.45	5.27	0.571E-03	0.571E-02
69	54062.0	901.0	38.54	5.36	0.541E-03	0.541E-02
70	54723.0	912.1	39.01	5.42	0.451E-03	0.451E-02
71	55413.0	923.6	39.60	5.50	0.501E-03	0.501E-02
72	55990.0	933.2	40.03	5.55	0.421E-03	0.421E-02
73	56958.0	949.3	40.74	5.64	0.461E-03	0.461E-02
74	58796.0	979.9	42.49	5.83	0.341E-03	0.341E-02
75	59765.0	996.1	43.20	5.93	0.341E-03	0.341E-02
76	61278.0	1021.3	44.36	6.08	0.260E-03	0.260E-02
77	62755.0	1045.9	45.55	6.22	0.240E-03	0.240E-02
78	64182.0	1069.7	46.76	6.36	0.230E-03	0.230E-02
79	65599.0	1093.3	48.36	6.50	0.191E-03	0.191E-02
80	67000.0	1116.7	49.45	6.64	0.220E-02	0.220E-01
81	68870.0	1147.8	50.83	6.83	0.800E-04	0.800E-03
82	70037.0	1167.3	51.72	6.94	0.180E-03	0.180E-02
83	71455.0	1190.9	52.84	7.08	0.250E-03	0.250E-02
84	73040.0	1217.3	54.09	7.24	0.250E-03	0.250E-02
85	75644.0	1260.7	56.02	7.50	0.200E-03	0.200E-02
86	77076.0	1284.6	57.11	7.64	0.210E-03	0.210E-02
87	78535.0	1308.9	58.23	7.79	0.200E-03	0.200E-02
88	79930.0	1332.2	59.32	7.93	0.210E-03	0.210E-02
89	83120.0	1385.3	61.43	8.25	0.130E-03	0.130E-02
90	85813.0	1430.2	63.49	8.51	0.170E-03	0.170E-02
91	97894.0	1631.6	72.12	9.71	0.761E-03	0.761E-02
92	100448.0	1674.1	75.27	9.96	0.291E-03	0.291E-02
93	136434.0	2273.9	102.56	13.53	0.820E-04	0.820E-03
94	169830.0	2830.5	127.88	16.84	0.350E-04	0.350E-03

Appendix P. Time, volume of effluent, pore volumes and concentrations for 252 cm depth of sampling, long-column.

#	MIN	HOURS	LITERS	PV	MEAS. CONC	REL CONC
1	16657.0	277.6	12.54	0.83	0.290E-04	0.290E-03
2	17063.0	284.4	12.78	0.84	0.400E-04	0.400E-03
3	18067.0	301.1	13.45	0.90	0.120E-03	0.120E-02
4	18461.0	307.7	13.67	0.92	0.541E-03	0.541E-02
5	18873.0	314.5	13.93	0.93	0.521E-03	0.521E-02
6	19615.0	326.9	14.42	0.97	0.190E-02	0.190E-01
7	19960.0	332.7	14.66	0.99	0.461E-02	0.461E-01
8	21100.0	351.7	15.45	1.05	0.190E-01	0.190E+00
9	21840.0	364.0	15.96	1.08	0.270E-01	0.270E+00
10	22505.0	375.1	16.38	1.11	0.420E-01	0.420E+00
11	23075.0	384.6	16.83	1.15	0.620E-01	0.620E+00
12	23791.0	396.5	17.38	1.18	0.660E-01	0.660E+00
13	24227.0	403.8	17.70	1.20	0.750E-01	0.750E+00
14	25296.0	421.6	17.99	1.25	0.821E-01	0.821E+00
15	25828.0	430.5	18.34	1.28	0.780E-01	0.781E+00
16	26700.0	445.0	18.96	1.33	0.831E-01	0.831E+00
17	27440.0	457.3	19.49	1.36	0.851E-01	0.851E+00
18	28207.0	470.1	20.01	1.40	0.821E-01	0.821E+00
19	28553.0	475.9	20.25	1.42	0.100E+00	0.100E+01
20	29586.0	493.1	20.92	1.46	0.841E-01	0.841E+00
21	30015.0	500.3	21.25	1.49	0.100E+00	0.100E+01
22	31112.0	518.5	22.03	1.55	0.100E+00	0.100E+01
23	31558.0	526.0	22.34	1.56	0.901E-01	0.901E+00
24	33027.0	550.4	23.38	1.64	0.100E+00	0.100E+01
25	33889.0	564.8	23.99	1.68	0.931E-01	0.931E+00
26	34379.0	573.0	24.31	1.70	0.981E-01	0.981E+00
27	35315.0	588.6	24.94	1.75	0.931E-01	0.931E+00
28	35880.0	598.0	25.30	1.78	0.921E-01	0.921E+00
29	36826.0	613.8	25.90	1.82	0.981E-01	0.981E+00
30	37519.0	625.3	26.38	1.86	0.981E-01	0.981E+00
31	38180.0	636.3	26.84	1.89	0.901E-01	0.901E+00
32	38617.0	643.6	26.94	1.91	0.100E+00	0.100E+01
33	39609.0	660.2	27.63	1.96	0.941E-01	0.941E+00
34	40028.0	667.1	27.92	1.99	0.100E+00	0.100E+01
35	41028.0	683.8	28.67	2.04	0.841E-01	0.841E+00
36	41651.0	694.2	29.09	2.06	0.100E+00	0.100E+01
37	42675.0	711.3	29.84	2.12	0.100E+00	0.100E+01
38	43288.0	721.5	30.29	2.14	0.861E-01	0.861E+00
39	43947.0	732.4	30.77	2.18	0.901E-01	0.901E+00
40	44464.0	741.1	31.10	2.21	0.941E-01	0.941E+00
41	45421.0	757.0	31.85	2.25	0.941E-01	0.941E+00
42	45970.0	766.2	32.20	2.28	0.800E-01	0.800E+00
43	46857.0	780.9	32.89	2.32	0.640E-01	0.640E+00
44	47300.0	788.3	33.20	2.35	0.500E-01	0.500E+00
45	48333.0	805.6	33.95	2.40	0.280E-01	0.280E+00
46	48735.0	812.3	34.24	2.41	0.220E-01	0.220E+00
47	49717.0	828.6	34.98	2.46	0.170E-01	0.170E+00
48	50221.0	837.0	35.34	2.49	0.200E-02	0.200E-01
49	51232.0	853.9	36.05	2.54	0.100E-02	0.100E-01
50	51716.0	861.9	36.39	2.56	0.140E-01	0.140E+00
51	52576.0	876.3	37.05	2.61	0.621E-02	0.621E-01
52	53095.0	884.9	37.45	2.63	0.541E-02	0.541E-01
53	54062.0	901.0	38.54	2.68	0.521E-02	0.521E-01
54	54723.0	912.1	39.01	2.72	0.390E-02	0.390E-01

55	55413.0	923.6	39.60	2.75	0.351E-02	0.351E-01
56	55990.0	933.2	40.03	2.77	0.370E-02	0.370E-01
57	56958.0	949.3	40.74	2.82	0.320E-02	0.321E-01
58	57795.0	963.3	41.36	2.86	0.331E-02	0.331E-01
59	58326.0	972.1	42.16	2.90	0.180E-02	0.180E-01
60	58796.0	979.9	42.49	2.91	0.230E-02	0.230E-01
61	59765.0	996.1	43.20	2.96	0.130E-02	0.130E-01
62	61278.0	1021.3	44.36	3.03	0.170E-02	0.170E-01
63	62755.0	1045.9	45.55	3.11	0.220E-02	0.220E-01
64	64182.0	1069.7	46.76	3.18	0.230E-02	0.230E-01
65	65599.0	1093.3	48.36	3.26	0.110E-02	0.110E-01
66	67000.0	1116.7	49.45	3.32	0.170E-02	0.170E-01
67	68870.0	1147.8	50.83	3.41	0.862E-03	0.862E-02
68	70037.0	1167.3	51.72	3.48	0.801E-03	0.801E-02
69	71455.0	1190.9	52.84	3.54	0.601E-03	0.601E-02
70	73040.0	1217.3	54.09	3.62	0.601E-03	0.601E-02
71	74165.0	1236.1	54.93	3.68	0.321E-03	0.321E-02
72	75644.0	1260.7	56.02	3.75	0.401E-03	0.401E-02
73	77076.0	1284.6	57.11	3.82	0.401E-03	0.401E-02
74	78535.0	1308.9	58.23	3.89	0.321E-03	0.321E-02
75	79930.0	1332.2	59.32	3.96	0.260E-03	0.260E-02
76	83120.0	1385.3	61.43	4.12	0.120E-03	0.120E-02
77	85813.0	1430.2	63.49	4.25	0.250E-03	0.250E-02
78	88545.0	1475.8	66.02	4.39	0.230E-03	0.230E-02
79	100448.0	1674.1	75.27	4.98	0.250E-03	0.250E-02
80	110259.0	1837.6	82.53	5.46	0.200E-03	0.200E-02
81	120488.0	2008.1	89.85	5.97	0.100E-04	0.100E-03
82	136434.0	2273.9	102.56	6.76	0.900E-04	0.900E-03
83	169830.0	2830.5	127.88	8.42	0.110E-03	0.110E-02

Appendix P. Time, volume of effluent, pore volumes, and concentrations for 330 cm sampling depth, long-column.

#	MIN	HOURS	LITERS	PV	MEAS. CONC	REL CONC
1	21100.0	351.7	15.45	0.80	0.150E-04	0.150E-03
2	21840.0	364.0	15.96	0.83	0.200E-04	0.200E-03
3	22505.0	375.1	16.38	0.85	0.200E-04	0.200E-03
4	23075.0	384.6	16.83	0.88	0.300E-04	0.300E-03
5	23791.0	396.5	17.38	0.90	0.300E-04	0.300E-03
6	24227.0	403.8	17.70	0.92	0.130E-03	0.130E-02
7	25296.0	421.6	17.99	0.96	0.340E-02	0.340E-01
8	25828.0	430.5	18.34	0.98	0.701E-02	0.701E-01
9	26700.0	445.0	18.96	1.01	0.230E-01	0.230E+00
10	27440.0	457.3	19.49	1.04	0.330E-01	0.330E+00
11	28207.0	470.1	20.01	1.07	0.480E-01	0.480E+00
12	28553.0	475.9	20.25	1.08	0.680E-01	0.680E+00
13	29586.0	493.1	20.92	1.12	0.600E-01	0.600E+00
14	30015.0	500.3	21.25	1.14	0.640E-01	0.640E+00
15	31112.0	518.5	22.03	1.18	0.740E-01	0.740E+00
16	31558.0	526.0	22.34	1.19	0.720E-01	0.720E+00
17	32468.0	541.1	22.99	1.23	0.720E-01	0.720E+00
18	33027.0	550.4	23.38	1.25	0.760E-01	0.760E+00
19	33889.0	564.8	23.99	1.28	0.650E-01	0.650E+00
20	34379.0	573.0	24.31	1.30	0.740E-01	0.740E+00
21	35315.0	588.6	24.94	1.33	0.851E-01	0.851E+00
22	35880.0	598.0	25.30	1.36	0.780E-01	0.781E+00
23	36826.0	613.8	25.90	1.39	0.901E-01	0.901E+00
24	37519.0	625.3	26.38	1.42	0.720E-01	0.720E+00
25	38180.0	636.3	26.84	1.45	0.720E-01	0.720E+00
26	38617.0	643.6	26.94	1.46	0.780E-01	0.781E+00
27	39609.0	660.2	27.63	1.50	0.780E-01	0.781E+00
28	40028.0	667.1	27.92	1.51	0.760E-01	0.760E+00
29	41082.0	684.7	28.67	1.55	0.650E-01	0.650E+00
30	41651.0	694.2	29.09	1.58	0.690E-01	0.690E+00
31	42675.0	711.3	29.84	1.62	0.790E-01	0.791E+00
32	43288.0	721.5	30.29	1.64	0.720E-01	0.720E+00
33	43947.0	732.4	30.77	1.66	0.720E-01	0.720E+00
34	44464.0	741.1	31.10	1.69	0.720E-01	0.720E+00
35	45390.0	756.5	31.82	1.72	0.780E-01	0.781E+00
36	45970.0	766.2	32.20	1.74	0.740E-01	0.740E+00
37	46857.0	780.9	32.89	1.78	0.700E-01	0.700E+00
38	47300.0	788.3	33.20	1.79	0.780E-01	0.781E+00
39	48333.0	805.6	33.95	1.83	0.800E-01	0.800E+00
40	48735.0	812.3	34.24	1.85	0.921E-01	0.921E+00
41	49717.0	828.6	34.98	1.88	0.740E-01	0.740E+00
42	50221.0	837.0	35.34	1.90	0.760E-01	0.760E+00
43	51232.0	853.9	36.05	1.94	0.720E-01	0.720E+00
44	51716.0	861.9	36.39	1.96	0.540E-01	0.540E+00
45	52576.0	876.3	37.05	1.99	0.440E-01	0.440E+00
46	53095.0	884.9	37.45	2.01	0.380E-01	0.380E+00
47	54062.0	901.0	38.54	2.05	0.240E-01	0.240E+00
48	54723.0	912.1	39.01	2.07	0.170E-01	0.170E+00
49	55413.0	923.6	39.60	2.09	0.100E-01	0.100E+00
50	55990.0	933.2	40.03	2.12	0.951E-02	0.951E-01
51	56958.0	949.3	40.74	2.16	0.741E-02	0.741E-01
52	57795.0	963.3	41.36	2.19	0.521E-02	0.521E-01
53	58326.0	972.1	42.16	2.21	0.340E-02	0.340E-01

54	58796.0	979.9	42.49	2.22	0.300E-02	0.300E-01
55	59765.0	996.1	43.20	2.27	0.170E-02	0.170E-01
56	61278.0	1021.3	44.36	2.32	0.901E-03	0.901E-02
57	62755.0	1045.9	45.55	2.37	0.701E-03	0.701E-02
58	64182.0	1069.7	46.76	2.43	0.451E-03	0.451E-02
59	65599.0	1093.3	48.36	2.49	0.320E-02	0.321E-01
60	67000.0	1116.7	49.45	2.54	0.441E-02	0.441E-01
61	68870.0	1147.8	50.83	2.61	0.281E-03	0.281E-02
62	70037.0	1167.3	51.72	2.65	0.350E-03	0.350E-02
63	71455.0	1190.9	52.84	2.71	0.260E-03	0.260E-02
64	73040.0	1217.3	54.09	2.76	0.200E-03	0.200E-02
65	74165.0	1236.1	54.93	2.81	0.130E-03	0.130E-02
66	75644.0	1260.7	56.02	2.86	0.150E-03	0.150E-02
67	77076.0	1284.6	57.11	2.92	0.180E-03	0.180E-02
68	78535.0	1308.9	58.23	2.98	0.150E-03	0.150E-02
69	79930.0	1332.2	59.32	3.03	0.150E-03	0.150E-02
70	83120.0	1385.3	61.43	3.15	0.110E-03	0.110E-02
71	85813.0	1430.2	63.49	3.25	0.120E-03	0.120E-02
72	88545.0	1475.8	66.02	3.35	0.110E-03	0.110E-02
73	94674.0	1577.9	69.70	3.58	0.820E-04	0.820E-03
74	95757.0	1595.9	70.50	3.62	0.940E-04	0.940E-03
75	100448.0	1674.1	75.27	3.80	0.740E-04	0.740E-03
76	110259.0	1837.6	82.53	4.17	0.620E-04	0.620E-03
77	120488.0	2008.1	89.85	4.56	0.550E-04	0.550E-03
78	136434.0	2273.9	102.56	5.17	0.390E-04	0.390E-03
79	169830.0	2830.5	127.88	6.43	0.170E-04	0.170E-03

Appendix Q.

```
**********************************************************************************
*                                                                                 *
*          NON-LINEAR  LEAST SQUARES ANALYSIS                                     *
*                                                                                 *
*          SEMI-INFINITE PROFILE, 3-TIPE BC                                       *
*long column, bottom effluent plate, bromide,v=1.25E-02cm/min                     *
*                                                                                 *
**********************************************************************************
```

INITIAL VALUES OF COEFFICIENTS

NO	NAME	INITIAL VALUE
1	peclet	165.000
2	RF	1.100
3	pulse	0.920

OBSERVED DATA

OBS.NO.	PORE VOLUME	CONCENTRATION
1	0.8000	0.0001
2	0.8300	0.0002
3	0.8500	0.0002
4	0.8800	0.0003
5	0.9000	0.0003
6	0.9200	0.0013
7	0.9600	0.0310
8	0.9800	0.0701
9	1.0100	0.2302
10	1.0400	0.3303
11	1.0700	0.4804
12	1.0800	0.6804
13	1.1200	0.6004
14	1.1400	0.6404
15	1.1800	0.7405
16	1.1900	0.7205
17	1.2300	0.7205
18	1.2500	0.7605
19	1.2800	0.6504
20	1.3000	0.7405
21	1.3300	0.8505
22	1.3600	0.7805
23	1.3900	0.9005
24	1.4200	0.7205
25	1.4500	0.7205
26	1.4600	0.7805
27	1.5000	0.7805
28	1.5100	0.7605
29	1.5500	0.6504
30	1.5800	0.6905
31	1.6200	0.7905
32	1.6400	0.7205
33	1.6600	0.7205
34	1.6900	0.7205
35	1.7200	0.7805
36	1.7400	0.7405
37	1.7800	0.7005
38	1.7900	0.7805
39	1.8300	0.8005

40	1.8500	0.9205
41	1.8800	0.7405
42	1.9000	0.7605
43	1.9400	0.7205
44	1.9600	0.5404
45	1.9900	0.4403
46	2.0100	0.3803
47	2.0500	0.2402
48	2.0700	0.1702
49	2.0900	0.1001
50	2.1200	0.0951
51	2.1600	0.0741
52	2.1900	0.0521
53	2.2100	0.0340
54	2.2200	0.0300
55	2.2700	0.0170
56	2.3200	0.0090
57	2.3700	0.0070
58	2.4300	0.0045
59	2.4900	0.0320
60	2.5400	0.0441
61	2.6100	0.0028
62	2.5500	0.0035
63	2.7100	0.0026
64	2.7600	0.0020
65	2.8100	0.0013
66	2.8600	0.0015
67	2.9200	0.0018
68	2.9800	0.0015
69	3.0300	0.0015
70	3.1500	0.0011
71	3.2500	0.0012
72	3.3500	0.0011
73	3.5800	0.0008
74	3.6200	0.0009
75	3.8000	0.0007
76	4.1700	0.0006
77	4.5600	0.0006
78	5.1700	0.0004
79	6.4300	0.0002

ITERATION	SSQ	peclet	Rf	pulse
0	1.5582838	165.00000	1.10000	0.92000
1	1.1488040	89.87866	1.10318	0.86525
2	1.0522065	72.22524	1.11803	0.83386
3	1.0013688	58.56924	1.12515	0.81933
4	0.9830856	52.99063	1.13117	0.80750
5	0.9761766	50.26592	1.13377	0.80195
6	0.9770367	49.10888	1.13502	0.79917
7	0.9767762	48.58963	1.13554	0.79796
8	0.9767119	48.36510	1.13578	0.79741
9	0.9766937	48.26614	1.13588	0.79717
10	0.9766876	48.22303	1.13592	0.79707
11	0.9766853	48.20413	1.13594	0.79702

CORRELATION MATRIX
==========

	1	2	3
1	1.0000		
2	0.2646	1.0000	
3	-0.2987	-0.6831	1.0000

NON-LINEAR LEAST SQUARES ANALYSIS, FINAL RESULTS

VARIABLE	NAME	VALUE	S.E.COEFF.	T-VALUE	95% CONFIDENCE LIMITS LOWER	UPPER
1	peclet	48.20413	7.0683	6.82	34.1258	62.2824
2	RF	1.13594	0.0170	66.81	1.1021	1.1698
3	pulse	0.79702	0.0234	34.03	0.7504	0.8437

ORDERED BY COMPUTER INPUT

NO	PORE VOLUME	CONCENTRATION OBS.	CONCENTRATION FITTED	RESIDUAL
1	0.800	0.000	0.040	-0.040
2	0.830	0.000	0.059	-0.059
3	0.850	0.000	0.074	-0.074
4	0.880	0.000	0.102	-0.102
5	0.900	0.000	0.123	-0.123
6	0.920	0.001	0.147	-0.146
7	0.950	0.034	0.201	-0.167
8	0.980	0.070	0.231	-0.161
9	1.010	0.230	0.279	-0.049
10	1.040	0.330	0.330	0.000
11	1.070	0.480	0.383	0.098
12	1.080	0.680	0.400	0.280
13	1.120	0.600	0.471	0.129
14	1.140	0.640	0.506	0.134
15	1.180	0.740	0.574	0.166
16	1.190	0.720	0.590	0.130
17	1.230	0.720	0.653	0.068
18	1.250	0.760	0.682	0.079
19	1.280	0.650	0.723	-0.072
20	1.300	0.740	0.748	-0.007
21	1.330	0.851	0.783	0.068
22	1.350	0.780	0.814	-0.033
23	1.390	0.901	0.841	0.060
24	1.420	0.720	0.865	-0.144
25	1.450	0.720	0.884	-0.164
26	1.480	0.780	0.890	-0.110
27	1.500	0.780	0.908	-0.128
28	1.510	0.760	0.911	-0.151
29	1.550	0.650	0.919	-0.268
30	1.580	0.690	0.918	-0.226
31	1.620	0.790	0.907	-0.117
32	1.640	0.720	0.898	-0.177
33	1.660	0.720	0.885	-0.165
34	1.690	0.720	0.861	-0.140
35	1.720	0.780	0.830	-0.050
36	1.740	0.740	0.806	-0.066
37	1.780	0.700	0.752	-0.051
38	1.790	0.780	0.737	0.044
39	1.830	0.800	0.673	0.127
40	1.850	0.921	0.640	0.281
41	1.880	0.740	0.589	0.152
42	1.900	0.760	0.554	0.207
43	1.940	0.720	0.485	0.236

ORDERED BY RESIDUALS

NO	PORE VOLUME	CONCENTRATION OBS.	CONCENTRATION FITTED	RESIDUAL
40	1.850	0.921	0.640	0.281
12	1.080	0.680	0.400	0.280
43	1.940	0.720	0.485	0.236
42	1.900	0.760	0.554	0.207
15	1.180	0.740	0.574	0.166
41	1.880	0.740	0.589	0.152
14	1.140	0.640	0.506	0.134
16	1.190	0.720	0.590	0.130
13	1.120	0.600	0.471	0.129
39	1.830	0.800	0.673	0.127
11	1.070	0.480	0.383	0.098
44	1.960	0.540	0.451	0.089
18	1.250	0.760	0.682	0.079
21	1.330	0.851	0.783	0.068
17	1.230	0.720	0.653	0.068
23	1.390	0.901	0.841	0.060
38	1.790	0.780	0.737	0.044
45	1.990	0.440	0.402	0.038
60	2.540	0.044	0.016	0.028
46	2.010	0.380	0.371	0.009
59	2.490	0.032	0.023	0.009
69	3.030	0.001	0.000	0.001
71	3.250	0.001	0.000	0.001
72	3.350	0.001	0.000	0.001
68	2.980	0.001	0.000	0.001
70	3.150	0.001	0.000	0.001
67	2.920	0.002	0.001	0.001
74	3.620	0.001	0.000	0.001
73	3.580	0.001	0.000	0.001
75	3.800	0.001	0.000	0.001
76	4.170	0.001	0.000	0.001
77	4.560	0.001	0.000	0.001
78	5.170	0.000	0.000	0.000
10	1.040	0.330	0.330	0.000
79	6.430	0.000	0.000	0.000
66	2.860	0.001	0.001	0.000
65	2.810	0.001	0.002	-0.001
64	2.760	0.002	0.003	-0.001
63	2.710	0.003	0.005	-0.002
62	2.650	0.004	0.007	-0.004
61	2.610	0.003	0.010	-0.007
20	1.300	0.740	0.748	-0.007
58	2.430	0.005	0.035	-0.031

44	1.960	0.540	0.451	0.089	22	1.360	0.780	0.814	-0.033
45	1.990	0.440	0.402	0.038	1	0.300	0.000	0.040	-0.040
46	2.010	0.380	0.371	0.009	57	2.370	0.007	0.053	-0.046
47	2.050	0.240	0.313	-0.072	9	1.010	0.230	0.279	-0.049
48	2.070	0.170	0.285	-0.115	35	1.720	0.780	0.830	-0.050
49	2.090	0.100	0.260	-0.160	37	1.780	0.700	0.752	-0.051
50	2.120	0.095	0.224	-0.129	2	0.830	0.000	0.059	-0.059
51	2.160	0.074	0.183	-0.109	56	2.320	0.009	0.072	-0.063
52	2.190	0.052	0.155	-0.103	36	1.740	0.740	0.806	-0.066
53	2.210	0.034	0.139	-0.105	19	1.280	0.650	0.723	-0.072
54	2.220	0.030	0.132	-0.101	47	2.050	0.240	0.313	-0.072
55	2.270	0.017	0.098	-0.081	3	0.850	0.000	0.074	-0.074
56	2.320	0.009	0.072	-0.063	55	2.270	0.017	0.098	-0.081
57	2.370	0.007	0.053	-0.046	54	2.220	0.030	0.132	-0.101
58	2.430	0.005	0.035	-0.031	4	0.880	0.000	0.102	-0.102
59	2.490	0.032	0.023	0.009	52	2.190	0.052	0.155	-0.103
60	2.540	0.044	0.016	0.028	53	2.210	0.034	0.139	-0.105
61	2.610	0.003	0.010	-0.007	51	2.160	0.074	0.183	-0.109
62	2.650	0.004	0.007	-0.004	26	1.460	0.780	0.890	-0.110
63	2.710	0.003	0.005	-0.002	48	2.070	0.170	0.285	-0.115
64	2.760	0.002	0.003	-0.001	31	1.620	0.790	0.907	-0.117
65	2.810	0.001	0.002	-0.001	5	0.900	0.000	0.123	-0.123
66	2.860	0.001	0.001	0.000	27	1.500	0.780	0.908	-0.128
67	2.920	0.002	0.001	0.001	50	2.120	0.095	0.224	-0.129
68	2.980	0.001	0.000	0.001	34	1.690	0.720	0.861	-0.140
69	3.030	0.001	0.000	0.001	24	1.420	0.720	0.865	-0.144
70	3.150	0.001	0.000	0.001	6	0.920	0.001	0.147	-0.146
71	3.250	0.001	0.000	0.001	28	1.510	0.760	0.911	-0.151
72	3.350	0.001	0.000	0.001	49	2.090	0.100	0.260	-0.160
73	3.580	0.001	0.000	0.001	8	0.980	0.070	0.231	-0.161
74	3.620	0.001	0.000	0.001	25	1.450	0.720	0.884	-0.164
75	3.800	0.001	0.000	0.001	33	1.660	0.720	0.885	-0.165
76	4.170	0.001	0.000	0.001	7	0.960	0.034	0.201	-0.167
77	4.560	0.001	0.000	0.001	32	1.640	0.720	0.898	-0.177
78	5.170	0.000	0.000	0.000	30	1.580	0.690	0.918	-0.228
79	6.430	0.000	0.000	0.000	29	1.550	0.650	0.919	-0.268

END OF PROBLEM
==========

P31C4.OUT

```
*****************************************************************************
*
*          NON-LINEAR  LEAST SQUARES ANALYSIS
*
*          SEMI-INFINITE PROFILE, 3-TYPE BC
*long column, porous cup #4, bromide, v=1.25E-02mc/min
*
*****************************************************************************
```

INITIAL VALUES OF COEFFICIENTS

NO	NAME	INITIAL VALUE
1	peclet	120.000
2	RF	1.100
3	Pulse	1.200

OBSERVED DATA

OBS.NO.	PORE VOLUME	CONCENTRATION
1	0.8300	0.0003
2	0.8400	0.0004
3	0.9000	0.0012
4	0.9200	0.0054
5	0.9300	0.0052
6	0.9700	0.0190
7	0.9900	0.0461
8	1.0500	0.1902
9	1.0800	0.2702
10	1.1100	0.4203
11	1.1500	0.6204
12	1.1800	0.6604
13	1.2000	0.7505
14	1.2500	0.8205
15	1.2800	0.7805
16	1.3200	0.8305
17	1.3600	0.8505
18	1.4000	0.8205
19	1.4200	1.0006
20	1.4600	0.8405
21	1.4900	1.0006
22	1.5500	1.0006
23	1.5600	0.9005
24	1.6400	1.0006
25	1.6800	0.9305
26	1.7000	0.9806
27	1.7500	0.9305
28	1.7800	0.9205
29	1.8200	0.9806
30	1.8600	0.9806
31	1.8900	0.9005
32	1.9100	1.0006
33	1.9600	0.9406
34	1.9900	1.0006
35	2.0400	0.8405
36	2.0600	1.0006
37	2.1200	1.0006
38	2.1400	0.8605
39	2.1800	0.9005

40	2.2100	0.9406
41	2.2500	0.9406
42	2.2800	0.8005
43	2.3200	0.6404
44	2.3500	0.5004
45	2.4000	0.2802
46	2.4100	0.2202
47	2.4600	0.1702
48	2.4900	0.0200
49	2.5400	0.0100
50	2.5600	0.1402
51	2.6100	0.0621
52	2.6300	0.0541
53	2.6800	0.0521
54	2.7200	0.0390
55	2.7500	0.0351
56	2.7700	0.0370
57	2.8200	0.0320
58	2.8600	0.0331
59	2.9000	0.0180
60	2.9100	0.0230
61	2.9600	0.0130
62	3.0300	0.0170
63	3.1100	0.0220
64	3.1800	0.0230
65	3.2600	0.0110
66	3.3200	0.0170
67	3.4100	0.0086
68	3.4800	0.0080
69	3.5400	0.0060
70	3.6200	0.0060
71	3.6800	0.0032
72	3.7500	0.0040
73	3.8200	0.0040
74	3.8900	0.0032
75	3.9600	0.0026
76	4.1200	0.0012
77	4.2500	0.0025
78	4.3900	0.0023
79	4.9800	0.0025
80	5.4600	0.0020
81	5.9700	0.0001
82	6.7600	0.0009
83	5.4200	0.0011

ITERATION	SSQ	peclet	RF	Pulse
0	0.5210072	126.00000	1.10000	1.20000
1	0.2590206	164.70780	1.14542	1.20832
2	0.2486382	189.66557	1.14183	1.20773
3	0.2466069	203.82070	1.14063	1.20936
4	0.2462268	210.24138	1.14002	1.20997
5	0.2461545	213.01815	1.13975	1.21025
6	0.2461400	214.18561	1.13963	1.21037
7	0.2461367	214.67147	1.13958	1.21042
8	0.2461358	214.87278	1.13956	1.21044
9	0.2461355	214.95605	1.13956	1.21045

CORRELATION MATRIX
==========

	1	2	3
1	1.0000		
2	0.1258	1.0000	
3	-0.0687	-0.7017	1.0000

NON-LINEAR LEAST SQUARES ANALYSIS, FINAL RESULTS.
==========

CORRELATION MATRIX

	1	2	3
1	1.0000		
2	0.1258	1.0000	
3	-0.0587	-0.7017	1.0000

NON-LINEAR LEAST SQUARES ANALYSIS, FINAL RESUL TS

VARIABLE	NAME	VALUE	S.E.COEFF.	T-VALUE	95% CONFIDENCE LIMITS LOWER	UPPER
1	peclet	214.95605	26.2905	8.18	162.6340	267.2761
2	RF	1.13956	0.0064	177.23	1.1268	1.1523
3	Pulse	1.21045	0.0091	133.23	1.1924	1.2285

ORDERED BY COMPUTER INPUT

O	PORE VOLUME	CONCENTRA TION OBS.	TION FITTED	RESI-DUAL
1	0.830	0.000	0.000	0.000
2	0.840	0.000	0.001	0.000
3	0.900	0.001	0.007	-0.006
4	0.920	0.005	0.013	-0.008
5	0.930	0.005	0.017	-0.012
6	0.970	0.019	0.047	-0.028
7	0.990	0.046	0.072	-0.026
8	1.050	0.190	0.197	-0.007
9	1.080	0.270	0.288	-0.018
10	1.110	0.420	0.392	0.028
11	1.150	0.620	0.538	0.083
12	1.180	0.660	0.641	0.019
13	1.200	0.750	0.704	0.046
14	1.250	0.821	0.832	-0.011
15	1.280	0.780	0.887	-0.106
16	1.330	0.831	0.946	-0.115
17	1.360	0.851	0.967	-0.117
18	1.400	0.821	0.984	-0.163
19	1.420	1.001	0.989	0.012
20	1.460	0.841	0.995	-0.155
21	1.490	1.001	0.997	0.003
22	1.550	1.001	0.999	0.001
23	1.580	0.901	0.999	-0.099
24	1.640	1.001	1.000	0.001
25	1.680	0.931	1.000	-0.069
26	1.700	0.981	1.000	-0.019
27	1.750	0.931	1.000	-0.069
28	1.780	0.921	1.000	-0.079
29	1.820	0.981	1.000	-0.019
30	1.860	0.981	1.000	-0.019
31	1.890	0.901	1.000	-0.099
32	1.910	1.001	1.000	0.001
33	1.960	0.941	1.000	-0.059
34	1.990	1.001	1.000	0.001
35	2.040	0.841	1.000	-0.159
36	2.060	1.001	0.999	0.002
37	2.120	1.001	0.991	0.010
38	2.140	0.861	0.983	-0.122
39	2.180	0.901	0.954	-0.053
40	2.210	0.941	0.914	0.027
41	2.250	0.941	0.830	0.110

ORDERED BY RESIDUALS

NO	PORE VOLUME	CONCENTRATION OBS.	FITTED	RESI-DUAL
41	2.250	0.941	0.830	0.110
50	2.560	0.140	0.039	0.101
11	1.150	0.620	0.538	0.083
42	2.280	0.800	0.745	0.055
53	2.680	0.052	0.004	0.048
13	1.200	0.750	0.704	0.046
51	2.610	0.062	0.016	0.046
52	2.630	0.054	0.011	0.043
54	2.720	0.039	0.002	0.037
56	2.770	0.037	0.001	0.037
55	2.750	0.035	0.001	0.034
58	2.860	0.033	0.000	0.033
57	2.820	0.032	0.000	0.032
43	2.320	0.640	0.609	0.031
10	1.110	0.420	0.392	0.028
40	2.210	0.941	0.914	0.027
64	3.180	0.023	0.000	0.023
60	2.910	0.023	0.000	0.023
63	3.110	0.022	0.000	0.022
12	1.180	0.660	0.641	0.019
59	2.900	0.018	0.000	0.018
66	3.320	0.017	0.000	0.017
62	3.030	0.017	0.000	0.017
61	2.960	0.013	0.000	0.013
19	1.420	1.001	0.989	0.012
65	3.260	0.011	0.000	0.011
37	2.120	1.001	0.991	0.010
67	3.410	0.009	0.000	0.009
68	3.480	0.008	0.000	0.008
70	3.620	0.006	0.000	0.006
69	3.540	0.006	0.000	0.006
73	3.820	0.004	0.000	0.004
72	3.750	0.004	0.000	0.004
74	3.890	0.003	0.000	0.003
71	3.680	0.003	0.000	0.003
21	1.490	1.001	0.997	0.003
75	3.960	0.003	0.000	0.003
77	4.250	0.003	0.000	0.003
79	4.980	0.003	0.000	0.003
78	4.390	0.002	0.000	0.002
80	5.460	0.002	0.000	0.002

42	2.280	0.800	0.745	0.055	36	2.060	1.001	0.999	0.002
43	2.320	0.640	0.609	0.031	22	1.550	1.001	0.999	0.001
44	2.350	0.500	0.500	0.000	76	4.120	0.001	0.000	0.001
45	2.400	0.260	0.326	-0.066	83	2.420	0.001	0.000	0.001
46	2.410	0.220	0.297	-0.077	47	2.460	0.170	0.169	0.001
47	2.460	0.170	0.169	0.001	82	6.760	0.001	0.000	0.001
48	2.490	0.020	0.114	-0.094	21	1.640	1.001	1.000	0.001
49	2.540	0.010	0.054	-0.044	34	1.990	1.001	1.000	0.001
50	2.560	0.140	0.039	0.101	32	1.910	1.001	1.000	0.001
51	2.610	0.062	0.016	0.046	44	2.350	0.500	0.500	0.000
52	2.630	0.054	0.011	0.043	61	5.970	0.000	0.000	0.000
53	2.680	0.052	0.004	0.048	1	0.830	0.000	0.000	0.000
54	2.720	0.039	0.002	0.037	2	0.840	0.000	0.001	0.000
55	2.750	0.035	0.001	0.034	3	0.900	0.001	0.007	-0.006
56	2.770	0.037	0.001	0.037	8	1.050	0.190	0.197	-0.007
57	2.820	0.032	0.000	0.032	4	0.920	0.005	0.013	-0.008
58	2.860	0.033	0.000	0.033	14	1.250	0.821	0.832	-0.011
59	2.900	0.018	0.000	0.018	5	0.930	0.005	0.017	-0.012
60	2.910	0.023	0.000	0.023	9	1.080	0.270	0.288	-0.018
61	2.960	0.013	0.000	0.013	28	1.700	0.981	1.000	-0.019
62	3.030	0.017	0.000	0.017	29	1.820	0.981	1.000	-0.019
63	3.110	0.022	0.000	0.022	30	1.860	0.981	1.000	-0.019
64	3.180	0.023	0.000	0.023	7	0.990	0.046	0.072	-0.026
65	3.200	0.011	0.000	0.011	6	0.970	0.019	0.047	-0.028
66	3.320	0.017	0.000	0.017	49	2.540	0.010	0.054	-0.044
67	3.410	0.009	0.000	0.009	45	2.400	0.280	0.328	-0.048
68	3.480	0.008	0.000	0.008	39	2.180	0.901	0.954	-0.053
69	3.540	0.006	0.000	0.006	33	1.960	0.941	1.000	-0.059
70	3.620	0.006	0.000	0.006	25	1.680	0.931	1.000	-0.069
71	3.680	0.003	0.000	0.003	27	1.750	0.931	1.000	-0.069
72	3.750	0.004	0.000	0.004	46	2.410	0.220	0.297	-0.077
73	3.820	0.004	0.000	0.004	28	1.730	0.921	1.000	-0.079
74	3.890	0.003	0.000	0.003	48	2.490	0.020	0.114	-0.094
75	3.960	0.003	0.000	0.003	23	1.560	0.901	0.999	-0.099
76	4.120	0.001	0.000	0.001	31	1.890	0.901	1.000	-0.099
77	4.250	0.003	0.000	0.003	15	1.280	0.780	0.887	-0.106
78	4.390	0.002	0.000	0.002	16	1.330	0.831	0.946	-0.115
79	4.980	0.003	0.000	0.003	17	1.360	0.851	0.967	-0.117
80	5.460	0.002	0.000	0.002	38	2.140	0.861	0.983	-0.122
81	5.970	0.000	0.000	0.000	20	1.460	0.841	0.995	-0.155
82	6.760	0.001	0.000	0.001	35	2.040	0.841	1.000	-0.159
83	8.420	0.001	0.000	0.001	18	1.400	0.821	0.984	-0.163

END OF PROBLEM
==========

P3LC2.OUT

```
*****************************************************************************
*
*          NON-LINEAR  LEAST SQUARES ANALYSIS
*
*          SEMI-INFINITE PROFILE, 3-TYPE BC
*long col, PULSE NOT FIXED, por. cop #2, br, v=1.25E-02cm/min
*
*****************************************************************************
```

INITIAL VALUES OF COEFFICIENTS

NO	NAME	INITIAL VALUE
1	peclet	63.000
2	RF	1.100
3	pulse	2.410

OBSERVED DATA

OBS.NO.	PORE VOLUME	CONCENTRATION
1	0.6200	0.0000
2	0.6500	0.0000
3	0.7100	0.0000
4	0.7600	0.0000
5	0.7900	0.0000
6	0.8300	0.0000
7	0.8800	0.0017
8	0.9000	0.0058
9	0.9400	0.0160
10	0.9800	0.0451
11	1.0700	0.1602
12	1.1400	0.2802
13	1.2400	0.4804
14	1.2600	0.5304
15	1.2900	0.5604
16	1.3600	0.2802
17	1.4000	0.2903
18	1.5100	0.6905
19	1.5700	0.7405
20	1.6500	0.7705
21	1.6900	0.6804
22	1.7900	0.6504
23	1.8700	0.8805
24	1.9500	0.7405
25	1.9800	0.5804
26	2.0900	0.8805
27	2.1700	0.9005
28	2.2300	0.8505
29	2.2900	1.0006
30	2.3600	0.8805
31	2.4000	0.9406
32	2.5100	1.0006
33	2.6500	1.0006
34	2.7200	0.9305
35	2.8000	0.8405
36	2.8300	1.0006
37	2.9400	0.9205
38	3.1300	1.0006
39	3.2200	1.0006

40	3.2700	0.9205
41	3.3600	0.9806
42	3.4100	0.9606
43	3.5000	0.8405
44	3.5600	0.6204
45	3.6500	0.4303
46	3.7200	0.3203
47	3.7900	0.2602
48	3.8300	0.1802
49	3.9300	0.1201
50	3.9700	0.0901
51	4.0700	0.0701
52	4.1300	0.0701
53	4.2300	0.0501
54	4.2900	0.0401
55	4.3600	0.0401
56	4.4100	0.0300
57	4.5000	0.0300
58	4.5600	0.0300
59	4.6500	0.0200
60	4.6900	0.0100
61	4.7900	0.0050
62	4.8300	0.0030
63	4.9300	0.0200
64	4.9800	0.0080
65	5.0800	0.0080
66	5.1300	0.0062
67	5.2100	0.0064
68	5.2700	0.0057
69	5.3600	0.0054
70	5.4200	0.0045
71	5.5000	0.0050
72	5.5500	0.0042
73	5.6400	0.0046
74	5.8300	0.0034
75	5.9300	0.0034
76	6.0800	0.0026
77	6.2200	0.0024
78	6.3600	0.0023
79	6.5000	0.0019
80	6.6400	0.0220
81	6.8300	0.0008
82	6.9400	0.0018
83	7.0800	0.0025
84	7.2400	0.0025
85	7.5000	0.0020
86	7.6400	0.0021
87	7.7900	0.0020
88	7.9300	0.0021
89	8.2500	0.0013
90	8.5100	0.0017
91	9.7100	0.0076
92	9.9600	0.0029
93	13.5300	0.0008
94	16.8400	0.0004

ITERATION	SSQ	peclet	RF	pulse
0	2.3544295	63.00000	1.10000	2.41000
1	0.8913751	15.86172	1.27962	2.35707

2	0.6395069	25.34514	1.41099	2.24221
3	0.6257789	29.42019	1.40500	2.23997
4	0.6245639	30.55924	1.40137	2.24449
5	0.6244543	30.79736	1.40009	2.24535
6	0.6244307	30.86469	1.39974	2.24573
7	0.6244265	30.88167	1.39964	2.24580
8	0.6244252	30.88641	1.39962	2.24583

CORRELATION MATRIX
==========

	1	2	3
1	1.0000		
2	0.1944	1.0000	
3	-0.1078	-0.0838	1.0000

NON-LINEAR LEAST SQUARES ANALYSIS, FINAL RESULTS
==========

VARIABLE	NAME	VALUE	S.E.COEFF.	T-VALUE	95% CONFIDENCE LIMITS LOWER	UPPER
1	peclet	30.88641	4.4409	6.95	22.0529	39.7199
2	RF	1.39962	0.0235	59.55	1.3529	1.4463
3	pulse	2.24583	0.0336	66.79	2.1790	2.3126

--------ORDERED BY COMPUTER INPUT---------

O	PORE VOLUME	CONCENTRATION OBS.	FITTED	RESIDUAL
1	0.620	0.000	0.000	0.000
2	0.650	0.000	0.001	-0.001
3	0.710	0.000	0.003	-0.003
4	0.750	0.000	0.007	-0.007
5	0.790	0.000	0.010	-0.010
6	0.830	0.000	0.017	-0.017
7	0.880	0.002	0.031	-0.029
8	0.900	0.006	0.038	-0.032
9	0.940	0.016	0.055	-0.039
10	0.980	0.045	0.076	-0.031
11	1.070	0.160	0.140	0.020
12	1.140	0.280	0.205	0.075
13	1.240	0.480	0.313	0.167
14	1.260	0.530	0.336	0.194
15	1.290	0.560	0.371	0.189
16	1.360	0.280	0.453	-0.173
17	1.400	0.290	0.499	-0.209
18	1.510	0.690	0.618	0.073
19	1.570	0.740	0.675	0.065
20	1.650	0.770	0.743	0.027
21	1.690	0.680	0.773	-0.093
22	1.790	0.950	0.837	-0.186
23	1.870	0.881	0.876	0.004
24	1.950	0.740	0.907	-0.167
25	1.980	0.580	0.917	-0.337
26	2.090	0.881	0.946	-0.065
27	2.170	0.901	0.961	-0.060
28	2.230	0.851	0.969	-0.119
29	2.290	1.001	0.976	0.024
30	2.360	0.881	0.982	-0.102
31	2.400	0.941	0.985	-0.045

----------ORDERED BY RESIDUALS----------

NO	PORE VOLUME	CONCENTRATION OBS.	FITTED	RESIDUAL
14	1.260	0.530	0.336	0.194
42	3.410	0.961	0.770	0.190
15	1.290	0.560	0.371	0.189
43	3.500	0.841	0.671	0.170
13	1.240	0.480	0.313	0.167
41	3.300	0.981	0.820	0.161
12	1.140	0.280	0.205	0.075
39	3.220	1.001	0.927	0.073
18	1.510	0.690	0.618	0.073
19	1.570	0.740	0.675	0.065
38	3.130	1.001	0.967	0.033
20	1.650	0.770	0.743	0.027
40	3.270	0.921	0.895	0.026
29	2.290	1.001	0.976	0.024
80	6.640	0.022	0.000	0.022
44	3.500	0.620	0.601	0.020
11	1.070	0.160	0.140	0.020
63	4.930	0.020	0.004	0.016
32	2.510	1.001	0.991	0.010
58	4.500	0.030	0.022	0.009
91	9.710	0.008	0.000	0.008
65	5.080	0.008	0.002	0.006
33	2.650	1.001	0.995	0.005
59	4.650	0.020	0.015	0.005
67	5.210	0.006	0.001	0.005
68	5.270	0.006	0.001	0.005
69	5.360	0.005	0.001	0.005
71	5.500	0.005	0.000	0.005
64	4.980	0.008	0.003	0.005
66	5.130	0.006	0.002	0.005
73	5.640	0.005	0.000	0.004

32	2.510	1.001	0.991	0.010
33	2.650	1.001	0.995	0.005
34	2.720	0.931	0.996	-0.066
35	2.800	0.841	0.998	-0.157
36	2.830	1.001	0.998	0.003
37	2.940	0.921	0.997	-0.076
38	3.130	1.001	0.967	0.033
39	3.220	1.001	0.927	0.073
40	3.270	0.921	0.895	0.026
41	3.350	0.981	0.820	0.161
42	3.410	0.961	0.770	0.190
43	3.500	0.841	0.671	0.170
44	3.550	0.620	0.601	0.020
45	3.650	0.430	0.496	-0.066
46	3.720	0.320	0.419	-0.099
47	3.790	0.260	0.349	-0.089
48	3.830	0.180	0.312	-0.132
49	3.930	0.120	0.231	-0.111
50	3.970	0.090	0.203	-0.113
51	4.070	0.070	0.145	-0.075
52	4.130	0.070	0.118	-0.048
53	4.230	0.050	0.081	-0.031
54	4.290	0.040	0.065	-0.025
55	4.360	0.040	0.049	-0.009
56	4.410	0.030	0.040	-0.010
57	4.500	0.030	0.028	0.002
58	4.560	0.030	0.022	0.009
59	4.650	0.020	0.015	0.005
60	4.690	0.010	0.012	-0.002
61	4.790	0.005	0.008	-0.003
62	4.830	0.003	0.007	-0.004
63	4.930	0.020	0.004	0.016
64	4.980	0.008	0.003	0.005
65	5.080	0.008	0.002	0.006
66	5.130	0.006	0.002	0.005
67	5.210	0.006	0.001	0.005
68	5.270	0.006	0.001	0.005
69	5.360	0.005	0.001	0.005
70	5.420	0.005	0.000	0.004
71	5.500	0.005	0.000	0.005
72	5.550	0.004	0.000	0.004
73	5.640	0.005	0.000	0.004
74	5.830	0.003	0.000	0.003
75	5.930	0.003	0.000	0.003
76	6.080	0.003	0.000	0.003
77	6.220	0.002	0.000	0.002
78	6.360	0.002	0.000	0.002
79	6.500	0.002	0.000	0.002
80	6.640	0.022	0.000	0.022
81	6.830	0.001	0.000	0.001
82	6.940	0.002	0.000	0.002
83	7.080	0.003	0.000	0.002
84	7.240	0.003	0.000	0.002
85	7.500	0.002	0.000	0.002
86	7.640	0.002	0.000	0.002
87	7.790	0.002	0.000	0.002
88	7.930	0.002	0.000	0.002
89	8.250	0.001	0.000	0.001
90	8.510	0.002	0.000	0.002
91	9.710	0.008	0.000	0.008

23	1.870	0.881	0.876	0.004
70	5.420	0.005	0.000	0.004
72	5.550	0.004	0.000	0.004
75	5.930	0.003	0.000	0.003
74	5.830	0.003	0.000	0.003
92	9.960	0.003	0.000	0.003
36	2.830	1.001	0.998	0.003
76	6.080	0.003	0.000	0.003
84	7.240	0.003	0.000	0.002
83	7.080	0.003	0.000	0.002
77	6.220	0.002	0.000	0.002
57	4.500	0.030	0.028	0.002
73	6.360	0.002	0.000	0.002
88	7.930	0.002	0.000	0.002
86	7.640	0.002	0.000	0.002
87	7.790	0.002	0.000	0.002
85	7.500	0.002	0.000	0.002
79	6.500	0.002	0.000	0.002
82	6.940	0.002	0.000	0.002
90	8.510	0.002	0.000	0.002
89	8.250	0.001	0.000	0.001
93	13.530	0.001	0.000	0.001
81	6.830	0.001	0.000	0.001
94	16.840	0.000	0.000	0.000
1	0.620	0.000	0.000	0.000
2	0.650	0.000	0.001	-0.001
60	4.690	0.010	0.012	-0.002
61	4.790	0.005	0.008	-0.003
3	0.710	0.000	0.003	-0.003
62	4.830	0.003	0.007	-0.004
4	0.760	0.000	0.007	-0.007
55	4.360	0.040	0.049	-0.009
56	4.410	0.030	0.040	-0.010
5	0.790	0.000	0.010	-0.010
6	0.830	0.000	0.017	-0.017
54	4.290	0.040	0.065	-0.025
7	0.880	0.002	0.031	-0.029
10	0.980	0.045	0.076	-0.031
53	4.230	0.050	0.081	-0.031
8	0.900	0.006	0.038	-0.032
9	0.940	0.016	0.055	-0.039
31	2.400	0.941	0.985	-0.045
52	4.130	0.070	0.118	-0.048
27	2.170	0.901	0.961	-0.060
26	2.090	0.881	0.946	-0.065
34	2.720	0.931	0.996	-0.066
45	3.650	0.430	0.496	-0.066
51	4.070	0.070	0.145	-0.075
37	2.940	0.921	0.997	-0.076
47	3.790	0.260	0.349	-0.089
21	1.690	0.680	0.773	-0.093
46	3.720	0.320	0.419	-0.099
30	2.360	0.881	0.982	-0.102
49	3.930	0.120	0.231	-0.111
50	3.970	0.090	0.203	-0.113
28	2.230	0.851	0.969	-0.119
48	3.830	0.180	0.312	-0.132
35	2.800	0.841	0.998	-0.157
24	1.950	0.740	0.907	-0.167
16	1.360	0.280	0.453	-0.173

92	9.960	0.003	0.000	0.003	22	1.790	0.650	0.837	-0.186
93	13.530	0.001	0.000	0.001	17	1.400	0.290	0.499	-0.209
94	16.840	0.000	0.000	0.000	25	1.980	0.580	0.917	-0.337

END OF PROBLEM
==========

```
*****************************************************************************
*                                                                           *
*            NON-LINEAR  LEAST SQUARES ANALYSIS                             *
*                                                                           *
*            SEMI-INFINITE PROFILE, 3-TYPE BC
*LONG COL. POROUS CUP#1, BR-, PULSE NOT FIXED,V=1.25E-02cm/min
*
*****************************************************************************
```

INITIAL VALUES OF COEFFICIENTS

NO	NAME	INITIAL VALUE
1	PECLET	31.500
2	RF	1.100
3	PULSE	4.820

OBSERVED DATA

OBS.NO.	PORE VOLUME	CONCENTRATION
1	0.1600	0.0000
2	0.3000	0.0000
3	0.4300	0.0000
4	0.5600	0.0000
5	0.6500	0.0000
6	0.7200	0.0000
7	0.8300	0.0000
8	1.0100	0.0921
9	1.0700	0.2802
10	1.1800	0.4103
11	1.2400	0.5904
12	1.3100	0.6204
13	1.4300	0.8005
14	1.5100	0.8005
15	1.6000	0.8005
16	1.6600	0.8005
17	1.7300	0.8305
18	1.8100	0.8605
19	1.8700	0.8605
20	1.9600	0.9406
21	2.1400	0.5004
22	2.2800	0.4804
23	2.4200	0.9606
24	2.5200	0.5904
25	2.5800	0.6504
26	2.7200	0.5404
27	2.8100	0.4704
28	3.0200	0.9406
29	3.1400	1.0006
30	3.3000	1.0006
31	3.3800	0.9706
32	3.5800	0.7805
33	3.7400	1.0006
34	3.8900	0.9406
35	3.9600	1.0006
36	4.1900	0.9406
37	4.3300	1.0006
38	4.4700	1.0006
39	4.8000	1.0006

10	5.0100	1.0000
11	5.1200	0.9400
12	5.2900	1.0000
13	5.3400	1.0000
14	5.5000	1.0000
15	5.6600	1.0000
16	5.8700	1.0000
17	5.9600	0.6504
18	6.1700	0.4003
19	6.4600	0.2202
20	6.4400	0.1582
21	6.5500	0.1201
22	6.7200	0.0601
23	6.8200	0.0401
24	7.0000	0.0401
25	7.1200	0.0300
26	7.3000	0.0200
27	7.4400	0.0200
28	7.5700	0.0200
29	7.6600	0.0050
30	7.8500	0.0050
31	7.9400	0.0050
32	8.1500	0.0020
33	8.2600	0.0020
34	8.4700	0.0050
35	8.5900	0.0040
36	8.7200	0.0030
37	8.9200	0.0030
38	9.0100	0.0020
39	9.1200	0.0020
40	9.2900	0.0020
41	9.3800	0.0010
42	9.5900	0.0005
43	9.6700	0.0004
44	9.8600	0.0010
45	9.9600	0.0010
46	10.1600	0.0020
47	10.2600	0.0014
48	10.4300	0.0014
49	10.5300	0.0012
50	10.7200	0.0014
51	10.8500	0.0011
52	10.9900	0.0010
53	11.1100	0.0007
54	11.3000	0.0007
55	11.6600	0.0007
56	11.6600	0.0006
57	12.1600	0.0006
58	12.1500	0.0007
59	12.7300	0.0007
60	13.2800	0.0026
61	13.6600	0.0029
62	13.8900	0.0007
63	14.1700	0.0007
64	14.4900	0.0009
65	14.7100	0.0009
66	15.0000	0.0007
67	15.2900	0.0007
68	15.5700	0.0007
69	15.8500	0.0007

100	16.4800	0.0010
101	17.0200	0.0008
102	17.5600	0.0010
103	18.7700	0.0009
104	19.9000	0.0008
105	21.8700	0.0006
106	23.8900	0.0004
107	27.0600	0.0000

ITERATION	SSQ	PECLET	RF	PULSE
0	1.9055673	31.50000	1.10000	4.82000
1	1.4569708	28.06241	1.23884	4.87182
2	1.4537093	26.74090	1.25173	4.85703
3	1.4521383	25.13398	1.25302	4.85609
4	1.4512704	24.06231	1.25455	4.85464
5	1.4507498	23.27203	1.25565	4.85389
6	1.4504281	22.67755	1.25656	4.85316
7	1.4502249	22.22116	1.25717	4.85257
8	1.4500945	21.86598	1.25770	4.85210
9	1.4500098	21.58671	1.25812	4.85172
10	1.4499542	21.36545	1.25846	4.85142
11	1.4499174	21.18911	1.25873	4.85117
12	1.4498929	21.04793	1.25895	4.85097
13	1.4498764	20.93450	1.25913	4.85081
14	1.4498653	20.84312	1.25928	4.85068
15	1.4498577	20.76933	1.25940	4.85057
16	1.4498525	20.70964	1.25949	4.85049
17	1.4498489	20.66130	1.25957	4.85042
18	1.4498464	20.62209	1.25963	4.85036
19	1.4498447	20.59027	1.25968	4.85031
20	1.4498434	20.56443	1.25973	4.85027
21	1.4498425	20.54342	1.25976	4.85024
22	1.4498419	20.52635	1.25979	4.85022
23	1.4498414	20.51245	1.25981	4.85020
24	1.4498410	20.50115	1.25983	4.85018
25	1.4498408	20.49195	1.25984	4.85017

CORRELATION MATRIX
==========

	1	2	3
1	1.0000		
2	0.3431	1.0000	
3	-0.1692	-0.6162	1.0000

NON-LINEAR LEAST SQUARES ANALYSIS, FINAL RESULTS
==========

VARIABLE	NAME	VALUE	S.E.COEFF.	T-VALUE	95% CONFIDENCE LIMITS LOWER	UPPER
1	PECLET	20.49195	5.3738	3.81	9.8351	31.1488
2	RF	1.25981	0.0423	29.75	1.1759	1.3438
3	PULSE	4.85017	0.0660	73.48	4.7193	4.9811

--------ORDERED BY COMPUTER INPUT----------

NO	PORE VOLUME	CONCENTRATION OBS.	FITTED	RESIDUAL
1	0.160	0.000	0.000	0.000

----------ORDERED BY RESIDUALS----------

NO	PORE VOLUME	CONCENTRATION OBS.	FITTED	RESIDUAL
46	5.870	1.001	0.758	0.243

2	0.370	0.000	0.000	0.000
3	0.430	0.000	0.000	0.000
4	0.560	0.000	0.003	-0.003
5	0.630	0.000	0.014	-0.014
6	0.720	0.000	0.031	-0.031
7	0.830	0.000	0.083	-0.083
8	1.010	0.092	0.232	-0.140
9	1.070	0.280	0.294	-0.014
10	1.180	0.410	0.413	-0.002
11	1.240	0.590	0.477	0.114
12	1.310	0.620	0.548	0.072
13	1.430	0.800	0.659	0.142
14	1.510	0.800	0.721	0.079
15	1.600	0.800	0.782	0.019
16	1.660	0.800	0.816	-0.015
17	1.730	0.831	0.850	-0.019
18	1.810	0.861	0.882	-0.022
19	1.870	0.861	0.902	-0.042
20	1.960	0.941	0.927	0.014
21	2.140	0.500	0.960	-0.459
22	2.280	0.480	0.975	-0.495
23	2.460	0.961	0.987	-0.026
24	2.520	0.590	0.989	-0.399
25	2.580	0.650	0.992	-0.341
26	2.720	0.540	0.995	-0.455
27	2.810	0.470	0.996	-0.526
28	3.020	0.941	0.998	-0.058
29	3.140	1.001	0.999	0.002
30	3.300	1.001	0.999	0.001
31	3.380	0.971	1.000	-0.029
32	3.580	0.780	1.000	-0.219
33	3.740	1.001	1.000	0.001
34	3.890	0.941	1.000	-0.059
35	3.960	1.001	1.000	0.001
36	4.190	0.941	1.000	-0.059
37	4.330	1.001	1.000	0.001
38	4.470	1.001	1.000	0.001
39	4.800	1.001	1.000	0.001
40	5.010	1.001	1.000	0.001
41	5.120	0.941	1.000	-0.059
42	5.290	1.001	1.000	0.001
43	5.440	1.001	0.995	0.006
44	5.600	0.951	0.958	-0.007
45	5.660	1.001	0.928	0.072
46	5.870	1.001	0.758	0.243
47	5.950	0.650	0.663	-0.013
48	6.170	0.400	0.442	-0.042
49	6.260	0.220	0.359	-0.139
50	6.440	0.150	0.225	-0.074
51	6.550	0.120	0.164	-0.044
52	6.720	0.060	0.098	-0.038
53	6.820	0.040	0.071	-0.031
54	7.000	0.040	0.039	0.001
55	7.120	0.030	0.026	0.004
56	7.300	0.020	0.014	0.006
57	7.440	0.020	0.008	0.012
58	7.570	0.020	0.005	0.015
59	7.660	0.005	0.004	0.001
60	7.850	0.005	0.002	0.003
61	7.940	0.005	0.001	0.004

13	1.430	0.300	0.659	0.142
11	1.240	0.590	0.477	0.114
14	1.510	0.800	0.721	0.079
12	1.310	0.620	0.548	0.072
45	5.660	1.001	0.928	0.072
15	1.600	0.800	0.782	0.019
58	7.570	0.020	0.005	0.015
20	1.960	0.941	0.927	0.014
57	7.440	0.020	0.008	0.012
56	7.300	0.020	0.014	0.006
43	5.440	1.001	0.995	0.006
54	6.470	0.005	0.000	0.005
55	7.120	0.030	0.026	0.004
65	8.590	0.004	0.000	0.004
61	7.940	0.005	0.001	0.004
62	7.850	0.005	0.002	0.003
67	8.820	0.003	0.000	0.003
65	8.720	0.003	0.000	0.003
91	13.660	0.003	0.000	0.003
90	13.280	0.003	0.000	0.003
76	10.160	0.002	0.000	0.002
70	9.290	0.002	0.000	0.002
69	9.120	0.002	0.000	0.002
68	9.010	0.002	0.000	0.002
63	8.280	0.002	0.000	0.002
29	3.140	1.001	0.999	0.002
62	8.150	0.002	0.001	0.001
59	7.660	0.005	0.004	0.001
80	10.720	0.001	0.000	0.001
78	10.430	0.001	0.000	0.001
77	10.280	0.001	0.000	0.001
79	10.530	0.001	0.000	0.001
30	3.300	1.001	0.999	0.001
81	10.850	0.001	0.000	0.001
54	7.000	0.040	0.039	0.001
102	17.560	0.001	0.000	0.001
82	10.990	0.001	0.000	0.001
75	9.960	0.001	0.000	0.001
74	9.860	0.001	0.000	0.001
71	9.380	0.001	0.000	0.001
100	16.480	0.001	0.000	0.001
103	18.770	0.001	0.000	0.001
94	14.490	0.001	0.000	0.001
95	14.710	0.001	0.000	0.001
104	19.900	0.001	0.000	0.001
101	17.020	0.001	0.000	0.001
89	12.730	0.001	0.000	0.001
88	12.450	0.001	0.000	0.001
85	11.660	0.001	0.000	0.001
84	11.300	0.001	0.000	0.001
83	11.110	0.001	0.000	0.001
93	14.170	0.001	0.000	0.001
42	5.290	1.001	1.000	0.001
98	15.570	0.001	0.000	0.001
97	15.290	0.001	0.000	0.001
99	15.850	0.001	0.000	0.001
96	15.000	0.001	0.000	0.001
33	3.740	1.001	1.000	0.001
92	13.890	0.001	0.000	0.001
105	21.870	0.001	0.000	0.001

62	8.150	0.002	0.001	0.001
63	8.250	0.002	0.000	0.002
64	8.470	0.005	0.000	0.005
65	8.590	0.004	0.000	0.004
66	8.720	0.003	0.000	0.003
67	8.820	0.003	0.000	0.003
68	9.010	0.002	0.000	0.002
69	9.120	0.002	0.000	0.002
70	9.290	0.002	0.000	0.002
71	9.380	0.001	0.000	0.001
72	9.530	0.001	0.000	0.000
73	9.570	0.000	0.000	0.000
74	9.850	0.001	0.000	0.001
75	9.960	0.001	0.000	0.001
76	10.160	0.002	0.000	0.002
77	10.260	0.001	0.000	0.001
78	10.430	0.001	0.000	0.001
79	10.530	0.001	0.000	0.001
80	10.720	0.001	0.000	0.001
81	10.850	0.001	0.000	0.001
82	10.990	0.001	0.000	0.001
83	11.110	0.001	0.000	0.001
84	11.300	0.001	0.000	0.001
85	11.060	0.001	0.000	0.001
86	11.660	0.001	0.000	0.001
87	12.160	0.001	0.000	0.001
88	12.450	0.001	0.000	0.001
89	12.730	0.001	0.000	0.001
90	13.260	0.003	0.000	0.003
91	13.660	0.003	0.000	0.003
92	13.890	0.001	0.000	0.001
93	14.170	0.001	0.000	0.001
94	14.490	0.001	0.000	0.001
95	14.710	0.001	0.000	0.001
96	15.000	0.001	0.000	0.001
97	15.290	0.001	0.000	0.001
98	15.570	0.001	0.000	0.001
99	15.850	0.001	0.000	0.001
100	16.480	0.001	0.000	0.001
101	17.020	0.001	0.000	0.001
102	17.560	0.001	0.000	0.001
103	18.770	0.001	0.000	0.001
104	19.920	0.001	0.000	0.001
105	21.870	0.001	0.000	0.001
106	23.890	0.000	0.000	0.000
107	27.060	0.000	0.000	0.000

35	3.960	1.001	1.000	0.001
87	12.160	0.001	0.000	0.001
86	11.660	0.001	0.000	0.001
37	4.330	1.001	1.000	0.001
38	4.470	1.001	1.000	0.001
39	4.800	1.001	1.000	0.001
40	5.010	1.001	1.000	0.001
72	9.590	0.001	0.000	0.000
106	23.890	0.000	0.000	0.000
73	9.670	0.000	0.000	0.000
107	27.060	0.000	0.000	0.000
1	0.160	0.000	0.000	0.000
2	0.300	0.000	0.000	0.000
3	0.430	0.000	0.000	0.000
10	1.180	0.413	0.413	-0.002
4	0.560	0.000	0.003	-0.003
44	5.000	0.951	0.958	-0.007
47	5.960	0.650	0.663	-0.013
5	0.650	0.000	0.014	-0.014
9	1.070	0.280	0.294	-0.014
16	1.660	0.800	0.816	-0.015
17	1.730	0.831	0.850	-0.019
18	1.810	0.861	0.882	-0.022
23	2.460	0.961	0.987	-0.026
31	3.380	0.971	1.000	-0.029
53	6.820	0.040	0.071	-0.031
6	0.720	0.000	0.031	-0.031
52	6.720	0.060	0.098	-0.038
19	1.870	0.861	0.902	-0.042
48	6.170	0.400	0.442	-0.042
51	6.550	0.120	0.164	-0.044
28	3.020	0.941	0.998	-0.058
34	3.890	0.941	1.000	-0.059
36	4.190	0.941	1.000	-0.059
41	5.120	0.941	1.000	-0.059
50	6.440	0.150	0.225	-0.074
7	0.830	0.000	0.083	-0.083
49	6.260	0.220	0.359	-0.139
8	1.010	0.092	0.232	-0.140
32	3.580	0.780	1.000	-0.219
25	2.580	0.650	0.992	-0.341
24	2.520	0.590	0.989	-0.399
26	2.720	0.540	0.995	-0.455
21	2.140	0.500	0.960	-0.459
22	2.280	0.480	0.975	-0.495
27	2.810	0.470	0.996	-0.526

END OF PROBLEM
==========

END OF PROBLEM